

ARS JOURNAL

RUSSIAN SUPPLEMENT

Igor Jurkevich, Editor
Julie Hight, Asst. Editor

One-Dimensional Problem of Temperature Stresses in an Elastoplastic Medium V. A. Lomakin 1034

Theory of Stabilized Systems With Three Self-Compensation Channels of Acceleration Due to Gravity V. A. Bodner and V. P. Seleznev 1036

Determination of Temperature Induced Stresses in a Conical Shell V. A. Sibiriakov 1041

Small Parameter Method for Second-Order Differential Equations With Discontinuous Terms T. S. Shteinberg 1047

Scattering of Light in a Medium Adjacent to a Reflecting Surface S. D. Gutshabash 1051

Investigation of Heat Exchange in Supersonic Flow of Air in Tubes A. E. Marenov 1055

Radio Astronomical Observations of the Second Soviet Space Rocket V. V. Vitkevich,
A. D. Kuzmin, R. L. Sorochenko and V. A. Udaltsov 1060

Failure of Metals Due to Thermal Fatigue Yu. V. Kostochkin and I. A. Oding 1062

Some Problems of Auroral Physics V. I. Krasovskii 1065

DIGEST OF TRANSLATED RUSSIAN LITERATURE 1068

Published Under National Science Foundation Grant-in-Aid

One-Dimensional Problem of Temperature Stresses in an Elastoplastic Medium

V. A. LOMAKIN

Several authors have considered one-dimensional problems of temperature stresses in an elastoplastic medium whose mechanical properties are independent of temperature. In particular Kachanov (1,2)¹ investigated problems on deformation of a hollow sphere and cylinder. In his study Kachanov assumed that the temperature was a given function of radius. Of interest are analogous problems in which the temperature field is nonsteady. In some cases (not too high temperature and absence of phase transformations) this formulation permits determination of residual stresses formed in the bodies upon cooling. It is necessary, however, that the active process of deformation and the load relaxation be considered simultaneously. In (3) the author considers the deformation of a sphere upon cooling with the assigned value of the surface temperature. The current work is concerned with the one-dimensional² problem under conditions of realistic heat exchange.

LET us solve the one-dimensional problem of temperature stresses in an elastoplastic medium; this problem comprises the problems of stresses in an infinite plate (with thickness equal to $2R$), and an infinite cylinder and sphere (with radii equal to R). Let us assume that the body is uniformly heated to the temperature T_0 and at the given time $t = 0$ is placed in a medium with temperature $T_i < T_0$, $T_i = \text{const}$; the heat transfer coefficient of the medium is $\beta = \text{const}$.

Let us designate the radial direction for the cylinder and the sphere as well as the normal toward the mean surface direction for the plate by the index "3," and the two other principal directions by the indexes "2" and "1" (the index "2" designates the tangential direction for the cylinder). The principal strains and stresses will be designated correspondingly by e_k , σ_k ($k = 1, 2, 3$).

Let r be the linear coordinate in the direction of the axis "3"; $w = w(r, t)$ is the displacement in the same direction. Then, the deformation can be expressed as follows

$$\begin{aligned} e_3 &= \frac{\partial w(r, t)}{\partial r} & e_2 &= \frac{n}{1 + (n-1)^2} \frac{w(r, t)}{r} \\ e_1 &= (n-1)^2 e_2 \end{aligned} \quad \dots \dots \dots [1.1]$$

It is assumed here and in the following pages that $n = 0$ for the plate, $n = 1$ for the cylinder and $n = 2$ for the sphere.

To solve the problem let us make use of the plasticity laws in the same form as in (3). Then, from the relation $e_1 + e_2 + e_3 = 3\alpha\theta(r, t)$, where $\theta(r, t) = T(r, t) - T_0$ (denoting by α the coefficient of linear expansion) we obtain the equation for w

$$\frac{\partial w}{\partial r} + n \frac{w}{r} = 3\alpha\theta(r, t) \quad [1.2]$$

By integrating this equation using the boundary condition

Translated from *Institut Mekhaniki Akademii Nauk SSSR, Inzhenernyi Sbornik* (Institute of Mechanics, Academy of Sciences USSR, Engineering Collection), vol. 25, 1959. Translated by Alexander G. Godlevsky.

¹ Numbers in parentheses indicate References at end of paper.

$w|_{r=0} = 0$ we find the displacement, and from Equation [1.1] also the strains, obtaining

$$\begin{aligned} w &= \frac{3\alpha r}{n+1} \theta^* & e_2 &= \frac{3\alpha n}{(n+1)[1+(n-1)^2]} \theta^* \\ e_3 &= 3\alpha \left[\theta - \frac{n}{n+1} \theta^* \right] \end{aligned} \quad \dots \dots \dots [1.3]$$

Here

$$\theta^*(r, t) = \frac{n+1}{r^{n+1}} \int_0^r r^n \theta(r, t) dr$$

is the mean value of the function θ in the volume bounded by the coordinate surfaces $r = 0$ and r . The effective strain will be expressed by the equation

$$e_i(r, t) = \sqrt{2\alpha \sqrt{(\theta - n_1\theta^*)^2 + (n_2\theta^*)^2 + [\theta - (n/2)\theta^*]^2}} \quad [1.4]$$

where

$$n_1 = \frac{n}{1 + (n-1)^2} \quad n_2 = \frac{n(n-2)}{2}$$

Thus, the effective strain and, consequently, the effective stress become known functions of r and t , provided the temperature field is known which, for the problem we are considering, will be determined as the solution of the heat condition equation

$$\frac{\partial \theta}{\partial t} = \kappa \left[\frac{\partial^2 \theta}{\partial r^2} + \frac{n}{r} \frac{\partial \theta}{\partial r} \right]$$

for the boundary conditions

$$\theta|_{t=0} = 0 \quad \left[\frac{\partial \theta}{\partial r} + h(\theta - c) \right] \Big|_{r=R} = 0 \quad \frac{\partial \theta}{\partial r} \Big|_{r=0} = 0$$

where

$$\begin{aligned} h &= \beta/\lambda \\ \lambda &= \text{coefficient of thermal conductivity} \\ \kappa &= \text{coefficient of thermal diffusivity} \\ c &= T_i - T_0 \end{aligned}$$

From $(\partial e_i / \partial t)|_{r=a} = 0$ we obtain the boundary of the active and passive deformation as function of time $a = \psi(t)$.

The surface of the body is the first to react to the load; therefore, the effective stress is

$$\begin{aligned} \sigma_i(r, t) &= \Phi[e_i(r, t)] \quad r < a = \psi(t) \\ \sigma_i'(r, t) &= \sigma_i[r, t_0(r)] + 3G\{\theta(r, t) - e_i[r, t_0(r)]\} \\ r &\geq a = \psi(t) \end{aligned} \quad [1.5]$$

where t_0 is determined by the relation $\psi(t_0) = r$.

In order to determine the stresses, we make use of the equilibrium equation

$$\frac{\partial \sigma_3}{\partial r} + \frac{n}{r} (\sigma_3 - \sigma_2) = 0 \quad [1.6]$$

and the corresponding equation for the stress deviators from which, for $r < a$, it follows

$$\begin{aligned} \sigma_2 &= \sigma_3 - (2\sigma_i/e_i)\alpha(\theta - n_1\theta^*) \\ \sigma_1 &= \sigma_2 + (2\sigma_i/e_i)\alpha n_2\theta^* \end{aligned} \quad [1.7]$$

and similar formulas hold, with σ_i replaced by σ_i' , for $r \geq a$.

Making use of Equation [1.7] and by integrating Equation [1.6] subject to $\sigma_3|_{r=R} = 0$ we obtain

$$\begin{aligned} \sigma_3(r, t) &= 2\alpha \int_a^r \frac{\sigma_i}{re_i} (n_1\theta^* - \theta) dr + 2\alpha \int_R^a \frac{\sigma_i'}{re_i} \times \\ &\quad (n_1\theta^* - \theta) dr \quad r < a \\ \sigma_3(r, t) &= 2\alpha \int_R^r \frac{\sigma_i'}{re_i} (n_1\theta^* - \theta) dr \quad r \geq a \end{aligned} \quad [1.8]$$

The relations [1.8, 1.7 and 1.5] determine the stresses in the body at any given time. The residual stresses will be found from these formulas by passing to the limit $t \rightarrow \infty$.

2 As an example, let us consider the cooling of a sphere. The examination of the relation [1.4] with $n = 2$ shows that with a fixed r , the intensity of deformations first increases, then diminishes and becomes zero when completely cooled.

The more intensive the heat transfer, the sooner the effective strain reaches its maximum and the larger this maximum is; with $\beta = \infty$ and $r = R$ it takes the limiting value

$$e_i^{\max} = 2\alpha(T_0 - T_i)$$

The intensity of heat transfer substantially influences the conditions of plastic deformation and the magnitude of the residual stresses. The maximum value of the quantity

$$\epsilon_i = \frac{e_i}{2\alpha(T_0 - T_i)} \geq 0$$

is a function only of Biot's number $\zeta = (\beta/\lambda)R$

$$\epsilon_i^{\max} = k(\zeta)$$

Therefore the condition for the occurrence of plastic deformations in a sphere can be expressed as follows

$$(T_0 - T_i) > \frac{1}{k(\zeta)} \frac{e_i}{2\alpha}$$

For some values of ζ the values of k have been calculated, and the following results were obtained: $k(\infty) = 1$, $k(4) = 0.25$, $k(1) = 0.12$. The first result corresponds to the in-

stantaneous cooling of the surface of the sphere down to the temperature of the medium; the second, to the cooling in water of a steel sphere with the radius $R = 6$ cm; the third, to the cooling of the same sphere in oil.

The examination of the expressions [1.7 and 1.8] shows that the tangential residual stresses assume their maximum on the surface of the sphere where they equal

$$\sigma_{20}^{\max} = \sigma_{10}^{\max} = \sigma_i'(R, \infty)$$

which, for example, in case of linear hardening gives

$$\sigma_{10}^{\max} = \sigma_s \lambda \left[1 - k(\zeta) \frac{2\alpha(T_0 - T_i)}{e_s} \right]$$

Given that for carbon steel α is equal to 13×10^{-6} per deg and e_s is equal to 12×10^{-4} , we find that plastic deformations (and consequently the residual stresses as well), in a sphere cooled in water will occur if the difference between the initial temperature of the body and the temperature of the medium $(T_0 - T_i)$ exceeds 200 C.

Assuming $\lambda = 0.95$ and $T_0 - T_i = 350$ C, we obtain

$$\sigma_{10}^{\max} = -0.85\sigma_s$$

If, in solution of this problem, we assume that the surface of the sphere acquires instantaneously the temperature of the medium, then the temperature drop at which plastic deformation occurs will equal only 50 C; in this case residual stresses will be considerable. This shows the importance of carrying out the calculations using realistic conditions of heat exchange.

Problems concerning the plate and the sphere can be solved with the consideration of the compressibility of material. This consideration, however, does not influence substantially the magnitude of residual stresses at high gradients of temperature arising in the body, since residual stresses are determined by maximal values of deformations. In such cases, the consideration of compressibility will only lead to an unjustified complication of computations.

3 Let us examine the semi-infinite space $z \geq 0$, every point of which has the temperature T_0 . The free surface [the plane (x, y)] at time $t = 0$ is brought into contact with a medium whose temperature is $T_i < T_0$. $T_i = \text{const}$; the coefficient of the heat transfer to this medium is $\beta = \text{const}$.

The solution of the boundary problem for $\theta = T - T_0$ gives (4)

$$\begin{aligned} \theta(z, t) &= (T_i - T_0) \times \left[\operatorname{erfc} \frac{z}{2\sqrt{at}} - e^{h^2 z^2 + h^2 at} \times \right. \\ &\quad \left. \operatorname{erfc} \left(\frac{z}{2\sqrt{at}} + h\sqrt{at} \right) \right] \end{aligned} \quad [3.1]$$

where

$$\operatorname{erfc} x = \frac{2}{\sqrt{\pi}} \int_x^\infty e^{-x^2} dx$$

For stresses and strains we have

$$\begin{aligned} X_x &= Y_y = \sigma_1(z, t) \quad Z_z = X_y = \dots = 0 \\ e_{zz} &= e_3(z, t) \quad e_{xx} = \dots = e_{zz} = 0 \end{aligned} \quad [3.2]$$

In this case the problem can be completely solved by the use of the following equations

$$\sigma_i = \Phi(e_i) \quad e = (\sigma/3k) + \alpha\theta \quad [3.3]$$

From Equation [3.3], considering [3.2 and 3.1] we find

$$\begin{aligned} e_i + \frac{4\Phi(e_i)}{9k} &= 2\alpha(T_0 - T_i) \left[\operatorname{erfc} \frac{z}{2\sqrt{at}} - e^{h^2 z^2 + h^2 at} \times \right. \\ &\quad \left. \operatorname{erfc} \left(\frac{z}{2\sqrt{at}} + h\sqrt{at} \right) \right] \end{aligned} \quad [3.4]$$

The equation [3.4] permits determining e_i ; after this the stresses can be found according to the formula

$$\sigma_i = \Phi(e_i) \quad [3.5]$$

Only active deformation takes place in the half-space; therefore, the residual stresses can be found from the foregoing relations at $t \rightarrow \infty$. In this case, the square bracket in [3.4] becomes unity, and for residual stresses σ_{10} we obtain

$$\sigma_{10} = \Phi(e_{i0}) \quad [3.6]$$

where e_{i0} is determined from

$$e_{i0} + [4\Phi(e_{i0})]/9k = 2\alpha(T_0 - T_i)$$

With linear hardening, taking for e_s , λ , α the same values as in the foregoing example for the sphere, and assuming $T_0 - T_i = 350^\circ\text{C}$, we obtain

$$\begin{aligned} \sigma_{10} &= 1.26\sigma_s & (k = 2G) \\ \sigma_{10} &= 1.30\sigma_s & (k = \infty) \end{aligned}$$

Let us note that the ultimate stress [3.6] in the half-space

Reviewer's Comment

Assuming a given effective stress-effective strain law $\sigma_i = \Phi(e_i)$, the author considers immersion of an incompressible elastoplastic plate, cylinder or sphere of temperature T_0 , into an atmosphere of temperature $T_i < T_0$, assuming a finite surface Biot number. Of prime interest are the residual stresses which remain after elapse of infinite time. The problem has been considered by incremental theory, and in

does not depend on the coefficient of the heat transfer β with the medium. (Quantity β affects only the time required to establish in a fixed region a state which is close to the limiting one.) For bodies of finite dimensions, as has been shown above in the example of the sphere, the intensity of heat transfer significantly influences the conditions under which the plastic deformation occurs as well as the magnitude of residual stresses.

References

1. Kachanov, L. M., *Mekhanika Plasticheskikh Sred* (The Mechanics of Plastic Bodies), Gostekhizdat, 1948.
2. Kachanov, L. M., *Uprugo-Plasticheskoye Ravnovesiye Neravnomernogo Nagretykh Tolstostennnykh Cylindrov, Nakhodiaschikhsia Pod Deystviem Vnutrennego Davleniya* (The Elastoplastic Equilibrium of the Nonuniformly Heated Thick-Walled Cylinders Under the Action of the Internal Pressure), *J. Tekhnich. Fiz.*, vol. X, no. 14, 1940.
3. Lomakin, V. A., *Uprugo-Plasticheskoye Ravnovesiye Shara v Nestatsionarnom Temperaturnom Pole* (Elastoplastic Equilibrium of the Sphere in a Nonstationary Temperature Field) *PMM, J. Appl. Math. and Mech.*, vol. XIX, no. 2, 1955.
4. Lykov, A. V., *Teoriya Teploprovodnosti* (Theory of Heat Conduction), Gostekhizdat, 1952.

—Original received March 29, 1955

more detail, by Weiner, Landau-Weiner, Landau-Zwicky (*J. Appl. Mech.*, vol. 23, Sept. 1956, p. 395; vol. 25, Dec. 1958, p. 459; vol. 27, Sept. 1960, p. 481), and also by D. R. Bland (*J. Mech. Phys. Sol.*, vol. 4, no. 4, 1956, p. 209), the latter for steady temperature, but including the effect of pressure.

—G. HORVAY
Metallurgy and Ceramics
G. E. Research Laboratory, Schenectady

Theory of Stabilized Systems With Three Self-Compensation Channels of Acceleration Due to Gravity

V. A. BODNER and
V. P. SELEZNEV

The guided motion of a body depends upon knowledge at any given time of its position, velocity and other navigation elements with respect to a definite coordinate system. Continuous determination of the navigational elements can be made by means of navigation systems that are based either on properties of physical fields (gravitational, magnetic, electric, etc.) or on measured fixes on celestial bodies. Among such systems, a special place is occupied by inertial systems frequently employed in conjunction with celestial systems. Carroll (1)¹ considered an astro-inertial system that combined the favorable properties of both the celestial and the inertial systems, but did not take into account properties of stabilized systems employing three channels of self-compensation, and did not estimate the errors of such systems. This paper considers certain problems in the theory of gyro-stabilized inertial systems operating in three-dimensional space, and analyzes their systematic errors.

1 Principles of Construction of Stable Systems

IN AN inertial system, the navigational elements are determined by integrating the accelerations measured by three

¹Translated from *Izvestiya Akademii Nauk SSSR, Otdeleniye Tekhnicheskikh Nauk, Energetika i Avtomatika* (Bull. USSR Acad. Sci., Div. Tech. Sci., Power and Automation), no. 1, 1960, pp. 76-85. Translated by J. George Adashko.

²Numbers in parentheses indicate References at end of paper.

accelerometers with mutually perpendicular axes. The accelerations are measured with respect to the inertial coordinate system, which is chosen such that it has no angular velocity with respect to stellar space, although its origin may move under the influence of gravitational forces. The accelerometers measure only the accelerations due to the drag and thrust of the engines, but not gravitational forces.

Let us select the coordinate system. The origin of an iner-

tial system can be placed at the center of inertia of any celestial body that moves in a gravitational field. When moving in the vicinity of the Earth, the inertial system of coordinates can be an equatorial system, in which two axes coincide with the plane of the equator and the third with the axis of the Earth's rotation. A shortcoming of such a system is that its axes change in position relative to stellar space, owing to the Earth's rotation.

For interplanetary flight, it is convenient to use an ecliptic system, $x_0y_0z_0$ (Fig. 1), the origin of which is at the center of the sun. Two axes (x_0 and y_0) are in the plane of the Earth's orbit (ecliptic), while the third is perpendicular to this plane. One of the axes (x_0) can be to the first-magnitude star "Spica" located near the plane of the ecliptic. The position of the vehicle is defined in such a system by the rectangular coordinates x and y and z . A spherical coordinate system can also be used, with the same origin, but using the astronomical latitude φ , longitude λ and radius vector R .

The ecliptic system of coordinates has greater stability. Thus, the change in astronomical latitude amounts to 0.07 microradian annually, and the change in longitude to less than 0.1 microradian annually.

The vehicle is acted upon by forces of thrust, drag and gravitation. The vector thrust and drag will be denoted by F , and that of gravitation by G . The components of these forces in the Cartesian system $x_0y_0z_0$ are F_x, F_y, F_z and G_x, G_y, G_z . We denote by x, y, z and x', y', z' the coordinates and the velocities of the center-of-mass of the vehicle in the chosen inertial coordinate system $x_0y_0z_0$.

The expressions for the components of the acceleration of the center of the mass of the vehicle can be obtained from the equations of motion

$$mx'' = F_x - G_x \quad my'' = F_y - G_y \quad mz'' = F_z - G_z \quad [1.1]$$

where m is the mass of the vehicle.

Using the expressions for the accelerations of the vehicle

$$a_{x0} = \frac{F_x}{m} \quad a_{y0} = \frac{F_y}{m} \quad a_{z0} = \frac{F_z}{m} \quad [1.2]$$

and introducing the corresponding accelerations due to gravity

$$g_x = \frac{G_x}{m} \quad g_y = \frac{G_y}{m} \quad g_z = \frac{G_z}{m} \quad [1.3]$$

we obtain from Equations [1.1]

$$a_{x0} = x'' + g_x \quad a_{y0} = y'' + g_y \quad a_{z0} = z'' + g_z \quad [1.4]$$

Accelerometers whose sensitive axes are aligned with the $x_0y_0z_0$ axes will measure the accelerations [1.4]. If the motion is produced only by gravitational forces ($F = 0$), the accelerations [1.4] vanish, and the accelerometers read zero.

The gyro-stabilized inertial system should include a stabilized platform, three accelerometers with mutually perpendicular sensitive axes, integrators, a computer and feedback elements (Fig. 2). The sensitive axes of the accelerometers form an orthogonal coordinate system xyz , which should be parallel to the inertial system $x_0y_0z_0$. However, owing to the gyro drift, the coordinate system xyz will be inclined with respect to the system $x_0y_0z_0$ by angles α, β and γ (Fig. 3).

The integrators are necessary to integrate the accelerations and to determine the velocities and the position coordinates. The computer in the feedback system generates the gravity compensation signals. A shortcoming of the gyro-inertial system is that it cannot eliminate autonomously the angles α, β and γ . External information must be provided for this purpose.

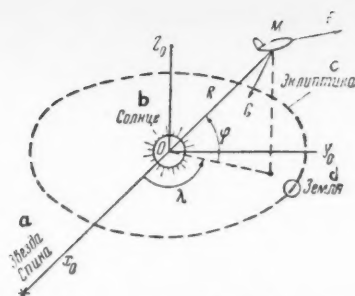


Fig. 1 Translations: a—star "Spica"; b—sun; c—ecliptic; d—Earth

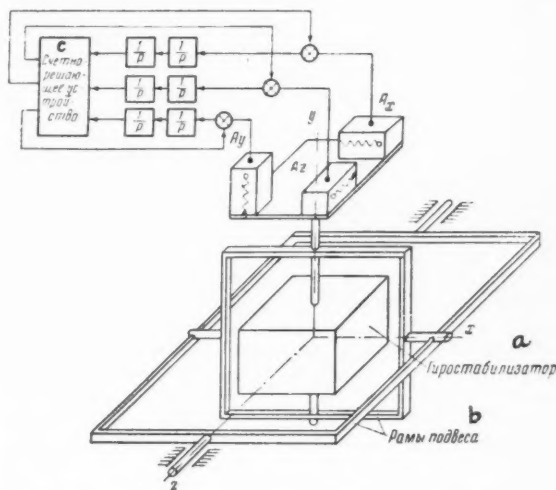


Fig. 2 Translations: a—gyro stabilizer; b—gimbals; c—computer

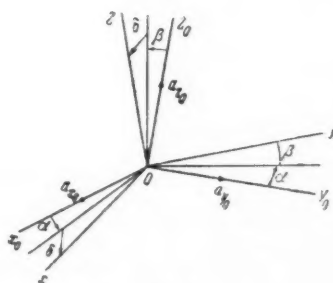


Fig. 3

Direction-cosine table

	x_0	y_0	z_0
x	$\cos \alpha \cos \beta$	$\sin \beta$	$-\sin \alpha \cos \beta$
y	$\sin \alpha \sin \gamma - \cos \alpha$	$\cos \beta \cos \gamma$	$\cos \alpha \sin \gamma + \sin \alpha$
	$\sin \beta \cos \gamma$		$\sin \beta \sin \gamma$
z	$\sin \alpha \cos \gamma + \cos \alpha$	$-\cos \beta \sin \gamma$	$\cos \alpha \cos \gamma - \sin \alpha$
	$\sin \beta \sin \gamma$		$\sin \beta \sin \gamma$

2 Equations of Motion of Stable Systems

To derive the equations of motion of an inertial system it is necessary to use the connection between the acceleration components in the $x_0y_0z_0$ and xyz systems. The acceleration components a_x, a_y and a_z measured by the accelerometers do not

equal the components of the acceleration of the center of mass of the vehicle, a_{x0} , a_{y0} and a_{z0} . The connection between these components is given by the direction-cosine table.

If we use the fact that under realistic conditions α , β and γ are small, the sines can be replaced by the angles themselves, the cosines can be set equal to unity and the products of the angles can be neglected as being of second order of smallness. Then the connection between the acceleration components in the xyz and $x_0y_0z_0$ systems will be

$$\begin{aligned} a_x &= a_{x0} + \Delta a_{x0} \\ a_y &= a_{y0} + \Delta a_{y0} \\ a_z &= a_{z0} + \Delta a_{z0} \end{aligned} \quad [2.1]$$

where

$$\begin{aligned} \Delta a_{x0} &= a_{y0}\beta - a_{z0}\alpha \\ \Delta a_{y0} &= a_{z0}\gamma - a_{x0}\beta \\ \Delta a_{z0} &= a_{x0}\alpha - a_{y0}\gamma \end{aligned} \quad [2.2]$$

The errors Δa_{x0} , Δa_{y0} and Δa_{z0} are due to the gyroscope drift, and consequently the sensitive axes of the accelerometers do not coincide with the axes of the inertial system.

The accelerometer output signals, as can be seen from the block diagram of Fig. 4, pass through the integrators with transfer functions k_{1x} , k_{1y} , k_{1z} , k_{2x} , k_{2y} and k_{2z} , and the computer, where the compensation signals g_{xc} , g_{yc} and g_{zc} are those computed to compensate for the gravitational accelerations.

The inertial system computes the position coordinates S_x , S_y and S_z and the velocities S'_x , S'_y and S'_z of the vehicle center of mass.

From the block diagram (Fig. 4) we obtain the following equations of motion for each of the inertial-system channels

$$\begin{aligned} \left[(a_x - g_{xc}) \frac{k_{1x}}{p} + x_0' \right] \frac{k_{2x}}{p} + x_0 &= S_x \\ \left[(a_y - g_{yc}) \frac{k_{1y}}{p} + y_0' \right] \frac{k_{2y}}{p} + y_0 &= S_y \\ \left[(a_z - g_{zc}) \frac{k_{1z}}{p} + z_0' \right] \frac{k_{2z}}{p} + z_0 &= S_z \end{aligned} \quad [2.3]$$

where x_0 , y_0 , z_0 and x_0' , y_0' , z_0' are the initial coordinates and velocities of the vehicle.

It is seen from the block diagram (Fig. 4) that the output signals of the first integrators are the components of the absolute flight velocity, and the second-integrator output signals are the components of the distance covered.

Let us transform Equations [2.3] by selecting the integrator transfer functions such as to satisfy the conditions $k_{1x}k_{2x} =$

$k_{1y}k_{2y} = k_{1z}k_{2z} = 1$. We obtain

$$\begin{aligned} \Delta x'' &= \Delta g_x + \Delta a_{x0} \\ \Delta y'' &= \Delta g_y + \Delta a_{y0} \\ \Delta z'' &= \Delta g_z + \Delta a_{z0} \end{aligned} \quad [2.4]$$

where

$$\Delta x = S_x - x \quad \Delta y = S_y - y \quad \Delta z = S_z - z \quad [2.5]$$

are the errors of the inertial system, and

$$\Delta g_x = g_x - g_{xc} \quad \Delta g_y = g_y - g_{yc} \quad \Delta g_z = g_z - g_{zc} \quad [2.6]$$

are errors that characterize inaccurate compensation for the accelerations due to gravity.

If the gravitational errors are fully compensated for in the inertial system ($\Delta g_x = \Delta g_y = \Delta g_z = 0$) and there is no gyroscope drift ($\Delta a_{x0} = \Delta a_{y0} = \Delta a_{z0} = 0$), then, as follows from Equation [2.4], the system error would be determined by the errors due to inaccurate specification of the initial conditions.

Since automatic compensation of the acceleration due to gravity cannot be exact, and the gyro platform does drift, various errors creep into the inertial system; these are analyzed in the material which follows.

3 Errors of the System for Automatic Compensation of the Gravitational Acceleration

The system errors of this kind arise because the compensation signals g_{xc} , g_{yc} and g_{zc} generated by the computer do not equal the acceleration components g_x , g_y and g_z . The errors arising are fed to an inertial system and, after going through the closed loop, again enter the computer. If the inertial system is stable, the automatic compensation errors will die out. Otherwise they will increase, resulting in an inexact determination of the position.

To generate the compensation signals it is necessary to know the analytic expressions for the acceleration components g_x , g_y and g_z due to the gravitational forces acting on the vehicle from the celestial bodies. If m_i , x_i , y_i and z_i ($i = 1, 2, \dots, n$) are the masses and coordinates of the centers of mass of the celestial bodies, causing the accelerations of the vehicle, then the acceleration components will be

$$\begin{aligned} g_x &= \sum_{i=1}^n f m_i \frac{x - x_i}{R_i^3} & g_y &= \sum_{i=1}^n f m_i \frac{y - y_i}{R_i^3} \\ g_z &= \sum_{i=1}^n f m_i \frac{z - z_i}{R_i^3} \end{aligned} \quad [3.1]$$

where

$$R_i = \sqrt{(x - x_i)^2 + (y - y_i)^2 + (z - z_i)^2} \quad [3.2]$$

and f is the gravitational constant, 6.67×10^{-8} cgs.

The computer will form compensation signals g_{xc} , g_{yc} and g_{zc} in accordance with formulas [3.1 and 3.2], in which one must replace the actual vehicle coordinates x , y and z by the coordinates S_x , S_y and S_z measured by the inertial system. Consequently, the computer will compute the compensation signals by means of the following formulas

$$\begin{aligned} g_{xc} &= \sum_{i=1}^n f m_i \frac{S_x - x_i}{\bar{R}_i^3} & g_{yc} &= \sum_{i=1}^n f m_i \frac{S_y - y_i}{\bar{R}_i^3} \\ g_{zc} &= \sum_{i=1}^n f m_i \frac{S_z - z_i}{\bar{R}_i^3} \end{aligned} \quad [3.3]$$

$$\bar{R}_i = \sqrt{(S_x - x_i)^2 + (S_y - y_i)^2 + (S_z - z_i)^2} \quad [3.4]$$

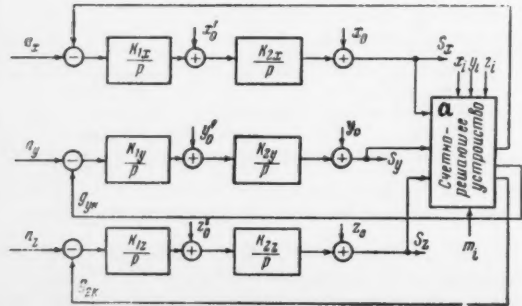


Fig. 4 Translation: a—computer

To perform the calculations it is also necessary to know the masses m_i and the coordinates x_i , y_i and z_i of celestial bodies, which can be obtained with high accuracy.

If one forms the differences Δg_x , Δg_y and Δg_z by substituting Equations [3.1 and 3.3] in [2.6], and if these differences are expanded in powers of the increments Δx , Δy and Δz , then, retaining only the linear terms, we obtain

$$\Delta g_x = - \sum_{i=1}^n \frac{fm_i}{R_i^3} \left\{ \left[1 - 3 \left(\frac{x - x_i}{R_i} \right)^2 \right] \Delta x - 3 \times \right. \\ \left. \frac{x - x_i}{R_i^2} [(y - y_i)\Delta y + (z - z_i)\Delta z] \right\}$$

$$\Delta g_y = - \sum_{i=1}^n \frac{fm_i}{R_i^3} \left\{ \left[1 - 3 \left(\frac{y - y_i}{R_i} \right)^2 \right] \Delta y - 3 \times \right. \\ \left. \frac{y - y_i}{R_i^2} [(x - x_i)\Delta x + (z - z_i)\Delta z] \right\}$$

$$p^2 + (\eta_x^2 + \eta_y^2 + \eta_z^2)p^4 + (\eta_x^2\eta_y^2 + \eta_x^2\eta_z^2 + \eta_y^2\eta_z^2 - A^2 - B^2 - C^2)p^2 +$$

$$\Delta g_z = - \sum_{i=1}^n \frac{fm_i}{R_i^3} \left\{ \left[1 - 3 \left(\frac{z - z_i}{R_i} \right)^2 \right] \Delta z - 3 \times \right. \\ \left. \frac{z - z_i}{R_i^2} [(x - x_i)\Delta x + (y - y_i)\Delta y] \right\}$$

Substituting Equations [3.5] in [2.4] we obtain

$$\begin{aligned} (p^2 + \eta_x^2)\Delta x - A\Delta y - B\Delta z &= \Delta a_{xg} \\ -A\Delta x + (p^2 + \eta_y^2)\Delta y - C\Delta z &= \Delta a_{yg} \\ -B\Delta x - C\Delta y + (p^2 + \eta_z^2)\Delta z &= \Delta a_{zg} \end{aligned}$$

where

$$\begin{aligned} \eta_x^2 &= \sum_{i=1}^n \frac{fm_i}{R_i^3} \left[1 - 3 \frac{(x - x_i)^2}{R_i^2} \right] \\ \eta_y^2 &= \sum_{i=1}^n \frac{fm_i}{R_i^3} \left[1 - 3 \frac{(y - y_i)^2}{R_i^2} \right] \\ \eta_z^2 &= \sum_{i=1}^n \frac{fm_i}{R_i^3} \left[1 - 3 \frac{(z - z_i)^2}{R_i^2} \right] \end{aligned}$$

$$A = 3 \sum_{i=1}^n \frac{fm_i}{R_i^3} \frac{(x - x_i)(y - y_i)}{R_i^2}$$

$$B = 3 \sum_{i=1}^n \frac{fm_i}{R_i^3} \frac{(x - x_i)(z - z_i)}{R_i^2}$$

$$C = 3 \sum_{i=1}^n \frac{fm_i}{R_i^3} \frac{(y - y_i)(z - z_i)}{R_i^2} \quad p = \frac{d}{dt}$$

Consequently, the errors of the inertial system, due to inexact automatic compensation of the accelerations due to gravity, are determined by a system of linear differential equations with variable coefficients.

Let us examine the behavior of the system [3.6] assuming no gyroscope drift. The behavior of the inertial system with respect to the errors Δx , Δy and Δz is determined by the form of the solution of Equation [3.6]. Obviously, if the system [3.6] is stable, then the errors in the automatic compensation will tend to zero. In the case of instability of the system, the errors will increase.

Let us investigate the stability of the system of automatic compensation of acceleration. For this purpose we consider a particular case, in which we assume that the coefficients of the system [3.6] vary slowly compared with the duration of the processes in the automatic compensation system. Using this assumption and taking, for the sake of simplicity, the coefficients of the system [3.6] to be constant, we can evaluate its stability on the basis of the properties of the characteristic determinant

$$\Delta = \begin{vmatrix} p^2 + \eta_x^2 & -A & -B \\ -A & p^2 + \eta_y^2 & -C \\ -B & -C & p^2 + \eta_z^2 \end{vmatrix}$$

Expanding this determinant and setting it equal to zero, we obtain the characteristic equation of the system [3.6]

$$\eta_x^2\eta_y^2\eta_z^2 - A^2\eta_z^2 - B^2\eta_y^2 - C^2\eta_x^2 - 2ABC = 0 \quad [3.10]$$

It follows from this equation that the system of automatic compensation for the acceleration due to gravity is unstable, since Equation [3.10] does not contain terms with odd powers of the operator $p = d/dt$.

Equation [3.10] can be transformed by calculating its coefficients with the aid of Equations [3.7 and 3.8]. It is assumed here for simplicity that the vehicle is in the gravitational field of a single celestial body, say the sun. If gravitation from several celestial bodies must be taken into account, one introduces the concept of an equivalent celestial body with

$$\frac{g}{R} = \sum_{i=1}^n \frac{fm_i}{R_i^3}$$

We have

$$\begin{aligned} \eta_x^2 + \eta_y^2 + \eta_z^2 &= 0 \\ \eta_x^2\eta_y^2 + \eta_x^2\eta_z^2 + \eta_y^2\eta_z^2 - A^2 - B^2 - C^2 &= -3(g^2/R^2) \\ \eta_x^2\eta_y^2\eta_z^2 - A^2\eta_z^2 - B^2\eta_y^2 - C^2\eta_x^2 - 2ABC &= -2(g^3/R^3) \end{aligned}$$

where

$$g = \sqrt{g_x^2 + g_y^2 + g_z^2}$$

Substituting Equation [3.11 in 3.10] and transforming, we obtain

$$(p^2 + \Omega^2)(p^2 - 2\Omega^2) = 0 \quad [3.12]$$

where

$$\Omega^2 = g/R$$

It follows therefore that the characteristic Equation [3.12] has two double imaginary roots and two real roots, one of which is positive. Consequently, the general motion of the system of automatic compensation consists of three motions: Harmonic oscillation with a period $T_1 = 2\pi/\Omega = 2\pi\sqrt{R/g}$, oscillations with the same period but with an amplitude increasing with time and, finally, an aperiodic exponentially increasing motion with a time constant $T_2 = 1/\sqrt{2\Omega} = T_1/2\sqrt{2}\pi$.

For a more detailed analysis of the character of the motion of this system, let us examine the flight of the vehicle in the sun's gravitational field in the direction of the y_0 axis. In this case $R = y$, $x = z = 0$, $g_x = g_z = 0$, $g_y = g$, and Equations [3.6] become

$$\begin{aligned}(p^2 + \Omega^2)\Delta x &= \Delta a_{xg} \\ (p^2 - 2\Omega^2)\Delta y &= \Delta a_{yg} \\ (p^2 + \Omega^2)\Delta z &= \Delta a_{zg}\end{aligned}\quad [3.13]$$

It follows, therefore, that in directions perpendicular to the resultant gravitational-force vector, the errors Δx and Δz vary sinusoidally with an amplitude that depends on the initial conditions, and with the period indicated in the foregoing. The error Δy in the direction of the gravitational vector increases exponentially. In the presence of coupling between the channels, as indicated in the foregoing, a third motion appears, with an increasing oscillation amplitude.

Let us note the analogy between the character of the variation of the error of the inertial navigation system and the motion of a satellite. The period of the errors (the period of oscillation) of the inertial system, $T_1 = 2\pi\sqrt{R/g}$, is equal to the period of revolution of a satellite moving in a circular orbit of radius R about a celestial body, with circular velocity

$$V_1 = R\Omega = \sqrt{gR} \quad [3.14]$$

For navigation at the surface of the Earth the period of variation of the errors Δx and Δz is $T_1 = 84.4$ min, and is called the Schuler period.

The error Δy in the automatic compensation of the acceleration due to gravity, along the direction of the resultant vector of the gravitational forces, varies exponentially with a time constant $T_2 = (1/\sqrt{2})\sqrt{R/g}$, which is $2\sqrt{2}\pi$ times smaller than the period of the inertial system. Under zero initial conditions, the error increases continuously, and this characterizes the instability of the automatic compensation system. Consequently, closing the automatic compensation loop of an inertial system, in which the accelerometer axis coincides with the direction of the gravitational force vector, makes the system absolutely unstable.

The analogy between an inertial system and the motion of a satellite can be continued. We note, in particular, that the relation for variation of the error Δy corresponds to that for the change in the radius vector R of the satellite, moving away from a celestial body (for example from the Earth) with escape velocity

$$V_2 = \sqrt{2}\Omega R = \sqrt{2gR} \quad [3.15]$$

Actually, only at the escape velocity does the vehicle (satellite) overcome completely the gravitation of the celestial body and move freely away from it. In an inertial system the signal in the automatic compensation channel, which measures the coordinate Δy , compensates completely for the acceleration due to gravity, and therefore the inertial system operates under conditions analogous to the physical absence of gravitation.

The analogy between the motion of an inertial system and that of a satellite can be used to simulate the motion of a satellite.

The effect of the initial error Δy_0 and the altitude above the Earth on the value of the error of the inertial system Δy may be determined from the second equation of [3.13] with Δa_{yg} set equal to zero. Fig. 5 shows the corresponding plot of $\Delta y/\Delta y_0 = f(t)$. Curves 1, 2 and 3 correspond to flight altitudes of 0, 1000 and 2000 km. With increasing flight altitude, the error accumulates less rapidly, since the effect of the gravitational forces diminishes.

The properties of the inertial system, considered here, correspond not only to a particular flight along a straight line,

but also to arbitrary flight, provided the sensitive axes of one of the accelerometers is maintained in the direction of the vector of the gravitational force. Under terrestrial conditions, this corresponds to orienting the sensitive axes of one of the accelerometers vertically, and locating the sensitive axes of the other two accelerometers in a horizontal plane. The error of the channel that measures the flight altitude will increase exponentially under nonzero initial conditions, and the errors of the channels that measure the position coordinates will vary harmonically with the Schuler period.

When a vehicle moves along an arbitrary trajectory, the automatic compensation system for the acceleration due to gravity, as follows from Equation [3.6], is unstable in all the channels. Under nonzero initial conditions the errors in all the channels have terms that increase with time, apart from the oscillating terms.

The instability of inertial systems with automatic compensation of acceleration due to gravity cannot serve as a criterion for the applicability of these systems. Under zero initial conditions there will be no errors, and in cases when the initial errors do exist, the rate of increase is slow. The buildup time is comparable here with the period of the system. In addition, the system can be made stable by introducing additional feedback or by supplying the system with supplementary external information (2), for example, from celestial navigational systems.

On the basis of the foregoing we can formulate the following theorems.

Theorem 1 Automatic compensation of acceleration due to gravity leads, in all three channels of an inertial system, to a characteristic equation

$$(p^2 + \Omega^2)^2(p^2 - 2\Omega^2) = 0$$

for the error in each of the channels.

Theorem 2 The period of the oscillation of the errors of an inertial system is equal to the period of rotation of a satellite moving in a circular orbit R about a celestial body with circular velocity $V_1 = \sqrt{gR}$.

Theorem 3 The time constant of the rise in the errors of an inertial system is equal to the time constant of the motion of a satellite, moving away from a celestial body with escape velocity $V_2 = \sqrt{2gR}$.

In the analysis of Equations [3.6] we used the method of "freezing" the coefficients to obtain a system with constant coefficients. For short time intervals, comparable with the period of oscillation of the inertial system, such an assumption can be considered valid and the foregoing conclusions are correct. For larger time intervals equations with variable coefficients must be considered. In this case the quantities T_1 and T_2 become variables, and lose the meaning of a period of oscillation and a time constant.

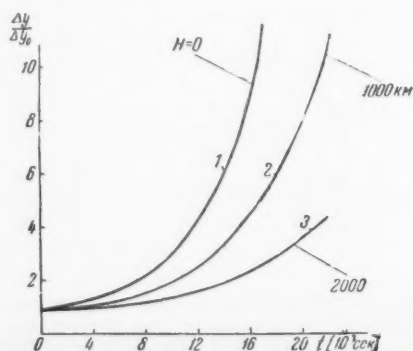


Fig. 5 Translations: KM = km; cek = sec

4 Instrument Errors

The instrument errors of an inertial system comprise the drifts of the gyro platform relative to the inertial system of coordinates, accelerometer errors, errors in the integrators, computer, etc. The drifts of the gyro platform comprise errors of two types: Errors due to the rotation of the coordinate system xyz relative to the inertial coordinate system $x_0/y_0/z_0$, and errors that are generated in the closed compensation system.

An idea of the effect of the instrumental errors on the accuracy of an inertial system can be gained from the following considerations.

For $\Delta a_{x0}, \dots, \Delta b_{x1}, \dots, \Delta b_{x2}, \dots$ (the errors of the accelerometer, first integrator and second integrator, respectively), Equations [2.3], which determine the computed coordinates, become

$$\begin{aligned} & \left[(x'' + \Delta g_x + \Delta a_{x0} + \Delta a_{x1}) \frac{k_{2x}}{p} + \Delta b_{x1} + x_0' \right] \frac{k_{2x}}{p} + \\ & \quad \Delta b_{x2} + x_0 = S_x \\ & \left[(y'' + \Delta g_y + \Delta a_{y0} + \Delta a_{y1}) \frac{k_{2y}}{p} + \Delta b_{y1} + y_0' \right] \frac{k_{2y}}{p} + \\ & \quad \Delta b_{y2} + y_0 = S_y \\ & \left[(z'' + \Delta g_z + \Delta a_{z0} + \Delta a_{z1}) \frac{k_{2z}}{p} + \Delta b_{z1} + z_0' \right] \frac{k_{2z}}{p} + \\ & \quad \Delta b_{z2} + z_0 = S_z \end{aligned} \quad [4.1]$$

It follows therefore that the instrumental errors of the elements of an inertial system affect directly the accuracy of the determination of the position coordinates. Under prolonged operation of an inertial system, the instrument errors may reach large values.

The principal methods of eliminating instrument errors are to reduce the errors in the components of the inertial system and to correct the system by introducing external and navigational information. In the latter case the correction may not be continuous, but discrete.

In conclusion, we note that an inertial system with three channels of automatic compensation of acceleration due to gravity is unstable for arbitrary motion of the vehicle, and its errors will increase under nonzero initial conditions. To eliminate the errors it is necessary to correct the system continuously or discretely by supplying it with external navigational information. In this case the inertial system, in addition to its basic task, serves also as a memory.

The analogy between the variation of the errors of an inertial system with three channels of automatic compensation and the motion of a satellite can be used to simulate the motion of a satellite.

References

- 1 Carroll, J., "Interplanetary Navigation by Optical Resection and Inertial Systems," *Aero/Space Engng.*, March 1959.
- 2 Bodner, V. A. and Seleznev, V. P., "On the Theory of Inertial Damped Systems with Arbitrary Period Invariant With Respect to the Maneuvering of a Vehicle," *Izvestiya Acad. Nauk SSSR, Otd. Tekh. Nauk, Energetika i Avtomatika* (Bull. USSR Acad. Sci., Div. Tech. Sci., Power and Automation), no. 3, 1959.
- 3 Wrigley, W., Woodbury, R. B. and Hovorka, J., "Inertial Guidance," Preprint no. 698, Institute of Aeronautical Sciences, New York, 1957.

—Original received August 27, 1959

Determination of Temperature Induced Stresses in a Conical Shell

V. A. SIBIRIAKOV

THE PRESENT article considers the determination of temperature induced stresses in a structurally orthotropic circular conical shell. The calculation is based on an idea advanced by Vlasov (1)¹ that the internal stresses in a thermally elastic free shell can be caused only by that part of the thermal load which corresponds to a bimoment state of the shell.

Translated from *Izvestiya Vysshikh Uchebnykh Zavedenii MVO, Seriya Aviatsonnaya Tekhnika* (Bull. of Institutions of Higher Learning, Aviation Technology Series), no. 1, 1960, pp. 72-82. Translated by J. George Adashko.

¹ Numbers in parentheses indicate References at end of paper.

The temperature problem is solved under the following assumptions:

- 1 The deformation takes place in the elastic region.
- 2 There are no general or local stability losses.
- 3 The Young's modulus and the coefficient of linear expansion of the material are assumed constant.
- 4 The temperature is constant over the thickness of the shell.
- 5 The law of cross sectional heating is the same over the entire length of the shell; all that changes is the "heating amplitude."

The stressed and deformed state of the orthotropic conical

shell is determined from the semimomentless shell theory. The equilibrium and Hooke's law equations for this case have the following form (3)

$$\begin{aligned} \left(\frac{\partial}{\partial t} + k\right) N_1 - \left(\frac{k^2}{Ar} \frac{\partial}{\partial t} - \frac{Ak}{r} \frac{\partial^2}{\partial \theta^2}\right) M_2 + A \frac{\partial S}{\partial \theta} &= 0 \\ \left(\frac{k}{r} \frac{\partial^2}{\partial t \partial \theta} - \frac{A^2}{r} \frac{\partial^3}{\partial \theta^3} - \frac{1}{r} \frac{\partial}{\partial \theta}\right) M_2 + \left(\frac{\partial}{\partial t} + 2k\right) S &= 0 \\ N_1 = Eh\epsilon_1 \quad S = 0.5Eh\omega \quad M_2 = -\frac{E\bar{h}^2}{12} \kappa_2 \end{aligned}$$

where

- $z(t), \theta$ = cylindrical coordinates of shell (Fig. 1)
- $z = z_0 e^{kt}$ = change-of-variable formula
- $r = kz$ = radius of conical shell
- $k = \tan \gamma$ = tangent of angle between generatrix and axis of cone
- $A = \sqrt{1 + k^2}$ = coefficient of first quadratic form
- N_1 = elastic normal stress
- S, M_2 = tangential force and bending moment
- E = modulus of elasticity of material
- h = thickness of shell along generatrix
- $\bar{h} = \eta h$ = reduced thickness of shell along parallel

The index "1" denotes the direction along the generatrix, the index "2" denotes the direction along the contour (along the parallel). We supplement system [1] by adding the equations connecting the total strain with the components of the total displacement vector

$$\begin{aligned} \epsilon_{1t} &= \frac{1}{Ar} \frac{\partial u}{\partial t} \quad \epsilon_{2t} = \frac{1}{Ar} \left(ku + A \frac{\partial v}{\partial \theta} + \omega \right) \\ \omega &= \frac{1}{r} \left[\frac{\partial u}{\partial \theta} + \frac{1}{A} \left(\frac{v}{r} \right) \right] \\ \kappa_2 &= -\frac{1}{A^2 r^2} \left(ku + w + k \frac{\partial w}{\partial t} + A^2 \frac{\partial^2 w}{\partial \theta^2} \right) \end{aligned}$$

and the equations that connect, in accordance with the hypothesis of Franz Neumann (2), the total, elastic temperature strains

$$\epsilon_{1t} = \epsilon_1 + \alpha T(t, \theta) \quad \epsilon_{2t} = \epsilon_2 + \alpha T(t, \theta) \quad [3]$$

We denote here

- u, v, w = components of vector of total displacement along generatrix, tangent to contour, and

outward normal, respectively. Positive directions are indicated in Fig. 1

- $\epsilon_{1t}, \epsilon_{2t}$ = components of total strain tensor
- $\epsilon_1, \epsilon_2, w, \kappa_2$ = components of elastic strain tensor
- α = coefficient of linear expansion of material
- $T(t, \theta) = T_1(t) \times T_2(\theta)$ = temperature function

Equations [1-3] are written in partial differential form, and in order to be able to separate the variables, one must put

$$\begin{aligned} N_1 &= \sum N_{1n} \cos n\theta \quad u = \sum u_n \cos n\theta \\ S &= \sum S_n \sin n\theta \quad v = \sum v_n \sin n\theta \\ M_2 &= \sum M_{2n} \cos n\theta \quad w = \sum w_n \cos n\theta \\ T_2(\theta) &= \sum \tau_n \cos n\theta \end{aligned}$$

The system [1-4] can be reduced to a simpler equation if a hypothesis is advanced that the contour of the transverse cross section of the shell is not stretchable. Analysis shows that no great difference is produced if the total strain (ϵ_{2t}) or the elastic strain (ϵ_2) are set equal to 0.

If it is considered that k varies from zero to unity, the solution of the system [1-4] for the n th term of the expansion can be reduced to a solution of the following linear differential equation with variable coefficients

$$u_n^{IV} - (k^2 + b_n e^{-2kt}) u_n'' + a_n e^{-kt} u_n = A^2 n \times \tau_n \times r \left(\frac{d}{dt} + k \right) \left(\frac{d}{dt} + 2k \right) \alpha T_1(t)$$

where

$$\begin{aligned} b_n &= \frac{n^2 \eta^3 (A^2 n^2 - 1)}{6} \left(\frac{h}{kz_0} \right)^2 \\ a_n &= \frac{A^6 n^4 (n^2 - 1)^2 \eta^3}{12} \left(\frac{h}{kz_0} \right)^2 \end{aligned}$$

A solution of [5], obtained by the method of successive approximation, can be written in the form

$$u_n = c_1 F_{11} + c_2 F_{12} + c_3 F_{13} + c_4 F_{14}$$

We denote here

$$\begin{aligned} F_{11} &= 1 + \sum_1^\infty a_m \quad a_m = \frac{(-1)^m p^4 m e^{-2mkt}}{2m! (2m+1)!} \prod_1^m [1 - 4(m-1)^2 \lambda] \\ F_{12} &= kt F_{11} + \sum_1^\infty a_m \gamma_m \quad \gamma_m = \left[\xi_1 + 4\lambda \sum_1^m \frac{m-1}{1 - 4(m-1)^2 \lambda} \right] \\ F_{13} &= \frac{1}{2} e^{-kt} + \sum_1^\infty \gamma_m \quad \gamma_m = \frac{(-1)^m p^4 (m+1) e^{-(2m+1)kt}}{(2m+1)! (2m+2)!} \prod_1^m [1 - (2m-1)^2 \lambda] \\ F_{14} &= kt F_{13} + e^{kt} + (1-\lambda) \sum_1^\infty \gamma_m \bar{\gamma}_m \quad \bar{\gamma}_m = \left[\xi_2 + 2\lambda \sum_1^m \frac{2m-1}{1 - (2m-1)^2 \lambda} \right] \\ p^4 &= \frac{a_n}{k^4} \quad \lambda = \frac{b_n k^2}{a_n} \\ \xi_1 &= \sum_1^m \frac{8m^2 - 1}{m(4m^2 - 1)} \quad \xi_2 = \sum_1^m \frac{2(2m+1)^2 - 1}{m(2m+1)(2m+2)} \end{aligned}$$

The system of functions for the determination of the arbitrary integration constants, obtained from the initial system [1-4] with allowance for the simplifications introduced in the derivation of [5], has the following form

$$N_{1n} = \frac{Eh}{Ar} \frac{du_n}{dt} \quad S_n = - \frac{Eh}{A^2 nr} \frac{d^2 u_n}{dt^2}$$

$$v_n = - \frac{12}{A^2 n^3 (n^2 - 1)^2 \eta^3 k^3} \left(\frac{r}{h} \right)^2 \left(\frac{d}{dt} + k \right) \frac{d^2 u_n}{dt^2}$$

From an analysis of the coefficients of Equation [5] it is seen that in the case of the design of thin shells ($h/r_0 \leq 1/30$), the terms of the coefficient preceding u_n'' exert different influences, depending on the extent to which the shell is conical. In shells of small taper, the dominating influence is that of the coefficient $b_n e^{-2kt}$, but starting with taper angles of 30 deg and above, the effect of this term is negligibly small compared with k^2 . In the calculation of the nose parts of a flight vehicle, it becomes necessary to deal with precisely such shells. Therefore Equation [5] can be simplified to yield an equation analogous to Equation [11] (3), derived under the assumption that there is no displacement in the central surface of the shell, i.e., $\omega = 0$. Written out in terms of the component of the vector of total displacement v_n for the temperature problem, this equation assumes the form

$$v_n^{IV} - k^2 v_n'' + a_n e^{-2kt} v_n' = A^2 n \times \tau_n r \alpha \left(\frac{d}{dt} + k \right) \left(\frac{d}{dt} + 2k \right) T_1(t) \quad [7]$$

and its solution is a particular case of expression [6] under the condition $\lambda = 0$. The series solution thus obtained reduces to Bessel functions of complex argument.

Let us list the complete system of equations for the arbitrary integration constants, inasmuch as in (3) an error crept in the listing

$$v_n = \sum_{i=1}^4 c_i \Phi_{1i} + v_n^*$$

$$\Phi_{11} = \frac{e^{0.5kt}}{p} \operatorname{Im} V \bar{i} I_1(V \bar{i} \varphi) \quad \varphi = 2pe^{-0.5kt}$$

$$\Phi_{12} = kt \Phi_{11} - 0.751 - 5.075 \frac{e^{0.5kt}}{p} \operatorname{Im} V \bar{i} I_1(V \bar{i} 0.898 \varphi)$$

$$\Phi_{13} = pe^{0.5kt} R V \bar{i} I_1(V \bar{i} \varphi)$$

$$\Phi_{14} = kt \Phi_{13} + e^{kt} - 0.113 p^4 e^{-kt} - 5.007 pe^{0.5kt} R V \bar{i} I_1(V \bar{i} 0.918 \varphi)$$

$$u_n = \frac{k}{An} \left[\sum_{i=1}^4 c_i \Phi_{2i} + u_n^* \right]$$

$$\Phi_{21} = -R I_0(V \bar{i} \varphi) \quad \Phi_{22} = kt \Phi_{21} + \Phi_{11} + 0.751 + 4.562 R I_0(V \bar{i} 0.898 \varphi)$$

$$\Phi_{23} = p^2 \operatorname{Im} I_0(V \bar{i} \varphi) \quad \Phi_{24} = kt \Phi_{23} + \Phi_{13} + 0.226 p^4 e^{-kt} - 4.673 p^2 \operatorname{Im} I_0(V \bar{i} 0.918 \varphi)$$

$$N_{1n} = \frac{Ehk e^{-kt}}{A^2 x_0 \eta} \cdot \left[\sum_{i=1}^4 c_i \Phi_{3i} + N_{1n}^* \right]$$

$$\Phi_{31} = -pe^{-0.5kt} R \sqrt{V \bar{i}} I_1(V \bar{i} \varphi)$$

$$\Phi_{32} = kt \Phi_{31} + 2\Phi_{21} + \Phi_{11} + 4.097 pe^{-0.5kt} R \sqrt{V \bar{i}} I_1(V \bar{i} 0.898 \varphi)$$

$$\Phi_{33} = p^3 e^{-0.5kt} \operatorname{Im} \sqrt{V \bar{i}} I_1(V \bar{i} \varphi)$$

$$\Phi_{34} = kt \Phi_{33} + 2\Phi_{23} + \Phi_{13} - 0.226 p^4 e^{-kt} - 4.284 p^3 e^{-0.5kt} \operatorname{Im} \sqrt{V \bar{i}} I_1(V \bar{i} 0.918 \varphi)$$

$$S_n = \frac{Ehk^2 e^{-kt}}{A^2 n^2 x_0} \left[\sum_{i=1}^4 c_i \Phi_{4i} + S_n^* \right]$$

$$\Phi_{41} = p^3 e^{-kt} \operatorname{Im} I_0(V \bar{i} \varphi)$$

$$\Phi_{42} = kt \Phi_{41} - 3\Phi_{31} - \Phi_{21} - \Phi_{11} - 3.688 p^2 e^{-kt} \operatorname{Im} I_0(V \bar{i} 0.898 \varphi)$$

$$\Phi_{43} = p^4 e^{-kt} R I_0(V \bar{i} \varphi)$$

$$\Phi_{44} = kt \Phi_{43} - 3\Phi_{33} - \Phi_{23} - \Phi_{13} - 0.226 p^4 e^{-kt} - 3.922 p^4 e^{-kt} R I_0(V \bar{i} 0.918 \varphi)$$

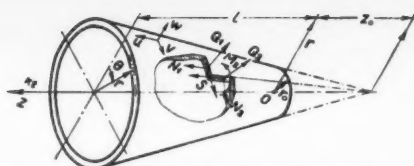


Fig. 1 Coordinate system and basic internal force factors of a semimomentless conical shell

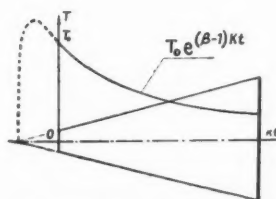


Fig. 2 Probable law of the distribution of the temperature of heating along the zero generatrix ($\theta = 0$) of the conical shell

We must dwell briefly on the expression for the function $T(t, \theta)$. Fig. 2 shows the probable variation of the temperature along the generatrix of a cone located in a gas stream. Since we are interested in a shell in the form of a truncated cone, the function approximating this law at a certain distance from the vertex can be written in the following form

$$T_1(t) = T_0 e^{-(\beta-1)kt}$$

The temperature variation along the shell contour, chosen on the basis of an analysis of the experimental data, is shown in

Fig. 3. This variation can be represented analytically by the expression

$$T_2(\theta) = \sum \tau_n \cos n\theta$$

where

$$\begin{aligned} \tau_0 &= \frac{2(1-\mu)}{\pi} & \tau_2 &= \frac{2(1-\mu)}{3\pi} & \tau_4 &= -\frac{2(1-\mu)}{15\pi} \\ \tau_1 &= \frac{(1-\mu)}{2} & \tau_3 &= 0 & \tau_5 &= 0 \text{ etc.} \end{aligned}$$

[9]

By assigning different values to the parameter μ , it is possible to obtain a sufficiently wide range of loads. The fact that at the points $\pm\pi/2$ of the contour the temperature is assumed to be zero does not change the nature of the problem. The whole curve of Fig. 3 can be shifted by an amount $\Delta T_2 > 0$, and only the coefficient τ_0 will change in the expansion [9].

The temperature stresses will be induced only by that part of the temperature of the thermal load which corresponds to the terms of expansion [9] with $n \geq 2$. The coefficient a_n in [7] becomes meaningful only if $n \geq 2$.

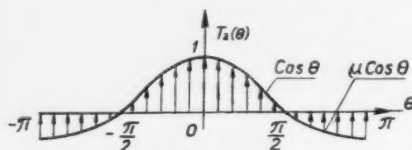


Fig. 3 Assumed law of the temperature distribution along the shell contour

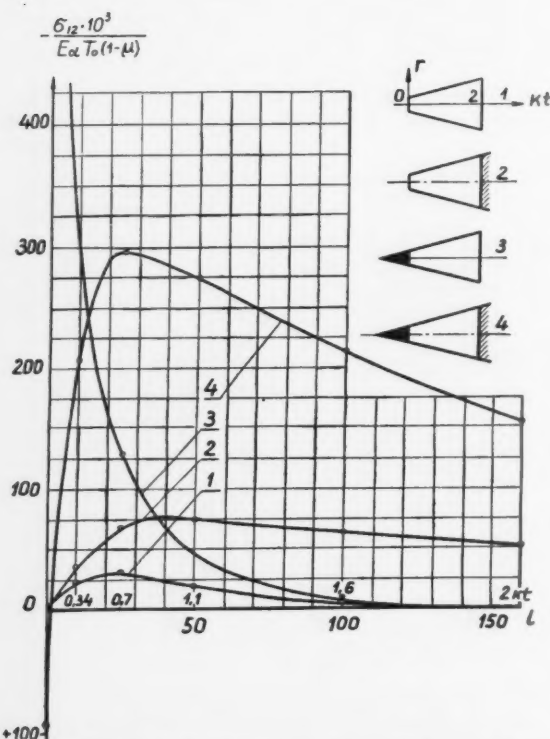


Fig. 4 Distribution of the normal temperature stresses along the zero generatrix of the conical shell. The shell has a deformable contour cross section. Several end boundary conditions are given. The temperature along the generating line is constant ($\beta = 1$)

Once the function $T_1(t)$ is specified, the right half of equation [7] becomes $qe^{\beta kt}$, where

$$q = A^2 [\tau_n k^3 z_0 \alpha T_0 \beta (\beta + 1)]$$

A particular solution in terms of the parameter β is written in the form

$$v_n^* = \frac{q}{k^4} \sum_0^m \frac{(kt)^{m+4}}{(m+4)!} B_m(\beta, p)$$

where $B_m(\beta, p)$ are coefficients that depend on the parameters β and p .

We can then obtain other partial solutions

$$u_n^* = \frac{q}{k^4} \sum_0^m \frac{(kt)^{m+2}}{(m+3)!} (B_m - B_{m-1}) \quad B_{-1} = 0$$

$$N_{1n}^* = \frac{q}{k^4} \left[\sum_0^m \frac{(kt)^{m+2}}{(m+2)!} (B_m - B_{m-1}) - \frac{e^{\beta kt}}{\beta(\beta+1)} \right]$$

$$S_n^* = \frac{q}{k^4} \left[- \sum_0^m \frac{(kt)^{m+1}}{(m+1)!} (B_m - B_{m-1}) + \frac{e^{\beta kt}}{(\beta+1)} \right]$$

[10]

The boundary conditions will be formulated in the following manner. In those cases when there is no compression of deplanation at the ends of the shell, the boundary conditions are that there be no normal and tangential bimoment stresses

$$N_{1n}(t^*) = 0 \quad S_n(t^*) = 0$$

On the other hand, if the end of the shell is rigidly secured over its entire contour to the remaining portion of the structure, which in turn is very rigid, in such a way that the bearing section remains plane and furthermore undeformed, then the boundary condition in the section $t = t^{**}$ will be equivalent to the condition of the absence of bimoment displacements

$$u_n(t^{**}) = 0$$

$$v_n(t^{**}) = 0$$

By way of an example, let us design a shell with the following geometric characteristics:

Angle at vertex = 35 deg ($k = 0.316$)

Length of shell $l = 160$ cm ($0 \leq kt \leq 2$)

$r_0 = 8$ cm $h = 0.25$ cm $p^4 = 1.61$

$\eta = 1.0$ $z_0 = 25$ cm $\varphi = 2.26e^{-0.5kt}$

We calculate only the second-order stresses ($n = 2$)

$$\sigma_{12} = (N_{12}/h) \cos 2\theta$$

since the stresses corresponding to $n \geq 3$ do not play an important role in this example ($\sigma_3 = 0$).

Let us calculate the values of the particular solutions from formulas [10], and the arbitrary integration constants will be obtained from the solution of the system [8].

The results of the calculations of the temperature stresses along the 0 generatrix $\theta = 0$ for different combinations of boundary conditions at the ends, at a constant heating temperature along the length of the shell ($\beta = 1$), are given in Fig. 4.

Fig. 5 shows the distribution of the normal stresses along the zero generatrix as a function of the different temperature distributions along the shell. The parameter β has the following range

$$-1 \leq \beta \leq +1$$

The boundary conditions provide for the absence of bimoment displacements along the ends of the shell. The curves on Figs. 4 and 5 are plotted in terms of the coefficient $E\alpha T_0 10^{-3} (1 - \mu)$. The factor $(1 - \mu)$ represents the temperature dis-

tribution along the contour of the transverse section of the shell, and the coefficient $E\alpha T_0$ represents the mechanical properties of the heated structural material. The magnitude of this coefficient for a given temperature T_0 , for various types of sheet materials, can be taken from Fig. 6.

An analysis of the curves in Fig. 4 shows that the internal compression in a given conical shell is small, and that the resultant temperature stresses (curve 1) do not play a practical role. The temperature stresses are greatly affected by the deformation compression along the edges, particularly on a narrow end, as can be seen from comparison of curves 2 and 3.

The absence of bimoment displacements at a narrow end causes a sharp rise in the temperature stresses in the region adjacent to this section (curves 3 and 4).

The curves in Fig. 5 indicate that the appearance and the character of the edge effect depend on the form of the external load. Another more important conclusion is that the temperature stresses in a conical shell, under the boundary conditions prevailing in practice, are considerable.

In order to determine the effect of the deformability of the contour of transverse cross section on the magnitude of the temperature stresses, let us perform the calculations for a conical shell with an undeformable contour.

We supplement the system of Equations [1-4] with the condition $\kappa_2 = 0$, perform all the necessary operations and obtain the differential equation

$$v_n^{IV} - 2\lambda_1^2 v_n'' + \lambda_2^4 v_n = - \frac{r\tau_n \alpha}{nk} \left[k^2 \left(\frac{d}{dt} + k \right)^2 - k \left(\frac{d}{dt} + k \right) - A^2 n^2 (A^2 n^2 - 1) \right] \left(\frac{d}{dt} + 2k \right) T_1(t) \quad [11]$$

the solution of which is written in the form

$$v_n = c_1 e^{\gamma_1 t} + c_2 e^{-\gamma_1 t} + c_3 e^{\gamma_2 t} + c_4 e^{-\gamma_2 t} + v_n^*$$

where

$$\begin{aligned} \gamma_1 &= \sqrt{\frac{\gamma_1^2 + \lambda_2^2}{2}} + \sqrt{\frac{\lambda_1^2 + \lambda_2^2}{2}} \\ \gamma_2 &= \sqrt{\frac{\lambda_1^2 + \lambda_2^2}{2}} - \sqrt{\frac{\lambda_1^2 + \lambda_2^2}{2}} \\ \lambda_1^2 &= \frac{A^2(A^2 n^2 - 1)(n^2 - 1)}{2k^2} \quad \lambda_2^2 = \frac{A^6 n^2(n^2 - 1)^2}{2k^2} \end{aligned} \quad [12]$$

We assume, as before, that $T_1(t)$ is equal to $T_0 e^{(\beta-1)kt}$. Therefore the right half of Equation [11] and its particular solution after simplification can be written, respectively

$$\alpha T_0 A^2 k z_0 n \tau_n (A^2 n^2 - 1)(\beta + 1) e^{\beta k t} = q e^{\beta k t}$$

$$v_n^* = \frac{q e^{\beta k t}}{\beta^4 k^4 - 2\lambda_1^2 \beta^2 k^2 + \lambda_2^4}$$

The solution [12], together with the equations given in the following material, forms a system from which, under suitable boundary conditions, one can determine the arbitrary integration constants

$$\begin{aligned} u_n &= \frac{1}{A n k} \left(k \frac{d}{dt} - A^2 n^2 + 1 \right) v_n \\ N_{in} &= \frac{E h}{A^2 n k r} \left[\frac{d}{dt} \left(k \frac{d}{dt} - A^2 n^2 + 1 \right) v_n - A^2 n k^2 z_0 \tau_n \alpha T_0 e^{\beta k t} \right] \\ S_n &= - \frac{E h}{A^2 n^2 k (n^2 - 1) r} \left\{ \frac{d^2}{dt^2} \left[k^2 \frac{d^2}{dt^2} - (A^2 n^2 - 1) \right] v_n - A^2 n k^2 z_0 \tau_n \alpha T_0 \beta [\beta k^2 + A^2 (n^2 - 1)] e^{\beta k t} \right\} \end{aligned}$$

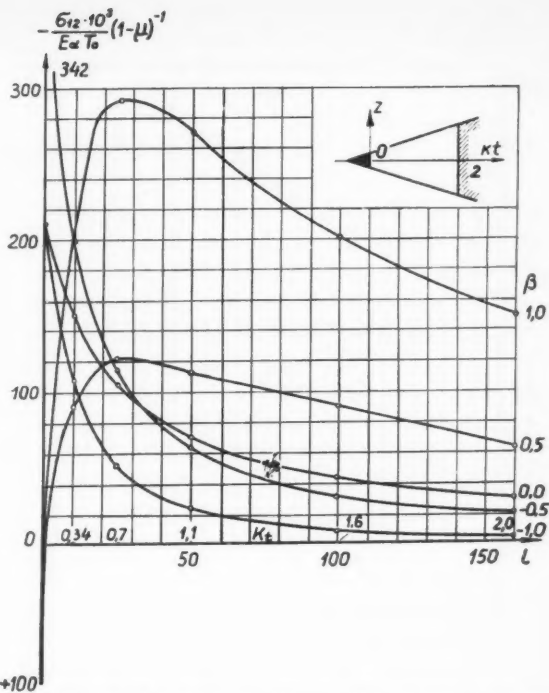


Fig. 5 Distribution of the normal temperature stresses along the zero generatrix of the conical shell. The shell has a deformable contour cross section. The dependence is given as a function of different temperature distributions along the length of the shell. The boundary conditions assume that there are no bimoment displacements at the ends

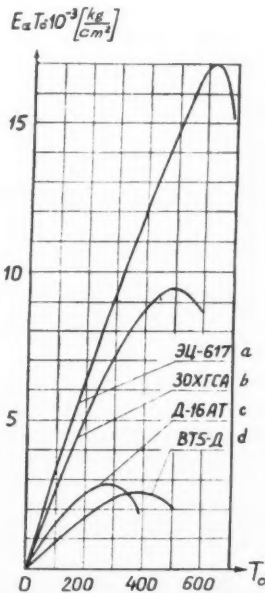


Fig. 6 Dependence of the generalized mechanical characteristics of the metals ($E\alpha T_0$) on the temperature of heating. a, b, c and d designate various types of sheet metals

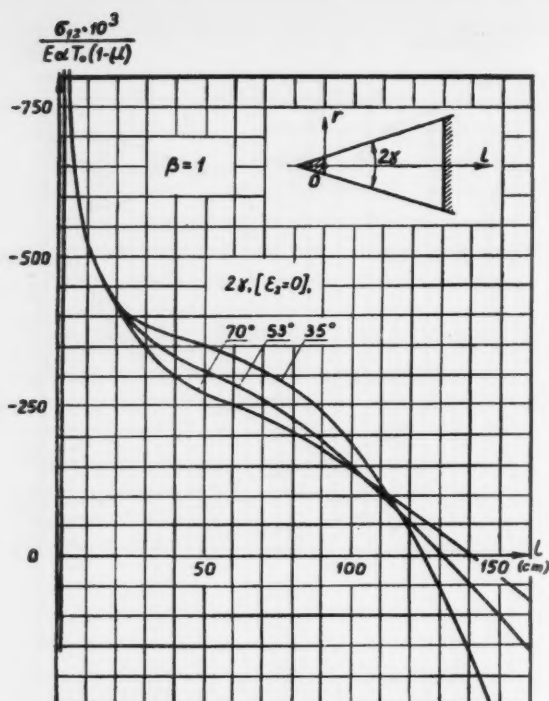


Fig. 7 Distribution of temperature stresses along the zero generatrix of a conical shell having a nondeformable cross sectional contour as a function of the vertex angle. The boundary conditions assume that there are no bimoment displacements at the ends. The temperature is constant along the length ($\beta = 1$)

The foregoing formulas were used to calculate several structurally orthotropic conical shells, with different vertex angles. The boundary conditions presuppose the absence of bimoment displacements at both ends of the shell. The temperature is constant along the shell.

The geometrical characteristics of the shell are as follows

$r_0 = 8 \text{ cm}$	1 $k = 0.7$ ($2\gamma = 70 \text{ deg}$)
$l = 160 \text{ cm}$	2 $k = 0.5$ ($2\gamma = 53 \text{ deg}$)
$h = 0.25 \text{ cm}$	3 $k = 0.32$ ($2\gamma = 35 \text{ deg}$)

The results of the calculations of the normal temperature stresses

$$\sigma_{12} = (N_{12}/h) \cos 2\theta$$

and also for the zero generatrix are shown in Fig. 7 as a function of the already known coefficient

$$E \alpha T_0 (1 - \mu) \times 10^{-3}$$

for the same boundary conditions as in Fig. 5.

An analysis of the curves shows that the temperature load causes considerable temperature stresses. The end sections, on which constraints are imposed on the deplanation and on the deformation of the contour, are a source of considerable disturbances. A certain reduction in the normal temperature stresses in the shell with increasing taper (within the limits

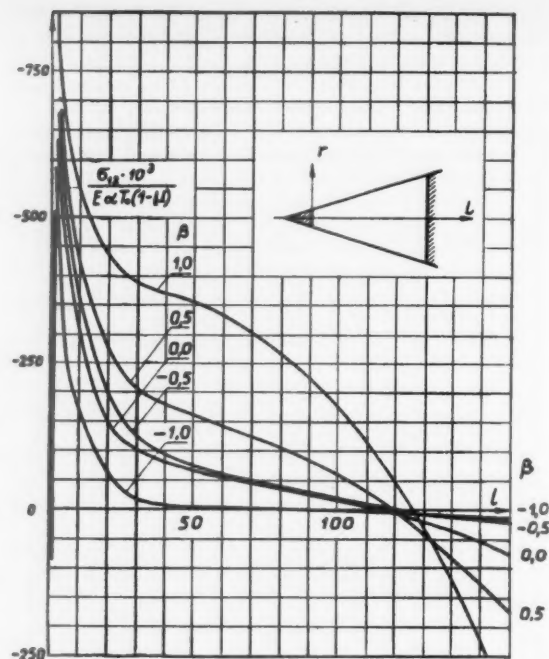


Fig. 8 Distribution of normal temperature stresses along the zero generatrix of the conical shell, having a nondeformable cross sectional contour. Dependence is given for several laws of distribution of heating along the length of the shell. The boundary conditions assume that there are no bimoment displacements at the ends

considered) can be explained by the character of the internal constraint in such a shell.

Fig. 8 shows the character of the distribution of the temperature stresses along the length of the shell under different laws of temperature distribution ($-1 \leq \beta \leq +1$) along the zero generatrix.

The geometrical characteristics and the boundary conditions of the given shell are the same as for the shell described in Fig. 5.

From a comparison of the curves of Figs. 5 and 8 it follows that the normal temperature stresses are differently distributed in shells having deformable and nondeformable transverse contours. The maximum stress along the length of the shell, in places where the edge effect can be considered absent, is greater in shells with a nondeformable contour.

References

- 1 Vlasov, V. Z., "Theory of Prestressed Rods, Plates and Shells," *Izvestiya Akad. Nauk SSSR, Otd. Tekh. Nauk* (Bull. Acad. Sci. USSR, Div. Tech. Sci.), no. 5, 1956.
- 2 Leibenson, L. S., "Kratkii Kurs Teorii Vprugost'" (Short Course in the Theory of Elasticity), GITTL, 1946.
- 3 Sibirskiy, V. A., "Calculation of Orthotropic Conical Shell for Arbitrary External Load by the Method of V. Z. Vlasov," *Izvestiya Vysshikh Uchebnykh Zavedeniy MVO, Aviatsonnaya Tekhnika* (Bull. of the Institutions of Higher Learning, Ministry of Higher Education, Aviation Technology), no. 2, 1959.

—Original submitted November 21, 1959

Small Parameter Method for Second-Order Differential Equations With Discontinuous Terms

T. S. SHTEINBERG

The small parameter method has been well worked out for finding periodic solutions of differential equations with discontinuous terms (1).¹ In another paper by the author (2), this method has been generalized to include a system of two equations, the right halves of which experience a first order of discontinuity along a certain curve; the present paper is a continuation of the earlier one.

Section 1

WE CONSIDER the equation

$$\ddot{x} + k^2(\dot{x})x = \mu F(x, \dot{x}) \quad [1.1]$$

where

$$k^2(\dot{x}) = \begin{cases} k_1^2 & \text{for } \dot{x} \leq f(x) \\ k_2^2 & \text{for } \dot{x} \geq f(x) \end{cases} \quad (k_1 = \text{const}) \\ (k_2 = \text{const})$$

Here $f(x)$ is a single valued analytic function, μ is a small parameter and $F(x, y)$ experiences a first-order discontinuity along the curve $y = f(x)$, and is analytic in x and y in all other points of the plane. We assume henceforth that the behavior of the system is described by the two equations

$$\begin{aligned} \ddot{x} + k_1^2 x &= \mu F_1(x, \dot{x}) \text{ for } \dot{x} \leq f(x) \\ \ddot{x} + k_2^2 x &= \mu F_2(x, \dot{x}) \text{ for } \dot{x} \geq f(x) \end{aligned} \quad [1.2]$$

We denote by W_1 and W_2 the regions on the phase plane for which $y \leq f(x)$ and $y \geq f(x)$ respectively, and replace each equation by the equivalent system

$$\dot{x} = y \quad \dot{y} = -k_i^2 x + \mu F_i(x, y) \quad [1.3]$$

in the region W_i , where

$$F_i(x, y) = F(x, y)$$

in the region W_i and is analytic in x and y in this region. The simplified system is obtained from the fundamental one when $\mu = 0$

$$\dot{x} = y \quad \dot{y} = -k_i^2 x \quad \text{in the region } W_i \quad (i = 1, 2) \quad [1.4]$$

By solutions of the systems [1.3] or [1.4] are meant continuous functions of t , satisfying Equations [1.3] or [1.4] everywhere in the phase plane in the region W_i , and continuously joined together on the curve $y = f(x)$. Only the case when all the solutions of the system [1.4] are periodic will be considered.² A sufficient condition of the periodicity

¹ Translated from *Izvestiya Akademii Nauk SSSR, Otd. Tekh. Nauk, Mekhanika i Mashinostroyeniye* (Bull. Acad. Sci. USSR, Div. Tech. Sci., Mechanics and Machine Construction), no. 1, 1960, pp. 106-112. Translated by J. George Adashko.

² Numbers in parentheses indicate References at end of paper.
³ The case when the simplified system has only one periodic solution is considered in another paper by the author (2).

of all the solutions of [1.4] is any of the conditions

$$k_1 = k_2 \quad f(x) = f(-x) \quad f(x) = -f(-x) \quad [1.5]$$

If none of the conditions [1.5] is satisfied, all the solutions cannot be periodic. The following notation will be used:

T_{0i} = time interval during which simplified system, described by Equation [1.4], is in the region W_i

T_i = analogous interval for fundamental system

Let $x_{0i}(t)$ and $y_{0i}(t)$ be that solution of the simplified system in the region W_i which is part of the periodic solution, and b_i the abscissa of the point of intersection of the trajectory (Fig. 1) of the periodic solution of the system [1.4] with the curve $y = f(x)$.

We assume that the trajectories of the periodic solutions of the systems [1.4] are not tangent to the curve $y = f(x)$, and consequently the following condition is satisfied

$$f(b_i)f'(b_i) + k_i^2 b_i \neq 0 \quad (i, l = 1, 2) \quad [1.6]$$

The representative point can move only clockwise.

The periodic solution of the simplified equation, satisfying in the region W_i the initial conditions

$$x_{0i}(0) = b_i \quad \dot{x}_{0i}(0) = f(b_i) \quad [1.7]$$

has the form

$$x_{0i}(t) = [f(b_i)/k_i] \sin k_i t + b_i \cos k_i t \quad [1.8]$$

and by virtue of the continuity of the periodic solution, ob-

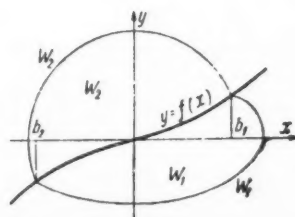


Fig. 1

tained by joining together the functions $x_{0i}(t)$ and $x_{0i}(t)$, as well as the continuity of its first derivative, the following conditions should be satisfied

$$x_{0i}(T_{0i}) = b_k \quad \dot{x}_{0i}(T_{0i}) = f(b_k) \quad (i, k = 1, 2 \quad i \neq k) \quad [1.9]$$

We denote by $x_i(t)$ the solution of the fundamental equation in the region W_i , satisfying the initial conditions

$$x_i(0) = b_i + \beta_i \quad \dot{x}_i(0) = f(b_i + \beta_i) \quad (i = 1, 2) \quad [1.10]$$

and becoming the generating solution [1.8] when $\mu = 0$; such a solution exists and will be analytic in t , in the parameter μ and in the initial values. As in the case of the simplified Equation [1.7], we choose for the initial time corresponding to initial conditions [1.10], the instant when the corresponding system is on the boundary between regions W_1 and W_2 .

In order for the set of solutions $x_1(t)$ and $x_2(t)$ to be a continuous periodic solution, it is necessary and sufficient that the following conditions be satisfied

$$x_i(T_i) = b_k + \beta_k \quad \dot{x}_i(T_i) = f(b_k + \beta_k) \quad (i, k = 1, 2 \quad i \neq k)$$

or, considering that x_i depends on the initial values and on μ , and that T_i is equal to $T_{0i} + \gamma_i$, we obtain the following four equations

$$\theta_i = x_i(T_{0i} + \gamma_i, \beta_i, \mu) - b_k - \beta_k = 0$$

$$D = \frac{k_2^2 - k_1^2}{\Delta_1 \Delta_2} \{ (b_2^2 f_1^2 - b_1^2 f_2^2) (f_1' f_2' f_1 f_2 - k_1^2 k_2^2 b_1 b_2) + f_2 f_2' b_1 [f_1^2 (f_2^2 + k_2^2 b_2^2) + k_1^2 b_2^2 (f_1^2 + k_2^2 b_1^2)] - f_1 f_1' b_2 [f_2^2 (f_1^2 + b_1^2 k_1^2) + k_2^2 b_1^2 (f_1^2 + k_1^2 b_2^2)] \} \quad [1.15]$$

$$U_i = \dot{x}_i(T_{0i} + \gamma_i, \beta_i, \mu) - f(b_k + \beta_k) = 0$$

$$(i, k = 1, 2 \quad i \neq k) \quad [1.11]$$

which are satisfied by the values $\mu = \beta_i = \gamma_i = 0$, for in this case the solution of the fundamental equation becomes the solution of the simplified equation, satisfying initial conditions [1.7]. Since x_i is analytic in μ and t and in the initial values [1.10], the quantity β_k will be small if β_i is also sufficiently small.

$$\begin{aligned} \theta_i &= \beta_i A_i^{(1)}(T_{0i}) - \beta_i + \gamma_i \dot{x}_{0i}(T_{0i}) + \beta_i^2 A_i^{(2)}(T_{0i}) + \gamma_i \beta_i \dot{A}_i^{(1)}(T_{0i}) + \frac{1}{2} \gamma_i^2 \ddot{x}_{0i}(T_{0i}) + \\ &\quad \mu [C_i(T_{0i}) + D_i(T_{0i}) \beta_i + \dot{C}_i(T_{0i}) \gamma_i + E_i(T_{0i}) \mu] + \bar{\theta}_i \\ U_i &= \beta_i \dot{A}_i^{(1)}(T_{0i}) - \beta_i f_i' + \gamma_i \dot{x}_{0i}(T_{0i}) + \beta_i^2 \dot{A}_i^{(2)}(T_{0i}) + \alpha_i \beta_i \ddot{A}_i^{(1)}(T_{0i}) + \frac{1}{2} \gamma_i^2 \ddot{x}_{0i}(T_{0i}) - \\ &\quad \frac{1}{2} \beta_i^2 f_i'' + \mu [\dot{C}_i(T_{0i}) + \dot{D}_i(T_{0i}) \beta_i + C_i(T_{0i}) \gamma_i + E_i(T_{0i}) \mu] + \bar{U}_i \end{aligned} \quad (l, i = 1, 2 \quad i \neq l) \quad [1.17]$$

The question of the existence of a periodic solution of the fundamental equation, satisfying the initial conditions [1.10] and becoming the periodic solution of the simplified equation when $\mu = 0$, is equivalent to the question of the existence of such solutions $\beta_i = \beta_i(\mu)$ and $\gamma_i = \gamma_i(\mu)$ of the Equations [1.11], which vanish when $\mu = 0$. As is known, a sufficient condition for the existence of such a unique solution is

$$D = \frac{\partial(\theta_1, \theta_2, U_1, U_2)}{\partial(\gamma_1, \gamma_2, \beta_1, \beta_2)} \neq 0 \quad \text{at } \mu = \beta_i = \gamma_i = 0 \quad [1.12]$$

To calculate D , we represent the solution $x_i(t)$ in the form of a series

$$\begin{aligned} x_i(t, \beta_i, \mu) &= x_{0i} + \beta_i A_i^{(1)} + \beta_i^2 A_i^{(2)} + \dots + \\ &\quad \mu [C_i + \beta_i D_i + \mu E_i + \dots] \\ \dot{x}_i(t, \beta_i, \mu) &= \dot{x}_{0i} + \beta_i \dot{A}_i^{(1)} + \beta_i^2 \dot{A}_i^{(2)} + \dots + \\ &\quad \mu [\dot{C}_i + \beta_i \dot{D}_i + \mu \dot{E}_i + \dots] \end{aligned} \quad [1.13]$$

which is substituted in [1.11] after first expanding $x_i(T_{0i} + \gamma_i)$ and $\dot{x}_i(T_{0i} + \gamma_i)$ in powers of γ_i . Making all the calculations, we obtain

$$D = \begin{vmatrix} A_1^{(1)}(T_{01}) & -1 & f(b_2) & 0 \\ A_1^{(1)}(T_{01}) & -f'(b_2) & -k_1^2 b_2 & 0 \\ -1 & A_2^{(1)}(T_{02}) & 0 & f(b_1) \\ -f'(b_1) & A_2^{(1)}(T_{02}) & 0 & -k_2^2 b_1 \end{vmatrix} \quad [1.14]$$

A differential equation for $A_i^{(1)}(t)$ is obtained by substituting [1.13] in [1.3]

$$\ddot{A}_i^{(1)} + k_i^2 A_i^{(1)} = 0$$

using the initial conditions $A_i^{(1)}(0) = 1$ and $\dot{A}_i^{(1)}(0) = f'(b_i)$, and taking into account the fact that $f(x)$ is analytic and can be expanded as

$$f(b_i + \beta_i) = f(b_i) + \beta_i f'(b_i) + \frac{1}{2} \beta_i^2 f''(b_i) + \dots$$

In calculating $A_i^{(1)}(T_{0i})$ and $\dot{A}_i^{(1)}(T_{0i})$, we make use of Equation [1.9]. Denoting

$$f_i = f(b_i) \quad f_i' = f'(b_i) \quad \Delta_i = k_i^2 b_i^2 + f_i^2 \quad (i = 1, 2)$$

and substituting the resultant values of $A_i^{(1)}(T_{0i})$ and $\dot{A}_i^{(1)}(T_{0i})$ in Equation [1.4], we obtain, after expanding the determinant

Considering that the points with coordinates b_1, f_1 and b_2, f_2 lie on one phase trajectory, the equation of which is

$$k_i^2 x^2 + y^2 = k_i^2 b_i^2 + f_i^2 \quad (l = 1, 2)$$

and therefore

$$k_i^2 b_i^2 + f_i^2 = k_i^2 b_l^2 + f_l^2 \quad (i, l = 1, 2) \quad [1.16]$$

we find that D vanishes in all three cases of Equation [1.5].

The question of the existence of a periodic solution remains unanswered. To answer this question we write out Equation [1.11] in expanded form, using the previously obtained series solution

$$M_{31} = -k_2^2 b_1 (k_1^2 b_2 + f_2' f_2) \quad M_{11} = f_1 (k_1^2 b_2 + f_2' f_2)$$

By definition, $k_i^2 b_k + f_k' f_k$ is unequal to 0 for all $i, k = 1, 2$. Therefore, all the minors cannot vanish simultaneously, and the rank of the matrix $\|a_{ki}\|$ is equal to three.

We multiply φ_k by the corresponding cofactors $A_{k1} = (-1)^{k+1} M_{k1}$ and sum over $k (k = 1, 2, 3, 4)$. In view of the vanishing of the determinant $\|a_{ki}\|$, the resultant equation will not contain terms linear in z_i . This yields

$$\varphi = \sum_{i=1}^4 u_{1i} z_i + \mu \left[u_\mu + \sum_{i=1}^4 u_{\mu i} z_i + u_{\mu\mu} \mu \right] + R \quad [1.19]$$

Here

$$u_{1i} = \sum_{k=1}^4 a_{ki}^{(k)} A_{k1} \quad u_\mu = \sum_{k=1}^4 d_k A_{k1}$$

$$u_{\mu i} = \sum_{k=1}^4 d_{ki} A_{k1} \quad u_{\mu\mu} = \sum_{k=1}^4 e_k A_{k1}$$

where R denotes a function containing terms of order not lower than third. We add to [1.19] the three equations of [1.18]

$$\varphi_k = 0 \quad (k = 1, 2, 3) \quad [1.20]$$

Since the rank of the matrix $\|a_{ki}\|$ is 3, we obtain from Eq. [1.20]

$$z_i = z_i(z_1, \mu) \quad (i = 2, 3, 4)$$

We seek z_i in the form of series

$$z_i = \alpha_1^{(i)} z_1 + \alpha_2^{(i)} \mu + \alpha_3^{(i)} z_1^2 + \alpha_4^{(i)} z_1 \mu + \alpha_5^{(i)} \mu^2 + \dots \quad [1.21]$$

whose coefficients are obtained by substituting Equation [1.21] in [1.20]. We then substitute the obtained values of z_i in Equation [1.19] and, returning to the previous notation, we obtain

$$m_1 \beta_1^2 + \mu [m_2 + m_3 \beta_1 + m_4 \mu] + \Phi = 0 \quad [1.22]$$

(Φ contains terms of order not lower than third in β_1 and μ .)

The question of the existence of the periodic solution of the fundamental equation is equivalent to the existence of a solution $\beta_1 = \beta_1(\mu)$ for Equation [1.22], which vanishes when $\mu = 0$. We seek only periodic solutions that can be expanded in integral powers of μ .

The necessary condition for the existence of an analytic solution $\beta_1 = \beta_1^{(u)}$ of Equation [1.22], and consequently of a periodic solution of Equations [1.1] analytic in μ , is the condition $m_2 = 0$ or, written out fully

$$A_{11} C_1(T_{01}) + A_{21} \dot{C}_1(T_{01}) + A_{31} C_2(T_{02}) + A_{41} \dot{C}_2(T_{02}) = 0 \quad [1.23]$$

Here A_{k1} is the cofactor of the determinant $\|a_{ki}\|$ previously calculated, and $C_i(t)$ is the solution of the equation

$$\ddot{C}_i + k_i^2 C_i = F_i[x_{0i}(t), \dot{x}_{0i}(t)] \quad [1.24]$$

satisfying the initial conditions $C_i(0) = \dot{C}_i(0) = 0$. Equation [1.23] contains two unknowns, b_1 and b_2 , and must be solved simultaneously with Equation [1.16].

The values obtained for b_1 and b_2 will be the initial values for the generating solution, provided the equation

$$m_1 \beta_1^2 + m_3 \beta_1 \mu + m_4 \mu^2 + \Phi = 0 \quad [1.25]$$

(where Φ contains terms of order not lower than third in μ and β) has an analytic solution $\beta_1 = \beta_1(\mu)$.

A sufficient condition for the existence of such a solution of Equation [1.25] is (3)

$$m_4^2 - 4m_1 m_3 > 0 \quad [1.26]$$

If the obtained values of b_1 and b_2 satisfy the inequality

[1.26], then the periodic solution of the simplified system, satisfying the initial conditions

$$x_{0i}(0) = b_i \quad \dot{x}_{0i}(0) = f(b_i)$$

will be the generating solution, which is the first approximation for the periodic solution of the basic fundamental system.

It is interesting to note that if m_1 is unequal to 0 and m_4 is unequal to 0, then each pair of values b_1 and b_2 , obtained from Equation [1.23] and satisfying [1.26], will correspond to two solutions of Equation [1.25] and, consequently, one and the same generating solution will be the first approximation for two different periodic solutions of the fundamental equation. The calculation of m_1, m_3 and m_4 presents no principal difficulties once the values of b_1 and b_2 have been obtained from [1.23].

For the particular case when the discontinuity takes place on the Ox axis, one can rewrite conditions [1.23 and 1.26] in a more compact form. Considering that $b_2 = -b_1 = -b$ we obtain

$$m_1 = 0 \quad m_2 = k_1^2 k_2^2 b^2 [C_2(T_{02}) - C_1(T_{01})]$$

$$m_3 = -k_1^2 k_2^2 b^2 [D_2(T_{02}) + D_1(T_{01})]$$

where $D_i(t)$ is the solution of the equation

$$\ddot{D}_i + k_i^2 D_i = \frac{\partial F_i(x_{0i}, \dot{x}_{0i})}{\partial x_{0i}} \cos k_i t - k_i \frac{\partial F_i(x_{0i}, \dot{x}_{0i})}{\partial \dot{x}_{0i}} \sin k_i t$$

satisfying the initial conditions $D_i(0) = \dot{D}_i(0) = 0$. The solutions $C_i(t)$ and $D_i(t)$ can be represented in the form

$$C_i(t) = \int_0^t F_i[x_{0i}(\tau), \dot{x}_{0i}(\tau)] \sin k_i(t - \tau) d\tau$$

$$D_i(t) = (-1)^{i+1} \int_0^t \left[\frac{\partial F_i(x_{0i}, \dot{x}_{0i})}{\partial x_{0i}} \cos k_i \tau - k_i \frac{\partial F_i(x_{0i}, \dot{x}_{0i})}{\partial \dot{x}_{0i}} \sin k_i \tau \right] \sin k_i(t - \tau) d\tau$$

Considering that $T_{01} = T_{02} = \pi/k$, the conditions [1.23] can be written as

$$P(b) = \int_0^{\pi/k} \{ F_1[x_{01}(\tau), \dot{x}_{01}(\tau)] \sin k_1 \tau - F_2[x_{02}(\tau), \dot{x}_{02}(\tau)] \sin k_2 \tau \} d\tau = 0 \quad [1.27]$$

Then condition [1.26] becomes

$$dP/db = 0 \quad [1.28]$$

It follows from all the foregoing that to each multiple root of Equation [1.27] there corresponds a unique periodic solution of the fundamental equation, which, being analytic in μ , becomes a periodic solution of simplified equation when $\mu = 0$.

As a particular case, one can obtain from conditions [1.27 and 1.28] the well-known (1) conditions for the existence of periodic solutions of a differential equation with continuous terms, for which it is enough to replace in the solution $x_{02}(t)$ the variable t by $t' = t + \pi/k$.

Section 2

By way of an application of the method developed, let us find the periodic solution of the equation

$$\ddot{x} + x = \mu [a_2 \dot{x} - (a_1 + a_3 \dot{x}^2) \text{sign } \dot{x}] \quad [2.1]$$

where a_1, a_2 and a_3 are known numbers. This equation can be considered as two different equations, which are correct for different parts of the phase half-plane

$$\dot{x} + x = \mu [a_1 + a_2 \dot{x} + a_3 \dot{x}^2] \text{ for } \dot{x} \leq 0$$

$$\dot{x} + x = \mu [-a_1 + a_2 \dot{x} - a_3 \dot{x}^2] \text{ for } \dot{x} \geq 0$$

On the phase half-plane, the boundary between these two

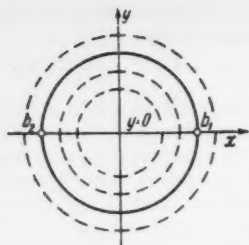


Fig. 2

equations is the Ox axis. The phase trajectories of the simplified system

$$\ddot{x} + x = 0 \quad [2.2]$$

are a family of circles that depend on a single parameter (Fig. 2).

As is known, equations of this type describe the oscillations of a mechanical system in the presence of "dry" friction forces.

The necessary condition for the existence of a periodic solution of Equation [2.1], analytic in μ and turning into a periodic solution of [2.2] when $\mu = 0$, as obtained in Section 1, Equation [1.23], has the form

$$C_2(T_{02}) - C_1(T_{01}) = 0 \quad [2.3]$$

Let us find $C_i(t)$ from Equation [1.24] and, considering that for a discontinuity on the Ox axis we have $T_{0i} = \pi$ when $k = 1$, we obtain the following equation for b

$$(8/3)a_3b^2 - \pi a_2b + 4a_1 = 0 \quad [2.4]$$

It has been shown in Section 1 that in the case of a discontinuity on the Ox axis, each multiple root of Equation [2.4] corresponds to the sought periodic solution of [2.1]. Let us find the root of [2.1]

$$b_{1,2} = \frac{3\pi a_2 \pm \sqrt{9\pi^2 a_2^2 - 384a_1a_3}}{16a_3}$$

In order for a periodic solution of Equation [2.1] to exist, it is necessary and sufficient that the roots of [2.4] be nonmultiple, real and positive. The inequality

$$3\pi^2 a_2^2 > 128a_1a_3$$

insures the presence of real roots; let us investigate all possible cases.

1 Let $a_1 = 0$; if $a_2a_3 > 0$ in this case, there exists one positive root of Equation [2.4], $b = (3/8)\pi a_2/a_3$, and conse-

quently there exists one periodic solution of [2.1], the first approximation of which has the form

$$x_0 = b \cos t = \frac{3}{8}\pi \frac{a_2}{a_3} \cos t$$

The limit cycle corresponding to this periodic solution will be stable if $a_2 > 0$ and unstable if $a_2 < 0$, as follows from an examination of the singular point at the origin and the behavior of the phase trajectories at infinity. If $a_2a_3 > 0$, there are no periodic solutions.

2 Let $a_2 = 0$; if $a_1a_3 < 0$ in this case, then there exists one positive root $b = \sqrt{3a_1/2a_3}$ and consequently there exists one periodic solution, the first approximation of which is

$$x_0 = \sqrt{3a_1/2a_3} \cos t$$

The corresponding limit cycle will be stable if $a_1 > 0$ and $a_3 < 0$, and unstable if $a_1 < 0$ and $a_3 > 0$. If $a_1a_3 > 0$, there are no periodic solutions.

3 All the coefficients are different from 0, and in this case the following cases are possible:

a Let $a_1a_3 > 0$; if $a_2a_3 > 0$ in this case, two positive roots of Equation [2.4] exist and consequently there are two periodic solutions of [2.1]. The limit cycle corresponding to the smaller root will be stable when $a_1 > 0$ and unstable when $a_1 < 0$, while the limit cycle corresponding to the larger root will be stable if $a_1 < 0$ and unstable if $a_1 > 0$.

If $a_2a_3 < 0$, then Equation [2.4] has no positive roots and consequently [2.1] has no periodic solutions.

b Let $a_1a_3 < 0$; in this case there exists one positive root. The limit cycle corresponding to this solution will be stable if $a_1 > 0$ and unstable if $a_1 < 0$.

It is interesting to consider the case when $a_3 = 0$, making Equation [2.4] linear in b . The positive root exists if $a_1a_2 > 0$

$$b = (4a_1/\pi a_2)$$

The exact value of b has been obtained for this case (4)

$$b = \mu a_1 \coth(\mu a_2 \pi / 4)$$

Using the expansion of $\coth x$ in powers of x , we find

$$b = \mu a_1 \left[\frac{4}{\mu a_2 \pi} + \mu \left(\frac{a_2 \pi}{12} + \dots \right) \right]$$

and when $\mu = 0$ the approximate values of b , obtained by different methods, coincide.

References

- 1 Malkin, I. G., "Nekotorye Zadachi Teorii Melineinykh Kolebaniy" (Certain Problems in the Theory of Nonlinear Oscillations), Gostekhizdat, 1956.
- 2 Shteinberg, T. S., "The Small Parameter Method in the Investigation of Periodic Motions of Systems With Friction," Tr. Ural'sk. Polit. In-ta (Transactions of Ural Polytechnic Institute), Collection no. 74, 1958.
- 3 Erugin, N. P., "Neyavnye Funktsii" (Implicit Functions), Leningrad State University Press, 1956.
- 4 Shteinberg, T. S., "Periodic Solutions of Differential Equations of Nonlinear Oscillations in the Presence of 'Dry' and 'Viscous' Friction Forces," Investia Akad. Nauk SSSR, Old. Tekh. Nauk (Bull. Acad. Sci. USSR, Div. Tech. Sci.), no. 4, 1954.

—Original received June 2, 1959

Reviewer's Comment

Dr. Shteinberg's paper is essentially devoted to a perturbation method for solving second-order differential equations with a small parameter. Although the method itself has features which bear some similarities to the Poincaré method of continuing periodic solutions, the particular treatment of first-order discontinuities in this paper appears to be novel but not original in light of Poincaré's method.

The author's principal goal in the treatment is to obtain the solutions of the original or fundamental set of equations with a small parameter in terms of the solutions of a simplified set where this parameter is set equal to zero. In addition, criteria are established for the determination of periodic solutions of the fundamental system in terms of those of the simplified system.

There are some points in the development of the paper where mathematical conciseness was lacking. More spe-

cifically, no mention was made of the fact that the solution of the fundamental equation, as well as its time derivative, are to be continuously dependent upon the original parameter μ and initial value perturbations.

As mentioned before, the entire treatment in this paper which centers around the questions of existence and determination of periodic solutions of the differential equations may be compared with the Poincaré treatment and theory. A discussion of the latter may be found in "Fundamentals of Poincaré's Theory" by K. O. Friedrichs in "Proceedings of the Symposium on Nonlinear Circuit Analysis," New York, April 23 and 24, 1953, p. 56.

The principal difference between Shteinberg's and Poincaré's theories is the following: The former method, treated in this paper, considers a periodic solution of the simplified system of differential equations with $\mu = 0$, and given initial conditions. The problem is to find a uniquely corresponding periodic solution of the fundamental set of equations whose initial conditions are those of the respective simplified set plus respective perturbations which are continuous functions of μ and which vanish when $\mu = 0$. In other words, the periodic solutions of the fundamental set reduce those of the simplified set when μ vanishes. The criterion which establishes such solutions is the vanishing of a certain Jacobian determinant of the initial solution and its time derivative with respect to the perturbations of initial conditions when they are zero. This eventually leads to the equivalent criterion that these perturbations are continuous functions of μ and vanish when $\mu = 0$, and, thereby, reduce to periodic solutions of the simplified equations.

Poincaré's treatment first considers the two sets of equations in the Shteinberg paper. However, the problem here is to consider a variational equation associated with the original equation, nonzero parameter, μ . Now the essence of this theory is that a periodic solution of the aforementioned simplified system may be continued to a periodic solution of the fundamental system if the above variational equation has no periodic solution. The above continued periodic solution in question depends continuously upon μ and reduces

to the periodic solution of the simplified system when $\mu = 0$.

Of course, the additional feature of the present paper of Shteinberg is the occurrence of discontinuous terms of the fundamental and simplified sets of equations. Although no particular mathematical difficulties arise because of these terms, their presence serves part of the intended purpose of Shteinberg's paper.

One important topic that was lacking in this paper was the discussion of stability of periodic solutions. However, the existence and stability of limit cycles were discussed in an example that was presented at the end of the paper.

Apart from occasional inconsistencies in the use of subscript symbols and some minor algebraic errors all of which were easily rectified, the paper is not at all difficult to follow.

From the point of view of the study and investigations in orbital mechanics and similar studies, the present paper appears to give a satisfactorily useful method for determining periodic solutions of second-order differential equations of special types. An example of a counterpart, nonperturbation method which has been used successfully for equations similar in type to those of this paper is van der Pol's method. As another example of a nonperturbative method for periodic solutions, the phase plane method is quite appropriate for the types of equations as Shteinberg's since they are autonomous systems.

There are no indications in the paper which point to decisively new contributions to the overall theory of periodic solutions of second-order differential equations. It is felt, though, that the material in this paper could be extended to systems somewhat more general than those treated here.

As a final comment, it might be stated that in comparing the method presented in Shteinberg's paper with Poincaré's method, the latter method does not make as stringent requirements on continuity and differentiability as the former does.

—ROBERT M. MEISEL
Engineering Section

Sperry Gyroscope Co., Great Neck

Scattering of Light in a Medium Adjacent to a Reflecting Surface

S. D. GUTSHABASH

IN this paper we will consider the problem of radiation transfer in a plane layer adjacent to a reflecting surface. Problems of this kind are encountered in astrophysics and geophysics, for example in the study of scattering of light by a planetary atmosphere bounded by the surface of the planet, and also in physics, in the study of diffusion of radiation in a gas or liquid contained in a vessel.

It was shown by Sobolev (1)¹ that the solutions of various problems of radiation transfer in a plane layer of finite optical

Translated from *Vestnik Leningradskogo Universiteta* (Bull. Leningrad University), no. 1, 1960, pp. 152-158. Translated by J. George Adashko.

¹ Numbers in parentheses indicate References at end of paper.

thickness τ_0 can be expressed, for different radiation sources, in terms of a single function $\Phi(\tau, \tau_0)$, which depends only on the optical depth τ (with τ_0 as a parameter).

In the present paper it is shown that the solution of analogous radiation transfer problems in the presence of a reflecting surface can also be expressed in terms of a similar function $\Phi(\tau, \tau_0)$. By way of example, two particular cases are considered. It is assumed in the first case that the incident rays are parallel, and in the second that the radiation sources are uniformly distributed within the medium.

We have solved this problem by using the probability method developed by Sobolev and the results of his papers (1 and 2).

1 Derivation of the Equation for the Resolvent

As is well-known (2 and 3), the calculation of the radiation field in an isotropic scattering medium, bounded by an orthotropic bottom, reduces to the determination of a function $B_1(\tau, \tau_0)$ from the integral equation

$$B_1(\tau, \tau_0) = \frac{\lambda}{2} \int_0^{\tau_0} B_1(\tau', \tau_0) [E_t |\tau - \tau'| + 2AE_{t_0}(\tau_0 - \tau)E_{t_0}(\tau_0 - \tau')] d\tau' + g_1(\tau) \quad [1]$$

where

$$\begin{aligned} \lambda &= \text{probability of survival of quantum} \\ A &= \text{albedo of bottom} \end{aligned}$$

$g_1(\tau)$ = function characterizing the arrangement of the radiation sources

$$E_{t_0} = \int_1^\infty e^{-xz} (dz/z^n) \quad [2]$$

With the aid of the resolvent $\Gamma_1(\tau, \tau', \tau_0)$, the solution of Equation [1] can be written in the form

$$B_1(\tau, \tau_0) = g_1(\tau) + \int_0^{\tau_0} \Gamma_1(\tau, \tau', \tau_0) g_1(\tau') d\tau' \quad [3]$$

The quantity $\Gamma_1(\tau, \tau', \tau_0) d\tau d\tau'$ represents the probability that a quantum, emitted between the optical depths τ and $\tau + d\tau$, will be subsequently emitted (after diffusion in the medium) between the optical depths τ' and $\tau' + d\tau'$.

Along with Equation [1], we shall consider an equation for the function $B(\tau, \tau_0)$, written out for the case when there is no reflecting surface

$$B(\tau, \tau_0) = \frac{\lambda}{2} \int_0^{\tau_0} B(\tau, \tau') E_t |\tau - \tau'| d\tau' + g(\tau) \quad [4]$$

and its solution

$$B(\tau, \tau_0) = g(\tau) + \int_0^{\tau_0} \Gamma(\tau, \tau', \tau_0) g(\tau') d\tau' \quad [5]$$

Starting out with this probabilistic meaning of the resolvent, we can write down the following equation for it

$$\Gamma_1(\tau, \tau', \tau_0) = \Gamma(\tau, \tau', \tau_0) + P(\tau_0 - \tau, \tau_0) \frac{A}{\pi} 2\pi \left[\int_0^{\tau_0} \Gamma_1(\tau'', \tau', \tau_0) d\tau'' \int_0^1 e^{-(\tau_0 - \tau'')/\eta} d\eta' + \int_0^1 e^{-(\tau_0 - \tau')/\eta} d\eta' \right] \quad [6]$$

where $P(\tau_0 - \tau, \tau_0)$ and $P(\tau, \tau_0)$ are the probability that a quantum absorbed at an optical depth τ will go out of the medium through the lower and upper boundaries respectively, in all directions.

The integral in the right half of Equation [6] can be calculated from the equation itself, by multiplying [6] by $E_{t_0}(\tau_0 - \tau) d\tau$ and integrating over τ in the interval from 0 to τ_0 . As a result we obtain, by using Equation [2]

$$\int_0^{\tau_0} \Gamma_1(\tau'', \tau', \tau_0) E_{t_0}(\tau_0 - \tau'') d\tau'' + E_{t_0}(\tau_0 - \tau') = \frac{\int_0^{\tau_0} \Gamma(\tau'', \tau', \tau_0) E_{t_0}(\tau_0 - \tau'') d\tau'' + E_{t_0}(\tau_0 - \tau')}{1 - AC} \quad [7]$$

where

$$C = 2 \int_0^{\tau_0} P(\tau, \tau_0) E_{t_0} \tau d\tau \quad [8]$$

If $p(\tau, \eta, \tau_0) d\omega$ is the probability that a quantum absorbed at an optical depth τ will go out of the medium through its upper boundary at an angle $\cos^{-1} \eta$ to the normal within a solid

angle $d\omega$, then

$$P(\tau, \tau_0) = 2\pi \int_0^1 p(\tau, \eta, \tau_0) d\eta \quad [9]$$

and the coefficient of reflection $\rho(\eta, \zeta)$ is

$$\rho(\eta, \zeta) = \frac{\pi}{\zeta} \int_0^{\tau_0} e^{-\tau/\zeta} p(\tau, \eta, \tau_0) \frac{d\tau}{\eta} \quad [10]$$

With the aid of these relations we obtain instead of Equation [8]

$$C = 4 \int_0^1 \eta \int_0^1 \rho(\eta, \zeta) \zeta d\zeta \quad [11]$$

Substituting [7] into [6], we get

$$\Gamma_1(\tau, \tau', \tau_0) = \Gamma(\tau, \tau', \tau_0) + \frac{2A}{1 - AC} P(\tau_0 - \tau, \tau_0) \left[\int_0^{\tau_0} \Gamma(\tau'', \tau', \tau_0) E_{t_0}(\tau_0 - \tau'') d\tau'' + E_{t_0}(\tau_0 - \tau') \right] \quad [12]$$

Since

$$\begin{aligned} p(\tau_0 - \tau', \eta, \tau_0) &= \frac{\lambda}{4\pi} e^{-(\tau_0 - \tau')/\eta} + \\ &\frac{\lambda}{4\pi} \int_0^{\tau_0} \Gamma(\tau', \tau'', \tau_0) e^{-(\tau_0 - \tau'')/\eta} d\tau'' \quad [13] \end{aligned}$$

integration of this equation with respect to η from 0 to 1 yields, considering the symmetry of the resolvent $\Gamma(\tau, \tau', \tau_0)$ with respect to τ and τ'

$$\begin{aligned} \int_0^{\tau_0} \Gamma(\tau'', \tau', \tau_0) E_{t_0}(\tau_0 - \tau'') d\tau'' + E_{t_0}(\tau_0 - \tau') = \\ \frac{2}{\lambda} P(\tau_0 - \tau', \tau_0) \quad [14] \end{aligned}$$

Instead of Equation [12] we shall have

$$\Gamma_1(\tau, \tau', \tau_0) = \Gamma(\tau, \tau', \tau_0) + \frac{4A}{(1 - AC)\lambda} P(\tau_0 - \tau, \tau_0) P(\tau_0 - \tau', \tau_0) \quad [15]$$

In view of the fact that the resolvent $\Gamma(\tau, \tau', \tau_0)$ of equation [14] is expressed in terms of the function

$$\Phi(\tau, \tau_0) = \Gamma(\tau, 0, \tau_0) \quad [16]$$

it follows from [14 and 15] that the resolvent of Equation [1] can also be expressed in terms of the function $\Phi(\tau, \tau_0)$.

2 Medium Illuminated With Parallel Rays

Assume that parallel rays are incident on a medium at an angle $\cos^{-1} \zeta$, and the flux per unit area perpendicular to the rays is πS .

Then

$$g_1(\tau) = \frac{\lambda}{4} S e^{-\tau/\zeta} + \frac{\lambda}{2} A S e^{-\tau_0/\zeta} E_{t_0}(\tau_0 - \tau) \zeta \quad [17]$$

and

$$g(\tau) = \frac{\lambda}{4} S e^{-\tau/\zeta} \quad [18]$$

Substituting [15 and 17] in [3], we obtain

$$B_1(\tau, \zeta, \tau_0) = B(\tau, \zeta, \tau_0) + \frac{A \times S}{1 - AC} \zeta \mu(\zeta) P(\tau_0 - \tau, \tau_0) \quad [19]$$

This demonstrates clearly the dependence of the "source function" $B_1(\tau, \zeta, \tau_0)$ and $B(\tau, \zeta, \tau_0)$ on the cosine of the angle of incidence of the external radiation ζ . The value of $\mu(\zeta)$ is

$$\mu(\zeta) = 2 \int_0^1 \sigma(\eta, \zeta) \eta d\eta + e^{-\tau_0/\zeta} \quad [20]$$

and the transmission coefficient $\sigma(\eta, \zeta)$ is determined by

$$\sigma(\eta, \zeta) = \frac{\pi}{\zeta} \int_0^{\tau_0} e^{-(\tau_0-\tau)/\zeta} p(\tau, \eta, \tau_0) \frac{d\tau}{\eta} \quad [21]$$

Since

$$p(\tau, \eta, \tau_0) = \frac{B(\tau, \eta, \tau_0)}{\pi S} \quad [22]$$

we obtain instead of [19]

$$B_1(\tau, \zeta, \tau_0) = B(\tau, \zeta, \tau_0) + \frac{2A}{1 - AC} \zeta \mu(\zeta) \int_0^1 B(\tau_0 - \tau, \eta', \tau_0) d\eta' \quad [23]$$

Thus, the "source function" in the presence of a reflecting surface, $B_1(\tau, \zeta, \tau_0)$, can be expressed in terms of a "source function" $B(\tau, \zeta, \tau_0)$ without a reflecting surface.

Using the obtained value of $B_1(\tau, \zeta, \tau_0)$ we can obtain the conditions of light inside the medium, i.e., the intensity of the diffused radiation at any optical depth, and also the intensity of the diffusely transmitted and diffusely reflected radiations (see diagram). The intensity of the diffused radiation at a certain optical depth is determined by the following formulas ($\eta > 0$)

$$I_1(\tau, \eta, \zeta) = \int_0^{\tau_0} B_1(\tau', \zeta, \tau_0) e^{-(\tau-\tau')/\eta} \frac{d\tau'}{\eta} \quad [24]$$

$$I_1(\tau, -\eta, \zeta) = \int_{\tau}^{\tau_0} B_1(\tau', \zeta, \tau_0) e^{-(\tau'-\tau)/\eta} \frac{d\tau'}{\eta} + A e^{-(\tau_0-\tau)/\eta} \left[2 \int_0^1 I_1(\tau_0, \eta', \zeta) \eta' d\eta' + S e^{-\tau_0/\zeta} \zeta \right] \quad [25]$$

In formula [25] we took into account the radiation propagated directly from the reflecting surface. Substituting in these formulas the values of $B_1(\tau, \zeta, \tau_0)$ as given by [23], we get

$$I_1(\tau, \eta, \zeta) = I(\tau, \eta, \zeta) + \frac{2A}{1 - AC} \zeta \mu(\zeta) \int_0^1 I(\tau_0 - \tau, -\eta, \eta') d\eta' \quad [26]$$

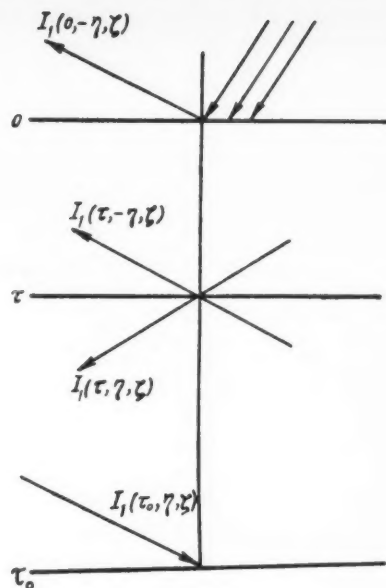
and

$$I_1(\tau, -\eta, \zeta) = I(\tau, -\eta, \zeta) + \frac{2A}{1 - AC} \zeta \mu(\zeta) \int_0^1 I(\tau_0 - \tau, \eta, \eta') d\eta' + A e^{-(\tau_0-\tau)/\eta} \left[2 \int_0^1 I_1(\tau_0, \eta', \zeta) \eta' d\eta' + S e^{-\tau_0/\zeta} \zeta \right] \quad [27]$$

In these formulas, $I(\tau, \eta, \zeta)$ and $I(\tau, -\eta, \zeta)$ are the intensities at an optical depth τ in the absence of a reflecting surface.

If we put in [27] for $I_1(\tau_0, \eta, \zeta)$ the value of Equation [26] with $\tau = \tau_0$ and use relation [11], we obtain

$$I_1(\tau, -\eta, \zeta) = I(\tau, -\eta, \zeta) + \frac{A}{1 - AC} \zeta \mu(\zeta) \left[2 \int_0^1 I(\tau_0 - \tau, \eta, \eta') d\eta' + S e^{-(\tau_0-\tau)/\eta} \right] \quad [28]$$



Putting $\tau = \tau_0$ in [26] and $\tau = 0$ in [28], we obtain the intensity of radiation of diffusely transmitted and diffusely reflected radiation from the medium

$$I_1(\tau_0, -\eta, \zeta) = S \zeta \left[\sigma(\eta, \zeta) + \frac{A}{1 - AC} \mu(\zeta) \nu(\eta) \right] \quad [29]$$

$$I_1(0, -\eta, \zeta) = S \zeta \left[\rho(\eta, \zeta) + \frac{A}{1 - AC} \mu(\zeta) \mu(\eta) \right] \quad [30]$$

where

$$\nu(\eta) = 2 \int_0^1 \rho(\eta, \eta') \eta' d\eta' \quad [31]$$

We make use here of the fact that the following relations hold along with [10 and 21]

$$I(0, -\eta, \zeta) = S \rho(\eta, \zeta) \times \zeta \quad I(\tau_0, \eta, \zeta) = S \sigma(\eta, \zeta) \times \zeta \quad [32]$$

Equations [26 and 28], and also Equations [29 and 30] which follow from them, are the ones we seek. Equations [29 and 30] were derived earlier by Sobolev (4) and Van de Hulst (5).

3 Medium With Uniformly Distributed Radiation Sources

Assume that the radiation sources are distributed uniformly inside the medium, i.e.

$$g_1(\tau) = 1 \quad [33]$$

With the aid of relation [3, 15 and 33] we obtain

$$B_1(\tau, \tau_0) = B(\tau, \tau_0) + \frac{4A}{(1 - AC)\lambda} P(\tau_0 - \tau, \tau_0) \int_0^{\tau_0} P(\tau_0 - \tau', \tau_0) d\tau' \quad [34]$$

The integral in the right half of this equation can be expressed in terms of the Abartsumyan functions (6) $\varphi(\zeta, \tau_0)$ and $\psi(\zeta, \tau_0)$

and their moments (for which purpose Eq. [9] is used), and the well-known relation

$$\int_0^{\tau_0} p(\tau, \eta, \tau_0) \frac{d\tau}{\eta} = \frac{\lambda}{4\pi} \frac{\varphi(\eta, \tau_0) - \psi(\eta, \tau_0)}{1 - (\lambda/2)(\alpha_0 - \beta_0)} \quad [35]$$

As a result we obtain

$$\int_0^{\tau_0} P(\tau_0 - \tau', \tau_0) d\tau' = \frac{\lambda}{2} \times \frac{\alpha_1 - \beta_1}{1 - (\lambda/2)(\alpha_0 - \beta_0)} \quad [36]$$

where

$$\alpha_n = \int_0^1 \varphi(\eta, \tau_0) \eta^n d\eta \quad \beta_n = \int_0^1 \psi(\eta, \tau_0) \eta^n d\eta \quad [37]$$

and consequently

$$B_1(\tau, \tau_0) = B(\tau, \tau_0) + \frac{2A}{1 - AC} \frac{\alpha_1 - \beta_1}{1 - (\lambda/2)(\alpha_0 - \beta_0)} P(\tau_0 - \tau, \tau_0) \quad [38]$$

The intensities at the optical depth τ are determined by the formulas

$$I_1(\tau, \eta) = \int_0^{\tau} B_1(\tau', \tau_0) e^{-(\tau-\tau')/\eta} \frac{d\tau'}{\eta} = I(\tau, \eta) + \frac{2A}{1 - AC} \times \frac{\alpha_1 - \beta_1}{1 - (\lambda/2)(\alpha_0 - \beta_0)} \times \int_0^{\tau} P(\tau_0 - \tau', \tau_0) e^{-(\tau-\tau')/\eta} \frac{d\tau'}{\eta} \quad [39]$$

$$I_1(\tau, -\eta) = \int_{\tau}^{\tau_0} B_1(\tau', \tau_0) e^{-(\tau'-\tau)/\eta} \frac{d\tau'}{\eta} + 2A \int_0^1 I_1(\tau_0, \eta') \eta' d\eta' = I(\tau, -\eta) + \frac{2A}{1 - AC} \frac{\alpha_1 - \beta_1}{1 - (\lambda/2)(\alpha_0 - \beta_0)} \times \int_{\tau}^{\tau_0} P(\tau_0 - \tau', \tau_0) e^{-(\tau'-\tau)/\eta} \frac{d\tau'}{\eta} + 2A e^{-(\tau_0-\tau)/\eta} \int_0^1 I_1(\tau_0, \eta') \eta' d\eta' \quad [40]$$

Formula [40] can be simplified somewhat by replacing $I_1(\tau_0, \eta)$ with the value of [39] at $\tau = \tau_0$. As a result we obtain

$$I_1(\tau, -\eta) = I(\tau, -\eta) + \frac{2A}{1 - AC} \times \frac{\alpha_1 - \beta_1}{1 - (\lambda/2)(\alpha_0 - \beta_0)} \times \left[\int_{\tau}^{\tau_0} P(\tau_0 - \tau', \tau_0) e^{-(\tau'-\tau)/\eta} \frac{d\tau'}{\eta} + e^{-(\tau_0-\tau)/\eta} \right] \quad [41]$$

As is known, on the boundaries of the medium we have

$$I(\tau_0, \eta) = I(0, -\eta) = \frac{\varphi(\eta, \tau_0) - \psi(\eta, \tau_0)}{1 - (\lambda/2)(\alpha_0 - \beta_0)} \quad [42]$$

We therefore obtain for the intensities on the boundaries of the medium, in the presence of a reflecting surface

$$I_1(\tau_0, \eta) = \frac{1}{1 - (\lambda/2)(\alpha_0 - \beta_0)} \times \left\{ \varphi(\eta, \tau_0) - \psi(\eta, \tau_0) + \frac{2A}{1 - AC} (\alpha_1 - \beta_1) \nu(\eta) \right\} \quad [43]$$

$$I_1(0, -\eta) = \frac{1}{1 - (\lambda/2)(\alpha_0 - \beta_0)} \times \left\{ \varphi(\eta, \tau_0) - \psi(\eta, \tau_0) + \frac{2A}{1 - AC} (\alpha_1 - \beta_1) \mu(\eta) \right\} \quad [44]$$

Equations [43 and 44] were derived earlier by Sobolev (2) in a somewhat different manner.

We note that the problem can be solved analogously for a different arrangement of the sources of radiation.

References

- 1 Sobolev, V. V., Doklady Acad. Nauk. SSSR (Trans. Acad. Sci. USSR), vol. 120, no. 1, 1958.
- 2 Sobolev, V. V., "Perenos Luchistoi Energii v Atmosferakh Zvezd i Planet" (Transfer of Radiant Energy in the Atmospheres of Stars and Planets), 1958.
- 3 Kuznetsov, E. S., *Izvestiya Acad. Nauk SSSR* (Bull. Acad. Sci. USSR), Geographic and Geophysics Series, no. 5, 1942.
- 4 Sobolev, V. V., Doklady Acad. Nauk SSSR (Trans. Acad. Sci. USSR), vol. 61, no. 5, 1948.
- 5 Van de Hulst, *Astrophys. J.*, vol. 107, p. 220, 1948.
- 6 Abartsumyan, V. A., Doklady Acad. Nauk SSSR (Trans. Acad. Sci. USSR), vol. 38, p. 257, 1943.

—Original submitted May 25, 1959

Reviewer's Comment

This paper is concerned with the diffusion of light through a medium which may emit, absorb and isotropically re-emit radiation. Problems of this type have recently been investigated because of the high radiation levels present in the solid fuel of rockets, in rocket nozzles (1) and in missile nose cones (1,2).

The mathematical apparatus for treating the diffusion of radiation in a medium has been extensively developed in connection with astrophysics (3) and neutron diffusion (4). However, the notation used in the present paper is quite different from any in the Western literature I have read and is only explained in an untranslated Russian source, Reference 2 of the text. Consequently, a word of explanation of the notation is appropriate here. The function $B(\tau, \tau_0)$ is the total intensity of radiation, integrated over all directions of travel, at the point τ . Here τ is a dimensionless coordinate in which the ordinary distance coordinate is divided by the radiation mean free path.¹ The quantity λ is the probability that a quantum will be re-emitted isotropically after

an absorption process. The albedo A is the probability that a quantum which leaves the surface of the medium will re-enter the medium, i.e., A is the specular reflectivity of the surface. The function $g(\tau)$ is the radiative intensity which would be produced by the sources in the medium present, were there no re-emission of radiation in the medium after an absorption process nor any reflection of radiation at the surface.² Finally, the function $\Gamma_1(\tau, \tau', \tau_0) + \delta(\tau - \tau')$ is the Green's function for integral Equation [1].

Notice also that in the present paper the word "absorb" may have the meaning "absorb and then re-emit isotropically" while the word "emit" may mean "re-emit after an absorption."

This paper is rather different in content from anything which appears in the recent Western literature. The author here considers, and elegantly solves, the problem of relating the intensity of radiation which would appear in a medium with a partially reflecting surface to the radiative intensity which would appear in the absence of the reflection. This type of work is exceedingly valuable because it considerably simplifies numerical computation. Once one has obtained

an approximate (analytical or numerical) solution to the radiation diffusion problem in a medium with a free surface, one can directly evaluate the solution with a reflecting surface.

This reviewer hopes and expects to see that results of this type will be incorporated in future Western work in radiative transport.

—LEO P. KADANOFF
Avco-Everett Research Laboratory

¹ This definition holds when the mean free path is independent of τ . For more general situations see (3 and 4).

² In Sec. 2 of the previously mentioned paper, an external beam of radiation has been replaced by an equivalent distribution of sources. This source distribution does depend explicitly upon the reflectivity of the surface.

1 Adams, Mac C., "Recent Advances in Ablation," *ARS JOURNAL*, vol. 29, no. 9, Sept. 1959, pp. 625-632.

2 Kadanoff, Leo P., "Radiative Heat Transfer in an Ablating Body," to be published in *ASME Heat Transfer Journal*. See also Adams, Mac C., Powers, William E. and Georgiev, S., "An Experimental and Theoretical Study of Quartz Ablation at the Stagnation Point," *J. Aero/Space Sci.*, vol. 27, no. 7, July 1960.

3 Chandrasekhar, S., *Radiative Transfer*, Clarendon Press, Oxford, Eng., 1950, chaps. I-III.

4 Davison B., *Neutron Transport Theory*, Clarendon Press, Oxford, Eng., 1957 chaps. IV-VI.

Investigation of Heat Exchange in Supersonic Flow of Air in Tubes

A. E. MARENOV

This paper contains certain results of an experimental investigation aimed at the determination of the local coefficients of heat exchange at supersonic speeds of gas flow in a cylindrical tube of constant cross section. The coefficients of heat exchange are expressed in terms of the numbers Nu_x , referred to the length of the experimental portion of the tube. It is known that in the region of steady-state flow the coefficient of heat exchange remains constant along the tube. In the initial portion of a straight tube, the dynamic and thermal boundary layers grow and cause the flow of gas to become unstable, and the coefficients of heat exchange to vary along the initial portion of the tube. The papers published thus far contain no computation formulas for the coefficients of heat exchange in the initial portion of the tube at supersonic speeds.

IF IT is assumed that the increase in the boundary layer in the initial portion of the tube is analogous to the increase of the boundary layer on a plate placed in a supersonic stream, then the experimental values of the coefficients of heat transfer in the initial portion of the tube can be verified against the analytical expressions for the coefficients of heat transfer of a plate.

In supersonic flow over a plate the formulas recommended for the heat transfer coefficients, expressed in terms of the Nusselt number, is

$$Nu = 0.274\sqrt{Re_x} \quad [1]$$

for a laminar boundary layer and

$$Nu = 0.037Re_x \times Pr^{1/4} \quad [2]$$

for a turbulent boundary layer.

Translated from *Institut Mekhaniki Akademii Nauk SSSR, Inzhenernyi Sbornik* (Institute of Mechanics, Academy of Sciences USSR, Engineering Collection), vol. 25, 1959, pp. 179-187. Translated by J. George Adashko.

The experiments covered flow with laminar, turbulent and transition boundary layers; the Mach number range was $1 \leq M \leq 3.5$, and the Re_x numbers referred to the length of the tube, ranged from 11×10^3 to 3×10^6 ; the air was heated to $T = 800$ K. The results of the experimental investigations are compared in the present paper with the Nusselt numbers expressed by relations [1 and 2].

1 Experimental Procedure

Our procedure for the determination of the local heat transfer coefficients makes use of the theory of steady-state temperature distributions. As is well known, under stationary thermal conditions the heat flowing from the moving gas through the wall of a tube is given by the equation

$$Q = 2\pi\lambda l \frac{(t_1 - t_2)}{\ln(r_2/r_1)} \quad [3]$$

where r_1 and r_2 are the radial distances at which the tube wall temperature is measured in a given section.

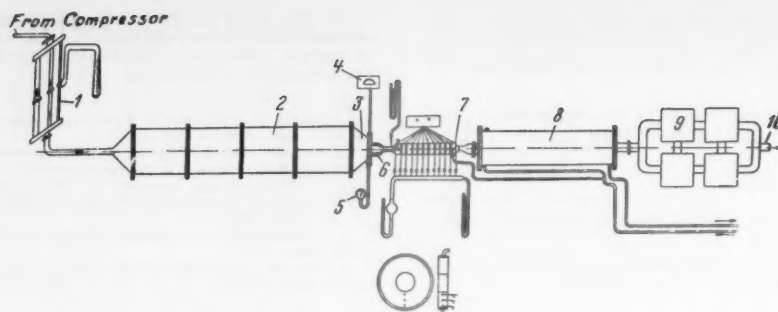


Fig. 1

The heat transfer coefficients α were determined from the expression for the specific heat flux per tube element

$$q = \alpha(t_0 - t_1) \quad [4]$$

where

α = local coefficient of heat transfer
 t_0 and t_1 = impact temperature of gas and wall temperature, respectively, in tube section under consideration

The resultant heat transfer coefficients are represented by the Nusselt numbers, referred to the length of the tube segment

$$Nu = (\alpha l / \lambda) \quad [5]$$

where

λ = coefficient of heat conduction of air, referred to impact temperature
 l = length of tube portion

The experiments were carried out with the apparatus going into the stationary thermal and gasdynamic modes.

The physical constants of the air, used in the different defining criteria, were referred to the impact temperature as determined on the tube length elements.

The Mach numbers were calculated from the measured values of the static pressures, wall temperature and impact temperature.

The increase in the boundary layer along the experimental segment of the tube was found by the method of (5)¹ and was compared with the Govorets formula for a boundary layer in the initial segment of the tube

$$\frac{\delta}{r} = 10.4 \frac{x}{d} \frac{1 + 0.795M^2}{\sqrt{Re}} \quad [6]$$

¹ Numbers in parentheses indicate References at end of paper.

2 Description of the Experimental Setup

A diagram of the experimental setup is shown in Fig. 1. Air from the compressor flows through measuring diaphragms 1 into a silite oven 2 and then into forechamber 3, where its temperature is measured with thermocouple and potentiometer 4, and the pressure is measured with manometer 5. The air flows from the forechamber into supersonic nozzle 6 and the experimental segment 7. It then goes through cooler 8 and vacuum pumps 9 and is exhausted to the atmosphere through port 10.

Fig. 2 shows the experimental segment, which consists of supersonic nozzle 1, joined through sleeve 2 with calibrated tube 3 (length $l = 658$ mm, ID 21 mm, and OD 25.5 mm). The transition sleeve is fitted to the nozzle and to the tube separately, so as to insure a smoother transition at the joint between the nozzle and the tube. Along the length of the tube are placed 13 brass rings 4, used to determine the local specific heat flux from the gas to the walls of the tube.

The entire ring area in contact with the tube was brazed to the latter with the aid of a special fixture. The rings were spaced 3 mm apart and insulated with asbestos. The first ring was located 85 mm from the junction of the nozzle with the tube. The rings had an outside diameter $d = 116$ mm and were $h = 40$ mm thick.

The rings were cooled on the outside with water flowing in special jackets 6, mounted on the rings. Each jacket had four inlets and four outlets for the cooling water, arranged in checkerboard fashion to insure uniform cooling.

To determine the heat flow from the air to the walls of the tube, three thermocouples 5 were mounted in each ring at fixed distances along the radius of the ring. All thermocouples were located in the same cross section. A fourth thermocouple, in the plane of the same cross section, was mounted in the wall of the tube.

The thermocouples were mounted in the middle of each ring, in holes of 1.2-mm diameter. The hot junctions of the

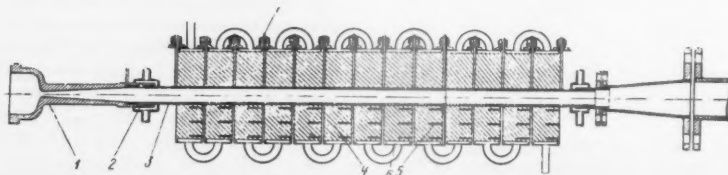


Fig. 2

thermocouples were soldered into the holes and the leads were insulated with two-duct porcelain tubing. The thermocouples were made of chromel-alumel wire 0.2 mm in diameter and were used with a PPTV-1 potentiometer. Outlets 7 were provided for the measurement of the static pressures in fifteen sections along the tube. The pressure was measured with a mercury vacuum meter. The experiments were carried out on three stainless steel nozzles with rated Mach numbers $M = 1.80, 2.5$ and 4.0 . The nozzles with $M = 2.5$ and 4 had a specially shaped supersonic part, while the nozzle with $M = 1.8$ was conical.

The impact temperature and the pressure of the air entering into the experimental segment were measured ahead of the nozzle in the forechamber. The temperature was measured with a diffusor thermocouple shielded against radiation.

The temperature of the oven was controlled by means of two "Norius" transformers (100 kw each) and monitored by an automatic-recording electronic potentiometer. In operation, the apparatus was first allowed to assume stationary temperature and pressure, after which the instrument readings were recorded.

3 Analysis of Experimental Data

The investigated flow conditions with turbulent, laminar and transition boundary layers are characterized by specific laws of heat transfer for each mode. For a detailed analysis let us examine one experiment for each of the different modes.

Fig. 3 shows the dependence of the parameter Nu_x on Re_x in one of the experiments where the flow had a developed turbulent boundary layer. The nozzle with $M = 1.80$ was used in this experiment. The flow remained supersonic only in a portion of the tube, after which it became subsonic. The experimental points were taken for the region of supersonic flow.

In the tested portion of the tube Re_x ranged from 0.9×10^6 to 3.5×10^6 ; the temperature factor varied very little over the length of the tube and could be assumed constant at $T_0/T_1 = 2$. It must be noted that the heat flux was measured not from the start of the tube, but from a distance 85 mm away from the junction between the tube and the nozzle.

As seen from the curve, the experimental points fit a certain straight line 1. Shown alongside is the theoretical heat transfer line 2 for a plate in a supersonic stream, with a turbulent boundary layer, as given by Equation [2]. The experimental points lie close to the indicated line, and are only slightly shifted towards larger Nu_x . The heat exchange conditions in the initial portion of the tube are characterized more clearly by the distribution of the specific heat fluxes.

Fig. 4 shows the dependence of the specific heat flux q on the Re for the experiment described in the foregoing. The experimental points were also taken only for the region of supersonic flow. As can be seen from the curve, the heat flux has a maximum at the beginning of the tube, where Re is a minimum, and diminishes towards the end of the tube with increasing Re_x .

Such a distribution of heat flux must be attributed to the growth of the boundary layer along the tube.

The character of the increase of the boundary layer thickness for this particular experiment is shown in Fig. 5.

The upper plot shows the experimental values of the relative thickness of the boundary layer δ/r as a function of Re_x . The lower plot shows the experimental Mach number as a function Re_x .

The first plot shows, for comparison, the increase in the boundary layer in the initial portion of the tube, calculated from Equation [6]. The experimental points are in good agreement with the theoretical relation. The values of the experimental points were taken from the start of the tube, i.e., from the joint between the nozzle and the tube.

The relations considered in the foregoing experiment are characteristic of the entire series of experiments carried out

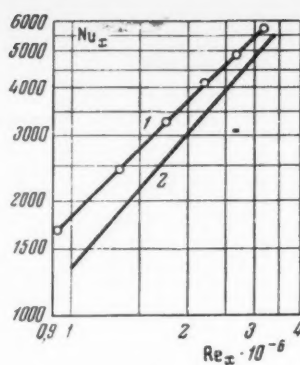


Fig. 3

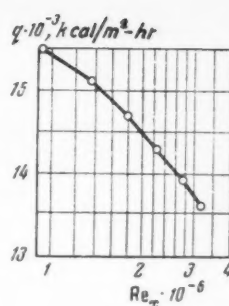


Fig. 4

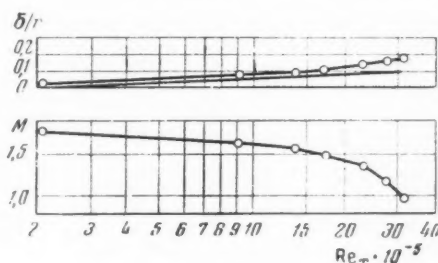


Fig. 5

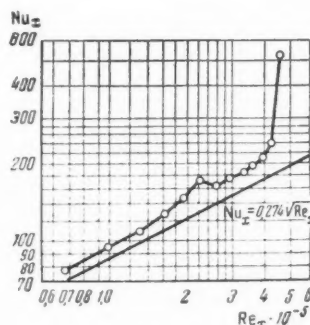


Fig. 6

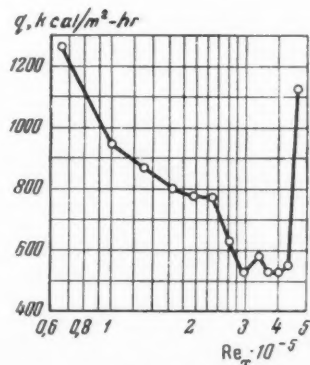


Fig. 7

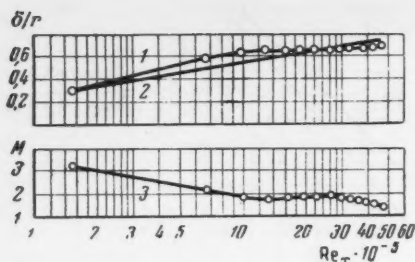


Fig. 8

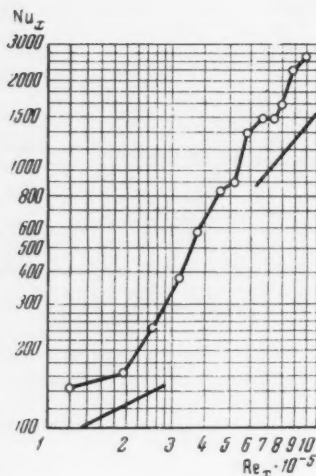


Fig. 9

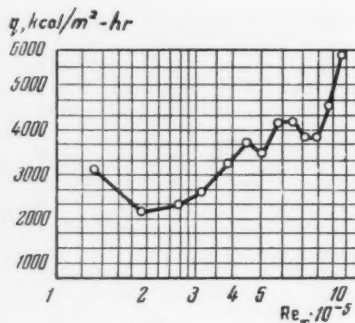


Fig. 10

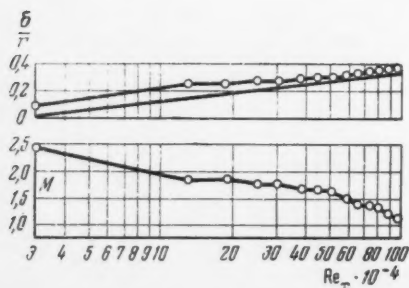


Fig. 11

for the region of supersonic flow in the initial portion of the tube for a turbulent boundary layer. Experiments were also carried out for supersonic flow in the presence of a laminar boundary layer. By way of illustration, we give the result of one of the experiments performed on the nozzle with $M = 4$. The parameter Re varied over the length of the tube from 67×10^3 to 461×10^3 , and the Mach numbers ranged from 3.45 at the start the tube to 1.32 at its end. The temperature factor varied little along the tube and its average was $T_0/T_1 = 2.4$.

Fig. 6 shows the experimental values of Nu as a function of Re_x (curve 1). For comparison, the theoretical values (curve 2), calculated from Equation [1], are also given. It is seen from the plot that Nu_x increases sharply when Re_x reaches a value on the order of 4×10^5 .

The value $Re_x = 4 \times 10^5$ is apparently critical, corresponding to the transition from a flow with a laminar boundary layer to a flow with a turbulent boundary layer.

Fig. 7 also gives an idea of the character of the heat transfer in supersonic flow in the initial portion of the tube, for a laminar boundary layer. It shows the experimental values of the specific heat flux q as a function of Re_x .

The specific heat flux has a maximum in the beginning of the tube. It diminishes along the tube up to the indicated critical value of Re_x , where it increases sharply.

In the transition region between the flow with laminar boundary layer and that with turbulent boundary layer, a change takes place in the structure of the boundary layer and the turbulence of the flow increases. This results in a sharp increase in heat transfer from the stream to the walls of the tube.

Fig. 8 shows the experimentally observed increase in the relative magnitude of the boundary layer (curve 1), and also in the Mach number (curve 3), as function of Re_x along the tube. For comparison, the line representing Equation [6] for the increase in the boundary layer is also plotted. Curve 2 deviates somewhat from the experimental data.

To illustrate the heat transfer in the transition from flow with laminar boundary layer to that with turbulent boundary layer, we give the result of one of the experiments with the $M = 2.5$ nozzle. The values of Re_x along the tube range from 30×10^3 to 10^6 while M ranges from 2.37 to 1.3. It is seen from Fig. 9 that the experimental value of Nu_x , as a function of Re_x , increases quite intensely near the critical value of Re_x . An analogous phenomenon takes place (Fig. 10) also for the experimental value of the specific heat flux q as a function of Re_x .

The change in the Mach numbers and in the relative thickness of the boundary layer δ/r is shown for the transition mode in Fig. 11 as a function of Re_x . The straight line corresponds to Equation [6].

Fig. 12 shows a summary plot of Nu_x vs. Re_x for the series of experiments including flow with laminar, turbulent and transition boundary layers, in which the critical values of Re_x range from 3×10^5 to 5×10^5 . For comparison, the plot shows the heat transfer (curves 1 and 2) for flow over plate with a laminar boundary layer and turbulent boundary layer, based on an empirical Equation [1] and Equation [2], respectively.

An analysis of the experimental heat transfer data for supersonic gas flow in the initial portion of the tube, shown in Fig. 12, suggests empirical relations analogous to Equations [1 and 2], but with different constants.

For flow with laminar boundary layer

$$Nu = 0.363 \sqrt{Re} \quad [7]$$

and for flow with turbulent boundary layer

$$Nu = 0.047 Re^{0.8} \times Pr^{1/4} \quad [8]$$

These formulas have been verified in many experiments and give grounds for assuming that the conditions of heat transfer

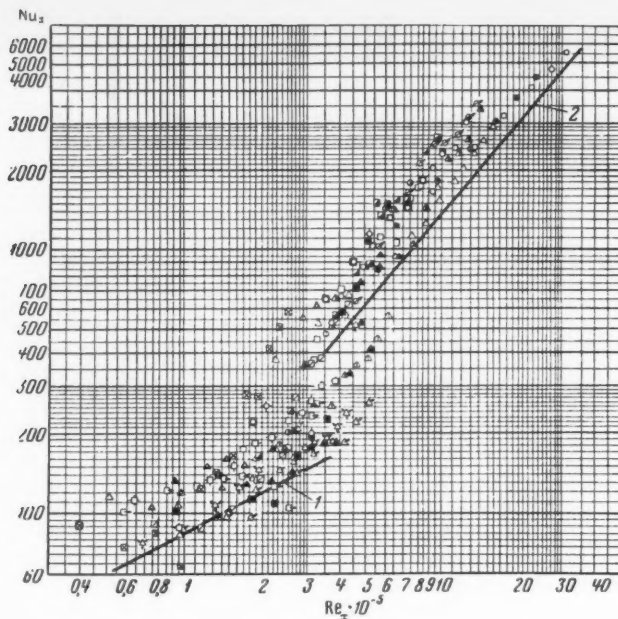


Fig. 12

are sufficiently accurately expressed in the investigated range of variation of the parameters M and T_0/T_1 .

References

- 1 Kalikhman, L. E., *PMM (Appl. Mech. and Math.)*, vol. 10, no. 4, 1946.

- 2 Kaye, J., Keenan, J. and McAdams, B. (Russian translation in "Problems of Rocket Engineering," no. 5, 1951).

- 3 Saunders, D. and Caulder, P. (Russian translation in "Problems of Rocket Engineering," no. 1, 1954).

- 4 Kaye, J., Keenan, J., Brown, G. and Shoulberg, R., *J. Appl. Mech.*, no. 3, 1955.

- 5 Kaye, J. and Brown, G., *J. Appl. Mech.*, no. 3, 1955.

—Original received May 28, 1957

Reviewer's Comments

The subject paper presents measurements of laminar transitional and turbulent heat transfer in a circular cylindrical tube attached to a supersonic nozzle. The results are shown to be in qualitative agreement with well-known flat plate theories. This is consistent with the fact that the boundary layer thicknesses were generally small with respect to the tube radius. Quantitatively, the measured Nusselt numbers were higher than the values given by the cited formulas. Although Mach numbers ranged from about 3.5 to 1.3 along the tube, no correction was made for pressure gradient effects or for the presence of an initial boundary layer due to the feed nozzle.

In addition to the references cited by the author, work along similar lines is described, for example, in the following: Deissler, R. G., "Turbulent Heat Transfer and Friction in Smooth Passages," Sec. E, chap. 1, pp. 288-313 in "Turbulent Flows and Heat Transfer," vol. 5 of "High Speed Aerodynamics and Jet Propulsion," Princeton University Press, 1959; and Eckert, E. R. G., "Introduction to the Transfer of Heat and Mass," McGraw-Hill Book Co., Inc., New York, 1950.

—MARTIN H. BLOOM
Department of Aeronautical Engineering
Polytechnic Institute of Brooklyn

Radio Astronomical Observations of the Second Soviet Space Rocket

V. V. VITKEVICH,
A. D. KUZMIN,
R. L. SOROCHENKO and
V. A. UDALTZOV

1 THE RADIO interference method widely used in radio astronomy (1-4)¹ is used to determine coordinates of discrete sources of radio emission, to examine the inhomogeneity of the ionosphere, to determine the coordinates of the artificial Earth satellites, etc. We have applied this method to observe the radio signals of the second Soviet cosmic rocket which reached the moon on Sept. 14, 1959. The angular coordinates of the container with scientific instruments have been measured, as well as the intensity of the received signal, and the character of the intensity variation in time has been determined.

2 These observations have been conducted on the frequency of the transmitter placed in the container, 183.6 mc. A radio interferometer has been used, similar to the one described already in literature (5); some unessential changes in the instrument have been introduced which are necessary for narrowing the reception bandwidth. It is obvious that if the sensitivity of instruments receiving a noisy signal increases in proportion to the root of the reception bandwidth, then, during the reception of a monochromatic signal, the sensitivity is inversely proportional to the square root of the bandwidth. We have used the transmission band of 10 kc. The first and the second heterodynes have been stabilized by quartz crystals. Near each of the two aerials, in the form of truncated parabolic mirrors (5) of about 200 m² each, have been placed preamplifiers with the noise figure of about 5. The reception has been accomplished by the method of phase modulation. To separate the variations of the signal's amplitude depending on the change of the direction to the source and on the change of intensity of the source itself, a twin radio interferometer has been used, similar to the one described previously (6). The distance between the aerials has been 175.9 m corresponding to the angular width of a single lobe 32 min of arc (in case of the normal incidence of the wave). The aerials have been placed approximately in the direction east-west and were receiving the signal with a horizontal polarization. The tracking of the container by the aerials and the determination of the number of the maximum in the interference diagram (the order of the interference) have been accomplished

according to the target commands received from the coordinate computing center.

3 By means of the radio interferometer we measure directly the angle β between the direction to the source of the signal and the normal to the base of the radio interferometer. The quantity β is determined from the order of interference n and the parameters of the interferometer using equation

$$\sin \beta = (\lambda/D)(n - \eta) \quad [1]$$

where

λ = wave length of the received signal

D = base of the interferometer

η = parameter determined by the difference of the electrical paths from each of the aerials to the point at which signals are added

When the electrical lengths are equal, η is equal to zero. The azimuth of the source A is connected with the angle β by the equation

$$\sin \beta = \sin \gamma \cos z + \cos \gamma \sin z \sin (A - \theta) \quad [2]$$

where

z = zenith angle of the source

γ = 2°44', angle between horizontal plane and base projection on vertical plane passing in direction east-west

θ = -14', angle between line east-west and projection of base on horizontal plane

Then

$$A = \theta + \arcsin \left[\frac{1}{\cos \gamma \sin z} \frac{\lambda}{D} (n - \eta) - \tan \gamma \cot z \right] \quad [3]$$

From five parameters (γ , θ , D , λ and η) entering Equation [3], one parameter γ is determined by the frequency of radiation corrected for the Doppler effect. Three others, λ , θ and D , which are constant, have been determined by a geodetical survey of the mutual position of the aerials and defined more exactly by adjusting. The parameter η , depending on the electrical lengths of cables and on phase characteristics of the input stages, can vary in time and

Translated from Doklady Akademii Nauk SSSR (Proceedings, USSR Acad. Sci.), vol. 132, no. 1, May 1960, pp. 85-88. Translated by Alexander G. Godlevsky.

¹ Numbers in parentheses indicate References at end of paper.

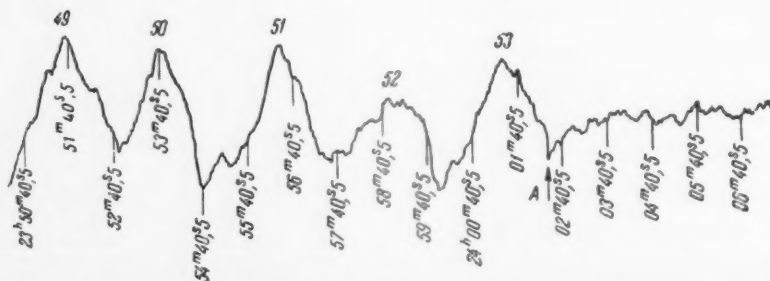


Fig. 1 Interference recording of the signal during the container's approach to the moon. A, the moment the signal stopped

Table 1

Source	$P_{183.6}$ watt · m ⁻² · cps ⁻¹	$\alpha_{1959.5}$	$\delta_{1959.5}$
Cygnus-A	70×10^{-24}	19 ^h 58 ^m 05 ^s	+40°36'.5
Taurus-A	18×10^{-24}	5 ^h 32 ^m 09 ^s	+21°59'
Virgo-A	9×10^{-24}	12 ^h 28 ^m 47 ^s	+12°34'

therefore had to be determined before each observation.

The adjustment of the radio interferometer was carried out using intense cosmic radio sources Cygnus-A, Taurus-A and Virgo-A whose accepted equatorial coordinates (epoch 1959.5) and flux of radiation P are shown in Table 1.

4 Reliable reception of the signal during the approach to the moon prior to impact has allowed the determination of the time of the impact with the moon's surface as well as the determination of the region of landing of the container with scientific instruments. A reproduction of the interference recording of the signal in the final section of the trajectory in one of the receiver channels is shown in Fig. 1. The moment the signal stopped, the sinusoidal character of the recording due to the interference changed into an exponential fall caused by the stopping of the signal and the presence of the time constant. This transition is clearly seen (Fig. 1, point A) and determines the time of the stopping of the signal as 0 hr 02 min 22 ± 1 sec (Sept. 14, 1959).

Taking into consideration that the time needed for the signal to reach Earth from the moon is equal to 1.2 sec, this corresponds to the time of the impact of the container with the lunar surface as 0 hr 02 min 21 ± 1 sec.

The stopping time of the signal (0 hr 2 min 22 sec) corresponds to the order of interference $n = 53.43$. For this value the curve A (z, n) computed according to the formula [3] intersects the visible disk of the moon. This line translated into the selenographic coordinates with the consideration of errors in measurements (equal to ±1 min of arc by averaging several readings) is transformed into a region shown in Fig. 2 with dashed lines.

Considering the data received by the automatized measuring complex (8), one should suppose that the landing region of the container with scientific instruments is that shown in Fig. 2 by the double cross hatching. The selenographic coordinates of this region are the following: Latitude +30 deg, longitude -3 deg (Archimedes' Crater).

5 The intensity of the received signal has been determined by comparison with the known radiation of the cosmic source

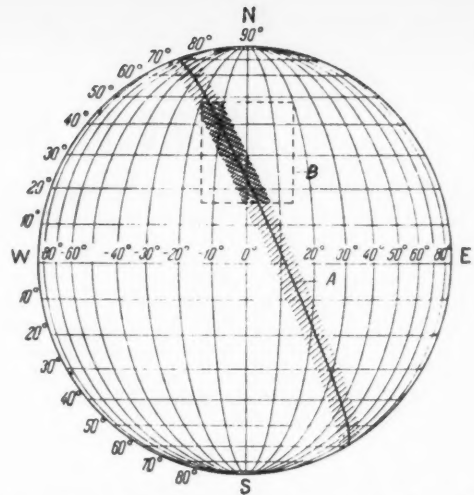


Fig. 2 Landing of the container. The single dashed lines show the data of the interferometer; B, the data of the automatized complex (8); the double cross-hatched lines, the region of the landing of the container. Selenographic coordinates

Cygnus-A. The time dependence of the variation of the signal reduced to an isotropic emitter at the distance of the container is shown in Fig. 3. Several characteristic periods of change in the intensity of the signal have been observed: A small one about 45 sec and a large one of 45 min on Sept. 12, 1959, and of 10-13 min on Sept. 13, 1959.

The existence of deep fading of the signal may be due to the periodical change of orientation of the container and the Faraday effect in the ionosphere.

—Original received October 2, 1959

References

- 1 Vitkevich, V. V., *J. Astron.*, vol. 29, no. 4, 1952, p. 450.
- 2 *Nature*, vol. 180, no. 4592, 1957, p. 879.
- 3 Vitkevich, V. V., *Radio Engineering and Electronics*, vol. 3, no. 4, 1958, p. 478.
- 4 Vitkevich, V. V. and Kokurin, Y. L., *Radio Engineering and Electronics*, vol. 2, no. 7, 1957, p. 826.
- 5 Vitkevich, V. V., *Proc. Fifth Conf. on Problems of Cosmogony*, edited by USSR Acad. Sci., 1956, p. 14.
- 6 Vitkevich, V. V., *Doklady Akad. Nauk SSSR*, vol. 86, no. 1, 1952, p. 39.
- 7 Vitkevich, V. V. and Kokurin, Y. L., *Radio Engineering and Electronics*, vol. 3, no. 2, 1958, p. 1373.
- 8 TASS Information, *Pravda*, Sept. 21, 1959

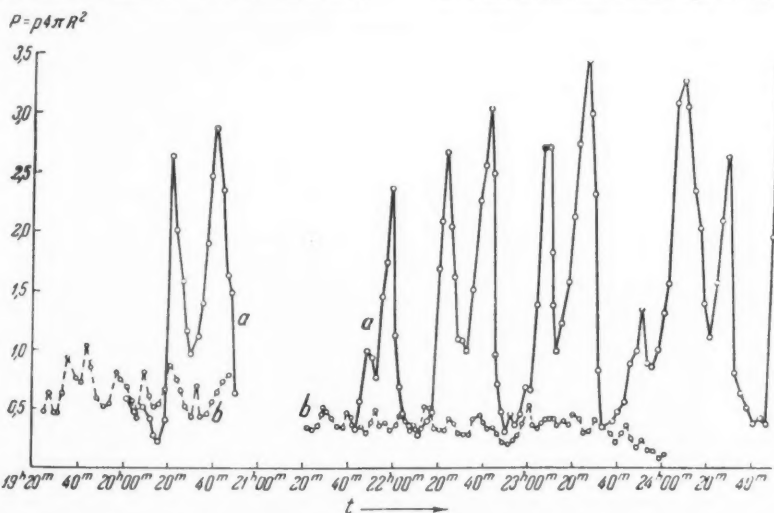


Fig. 3 Temporal run of the variation of the signal corrected for the distance effect. a: Sept. 12-13, 1959; b: Sept. 13-14, 1959

Failure of Metals Due to Thermal Fatigue

YU. V. KOSTOCHKIN
and I. A. ODING

Repeated heating and cooling of a machine part or a metallic sample produces a network of tiny fissures on the surface of the sample and reduces its strength. The rate of fissure formation and the decrease of strength under conditions of thermal fatigue depend on the properties of the metal, the shape and size of the part, and very significantly on heat transfer. In experimental studies of thermal fatigue it is therefore desirable to hold the test conditions as close to the operating ones as possible.

In most previous studies (1-3)¹ experiments were conducted on the conventional cylindrical or prismatic samples. These were heated either in a furnace or by electrical currents, and cooled by a blast of cold air or by immersion in water. The number of heating and cooling cycles generally exceeded those possible in actual operation. Under such conditions the sample developed easily recognizable surface flaws which decreased both the strength and the ductility.

In actual operation parts experience milder temperature changes, which lead to microfissures that are difficult to detect, and more frequently an increase in distance between grain boundaries near the surface. These can be considered as incipient fissures (4). When this occurs one is faced with an evaluation of the likely failure of the part in order to ascertain its further usefulness.

The effect of cyclic heating and cooling on the strength of the EI-765 nickel-chrome alloy and EI-612 austenitic steel used in the manufacture of gas-turbine blades was investigated at the Central Institute of Technology and Machine Building.

NORMAL cylindrical specimens and specimens used in tests for impact viscosity were heated in a special installation (5) in a stream of hot gas (750 deg) and cooled with 70-deg air to simulate the thermal operating conditions of a gas-turbine blade. The specimens withstood up to 6000

Translated from *Izvestiya Akademii Nauk SSSR, Otd. Tekh. Nauk, Metallurgiya i Toplivo* (Bull. USSR Acad Sci., Div. Tech. Sci., Metallurgy and Fuel), no. 1, 1960, pp. 101-104. Translated by J. George Adashko.

¹ Numbers in parentheses indicate References at end of paper.

thermal cycles, but neither macroanalysis nor microanalysis disclosed visible fissures. After withstanding varying numbers of temperature change cycles, the specimens were tested for failure with an IN-4R testing machine and with a drop hammer. The results of the tests are listed in Tables 1, 2, 3 and 4.

It is seen from the tables that under the thermal conditions used in the tests and the number of cycles employed, taking into account the great spread in the tests results (which in general is typical of thermal fatigue), the mechanical proper-

Table 1 Results of short term rupture tests
(alloy EI-765)

Brand of sample	Number of cycles 750-70-750 deg	Test temperature, deg C	Mechanical properties			
			$\sigma_{0.2}$, kg/mm ²	σ_s , kg/mm ²	δ , %	ψ , %
5	0	20	71.6	115.5	29.3	41.8
8	0	20	72.3	116.3	31.0	41.2
E8	800	20	74.7	117.8	22.0	33.0
3	1382	20	73.1	117.0	25.7	30.6
4	2043	20	87.5	126.8	26.0	27.8
2	3000	20	84.9	119.3	26.3	33.0
1	3500	20	77.1	121.1	27.0	28.2
A3	4500	20	76.7	119.8	—	32.0
E1	6037	20	84.3	—	23.7	33.0
E5	0	750	55.6	81.6	16.7	24.9
E10	0	750	65.8	73.3	16.3	33.0
E11	0	750	64.2	69.4	17.3	38.6
E12	0	750	60.7	67.1	19.3	43.5
E2	800	750	56.6	69.9	10.0	22.0
7	1382	750	67.1	81.6	13.0	22.0
E3	2043	750	65.1	76.8	7.7	24.9
12	3000	750	68.9	81.1	12.3	22.0
10	3500	750	61.4	84.2	12.3	16.0
6	4500	750	72.8	86.5	9.3	16.0
9	6037	750	71.2	81.9	8.3	16.0
11	6400	750	73.7	84.2	7.3	12.9

Table 2 Results of impact viscosity tests
(alloy EI-765)

Brand of sample	Number of cycles 750-70-750 deg	Test temperature, deg C	a_k , kg-m/cm ²
E29	0	20	7.8
E19	0	20	7.7
E9	800	20	7.7
E17	1382	20	6.8
E4	3411	20	6.5
E20	4500	20	6.1
E27	6037	20	5.5
E22	0	750	9.1
E23	0	750	9.1
E21	800	700	8.9
E16	1382	750	8.1
E28	2043	750	8.4
E2	3000	750	7.9
E14	3411	750	7.5
E7	4500	750	6.6
E13	6037	750	5.6
E24	6400	750	5.1

Table 3 Results of short term rupture tests
(steel EI-612)

Brand of sample	Number of cycles 750-70-750 deg	Test temperature, deg C	Mechanical properties			
			$\sigma_{0.2}$, kg/mm ²	σ_b , kg/mm ²	δ , %	ψ , %
I5	0	20	50.4	82.4	24.3	48.6
I4	0	20	45.9	79.4	26.3	45.9
I11	1503	20	50.0	82.0	23.7	43.5
I30	3091	20	54.4	83.7	21.3	38.6
I3	3987	20	57.7	86.7	25.0	33.0
I29	0	650	43.2	63.2	20.3	33.0
I24	0	650	39.6	56.5	20.0	30.6
I18	1503	650	35.1	53.3	20.0	30.6
I7	3091	650	48.2	62.0	16.3	30.6
I8	3987	650	35.8	53.7	20.0	30.6
I26	5250	650	44.1	61.2	12.0	30.0

Table 4 Results of impact viscosity tests
(steel EI-612)

Brand of sample	Number of cycles 750-70-750 deg	Test temperature deg C	a_k , kg-m/cm ²
I12	0	20	14.4
I15	0	20	15.1
I17	1503	20	14.3
I2	3091	20	13.5
I27	3987	20	13.8
I26	5250	20	11.9
I18	0	650	12.7
I3	0	650	12.2
I4	1503	650	11.7
I22	3091	650	10.0
I5	3987	650	11.3
I13	5250	650	11.7

ties of the specimen remain almost constant, except for a slight reduction in ductility. Consequently, from the results of such experiments it is difficult to judge of the tendency of a metal that has withstood a definite number of heat cycles to failure.

Consequently, in subsequent experiments the specimens used were in the form of active gas-turbine blades, alternately exposed to blasts of hot gas and cold air. The construction of the experimental apparatus, the shape of the specimens and the test procedure have been described previously (5).

Blades that withstood a different number of heating and cooling cycles were tested for long term strength. Fig. 1 shows the time required for failure vs. the number of heat cycles. It is seen from this figure that as the number of temperature change cycles increases, the long term strength—time required for failure—decreases, and as the number of cycles increases the decrease in time required for failure slows down. In addition, the greater the tensile stress, i.e., the shorter the time before failure, the less intense is the reduction in long term strength. Obviously, such short duration tests approach conditions of short time tensile tests, at which a slight change in the strength is already observed.

The macro- and microstructural analysis of the point of blade failure has shown that fracture occurs not immediately, but develops gradually, approximately in the middle of the section, in the form of a fissure perpendicular to the blade axis. The development of the fissure follows the grain boundaries. Final rupture occurs when the supporting section is reduced to approximately half its size. The fracture plane makes in this case an angle of 45 deg with the horizontal; the fracture is produced by a cut across the body of the grain, similar to what takes place usually in tests for short duration rupture. Blades which are not subjected to the heat cycles fail simultaneously over the entire cross section. In this case the specimen fails by rupture between the crystals, which is generally typical of blades damaged when the long term strength is exhausted.

The low sensitivity of short term strength characteristics to thermal fatigue is explained by the fact that under such thermal conditions and for these numbers of heating and cooling cycles, the microscopic damage produced in the specimen can exert a substantial effect on the mechanical properties, which are determined for a rather rapid application of the load. When testing for long term strength, a long exposure of the specimen to load at high temperature favors the development of microscopic damages and micro cracks, which reduce sharply the long term strength.

Figs. 2 and 3 show the primary long term strength curves. It is seen that the greater the number of heat cycles that the blade has withstood the more rapid is the increase in the strain and the greater is the final strain preceding the rupture. Such a behavior of the primary curves is obviously due to the fact

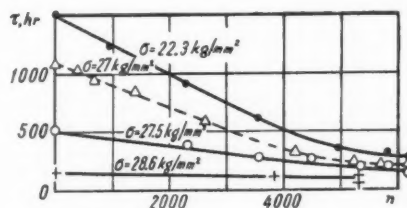


Fig. 1 Results of tests of blades for long term strength: Alloy EI-765, 750 deg (solid lines); steel EI-612, 650 deg (dotted lines); τ = time required for failure; n = number of heat cycles

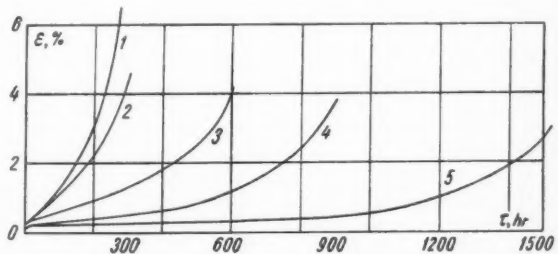


Fig. 2 Initial curves of long term strength of EI-765, tested at 750 deg. $\sigma = 22.3$ kg/mm²

- 1 Blade E16, $\tau = 276$ hr, $\epsilon = 6.45$ per cent, $n = 6200$
- 2 Blade E17, $\tau = 306$ hr, $\epsilon = 4.55$ per cent, $n = 5817$
- 3 Blade E2, $\tau = 605$ hr, $\epsilon = 4.20$ per cent, $n = 3580$
- 4 Blade E1, $\tau = 912$ hr, $\epsilon = 3.95$ per cent, $n = 2315$
- 5 Blade E21, $\tau = 1520$ hr, $\epsilon = 3.00$ per cent, $n = 0$

that the blade failure due to the heat cycles is produced over a smaller cross section (owing to the developing cracks), and consequently under a greater stress. It is known that in ordinary tests for long term strength the first curves rise more steeply with increasing stress, and the final total strain increases.

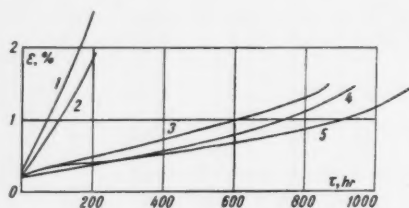


Fig. 3 Initial curves of long term strength of EI-612 steel, tested at 650 deg. $\sigma = 22.3 \text{ kg/mm}^2$

- 1 Blade I5, $\tau = 203 \text{ hr}$, $\epsilon = 2.50 \text{ per cent}$, $n = 6200$
- 2 Blade I1, $\tau = 209 \text{ hr}$, $\epsilon = 1.94 \text{ per cent}$, $n = 5722$
- 3 Blade I14, $\tau = 856 \text{ hr}$, $\epsilon = 1.44 \text{ per cent}$, $n = 1420$
- 4 Blade I15, $\tau = 942 \text{ hr}$, $\epsilon = 1.47 \text{ per cent}$, $n = 710$
- 5 Blade I17, $\tau = 1091 \text{ hr}$, $\epsilon = 1.40 \text{ per cent}$, $n = 0$

Reviewer's Comment

This paper reports the results of experiments pertaining to the behavior of metals under cyclic thermal stresses. The general subject is of wide interest throughout the world's technical literature because of its importance to high temperature equipment. In this country considerable attention has been given to the nature of thermal stress fatigue in metals (1, 2), the behavior of real materials subjected to these conditions (1, 3, 5) and the establishment of design procedures for the prevention of failure by fatigue (6, 7).

More specifically, the present work reports experiments on the effect of thermal stress fatigue on subsequent mechanical properties, an area not widely treated in this country. The reviewer has published information on tension tests subsequent to thermal stress fatigue tests for AISI type 347 stainless steel (1), which show a much greater sensitivity to the prior cyclic straining than reported by Kostochkin and Oding. This is probably due to the geometry of the test specimen. Fatigue damage in the form of micro cracks can be shown to be an important factor in subsequent mechanical strength, particularly when the crack size may be a significant ratio of the specimen thickness, i.e., in thin sheets and tubes, and when a fair fraction of the fatigue life has been consumed.

Of significant technical interest in this paper is the pronounced effect of thermal stress cycling on the subsequent creep and rupture properties of the alloys tested. However, the reviewer is in disagreement with the views of the authors concerning interpretation of the results. It seems more reasonable to assume that modifications in the structure are

Thus, the tendency of thermally fatigued gas-turbine blades to failure must be estimated by testing for long term strength. The experimental conditions must be made here as close as possible to the operating conditions of the real blade. The strength characteristics obtained in short duration tests depend little on the cyclic temperature variations. The results of such tests give a much greater dispersion than tests for long term strength.

References

- 1 Kostochkin, Yu. V., "Structural Strength of Materials Operating at Variable Temperatures," in "Advanced Scientific-Technical and Manufacturing Experience," no. M-58-328/10, published by Branch of Institute for Scientific and Technical Information, 1958.
- 2 Kurganov, G. V. and Sutina, Yu. L., "Failure of Refractory Alloys Under Cyclic Changes in Temperature and Stress," *Metallurgy and Metal Working*, no. 10, 1958.
- 3 Kishkin, S. T. and Klypin, A. A., "Effect of Repeated Heating and Cooling on Change in the Properties of Steels and Alloys," *Ibid.*, no. 5, 1959.
- 4 Chernyavskii, L. L. and Kostochkin, Yu. V., "Setup for Testing Gas-Turbine Blades Under Extreme Temperature Changes," in "Advanced Scientific-Technical and Manufacturing Experience," no. M-58-143/5, published by Institute for Scientific and Technical Information, 1958.
- 5 Oding, I. A. and Kostochkin, Yu. V., "Tests of Turbine Blades in a Gas Stream of Variable Temperature," *Plant Laboratory*, no. 7, 1959.

—Original received October 6, 1959

being produced by the cyclic strain, as for example, overaging as discussed by Hanstock (8) and Forsyth (9). These effects can be very subtle in their effect on subsequent creep properties. Unfortunately no mention is made of the chemical composition of the alloys studied and there is a complete lack of metallography. The behavior shown by the authors should be very specific to the particular alloy and heat treatment employed and caution should be exercised regarding generalizations on the loss of creep strength by cyclic thermal stress.

—LEWIS F. COFFIN, JR.
Metallurgy and Ceramics

General Electric Research Laboratory, Schenectady

- 1 Coffin, L. F., Jr., "A Study of the Effects of Cyclic Thermal Stresses on a Ductile Metal," *Trans. ASME*, vol. 76, 1954, pp. 923-930.
- 2 Manson, S. S., "Behavior of Materials under Conditions of Thermal Stress," *NACA Rep.* 1170, 1954.
- 3 Claus, F. J. and Freeman, J. W., "Thermal Fatigue of Ductile Metals I—Effect of Variations in the Temperature Cycle on the Thermal-Fatigue Life of S-816 and Inconel 550," *NACA TN* 4160, Sept. 1958.
- 4 Majors, H., Jr., "Thermal and Mechanical Fatigue of Nickel and Titanium," Preprint no. 105, American Society for Metals, 1958.
- 5 Swindeman, R. W. and Douglas, D. A., "The Failure of Structural Metals Subjected to Strain Cycling Conditions," Paper 58-A-198, American Society of Mechanical Engineers, 1958.
- 6 Coffin, L. F., Jr., "Design Aspects of High Temperature Fatigue with Particular Reference to Thermal Stresses," *Trans. ASME*, vol. 78, 1956, p. 527.
- 7 Manson, S. S., "Thermal Stress in Design," *Machine Design*, various issues 1959-1960.
- 8 Hanstock, R. F., "Fatigue Phenomena on High Strength Aluminum Alloys," *J. Inst. Metals*, vol. 83, 1954, p. 11.
- 9 Forsyth, P. J. E. and Stubbington, C. A., "The Mechanism of Fatigue in Some Binary and Ternary Aluminum Alloys," *J. Inst. Metals*, vol. 85, 1956-57, p. 339.

Some Problems of Auroral Physics

V. I. KRASOVSKII

THE SPECTRAL analysis is one of the effective means of studying the upper atmosphere. Its use in studying the emission of radiation of the night sky and the aurora borealis has permitted us to discover various microprocesses arising as the result of the photodissociation, ionization and recombination under the influence of hard ultraviolet, x-ray and corpuscular radiation of the sun, as well as numerous macroscopic processes and characteristics of the upper atmosphere, for example the temperature, the nonuniformity of its atomic and allotropic composition, etc.

In the Soviet Union this kind of research has been developed at the Institute of Physics of the Atmosphere of the Academy of Sciences of the USSR, and has increased as a result of the International Geophysical Year thanks to the development of high quality spectrographs, interferometers and fast spectro-electrophotometers. Earlier, the emission of the night sky was recorded in the visible and the nearest infrared parts of the spectrum (from 4000 to 8000 Å) with the dispersion of only several hundreds of angstroms per 1 mm and with resolution of tens of angstroms. To photograph spectra in this region, long exposures lasting one or even several nights were needed, and only a few tens of emission lines could be recorded. At the present time, the domain of this spectral research is widened up to 12,000 Å; in the case of night emissions it became possible to reduce the time of exposure to one hour, or even to a few tens of minutes, guaranteeing resolution of 2 Å with dispersion up to 80 Å/mm. This success has been achieved in considerable degree by the use of photocontact tubes—electronic optical converters in which the fluorescent screen is deposited on a very thin mica window (about 20 μ thick). The photographing is done by pressing the photofilm to the mica on the external side of the converter.

Thanks to this, we have now at our disposal a high quality collection of photographs of spectra of the night sky radiation, containing more than three hundred emission lines instead of the few tens known before. No less rich is the material collected about the spectra of brighter aurorae borealis.

It is impossible to treat even the most basic results of the completed observations in a short article. Therefore, we will limit it to a description of only those conclusions which the recently obtained material permits us to make concerning the energetics of the upper atmosphere, essentially from the spectra of aurorae.

In recent years, one of the essential problems of physics of the upper atmosphere has been that of the sources of its heating and ionization. In order to explain the insignificant content of helium in the Earth's atmosphere, liberated by radioactive disintegration of the Earth's crust long before the examination by rockets, one had to assume a temperature of several thousand degrees in the zone of the dissipation of the atmosphere at a height of 500–800 km. It was also assumed that, beginning with the level of approximately 100 km, the temperature rose by 5 deg per km. As shown by Bates and Chapman, with such a gradient a large flux of heat

is necessarily flowing from the upper parts of the atmosphere toward the 100-km level, where an intensive cooling occurs at the expense of microwave radiation of the atomic oxygen. This flux of heat has been estimated to have the value of $1 \text{ erg/cm}^2 \times \text{sec}^{-1}$.

When with the help of rockets the intensity of the sun's radiant energy in the hard ultraviolet and x-ray parts of the spectrum was actually measured, it became obvious that the energy absorbed in the atmosphere above 200 km was insufficient to explain the necessary flux of heat. The first estimates of the density of the upper atmosphere by the ionization manometers up to the altitude of 200 km agreed with the existence of temperature gradients of 5 deg per km. To avoid difficulties with a large flux of heat from the upper regions, it became popular to consider the atmosphere above the 200-km level as isothermal with the temperature not higher than 900 K. This point of view, however, brought forth serious doubts since it did not correspond to certain observational data.

The heating of the upper atmosphere could, naturally, be explained by the penetration of high speed charged and neutral particles: Electrons, protons, atoms of hydrogen and helium, as the result of the influence of direct and indirect products of the solar activity. Thus, we are discussing the assumption that, at very great altitudes, frequent and long-lasting aurorae exist which cannot be detected visually without special instruments. It was natural to assume such sources of heating for polar regions. For the lower latitude regions these sources seemed to be less probable. We will limit ourselves to the problems directly concerned with the heating of the upper atmosphere.

The first type of auroral spectrum is that common to the night sky with strengthened red forbidden oxygen emission from the state with an average lifetime of 100 sec and an excitation energy of 2 ev. This emission is followed by the weaker forbidden emission of the atomic nitrogen of about 5200 Å from the state with an average lifetime of 26 hr and an excitation energy of 2.4 ev. The intensities of both emissions correlate with each other and also with the magnetic activities. The next type of the auroral spectrum is the one in which, beside the above mentioned emissions, a strengthening is observed of the green forbidden emission of the atomic oxygen from the level with a lifetime of 1 sec and the excitation energy of 4.2 ev, and the emission of neutral and ionized molecules of nitrogen and atoms of nitrogen and oxygen with considerably greater excitation energies—up to 25 ev. And finally, the last type of spectrum is one in which, beside the above mentioned emissions, bands of ionized oxygen molecules appear with a slightly smaller excitation energy of 18 ev.

The foregoing classification of the auroral spectra is most easily explained by the depth of penetration of a certain active agent. The first type of aurora, usually barely noticeable visually, corresponds to the radiation of the very high rarefied layer of the atmosphere of mostly atomic composition, where it is possible for metastable levels to exist longer. The next bright and easily observed visually type of aurora, with a strengthened green oxygen line and numerous emissions of the neutral and ionized nitrogen molecules, is connected with the layer of the atmosphere with

Translated from *Izvestiya Akademii Nauk SSSR* (News of the Acad. Sci. USSR), vol. 30, no. 5, pp. 10–16, 1960. Translated by Alexander G. Godlevsky.

molecular nitrogen. And finally, the last type of aurora, with the emission of the ionized oxygen molecules, is present in the layer where there is molecular oxygen. The lowest limit of auroral lights easily detected by optical means is situated in the layer where oxygen is present in molecular form.

It turns out that the major part of the radiation energy of auroral lights is concentrated not in the bright and sharply defined patterns which occupy an insignificant space, but in the surrounding weak diffused glow which fills enormous surfaces above the Earth and is difficult to observe visually because of the small contrast sensitivity of our eyes in conditions of low illumination. As the result of observations conducted

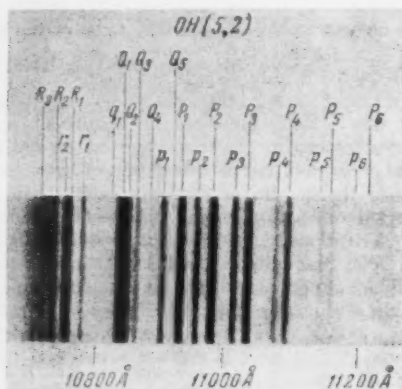


Fig. 1 Photograph of the spectrum of one of the vibration rotation bands of hydroxyl. The distribution of intensities among separate lines of the band permits us to determine temperature of upper atmosphere. Standard symbols of the rotation lines (R, r, Q, q, P, p) are shown at the top

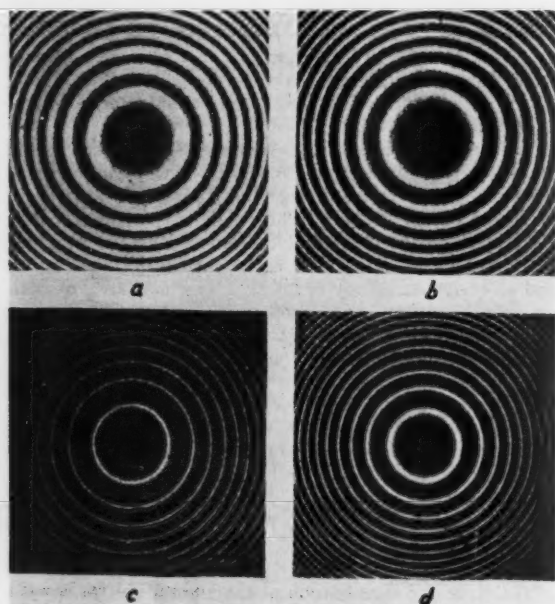


Fig. 2 Photographs of interference pictures from the emissions of auroral lights and krypton made by use of Fabry-Pero standard. The width of the rings characterizes temperature of upper atmosphere. a—red oxygen emission of 6300 Å for the case of very bright lights ($T = 3400$ K). b—weak lights ($T = 1500$ K). d—green oxygen emission of 5577 Å corresponding to strong auroral lights occurring at small altitudes where the temperature is not high (250 K). c—krypton emission of 5870 Å obtained from a laboratory gas discharging source

outside the polar zone—in the regions of lower latitudes—it was found that there also, characteristic spectral types of the radiation of the upper atmosphere at the time of auroral lights could be observed. However, in the great majority of cases, the observed types belong to the high altitude ones. Spectra corresponding to lower altitudes are rare in the lower latitudes. It should be noted that the first type of lights characterized by the stronger red forbidden oxygen emission and the forbidden green nitrogen emission is usual for Moscow, even in the absence of visually detectable auroral lights in the regions of higher latitudes. In the region of Murmansk there very often occurs a weak diffused glow of the whole sky and a strengthened green oxygen emission in which the emission of ionized nitrogen molecules is easily detected.

The obvious conclusion is that either the energy of corpuscles over the regions of lower latitudes is smaller than over the regions of higher latitudes, or that the depth of their penetration is shallower because of the geomagnetic barrier.

It is easy to determine the temperature of the surrounding medium according to the distribution of intensities in the vibration-rotation spectrum of hydroxyl. The sample of such a spectrum obtained by N. N. Shefov is shown in Fig. 1. We have discovered that even at the level of about 100 km where the radiation of the hydroxyl occurs, the temperature rises from about 200 K above Armenia to 350 K above Murmansk. Near Leningrad one can detect the rise of the rotation temperature of the hydroxyl from the emission arriving from the northern side of the sky in comparison with the emission from the south. This difference is still greater above Murmansk. Using the interferometer it is easy to determine the spectral width of the emission lines and, consequently, the temperature of the radiating medium. In Fig. 2 are shown sample photographs of the interference picture in the auroral light emissions, made by T. M. Muliarchik. It has been established that at the time of strong auroral lights, the temperature of the layers where these emissions occur rises by several thousand degrees. The rise in temperature of the upper atmosphere has also been detected above the Moscow region according to the emissions of the ionized nitrogen molecule; the rotation temperature of these emissions at the time of auroral lights sometimes reached several thousand degrees.

As is well known, the radiant formations of auroral lights (see Fig. 3) are of very large dimensions in height—sometimes exceeding 1000 km. It is characteristic that the intensity of ray glow at different altitudes is not subject to any substantial changes. Since the concentration of neutral nitrogen molecules decreases sharply with altitude, the preservation of the intensity of the ray can only be explained by an increase of the streams of the ionizing agent. In initial investigations of auroral lights this phenomenon was explained as collision of rapid electrons with the atmosphere of the Earth. In the last decade, however, after the discovery of the wide lines of hydrogen emission displaced toward the blue part of the spectrum when observed in the magnetic zenith, it became popular to explain this phenomenon by the motion toward the Earth of rapid streams of hydrogen atoms ejected from the sun.

The use of sensitive instruments with a high resolving power permits us to accomplish a regular recording of the wide hydrogen emission. This emission can be recorded with some intensity in almost all types of auroral lights. The hydrogen emission usually covers large parts of the sky and is only slightly connected with the sharpest formations of auroral lights. This emission, as a rule, can be observed several hours before the appearance of strong polar lights, and sometimes it disappears without polar lights appearing at all. Such nonconcentrated luminosity of hydrogen is easily explained by the disturbance of the motion of protons in the proximity of magnetic force lines as a result of their effective recharging with the atomic oxygen. Fig. 4 shows a sample

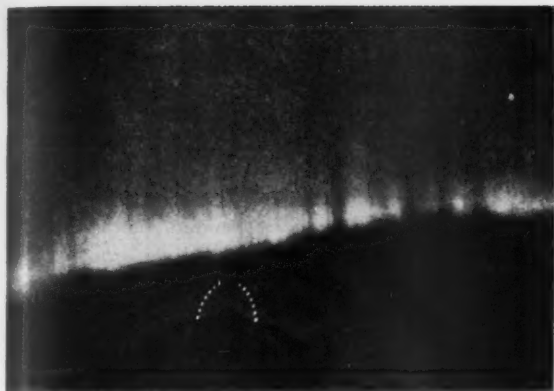


Fig. 3 Photograph of radiant arc of auroral lights. On the left side one sees long rays with a rather constant brightness

hydrogen spectrum and the outline of hydrogen emissions in comparison with the spectrum containing the usual hydrogen emission of atmospheric origin. It is particularly interesting that the maximal intensity of the hydrogen emission in the magnetic zenith corresponds to very low speeds (3000 km/sec) of the incoming hydrogen atoms, which is difficult to reconcile with the retardation of the appearance of the hydrogen emission relative to characteristic formations of the solar activity. The observed outline of the hydrogen emission can be explained only by the dispersion of speeds of corpuscles which cannot be the primary particles ejected from the sun.

Although a wide hydrogen emission of some intensity can be observed in most auroral lights in all stages of development, we find that brightest auroral lights with strong molecular emissions are not followed by such hydrogen emission. As a rule, a wide hydrogen emission is more often observed simultaneously with the spectra of the high altitude type which, however, often do not have this wide emission. It is natural therefore to assume that a considerable part of auroral light is caused by the penetration of the atmosphere by electrons with energies of about 10 kev. This assumption is based on the fact that electrons possessing such energies are able to penetrate to the level of 100–120 km, and just at this altitude auroral lights are observed.

To prove the existence of such electrons in the upper layers of the atmosphere even in the absence of visually observed polar lights, we made use of the third artificial Earth satellite. Special instruments have been developed and constructed which succeeded in recording streams of expected electrons, but with an intensity not supposed previously. Most of the time the instruments were overloaded. In cases where data were received from two indicators, one could estimate the equivalent energy of electrons by the ratio of the intensity of the indicators' signals. The value of such equivalent energy proved to be about 10 kev. If at the time when saturation occurred the electrons possessed the same energy, the total energy of the streams of electrons would attain thousands of $\text{erg/cm}^2 \times \text{sec}$. The direction of motion of the majority of energetic electrons formed an angle exceeding 50 deg with the

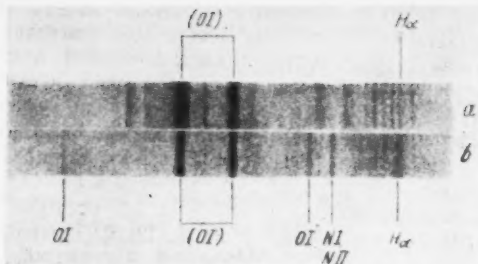


Fig. 4 Photograph of spectra of night sky glow in magnetic zenith in red part of spectrum. Exposure during time of auroral lights was considerably smaller than during time of their absence. Therefore there are no hydroxyl bands in auroral light spectrum. In radiation of night sky, there exists a narrow hydrogen emission line $H\alpha$; in auroral light radiation it is wider and its center is displaced to blue part of spectrum by 6 Å. a—glow of the night sky; b—auroral lights

magnetic force line. Because of the magnetic barrier, these electrons cannot penetrate into the lower part of the atmosphere. Only a few energetic electrons move into ionospheric layers at an angle smaller than 50 deg to the magnetic force line. The stream of energy carried by these equals about $1 \text{ erg/cm}^2 \times \text{sec}$, and it is sufficient to assure the temperature gradient of 5 deg per km.

Thus, it has been found that at high altitudes, especially in high latitude regions, there is a higher concentration of electrons with an energy of about 10 kev which cannot be primary solar corpuscles. At the time of auroral lights and geomagnetic perturbations, the zone with energetic electrons moves down. Because of the heating, the upper atmosphere, especially in high latitude regions, is more extended and has more contact with rapid electrons. Because of the small density, the higher layers of the atmosphere heat considerably faster and use much less energy than the lower ones. Now, the retardation of the artificial Earth satellites permits us to establish the higher density and, consequently, the higher temperature of the atmosphere at the altitude above 200 km, particularly above the high latitude regions.

Protons and electrons which cause the phenomenon of auroral lights, as well as the heating of the upper layer of the atmosphere, have velocities which do not correspond with the delay of the onset of characteristic active formations on the sun. Therefore, such protons and electrons cannot be primary particles ejected from the sun. They are the result of a complex interaction between clouds of ionized gas ejected from the sun and the ionized gas held by the geomagnetic field. Although at the present time very interesting peculiarities have been discovered in the spectra of polar lights, and rapid active particles have been recorded directly in the outer atmosphere of the Earth, further systematic observations of all described phenomena are nevertheless very necessary. Then it will be possible to find out to what degree they are constant during the cycle of solar activity. Therefore, the continuation of the research begun during the International Geophysical Year is of great scientific and practical interest.

Digest of Translated Russian Literature

The following abstracts have been selected by the Editor from translated Russian journals supplied by the indicated societies and organizations, whose cooperation is gratefully acknowledged. Information concerning subscriptions to these publications may be obtained from these societies and organizations. Note: Volumes and numbers given are those of the English translations, not of the original Russian.

ASTRONOMICAL JOURNAL (*Astronomicheskii Zhurnal*). Published by American Institute of Physics, New York.

Vol. 4, no. 1, July-Aug. 1960.

The Scattering of Light in a Medium With a Moving Boundary, by S. A. Kaplan, I. A. Klimishin and V. N. Sivers, pp. 7-12.

Abstract: In order to study the interaction between gas motion and radiation by the methods of the modern theory of light scattering, it is necessary to solve the problem of light scattering in a medium with a moving boundary. The calculation of the probability of escape of a quantum from the medium after scattering is reduced to the solution of integral Equations [6 and 15] (if the quantum is in the absorbed state for most of the time), or Equation [18] (if the quantum is in the free state for most of the time). The solution of these equations is given by formulas [11-14] in the case of [6], [16] in the case of [15], and [20-21] in the case of [18]. The theory of light scattering as applied to the study of the interaction between gas motion and radiation will be given in future papers.

The Origin of Cometary Nebulae, by É. A. Dibai, pp. 13-18.

Abstract: From a review of available observational data, it can be concluded that cometary nebulae obey the following statistical regularities: 1) The nuclei of cometary nebulae are, in many cases, *T* Tauri type variable stars; 2) cometary nebulae are often associated with emission nebulae; 3) in the latter case, the tip of the cometary nebula is directed, as a rule, toward the hot star exciting the emission nebula.

The last two circumstances lead to the idea of a possible analogy between cometary nebulae and structural details observed in diffuse nebulae—"bays" or "elephant trunks"—dense, dark objects located on the boundary of regions of ionized and neutral hydrogen. The "trunks" are often outlined by bright luminous rims. A typical example of a "trunk" is the Horsehead nebula in the constellation Orion.

As is known, the appearance of such structures on the boundary of ionized and neutral hydrogen is a result of the encounter of a moving front of ionization with some condensations in the nebula. The ionized front, moving in the neutral gas, is retarded by the density fluctuations, and flows around them; the result of such an interaction is cone-shaped "trunks" with vertices pointing toward the star which is the source of ionization.

The denser neutral gas, which retards the movement of the ionized front, is subjected to inevitable compression, and it is easily seen that this compression will be maximum in that part which is directed toward the exciting star. The progressive increase in density can, apparently, in favorable cases, promote the process of formation of a star from diffuse matter. The developing star begins to illuminate the cone-shaped cloud surrounding it; the dark "trunk" becomes a bright cometary nebula.

The Solar Supercorona From the Observations of 1951-1958, by V. V. Vitkevich, pp. 31-39.

Abstract: The observations of the solar supercorona, made at the Crimean station of the Institute of Physics, USSR Academy of Sciences, are summarized. These observations were made on different wave lengths and with different interferometer base lines during 1951-1958. The average properties of the supercorona at the minimum phase of solar activity have been found. During the period of maximum solar activity, the electron density of nonuniformities increases, on the average, by a

factor of 2. An increase of the electron density is observed for the outer, as well as the inner, regions of the supercorona. The lower limit to the velocity of the plasma ejected from the sun during the period of maximum solar activity, and reaching the outer regions of the supercorona, is 1 km per sec.

The Structure of the Sun, by A. G. Masevich and T. G. Volkonskaya, pp. 40-48.

Introduction: The "Strela" computer at Moscow University was used to compute a new model of the sun. The model consists of three parts differing in chemical composition: 1) An outer shell without energy sources. The mean molecular weight μ of this layer is, at the same time, the initial chemical composition of the entire model. 2) An intermediate layer in which energy release is due to the proton reaction. The energy contribution attributed to reactions of the carbon-nitrogen cycle is negligible. 3) A central nucleus in which the energy yield is governed by the proton reaction and reactions of the carbon-nitrogen cycle.

It is suggested that mixing between discrete layers does not occur. No inference is offered in advance as to the state of equilibrium of the three parts of the model. Numerical integration of the model proceeds from the surface into the interior, and tests are made for convective instability at each point.

A Comparison of the Curves of Growth for the Center and the Limb of the Solar Disk, by R. B. Teplitskaya, pp. 49-59.

Abstract: The variation of the equivalent widths of FeI and TiII toward the solar limb is studied by means of the curves of growth. The theoretical curves of growth for the solar center and the limb were computed using two models of the photosphere: Vitense II and Voigt, and de Jager VII. It was found that the first of these two models is in better agreement with observations. A small increase in the turbulence velocity toward the outer layers of the solar atmosphere was detected. The existence of the parity effect in the broadening of spectral lines is confirmed.

The Relation Between the Delay Time of Geomagnetic Disturbances and the Relative Sunspot Number, by O. N. Mitropol'skaya, pp. 60-63.

Abstract: Figs. 1 and 2 of the present study show that the time delay Δt of a disturbance relative to the GMP of the plage depends on the sunspot numbers, rather than on the phase of solar activity. The divergence of the curves in the right part of Fig. 2 is due to the numbers R not being an adequate measure of the level of solar activity for the very minimum of activity (low R). The statistical curves (Fig. 3) are given for different intervals of R , and are based on plages of the periods 1929-1933, 1942-1944 and 1950-1953. The upper curve includes plages for the period April 1950-Dec. 1950; the second, Oct. 1929-Sept. 1930, April 1942-June 1942, June 1951-June 1952; the third, Oct. 1930-Dec. 1931, July 1942-June 1943, July 1952-Sept. 1953; the fourth (bottom), Jan. 1932-Sept. 1933, July 1943-March 1944, Oct. 1953-Dec. 1953. The curve in Fig. 4 was drawn for the interval $15 < R < 90$, and is based on data for Oct. 1929-Dec. 1931, April 1942-June 1943, June 1951-Sept. 1953. Notwithstanding the sharply defined left maximum for the periods 1929-1933 and 1942-1944, the second and third curves of Fig. 3 and the curve of Fig. 4 have almost no noticeable left maximum. This agrees with the interpretation of the statistical curves given in other papers. The scheme was computed for the case when pairs of plages were different ΔL are present on the sun during a long period. At the same time, these curves contradict the hypothesis that there is a cone of avoidance. Fig. 5 is based on Fig. 3, and gives the delay time of a disturbance

Δt as a function of the number R . This figure can serve as a basis for the prediction of M -disturbances.

General Principles for the Realization of a Model of a Black Body at a High Temperature, by G. F. Sitnik, pp. 74-82.

Abstract: A discussion is given of the general principles for the realization of a model of a black body, to be used as a primary standard in the calibration of spectrophotometric measurements in absolute energy units. The various factors which influence the degree of correspondence between the practical model and the perfect black body are discussed. The effect of a nonuniform temperature distribution on the accuracy of the model is considered again. A theoretical treatment has led to a rational scheme for constructing a model of a black body whose radiation is identical with the thermal equilibrium radiation at the given temperature.

Formation of an Ionized Meteor Trail, by V. P. Dokuchaev, pp. 106-109.

Abstract: The distribution of ionized gas in the wake of a meteor trail through the upper layers of the atmosphere is discussed. A solution is found for the diffusion equation in the presence of an ion source traveling at constant velocity at a small angle to the horizon. It is shown that the plasma concentration in the vicinity of the moving meteor is appreciably greater than in the remainder of the meteor wake. The conditions under which the trail may be approximated to a cylinder with a Gaussian distribution for the plasma concentration with radius are found.

Radar-Echo Observations of Meteors Using Two Receivers of Different Sensitivity, by L. A. Katasev, V. N. Korpusov and A. D. Orlyanskii, pp. 110-113.

Abstract: Results are given of a study of the S parameter of the distribution of meteoric bodies with respect to mass for the 1959 Quadrantid shower. It is shown that S did not remain constant, but varied with time, and reached a peak value of 2.96 at about 5^h-7^h UT on Jan. 4, 1959. A derivation of a formula for determining the diffusion coefficient D on the basis of radar-echo observations of meteors, using two receiving sets of unequal sensitivity, is given.

The Night Airglow Infrared Emission Spectrum to 3.4 μ , by V. I. Moroz, pp. 118-124.

Abstract: An infrared spectrometer with a PbS photoconductive cell was used to record the night airglow emission spectrum in the broad spectral interval from 1.2 to 3.4 μ . In the 1.2-2.0 μ region, the results were found to be in excellent agreement with the findings of Gush, Jones and Harrison. The region $\lambda > 2.0 \mu$ was studied for the first time. No intense emission bands of any kind were found in the 2.1-2.5 μ region, which is comparatively free from tropospheric absorption lines. A weak maximum near 2.1-2.2 μ was identified with the 9-7 OH band at $\lambda 2.145 \mu$. The thermal emission spectrum of the troposphere was recorded in the 2.6-3.4 μ region. Near 3.2 μ , a clearly delineated band structure was observed, and was identified with the inverted absorption spectrum of water vapor in the troposphere. Absolute intensities were found for the 8-5, 3-1, 4-2, 5-3 and 9-7 bands of OH, and were compared to theoretical predictions. The intensity ratios of bands having common upper levels, obtained by drawing upon observational data reported by other authors, show better agreement with the Einstein coefficients computed by Shklovskii than with the second approximation of Heaps and Herzberg. The intensities of the bands which were not studied (3-2, 4-3, 5-4 and 9-8) were calculated, and the possibility of studying the band sequence $\Delta V = 1$ is discussed.

Determination of Earth's Albedo, by É. K. Dzhasybekova, V. M. Kazachevskii and A. V. Kharitonov, pp. 125-128.

Abstract: The article contains a short exposition of the principle applied in determining the albedo of Earth by observations of the Earthlight on the moon, with a brief description of the instrumentation and procedure used in the observations. Results and description of laboratory studies of the instrument are also given.

Albedo values of 17 dates are tabulated, with the geographic position of the moon indicated for each date.

The mean value for the albedo was found to be 0.391 ± 0.014 . An accompanying table gives all known determinations of Earth's albedo.

The Diurnal Sunlit Component of F2 Layer Ionization During the First Half of the Day, by A. I. Likhachev, pp. 129-133.

Abstract: Results are given of research on the diurnal variation of ionization in the F2 ionospheric layer during the first half of the day. It is shown that the variation of the diurnal sunlit component over a year's time correlates excellently with the sine of the sun's zenith angle. The annual amplitudes of the diurnal sunlit component are correctly determined by the mean annual values of sunspot numbers. During the summer months, ionization in the F2 layer reaches saturation at the latitude of Tomsk.

Introduction of the parameter $f^\circ F2 \sim$ for the F2 ionization layer makes for a rather accurate prognosis of the state of ionization over a protracted period.

Long Focus Cameras for Determining Coordinates of Faint Artificial Earth Satellites, by M. K. Abele, pp. 134-139.

Abstract: The use of long focus cameras of low aperture for photographic tracking of Earth satellites is discussed. Two ways of increasing the limiting stellar magnitude, using special plate holders with moving plates, are described. A cam, dimensioned to specifications, is rotated by a synchronous motor to move the plate in the first method. Instants of time are recorded on a chronograph. The second method utilizes sinusoidal oscillations of the plate, excited by a special electromagnet. Moments of time are recorded by an electronic oscillograph. Photographs obtained by both techniques are reproduced, and an evaluation of the precision of the techniques is made.

An Oscillographic Apparatus for the Reception of Time Signals, by M. A. Ishchenko, Yu. P. Platomov and V. B. Sukhov, pp. 150-153.

Abstract: A brief description is given of a device for the reception of second-pulses and rhythmic time signals, using an oscillograph with continuous circular scanning. The latter is convenient for reading off the position of the radio signal. The change in the rate of scanning in transferring from the reception of second-pulses to the reception of rhythmic signals is made with the aid of a gear reducer connecting the selsyn motor (which controls the uniform scanning) to the deflecting system. The error involved in the reception of time signals with the aid of this device can be reduced to 0.3 to 0.6 msec.

The Application of Geodetic Principles to Practical Astronomy, by A. V. Butkevich, pp. 154-165.

Abstract: The possibility of carrying over the principles and techniques of geodesy to practical astronomy is demonstrated as an example of the effectiveness achievable in relating two adjacent disciplines. This possibility is fraught with great practical and methodological significance. Three questions are taken up: 1) Application of Legendre's theorem for computing azimuth and latitude from observations of Polaris; 2) use of the principle of the general arithmetic mean for computing and estimating the precision of chronometer corrections; and 3) computing and evaluating scale values of ocular-micrometer-screw turns from the adjustment of directions and angles.

Choice of Celestial Body for Compass Error Determinations in the Case of Dead Reckoning Errors, by N. N. Ezhov, pp. 166-173.

Abstract: This paper discusses the effect of dead reckoning errors on the accuracy of calculations of the compass course to be made good by a ship (airplane or any other locomotive object carrying a compass on board as course indicator), from point of departure to point of arrival, for which a formula [6] is derived, giving the relation between the error in compass correction and the extent of the dead reckoning error.

It is shown that, in the presence of unavoidable errors in dead reckoning, the term "compass correction error" generally used in marine navigation for solving the problem of calculating compass course, does not correspond to reality, since this quantity is not an error in the sense indicated, but an indispensable quantity.

From an analysis of formula [6], the author reaches the conclusion that determination of compass correction as a course correction necessitates selecting some heavenly body whose zenith angle is equal to the length of the ship's track on this course; the required heavenly body must be found at the zenith of the point of arrival. This choice of heavenly body simplified the task of determining the necessary course, reducing it to one of taking the compass bearing of the heavenly body.

The choice of heavenly body is of no consequence when determining compass correction as a bearing correction, in sightings where three bearings are taken, since any quantity arrived at for the compass correction, including an erroneous one,

will in that case be excluded from the results of the round of sightings, after the lines of position are plotted on the chart or on paper. A fix based on two lines of position requires choosing a low altitude heavenly body.

This article refutes the main conclusions arrived at by Marinbakh.

Radio Image of the Moon at 8 mm, by N. A. Amenitskii, R. I. Noskova and A. E. Salomonovich, pp. 177-179.

Abstract: A report of the two-dimensional distribution of radio brightness of the moon in the 8-mm range, obtained using the 22-meter radio telescope of the Physical Institute. A noticeable phase dependence of the radio brightness distribution, lagging the phase variation of the moon by $\sim 30^\circ$, was noted. Limb darkening was also recorded.

AUTOMATION AND REMOTE CONTROL (*Avtomatika i Telemekhanika*). Published by Instrument Society of America, Pittsburgh, Pa.

Vol. 20, no. 10, Oct. 1959.

Evaluating the Quality of Nonlinear Automatic Systems With Random Interference, by E. P. Popov, pp. 1281-1287.

Introduction: The method of statistical linearization and its further development from the aspect of harmonic linearization for self-oscillating systems are the most effective means for an approximate investigation of the dynamics of automatic systems with typical nonlinearities (relay, saturation, insensitivity zone, cubic dependence, etc.). However, the solution of the given problem, as was shown elsewhere, is still in an initial stage of development.

A new application of a combination of the methods of statistical and harmonic linearization to the problem of investigating the influence of random interference on the stability and dynamic properties of nonlinear automatic control systems is given in this article. It is known, for example, that a decrease of the amplification factor of the useful signal under the influence of noise is observed in the presence of saturation nonlinearity. It is evident that if such an amplifier is included in a closed automatic system the latter can substantially change its dynamic properties in relation to the useful signal under the influence of random interference up to the point of possible loss of stability, ultimately. In connection with this, an attempt to develop an approximate theory of the forementioned phenomena is undertaken here, and is illustrated with an example of the calculation of a concrete automatic system.

L. S. Pontryagin Maximum Principle in the Theory of Optimum Systems. I, by L. I. Rozonoer, pp. 1288-1302.

Abstract: Questions are discussed which are associated with the proof and use of the Pontryagin maximum principle in the theory of optimum systems. The work also contains some new results. The problem of optimization for the case of a free right end of a trajectory is examined in the first part of the work. In the second part, the maximum principle is formulated for boundary conditions of a more general type. The connection between the method of dynamic programming and the maximum principle is established in the third part; a method of solving optimization problems in linear discrete systems is given, and a number of considerations concerning the use of the maximum principle in the solution of a definite class of problems associated with the theory of dynamic accuracy of control systems are also discussed.

The Problem of Optimizing Systems Which Contain Essentially Nonlinear Elements, by E. P. Merkulova, pp. 1303-1313.

Abstract: A method is given for finding the optimal weight function of the linear portion of a stationary system which contains an arbitrary number of essentially nonlinear elements. The problem is solved for various methods of connecting the linear portions and the nonlinear elements. The input is a stationary random function of time consisting of signal plus noise. The linearization of the nonlinear elements is carried out by a statistical method.

Optimal Control of an Object With Two Controlling Stimuli, by E. A. Rozenman, pp. 1314-1318.

Abstract: The problem considered is that of the optimal transient response in an object at whose input the product of two independent controlling functions acts, namely, an electric motor controlled by the independent variation of the armature current

and the excitation current. It is shown that the external are combinations of δ -functions.

A Method of Synthesizing Linear Sampled-Data Automatic Control Systems to Accord With Dynamic Criteria, by L. N. Volgin, pp. 1319-1326.

Abstract: A method of synthesizing sampled-data systems is proposed. The transfer function of a system is written as the product of the so-called "minimal polynomial," to which the given portion of the system is reduced, by an artificial portion which is introduced in order to obtain the desired quality. The method presented permits the use of a digital computer for the design of linear sampled-data automatic control systems.

Increasing Telemetering Effectiveness, by N. V. Pozin, pp. 1369-1373.

Abstract: Ways are considered for increasing the effectiveness of information transmission by telemetry on the basis of taking into account such spectral characteristics of the measured parameter as the dependency on frequency of oscillation of the amplitude of the oscillations and the measurement errors.

The paper presents a method of transmission with automatic changeover of the coding system. Estimates are made of the increase in speed of transmission and of the possible decrease in bandwidth.

Summary: The advantages of special measures directed toward increasing telemetry efficiency are defined, certainly, by a number of factors and, in the first instance, by the simplicity of their technological implementations. Together with such well-known methods for fuller use of communications channels as improving the quality of elements and components (stability of filters, generators, etc.), increasing telemetering efficiency on the basis of taking the spectral characteristics of the measured parameter into account allows an additional manifold decrease in bandwidth or increase in teletransmission speed.

To match the information source with the channel in telemetry, it is advantageous to use an automatically changed-over coding system which varies the number of transmitted gradations and the rate of telemetering as functions of the speed of parameter variation.

It is necessary to mention that although the basic types (second and third) of spectral characteristics considered contain decreasing functions of numbers of gradations on frequency, i.e., $N(f)$, nonetheless the difference in characteristic $A(f)$, and also $\Delta(f)$, determines the specific features of the transmissions systems for parameters of each type.

Whether some spectral characteristics of parameters or others are typical cannot be definitely decided today. However, it seems most probable that, in industrial telemetry, the most widespread will be the parameters with characteristics of the fourth type where, with increases in frequency, there are permitted not only increases in the measurement errors, but also decreases in the amplitude of parameters oscillations.

Switching Circuit Operation During Transition Periods, by V. N. Roginskii, pp. 1374-1381.

Abstract: A method is given for disclosing the possible disruptions in switching circuit operation during the periods of operation or release of the individual relays in the circuit, and recommendation are made for avoiding these disruptions.

One Method of Analyzing Complex Switching Circuits, by V. F. D'yachenko, pp. 1382-1390.

Abstract: A method is presented for the analysis of switching circuits which is based on the finding of the intermediate relay windings and executive elements carrying current, and their interconnections, for each state of the circuit's contacts.

Two-terminal, class P and N switching circuits with multi-winding relays and parametric dependencies are considered.

Use of Magnetic Amplifiers in Integrating Circuits, by S. B. Negnevitskii, pp. 1396-1400.

Abstract: Two basic circuits employing magnetic amplifiers as integrators are considered. Approximate expressions are derived for the transfer functions of these amplifiers, both without the amplifier time constant being taken into account, and with it. The disadvantages and advantages of integrating magnetic amplifiers are given.

Summary: Magnetic amplifiers have a host of specific special features, thanks to which integrating MA's have their disadvantages and advantages in comparison with vacuum-tube amplifiers. One of the fundamental disadvantages of integrating

MA's is the decrease in the band of possible integrating frequencies, since an MA has a comparatively large time constant. Moreover, in an integrating amplifier with parallel feedback, the system time constant is decreased by a factor of $(1 + R/R_0)$; this decrease will be significant in cases where an MA is used, since its input impedance R_0 is comparatively small.

The advantages of an integrating MA are the greater reliability of operation, the lower expenditure of energy, the lower influence of the condenser bleeder resistance in the feedback circuit and of the impedance of the isolation circuit, since the comparatively low input impedance of the MA causes a correspondingly low value of impedance in the remaining circuits. In the integrating MA with magnetic feedback, the polarity of the output voltage is not rigidly related to the polarity of the input voltage. In such an amplifier, the input quantity may be applied from a current generator, while an integrating amplifier with parallel feedback is useless in principle in such a case. The input impedance, in comparison with all other schemes, has a comparatively low value and can be easily matched with the transducer's internal impedance. By means of an integrating amplifier with parallel feedback, one can integrate the sum of several signals from different sources without interconnecting them galvanically. The absence of any galvanic connection between amplifier input and output simplifies its use in complicated interconnected circuits.

Vol. 20, no. 11, Nov. 1959.

L. S. Pontryagin's Maximum Principle in Optimal System Theory. II, by L. I. Rozonoër, pp. 1405-1421.

Abstract: Questions are treated which are related to the proofs and applications of Pontryagin's maximum principle in optimal system theory. The work also contains certain new results. The first portion of the work deals with the optimization problem for the case of a trajectory with a free right end. In the second portion, the maximum principle is formulated for a more general type of boundary conditions. The third part establishes the connection between the method of dynamic programming and the maximum principle, provides a method of solving the optimization problem for linear discrete systems, and also presents a number of considerations in the use of the maximum principle for solving a definite class of problems, related to the theory of dynamic accuracy of control systems.

A Multichannel Automatic Optimizer for Solving Variational Problems, by R. I. Stakhovskii, pp. 1435-1445.

Abstract: The block schematic, as well as several functional schematics of the component blocks, are described for an electronic variant of a 12-channel optimizer. Results of testing it as an automatic approximator of a given function of time are provided. A search method is given when "false" extrema of the "ridge" and "saddle" types are present.

Summary:

1 The instrument described may be used for solving by direct methods a broad class of variation problems, both with limitations and without them. The simplest examples were given in the paper.

2 The number of independent variables (12, in our case) can, if necessary, be greatly increased without undue complication of the instrument.

Shift Registers With Logical Feedback and Their Use as Counting and Coding Devices, by A. N. Radchenko and V. I. Filippov, pp. 1467-1473.

Abstract: Methods are considered for increasing the efficiency of counting and coding devices based on shift registers. The distinguishing feature of such devices is that the shift register is closed into a ring, whereby the closing link is a logical circuit, whose state is a function of the code introduced into the register. Methods are presented for constructing logical feedback circuits in order to obtain counting devices or coding devices of arbitrary capacity, and methods of reading out information are also given.

Calculating Function—Generating Shunted Potentiometers for Chebyshev Approximations, by S. G. Kisil'syn and F. L. Litvin, pp. 1474-1483.

Abstract: A method is presented for the calculation of a shunted potentiometer intended to reproduce a nonlinear function. The potentiometer is chosen so as to provide the best (Chebyshev) approximation to the function to be reproduced. The design method presented is extended to potentiometers with

finite and with infinite load impedances. The method presented in the paper is illustrated by a design example.

Vol. 20, no. 12, Dec. 1959.

The Maximum Principle of L. S. Pontryagin in Optimal-System Theory. Part III, by L. I. Rozonoër, pp. 1517-1532.

Abstract: The paper deals with questions related to the proof and employment of L. S. Pontryagin's maximum principle in optimal system theory. Certain new results are also contained in this work. The first part of the work deals with the optimization problem for the case of free trajectory right ends. In the second part, the maximum principle is formulated for a more general type of boundary conditions. In the third part, the connection between the method of dynamic programming and the maximum principle is established, a method of solving the optimization problem in discrete linear systems is given, and a number of considerations are presented concerning the use of the maximum principle for solving a definite class of problems which are related to the theory of dynamic accuracy of control systems.

The Synthesis of Linear Automatic Control Systems With Variable Parameters, by S. V. Mal'chikov, pp. 1543-1549.

Abstract: A method is presented for determining, from the optimal weight function of an entire system and the weight functions of the known links in the system, the optimal weight function of the system's correcting link, which may be placed either on the forward path or in a feedback path. The method presented here allows one to circumvent the difficulties associated with the necessity of solving Volterra integral equations of the first type.

Synthesizing the Elements of Linear Automatic Control Systems, by I. A. Orurk, pp. 1550-1557.

Abstract: A method is proposed for synthesizing the elements of linear automatic control systems. The method is based on the use of time characteristics and relationships obtained from the system's (and links') integral equations with kernels in the form of polynomials, in conjunction with the D-decomposition of parameter space.

The method can be used, in particular, for programming the synthesis problem for computer solution.

Frequency Characteristics of Relay Servo Systems, by Ya. Z. Tsypkin, pp. 1558-1565.

Abstract: A method is presented for constructing exact amplitude-frequency and phase-frequency characteristics of relay servo systems with arbitrary forms of external periodic stimuli. At the base of this method is the concept of the generalized characteristic of a relay system, a particular case of which was used elsewhere for the investigation of periodic modes.

Examples are given which illustrate the method described.

Analysis of Tracking Failure in Automatic Control Systems in the Presence of Fluctuating Noise, by I. A. Bol'shakov, pp. 1566-1576.

Abstract: The failure of tracking in automatic control systems under the action of intense fluctuating noise is investigated by means of the Fokker-Planck equation. The Ritz-Galerkin method is used to solve the boundary problem where, by a failure, we understand an increase of the error in the system above some definite quantity. For a system with a smoothing circuit in the form of an integrator, formulas are found for the probabilities of absence of failures in the system as functions of the system parameters, noise level and time. The results are used in the analysis of the noise stability of the AFC (automatic frequency control) system of a receiver of continuous signals.

The Computation of the Mean Square Error of Processing a Stationary Random Signal by a Linear Automatic Control System, by N. I. Sokolov, pp. 1577-1588.

Abstract: A formula is presented for the approximate computation of a convolution integral (a Duhamel integral) which has a high degree of accuracy for a large integration step.

A method is given for the approximate solution (evaluation) of a double-convolution integral which permits the rapid computation of the magnitude of the mean square error of processing a stationary random signal by an automatic control system.

Summary:

1 The approximate formula for computing a convolution integral has a high degree of accuracy for a large integration step, and permits the transient response of a linear automatic

control system to be determined when an arbitrary function of time, given either analytically or graphically, is impressed on its input.

2 The computation of the mean square error of processing a stationary random signal by a linear automatic control system leads to the solution (evaluation) of some double-convolution integrals.

The approximate formula given here for computing convolution integrals allows this given double convolution integral to be solved with a high degree of accuracy with a small amount of computational work.

Jet Power Effect in Nozzle-Flapper Hydraulic Amplifiers, by I. M. Krassov and B. G. Turbin, pp. 1589-1595.

Abstract: The experimental results are given for an investigation of a hydraulic amplifier of the nozzle-flapper type for various combinations of its parameters. Basic attention was paid to the power interaction of the jet and the flapper. A short description is given of the objects tested, the program, the setup, and the methods of carrying out the tests.

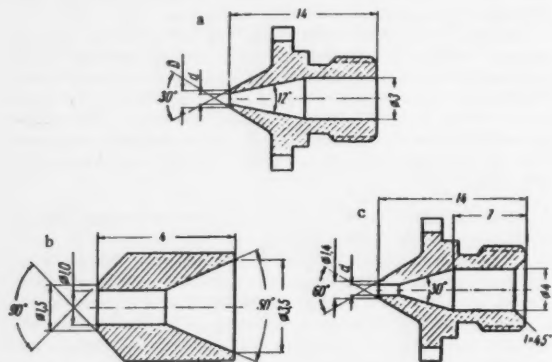


Fig. 1. Types of nozzles investigated.

Magnetic Logical Elements for Automatic Control Circuits, by N. P. Vasil'eva and N. L. Prokhorov, pp. 1601-1610.

Abstract: The functional schematics of basic systems of logical elements based on magnetic cores and semiconducting diodes are considered.

Comparative evaluations of these systems are made.

Determining the Optimal Coefficients of Impulsive Responses, by A. M. Perel'man, pp. 1622-1625.

Abstract: A formula is presented for determining the impulsive response of a system which will be optimal for "white noise."

Summary: The formula presented allows one to determine easily the coefficients γ_i of the impulsive response, optimal for "white noise," which satisfies given forces. This same formula can also be used for solving systems of linear algebraic equations whose numerical coefficients, reading from right to left and from top to bottom, comprise the number series $1/1, 1/2, 1/3, 1/4$, etc.

An Instrument for Determining the Frequency Characteristics of Nonlinear Systems, by K. V. Zakharov and V. K. Svyatodukh, pp. 1630-1637.

Abstract: The theory of operation as well as the device itself are described for a new electronic instrument which permits the forementioned frequency characteristics to be determined with high accuracy in the frequency range $f = 0.25$ to 50 cps, directly in the experimental process.

BULL. ACAD. SCI. USSR, GEOPHYSICS SERIES (Izvestiia Akademii Nauk SSSR, Seriya Geofizicheskaya). Published by American Geophysical Union, Washington, D. C.

No. 11, Nov. 1959.

Magnetoelastic Waves and the Boundary of the Earth's Core, by V. I. Keilis-Borok and A. S. Munin, pp. 1089-1095.

Abstract: The dispersion, damping, polarization and excitation

conditions for plane magnetoelastic waves are investigated. As the field strength H_0 increases, the damping of waves passes a certain maximum and then tends toward zero. Two waves are possible in strong fields: A slow wave, the velocity of which lies between the velocities of longitudinal and transverse elastic waves, and a fast wave, the velocity of which is proportional to H_0 . It is only in the slow wave that there is intensive mechanical vibration. Whether these waves are close to longitudinal or transverse waves is dependent on the orientation of the field in relation to the direction in which the waves are propagated and is practically independent of whether the initial impulse was longitudinal or transverse. The observed distribution for the velocities of seismic waves in the D'' layer can be explained by assuming a linear increase in the gradient k/ρ and a decline in u/ρ compensated by the magnetic field.

Conclusions:

1 The following properties of magnetoelastic waves are those of the greatest interest for seismology: Their velocity and damping increase with increase of ψ up to a definite limit, and more strongly for longitudinal than for transverse waves; for large ψ the waves are divided into two groups (slow and fast) the properties of which are mainly dependent only on the direction of propagation in relation to the field strength.

2 The observed distribution of the velocities of seismic waves in the D'' layer can be explained as being due to increase in the gradient of k/ρ and decline in the gradient of u/ρ compensated by the magnetic field (see the table). The required field strength is 10^6 oerst.

This explanation is more feasible physically than the usual explanation (decline in the gradient of k/ρ). If it is true, there should be marked anisotropy in the propagation of S and P waves in the D'' layer.

3 The absence of transverse waves in the core could be explained by the influence of the magnetic field if there were to be either a layer of increased (up to $\sim 0.4 \times 10^{-3}$ sec) resistivity 20-80 km thick at the surface of the core or a radial field of strength $\sim 10^9$ - 10^{10} oerst.

Both of these figures are extremely high in relation to existing views; it would be interesting to investigate the variation that would be introduced into these figures if electric currents were to be taken into account.

4 Data on the mechanical and magnetic properties of Earth's core and mantle are very closely connected. A definitive description of the mechanical properties of matter at the boundary of the core therefore requires that the magnetic field in this region should be quantitatively described, even if only approximately.

In particular, the influence of the magnetic field should cause marked anisotropy in the propagation of seismic waves.

The existence and nature of this anisotropy can be determined from seismic observations; the task would, however, be extremely laborious in the absence of quantitative data on the magnetic field.

An Apparatus for Recording Inclinations and Accelerations in the Determination of Gravity at Sea, by V. V. Sukhodol'ski, pp. 1114-1119.

Abstract: The construction of the RNVU apparatus is described. This apparatus is for recording the inclination and acceleration of the mounting of a gravimetric device for determining the gravity at sea. The basic data and characteristics of the apparatus are given.

The Diffraction of Electromagnetic Waves by a Sphere Located in a Half-Space, by B. P. D'Yakonov, pp. 1120-1125.

Abstract: The problem is solved of the diffraction of electromagnetic waves at a sphere of arbitrary conductance which is located in a conducting half-space with a plane boundary. The solution is obtained in a form that is applicable to calculations that are relevant to the low frequency method of electric geophysical exploration.

Conclusions:

1 The solution of the problem has been obtained in the form of an infinite system of algebraic equations with a normal determinant.

2 The first approximation obtained for the solution of the system of equations by iteration has a simple form, and shows not only the influence of the homogeneous half-space on the original wave, but also the effect of the interaction of the sphere with the plane separating the two media, i.e., it shows the influence of the reflections of the diffracted waves from the boundary of the half-space on the distribution of the current both in the sphere and in the medium surrounding the sphere.

Remanent Magnetization of Tertiary and Quaternary Volcanic Rocks, by G. A. Pospelova, pp. 1126-1130.

Abstract: The author investigates the remanent magnetization of Tertiary and Quaternary lavas in Armenia, the Kurile Islands and in Kamchatka. It is established that the Quaternary rocks display normal magnetization; the rocks contemporaneous with the Pliocene/Pleistocene boundary, however, reverse magnetization. This agrees with the assumption of inversion of Earth's magnetic field. The pole positions during the time of formation of these rocks are calculated and coincide well with data by other investigators. Based on these results, the age of certain rocks is determined more accurately.

Conclusions: The results presented here allow the following conclusions.

1 The specimens of Upper Quaternary magmatogenic rocks from Armenia, the Kurile Islands and Kamchatka possess a mean magnetization in the direction of the present magnetic field, which confirms the ability of rocks to acquire during formation remanent magnetization directed parallel to the effective local magnetic field. The remanent magnetization allows, therefore, determination of changes in the direction of the geomagnetic field of the past.

2 The presence of reversely magnetized lavas of early Quaternary/Upper Pliocene age among the volcanogenic strata of Armenia and the Kurile Islands is another fact in favor of the hypothesis of a changing geomagnetic field.

3 The geomagnetic pole positions as determined from the remanent magnetization vector of various age rocks agree with the findings of other investigators.

4 Proceeding from the alternation of normally and reversely magnetized rocks, the paleomagnetic method allowed a definite determination of the age of rocks which was doubtful from geological data.

A Nomographic Method for Output Signal Determination in Linear Filtering Systems, by T. B. Kalinina and F. M. Holzmann, pp. 1136-1142.

Abstract: An approximate nomographic method for calculating the convolution integral for discrete values of the given functions is proposed. The calculation error is estimated. Examples of the application of the method to the solution of various physical problems are examined.

Conclusions: These examples are far from exhausting all the problems which can be reduced to the calculation of a convolution integral. Thus, for example, this method of calculation can be used to calculate correlation functions and to determine the output signals of various interference systems in, for example, grouping regulated by directional reception, wave displacement, etc.

It does not usually take more than an hour to determine the signal $F_{out}(t)$ with the working nomogram. Additional calculations are necessary to determine the errors $\Delta F(t)$ and $\Delta h(t)$.

To reduce the calculation time, the errors ΔF and Δh need only be found close to those values of t for which the sharpest variation in the given functions $F(t)$ and $h(t)$ is observed (maxima, break, discontinuity) since it is near these values of t that the errors ΔF and Δh will be the greatest. In the overwhelming majority of cases the values of ΔF and Δh need not be determined since the approximate criteria for the selection of Δt given above are sufficiently rigorous and do not need additional checking.

A considerable economy in time can be effected by using a computer with memory cells. Several versions of this type of apparatus are being developed at the present time in the Laboratory for the Dynamics of Elastic Media at the Leningrad State University. The theoretical foundation for the replacement of the convolution integral by the sums given, and for the estimation of error given above are of use in the design and application of these machines.

An Airborne Technique for Measuring Sizes and Charges of Aerosol Particles, by G.D. Petrov, pp. 1170-1172.

Abstract: A technique used to measure the charges and sizes of individual aerosol particles in the free atmosphere is described. Data obtained in cumulus clouds are presented. The range of applicability of the technique is indicated.

Geomagnetic Effectiveness of Chromospheric Flares From Data of 1957, by O. M. Barsukov, 1186-1188.

Use of Magnetic Modulation Probes for Measuring Magnetization of Rock Samples, by V. N. Mikhailovsky and Yu. I. Spektor, pp. 1195-1198.

Influence of the Coriolis Force on Shore Currents in Narrowing and in Widening Channels, by V. G. Labeish, pp. 1204-1205.

No. 12, Dec. 1959.

The Theory of Linear Transformations of Two-Dimensional Magnetic and Gravitational Fields, by T. B. Kalinina, pp. 1245-1251.

Abstract: The theory of linear transformations of potential fields is studied on the basis of frequency analysis and Fourier synthesis. A method is proposed for estimating the errors arising in connection with the transformation to a discrete method of calculation and also those caused by the accumulation of random errors.

Conclusions: The integral transformation can be replaced by an approximate formula. From the point of view of the frequency, this is equivalent to replacing the characteristic $H(\omega)$ in the spectral equality by the periodic characteristic $H_{per}(\omega) =$

$\sum_{k=-\infty}^{\infty} H(\omega - 2k\omega_0)$. If bounded characteristics $H'(\omega)$ are used to construct characteristics $H'_{per}(\omega)$, this is equivalent to replacing the discrete kernel $\Delta x h(k\Delta x)$ in a given formula by the auxiliary kernel $\Delta x h'(k\Delta x)$. In the latter case the accuracy of the calculation can be substantially increased without changing Δx , or the length of the interval Δx can be increased while retaining the same accuracy.

Methods are proposed for estimating the error arising in the discrete method of calculation, and also for estimating the cumulative error due to random errors in the given original field. It is shown that the effectiveness and accuracy of linear transformations depend essentially on these random errors. In particular the application of analytic continuation in the lower half-plane, and also the calculation of derivatives of higher order, are restricted by the presence of these errors. Analytic expressions are proposed for the kernels of certain linear transformations and the errors involved in the use of these kernels for the transformation of the fields of certain model bodies are investigated.

Marine Measurements With the "GAL" Gravity Meter, by E. I. Popov, pp. 1256-1260.

Abstract: The paper sets out the results of measurements made with marine gravity meters on board a vessel of approximately 6000 tons displacement. It was shown that the mean quadratic errors of the observation points varied within the limits ± 3.5 to ± 14.0 milligals, depending on the amount of acceleration due to wave disturbance.

The Nature of Corpuscular Radiation in the Upper Atmosphere, by I. S. Shklovski, V. I. Krassovsky and Yu. I. Gal'perin, pp. 1261-1265.

Abstract: The analysis of the spatial distribution of "Earth's corona" belts permitted one to make some conclusions on the mechanisms of generation and "leakage" of the hard corpuscles. It was shown that the particle concentration in the solar corpuscular flux is sufficient for the replenishment of corpuscles of the outer belt in a matter of a few hours. A calculation was made of the energy spectrum of the protons and the rate of generation of the hard corpuscles in the inner belt on the basis of neutron star formations with the consideration of their deceleration during diffusion through the atmosphere. It was shown that the record of the hard charged particle products of nuclear explosions within a certain time markedly alters the intensity measurement of the corpuscular radiation in "Earth's corona," particularly in the high energy region.

The Solution of an Equation for the Forecasting of an Atmospheric Pressure Field, by S. V. Nemchinov, pp. 1274-1278.

Abstract: An approximate solution is given for an equation describing variation of the atmospheric pressure field. For this purpose partial derivatives with respect to the ventral coordinate are replaced by finite differences. The resulting system of nonhomogeneous system of partial differential equations in two variables with constant coefficients is set out in canonical form and solved in closed form. The suggested method of solution makes it possible to use in the solution the most general assumptions in regard to the stratification of the atmosphere as well as to allow for the presence of pseudoadiabatic processes in a real atmosphere.

Temperature Gradient in the Upper Layers of Earth and on the Possibility of an Explanation of the Low Velocity Layers, by E. A. Lyubimova, pp. 1300-1301.

The Solution of the Inverse Problem of the Theory of Electromagnetic Soundings, by A. I. Chetaev, pp. 1302-1304.

Introduction: An algorithm is adduced for analytic interpretation of the observation results during electromagnetic soundings in the case of the field generated by a vertical magnetic dipole, similar to the algorithm of Langer-Belluigi for the soundings with a constant current. Thereby, the determination of the geoelectric cross section reduces to the solution of a Cauchy problem for the infinite dynamic system of triangular form.

The Variation Spectrum of the Natural Electromagnetic Field of Earth, by N. P. Vladimirov and N. N. Nikiforova, pp. 1305-1307.

Introduction: In recent years interest on the variable natural electromagnetic field of Earth increased due to the investigations, which showed more prospective use of the variation of this field for geological surveys. The spectral study of the variation of the natural field has not only theoretical but also practical importance.

Principally the low frequency variation of the field with frequencies less than 0.1 cps was studied up to now and used practically. Very little work was done on investigating the distribution with time of the variation with a frequency higher than 1 cps. The first undertakings in this direction, completed in 1940, established the presence of Earth's currents with a period of 0.01-0.03 sec. Field variations of various frequencies in the range from 2 to 300 cps were noted in 1952-1954 with the help of selective amplifiers.

With 1957 according to the program of the International Geophysical Year at the Institute of Physics of the Earth, Acad. Sci. USSR, the study of the natural field variations was carried out on a large scale. For the reception of the signals a station was developed and readied, which permitted the recording of the oscillation in the 0.3-1000 cps range. The results of the investigations, completed with the help of this station in 1957-1958 in the 0.3-100 cps frequency interval, is written up in this article.

The Relative Velocity of the Motion of Solid Particles in a Liquid Flow, by A. E. Smoldyrev, pp. 1313-1316.

Introduction: This article adduces the investigational results for the establishment of a general relationship connecting the relative velocity of motion of the solid particles with the hydraulic characteristics of the flow and the particle.

New Method of Measuring the Height of a Homogeneous Atmosphere, by E. I. Fialko, pp. 1326-1328.

The Analysis of Atmospheric Motions by Means of the Pressure Field, by M. I. Ruzin, pp. 1329-1333.

Introduction: One of the methods of analysis of the atmospheric processes in general and their kinematics in particular is the construction of air particles trajectories. In another paper we obtained from the equations of motion formulas for calculating more precisely the trajectories of air particles in the free atmosphere by means of the pressure field and the ageostrophic deviations of the trajectory δ_{dev} and acceleration δ_{acc} . The effect of turbulence friction was also taken into account. It follows from Ref. (1) that the calculation of δ_{dev} and δ_{acc} should introduce appreciable precision in the computation of trajectories longer than 2-3 days, and from (2) that the calculation of turbulence friction is only necessary in the boundary layer. Thereby, however, the effect of the turbulence friction on the air motion in the region of the surface discontinuity at a front, for whose neglect a priori there is no basis, is not considered.

BULL. ACAD. SCI. USSR, PHYSICAL SERIES
(*Izvestiia Akademii Nauk SSSR., Seriya Fizicheskaya*). Published by Columbia Technical Translations, White Plains, N. Y.

Vol. 23, no. 4, 1959.

Instrument for Measuring the Resolution and Light Yield of Fluorescent Screens (PRS), by B. I. Pochtarev, K. K. Raspletin and D. V. Fetisov, pp. 445-448.

Introduction: We describe an instrument—designated PRS—intended for determining the resolution, measuring the efficiency and investigating the spectral composition of the radiation of fluorescent screens on the unbombarded side with stimulation by

electrons with potentials in the range from 5 to 30 kv. The resolution of the instrument itself exceeds 500 lines per mm.

Conclusions: Use of the PRS equipment for investigating the properties of cathodoluminescing phosphor screens greatly facilitates measurements of their basic parameters, namely, the resolution, brightness, efficiency and spectral characteristics of the luminescence.

In view of its efficient design, the instrument can be used not only for research purposes but for industrial control and inspection of various screens and similar products. To this end the instrument can be equipped with suitable interchangeable disks with special recesses for the samples to be inspected.

X-Ray Shadow Microscope, by G. O. Bagdyk'yants and A. V. Shishatskii, pp. 464-468.

Introduction: In the present article is described an experimental model of an x-ray shadow microscope developed by the authors.

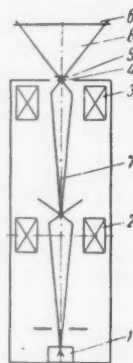


Fig. 1 Diagram of the x-ray shadow microscope. 1—electron source, 2—first demagnifying lens, 3—second demagnifying lens, 4—anticathode, 5—specimen, 6—photographic film, 7—electron beam, 8—x-rays

Cell for Electron Microscopic Study of Objects in a Gaseous Medium, by I. G. Stoyanova, pp. 472-476.

Conclusions: Exhaustive tests of the experimental gas cell and techniques developed by us showed that it is feasible to carry out electron microscopic studies of objects in a gaseous medium with a resolution not inferior to 120 Å at pressures close to atmospheric. The cell can also be used for investigation with the aid of an electron microscope of reactions between a gaseous and a solid phase.

High Voltage Electron Gun, by N. M. Popov, pp. 477-487.

Introduction: This report contains some observations and conclusions regarding the design and construction of an electron gun with an accelerating potential exceeding 100 kv and regarding electron guns with V-type tungsten cathodes in general, arrived at in the process of developing and testing the illuminating system of the 400-kv electron microscope reported on earlier.

Computer for Design Calculation of Fields in Electron-Optical Systems, by G. V. Der-Shvarts and K. A. Netrebenko, pp. 488-491.

Introduction: One of the fundamental problems arising in the design of electron-optical systems is calculation of the electric and magnetic fields. Ordinarily the calculations reduce to numerical solution of the Laplace and Poisson equations for different boundary cases.

It can be shown that for solution of such problems it is expedient to use special purpose calculating equipment combining digital and analog computation principles.

At present we have designed and partially constructed a special purpose computer intended for the calculation of fields possessing rotational symmetry. The salient features of the computer are described.

Vol. 23, no. 5, 1959.

Absorption Coefficient of Soft X-Rays in Beryllium, by D. M. Zhukovskaya and Yu. K. Ioffe, pp. 524-527.

Conclusions:

1 The values of the mass absorption coefficient of beryllium for soft x-rays (2.3-1.5 Å) obtained in the present work differ from those published earlier by a factor of about 1.5.

2 The accuracy of our results is substantiated by the good

agreement of measurements carried out on single crystal and twin crystal spectrometers and with recording by means of Geiger and scintillation counters, by the agreement of the values of μ/ρ for aluminum obtained with our equipment with the values in the literature and by the data of comparative measurements of the absorption of domestic and foreign beryllium.

3 Published data on μ/ρ of beryllium for soft x-rays diverge appreciably; presumably most published data are overestimates due to impurities present in the beryllium specimens. This inference is supported by the fact that there is generally good agreement among the different authors and as regards the present work where the values of μ/ρ for the hardest of the investigated radiations (Mo K α) is concerned.

4 The 0.7–0.8-mm thick beryllium windows of domestic commercial x-ray tubes are equivalent as regards absorption of 5–10 keV x-rays to the 0.4–0.5-mm thick beryllium windows in foreign x-ray tubes.

5 The domestic commercial vacuum grade beryllium has an appreciably higher degree of purity than beryllium produced abroad.

Electron-Optical X-Ray Image Intensifier, by M. M. Butslov, pp. 535–539.

Investigation of the L-Series of Germanium—Influence of Impurities, by G. P. Borovikova and M. I. Korsunskii, pp. 546–550.

Introduction: Transitions of matter into different physical and chemical states are accompanied by certain specific changes in the state of its atomic electrons. These changes must obviously be evinced in the structure of the x-ray spectrum. Of greatest interest are the spectrum lines corresponding to transitions of valence electrons, the energy states of which are subject to the greatest alterations incident to transition of the material from one state to another. In earlier contributions, we reported that in investigating the L emission spectrum of metallic germanium, we detected the $L\beta_6$ and $L\gamma_8$ lines associated with the $L_{II} \rightarrow N_I$ and $L_{II} \rightarrow N_I$ transitions, respectively. It was found that the $L\beta_6$ and $L\gamma_8$ lines are very sensitive to changes in the physical and chemical state of the material. In particular, we noted a substantial change in the appearance of the spectrum as a result of prolonged work with one and the same sample (we studied the spectral regions in the vicinity of the $L\alpha_{1,2}$ and $L\beta_6$ and $L\beta_1$ and $L\gamma_8$ lines). To determine the reason for the change in the spectrum of metallic germanium under the influence of prolonged irradiation incident to fluorescence analysis, we also studied the emission spectrum of germanium dioxide, GeO_2 . Comparison of the spectra showed that the spectrum of metallic Ge changed as though the surface of the sample was gradually oxidized in the process of excitation.

Contribution to the Theory of Diffuse Scattering of X-Rays and Slow Neutrons by Multiple Component Alloys, by V. V. Geichenko, V. M. Danilenko, M. A. Krivoglas, Z. A. Matysina and A. A. Smirnov, pp. 619–622.

Introduction: The purpose of the present work was derivation of equations for the scattering probability of waves in the general case of solid solutions with any number of components, having in the disordered state any type of Bravais lattice, any composition and long range order, and taking into account correlation in the substitutional occupation of regular and interstitial lattice sites by atoms of different types in all coordination spheres.

Theory of Scattering of X-Rays and Thermal Neutrons by Fluctuation Heterogeneities in Solid Solutions, by M. A. Krivoglas and E. A. Tikhonova, pp. 640–643.

Introduction: The aim of the present work is to investigate in the framework of kinematic theory the scattering of monochromatic x-rays and thermal neutrons by single crystal solid solutions. We consider diffuse scattering by the static heterogeneities which are produced, first, by the difference between the atomic scattering factors of atoms of different types and, second, by geometric distortions connected with the difference between atomic radii. We also consider the weakening of regular reflections connected with the difference between atomic radii. In contrast to other studies wherein geometric distortions were correctly taken into account only for weak and ideal solutions, herein we consider the general case of solutions of arbitrary composition with arbitrary values of the long- and short-range order parameters. Calculations have been carried out for binary and multiple component solutions. In considering distortions, we have explicitly taken into account the anisotropy of the

crystal and its atomic structure. This (as well as taking into account departure of the solution from the ideal) enabled us to bring out certain effects which are glossed over in the case of the familiar model of an isotropic continuum.

INDUSTRIAL LABORATORY (Zavodskaya Laboratoriya). Published by Instrument Society of America, Pittsburgh, Pa.

Vol. 25, no. 5, May 1959.

Force Method of Determining Residual Stresses, by D. M. Shur, pp. 614–617.

Introduction: The existing mechanical methods of determining residual stresses of type I are based, as we know, on the principle of the destruction of the geometrical integrity of the test object by some means (by abrading or etching layers from the surface, turning or boring and so on).

The residual stresses are calculated as a function of the measured deformations by using the generalized Hooke's law. Hence, all these methods can be considered as fundamentally a single "deformation" method.

However, the solution to the problem of determining residual stresses may be reached by a totally different approach, which does not require the measurement of deformations and the employment of approximate relationships between stresses and deformations on the basis of Hooke's law.

The method proposed can be called the "force" method; it is based on the following argument. If part of a test object, obtained from the latter by one of the methods mentioned and deformed as a result of removal of the residual stresses, is subjected to an external load which will restore to the separated parts its former geometrical dimensions and shape (i.e., the dimensions and shape it had before separation from the object), then from the magnitude of this load we can determine the magnitude and direction of the internal stresses occurring on the faces or external surfaces of the part of the object before it was removed.

We will consider the application of this method to an investigation of the field of residual tangential stresses arising in the plastic torsion of round cylindrical components.

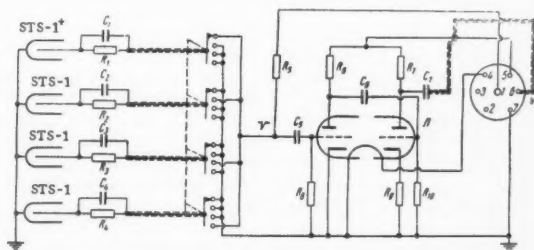
Use of Method of High Temperature Uniform Upsetting for Determining Deformation Resistance, by M. V. Rastegaev, pp. 622–623.

X-Ray Photography at Low Temperatures, by P. N. Aronova, Ya. E. Gegusin and N. N. Ovcharenko, pp. 646–647.

Adaptation of the "TISS" Radiometer for Dosimetry Work With Gamma Radiation, by V. I. Andreev, pp. 650–651.

Introduction: Lately dosimeters of gamma radiation using counter tubes instead of ionization chambers have obtained widespread use, because they are dependable, simple to operate and have high sensitivity.

For work in small laboratories, it is possible to use standard radiometers for dosimetry of gamma radiations. For this purpose, it is only necessary to provide the radiometer with external sensor elements which contain small size counters of gamma radiation. Such an arrangement, designed to be used with the "TISS" radiometer, is described.



Circuit diagram of attachment to "TISS" radiometer. D) 6P9S tube 6AG7; C_1, C_2, C_3 and C_4 10 μ f; C_5 0.01 μ f; C_6 and C_7 0.05 μ f; R_1, R_2, R_3 and R_4 8.2 meg R_5 47 kohm; R_7 30 kohm; R_9 100 kohm; R_8 10 kohm; R_{10} 100 kohm.

Simplification in Design of Radioactivity Alarms, by K. S. Klemppner, V. A. Machkovskii and E. S. Shlyakhovetskii, pp. 651-652.

Introduction: We have eliminated stabilization of the counter tube supply voltage in transducers of radioactivity alarm devices, which have large absorbers ($\mu d > 4$) and time constants of the order of a second for the integrating circuit (such as are being used in alarms of high radioactivity levels). As a result, the construction of these alarms has been simplified.

Direct Determination of the Cooling Capacity of a Medium, by L. B. Medinskii, pp. 657-658.

Introduction: We have developed a method and apparatus for direct determination of cooling capacity of a material in heat treatment, whereby it is made possible to determine the quantity α , in cal per $\text{cm}^2 \times \text{sec} \times \text{deg C}$, in the needed temperature range and at the required travel velocity of the medium.

A Measuring Element for Measuring Vacuum and High Pressures, by B. Z. Votlokhin, p. 662.

Vol. 25, no. 6, June 1959.

Internal Flaw Detection in Opaque Materials, by P. K. Oshchepkov, pp. 716-720.

Determining Grain Orientation by Means of Electron Microscope Photographs of Etching Figures, by V. I. Shalaev and E. S. Yakovleva, pp. 729-730.

Statistical Processing of Static Long Time Tests, by S. V. Serensen and N. A. Borodin, pp. 752-756.

Introduction: For a given time and temperature the ultimate static long-time strength is usually determined from the long-time strength curve plotted from the results obtained in testing 6 to 8 specimens.

However, the test results are affected by the scatter of the strength values caused by deformations and rupture due to the nonuniformity of the metal, and the occasional differences in test conditions.

The effect of this scatter upon the time needed to produce a rupture at a given stress is particularly great (this is also observed in fatigue tests with regard to the number of cycles).

In this connection several investigators suggest that for obtaining sufficiently reliable long-time strength and plasticity characteristics 15 to 20 specimens should be tested at several stress levels and the results obtained processed statistically.

This processing is based on the assumption that the scatter of experimental data obtained in identical conditions obeys a certain law of distribution density of probabilities.

It is the object of this work to analyze the law governing the distribution of durations τ of tests needed to produce a rupture at the given stress, and of the percentage contraction of cross-sectional area ψ_k in the neck of the specimen at the rupture.

Criteria of Linearity of the σ -lg N Curve of Titanium, by E. Reinberg, pp. 761-764.

Introduction: The functional relationship between the amplitude of the stress σ_a and the number of cycles to rupture N is usually represented graphically as a broken straight line in semilogarithmic coordinates.

The sloping section σ -lg N of the curve is usually drawn in such a manner that the experimental points form a straight line. Very often, however, owing to the scatter of the endurance limit values N_1 , the experimental points are far from being a straight line. In such cases the question arises as to whether it is permissible to draw a straight line to represent the σ -lg N function.

An Equipment for Thermal Analysis, by V. V. Pudikov, pp. 778-780.

Introduction: We have developed an equipment for thermal analysis based on the use of the electronic potentiometer EPP-09 which records simultaneously three curves. The standard temperature chart of the instrument is used for recording simultaneously the differential heating curves in coordinates of "time against the temperature difference between sample and the standard" and the simple heating curve in coordinates of "time against temperature." The temperature range is 0 to 1600 C. The schematic of the equipment is shown in Fig. 1.

The equipment consists of a differential thermocouple, an optical amplifier, an electronic potentiometer and a heating device.

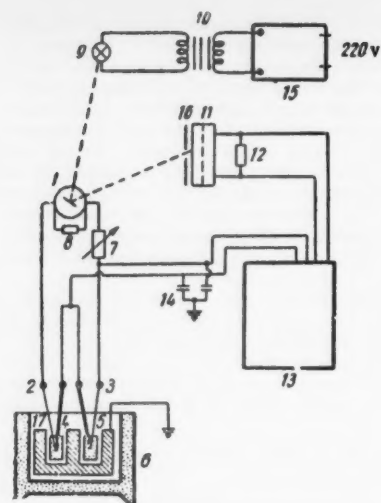


Fig. 1. Schematic of the equipment for thermal analysis: 1) mirror galvanometer M21 $R_{in} = 339$ ohm; 2 and 3) platinum and platinum-rhodium thermocouples; 4) samples; 5) standard; 6) oven; 7) variable resistance (resistance box KMS-4); 8) galvanometer shunt $R = 40$ ohm; 9) illuminator bulb, 26 v, 26 w; 10) transformer 127/24 v; 11) selenium photocell AFI-20; 12) resistance of 1 kilohm 2 w; 13) electronic potentiometer EPP-09 which records 3 curves simultaneously, calibrated to PP; 14) 2 μ f capacitor; 15) voltage stabilizer STN-35; 16) slit diaphragm; 17) steel block.

The Use of an Electronic Potentiometer as a Programming Regulator, by V. B. Shvetsov, pp. 782-783.

An Instrument for Measuring Deformations, by M. G. Shtarkov, pp. 784-785.

Precise Measurement of Deformation on Rotating Devices, by S. B. Stopskii, p. 786.

Apparatus for Measuring Elongation in Samples Subjected Simultaneously to Both Stretching and Torsion, by Yu. I. Yagn and P. A. Pavlov, pp. 789-790.

Much of the apparatus used for measuring longitudinal deformations produced by stretching (such as the Martenson mirror apparatus, the Gugenberg tensiometer, various apparatus for measuring real plastic deformations, the MIL apparatus, etc.) does not give accurate results when the samples are simultaneously subjected to torsion. Errors are found in the measurements because the normal operation of the apparatus has been disrupted and the position of the apparatus in relation to the sample axis has been changed.

The mechanical operations of the apparatus are disrupted because of a structural defect: The apparatus is built in such a manner that it is not a statically determined system, which would be capable of observing any shifts in position on the surface of the sample without changing the points of contact with the sample and without the creation of appreciable stresses. An apparatus satisfying these conditions may be constructed by making relatively simple changes in the structural design.

By way of example a variation in the bar device for the Martenson mirror apparatus or similar apparatus is shown in Fig. 1.

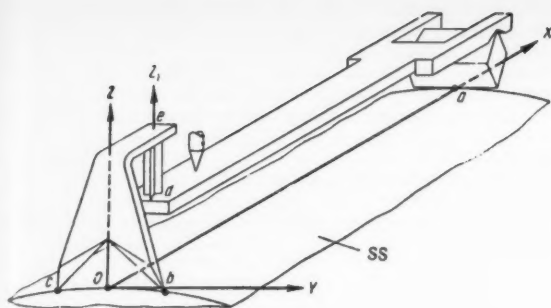


Fig. 1. The Martenson apparatus with the addition of an elastic element *de*; SS is the sample surface.

INSTRUMENTS AND EXPERIMENTAL TECHNIQUES (Pribory i Tekhnika Eksperimenta). Published by Instrument Society of America, Pittsburgh, Pa.

No. 5, Sept.-Oct. 1959.

Calculations Dealing With a Klystron Buncher for a Linear Electron Accelerator, by E. L. Burshtein and A. D. Vlasov, pp. 722-725.

Abstract: A method is presented for calculating optimal parameters for a buncher of klystron type for a linear electron accelerator, guaranteeing a given standard dispersion of outgoing energy for a maximal portion of injected particles.

A Fast Neutron Spectrometer, by E. A. Zherebin, L. G. Andreev and D. V. Timoshuk, pp. 725-729.

Abstract: A neutron spectrometer of telescopic type using two scintillation counters is described. The energy of neutrons is determined by the sum of amplitudes of the pulses from these counters from recoil protons formed in the first organic crystal and losing the energy residue in the second one. The combination of the radiator and detector functions in one of the scintillation counters, and the addition method, give a possibility of using crystals of working thickness equal to the maximum range of recoil proton that considerably increases the efficiency and eliminates the marginal effects. A few spectra are cited, characterizing the basic parameters of the spectrometer.

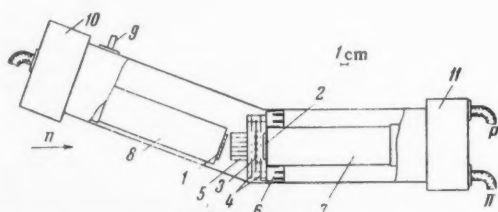


Fig. 1. Schematic drawing of the spectrometer. 1) Crystal radiator and light reflector of the first scintillation counter; 2) crystal and light reflector of the second scintillation counter; 3) collecting electrodes (wires) of the proton proportional counter; 4) negative electrodes (grids) of the proton counter; 5) proton collimator; 6) flange centering the photomultiplier, being also the base of the proton counter with collimator; 7) and 8) photomultipliers FEU-S; 9) pipe for filling the system with methane; 10 and 11) cathode followers of the scintillation counters and preamplifier of the proton counter.

Apparatus With Circular Target for Studying Scattering of High-Energy Neutrons at Low Angles, by B. M. Golovin, V. P. Dzhelepov, Yu. V. Katyashev, A. D. Konin and S. V. Medved', pp. 729-732.

Abstract: An apparatus with a ring target for studying scattering of neutrons with energies of hundreds of Mev is described.

The detector for the scattered neutrons is a telescope which uses scintillation counters with aluminum converters ("neutron" telescope). A system of this kind makes it possible to carry out measurements with neutron beams of relatively low intensity and is especially useful in experiments on small angle scattering.

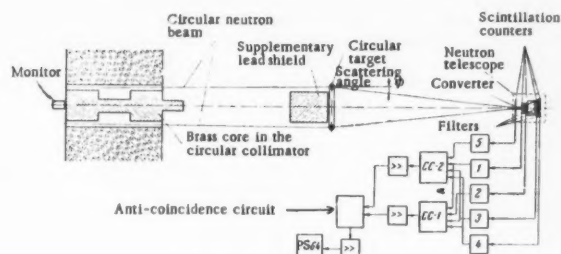


Fig. 1. Experimental arrangement.

Mean Light Yield of Scintillators, by A. M. Ratner, pp. 742-745.

Abstract: The relation between the physical and technical yield of luminescence is discussed. A calculation is made for the mean light yield of a scintillator of cylindrical form with arbitrary values taken for the light absorption coefficient in the scintillator, the reflection factor from its internal surface, and the relative refractive index at the boundary between the scintillator and photomultiplier.

Measurement of the Vapor Pressure in a High Vacuum Pump, by M. G. Manov, pp. 798-802.

Abstract: Two methods for measuring low pressures of lightly condensed vapors at high temperatures are described: By means of a condensation manometer and a manometer with intermediate air "cushion." On finds that it is possible to measure the vapor pressure in the jets of high vacuum vaporjet pumps with an accuracy meeting the demands of engineering calculations.

Calculation of the Thickness of the Films Resulting From Vaporization in a Vacuum, by A. P. Rummyantsev, pp. 802-805.

Abstract: Distribution functions for the thickness of thin films deposited by vaporization in a vacuum are derived, taking into account the commensurability of the dimensions of the vaporizer and the distance from it to the point of condensation h , as well as the spatial distribution law (Knudsen) for the vaporization products. It is shown that the consideration of these factors provides a considerable correction to the distribution function, which increases with a decrease in the "sighting" distance h_0 , with an increase in the distance h from the point of condensation to the vaporizer, and with an increase in the dimensions of the latter. For example, with $h_0 = 15.0$ mm, $r = 4.0$ mm, the correction becomes as large as 25 per cent, even with $h \sim 300$ mm.

Measurement of Work Function by the Initial Current Method, by M. D. Malev, pp. 806-808.

Abstract: A simple method is described which makes it possible to obtain, to semilogarithmic scale, a linear characteristic of initial current in an instrument with arbitrary configuration of the electrodes. Linearization of the characteristic is achieved by moving the instrument in a magnetic field. The error in measurement of the contact difference in potentials comprises ± 0.01 v.

Cavities for Observing Electronic Paramagnetic Resonance at Low Temperatures, by S. D. Kaitmazov and A. M. Prokhorov, pp. 808-811.

Abstract: A description is given of cavities which are designed for observation of electronic paramagnetic resonance at low temperatures in the centimeter ($\lambda = 2.5$ and $\lambda = 3.2$ cm) and the decimeter range. The design allows the sample to be placed in the refrigerated cavity. The cavity for the centimeter region can be tuned. The dimensions of the cavities are suitable for operation in a standard Dewar (1 liter).

Finite Pulse Train Generator, by V. V. Okorokov, pp. 767-773.

Abstract: A finite pulse train generator is described with crystal control of the interval between the pulses of the train, which is equal to 1 microsec. The use of synchronizing pulses with an 8-megacycle frequency makes the time jitter of the 1-

microsec train equal to 0.12 microsec. The presence of a phenomenon somewhat analogous to self-phasing in accelerators, which exists in the described circuit, eases the necessity for any changes of the parameters of the circuit which characterize its normal operation. The conditions for maximum attenuation of transients, which arise unavoidably in the circuit in generating the first pulses of the train because of the different position of the start signal relative to the synchronizing pulses, are examined in this article. The generator can be used for generating a time scale in amplitude and time analyzers, and also as a circuit for phasing signals relative to high frequency (4-20 mc) reference pulses.

A Double-Beam Spectrometer for the Investigation of Spectra of Combination Scattering of Light, by V. A. Zubov, G. G. Petrash and M. M. Sushchinskii, pp. 819-821.

Abstract: This article describes a photoelectric spectrometer for the investigation of spectra of combination scattering of light, which has a diffraction grating and a dispersion of 5.5 \AA per mm. The instrument can operate in the single-beam as well in the double-beam variants. In the latter case, the ratio of the line intensities of the spectrum under investigation to the excitation line intensity is recorded, which makes it possible to eliminate the instability in tube operation and the instability of the photo-multiplier sensitivity.

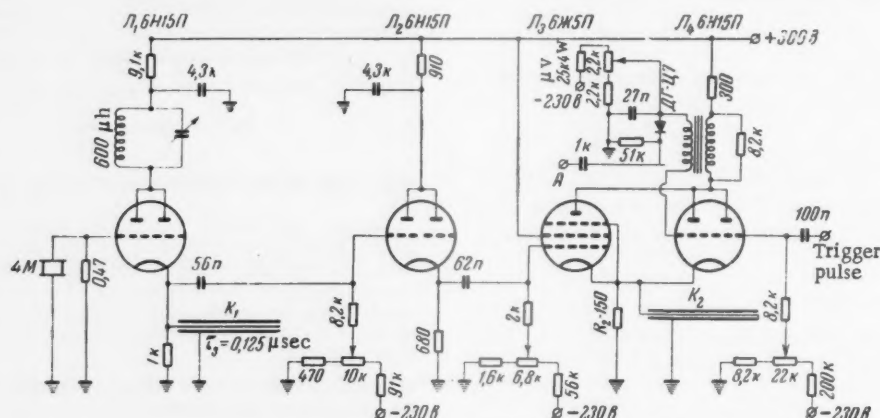


Fig. 1. Generator circuit. The stop signal, 1 to 2 microseconds in duration, is impressed on point A. The blocking-oscillator transformer is wound on a ferrite toroid made of Oxifer-1000, 18 mm in diameter; plate winding - 15 turns, grid winding - 20 turns.

The following Russian abbreviations are retained in the figure: Л = tube, Тр = transformer, М = megohm, к = kilohm, мк = μf or μh , н = $\text{m}\mu\text{f}$ or $\text{m}\mu\text{h}$, н = μf or μh , and ε = volt. For individual tube designations see appendix to No. 1 of this year.

High Voltage Rectangular-Pulse Generator, by G. A. Martynov, pp. 840-841.

Abstract: It is recommended that the circuit of the high voltage pulse generator described in another paper be modified to permit a considerable increase in the amplitude of the output voltage.

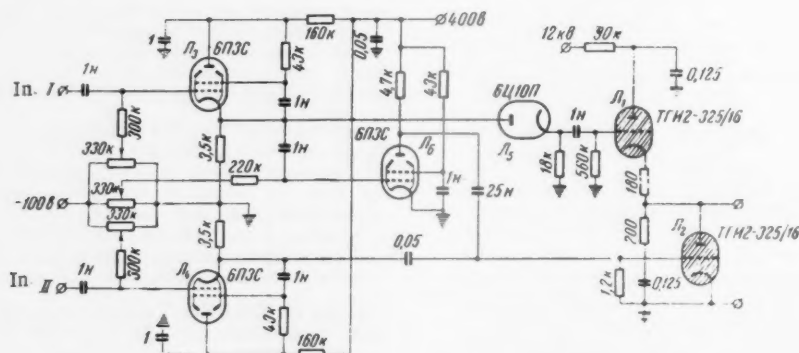


Fig. 3. Circuit for a modernized high-voltage pulse generator.

The following Russian abbreviations are retained in the figure: Л = tube, Тр = transformer, М = megohm, к = kilohm, мк = μf or μh , н = $\text{m}\mu\text{f}$ or $\text{m}\mu\text{h}$, н = μf or μh , and ε = volt. For individual tube designations see appendix to No. 1 of this year.

Wire Construction Gaseous Source Counters, by Yu. A. Prokof'ev and A. N. Sosnovskii, pp. 825-827.

Abstract: A description is given of reliable gaseous source counters with cathodes constructed from a system of metallic wires and two types of "carpets" made up of such counters; some of their characteristics are given.

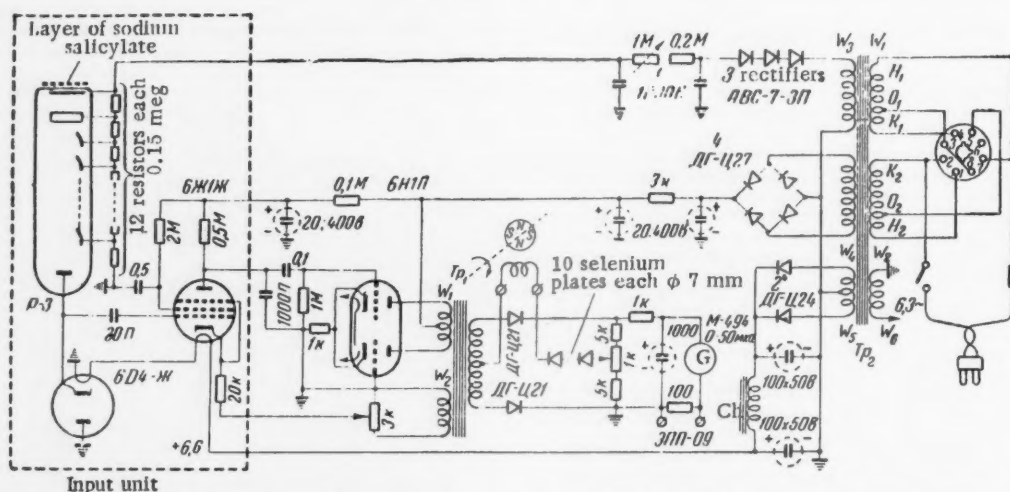
An Effective Method for Regulating Filament Current, by A. N. Tkachenko, pp. 845-846.

Abstract: In a whole series of electronic and photoelectric equipment it is necessary to regulate the filament current of the electronic tubes and illuminating lamps. This is accomplished

1079

Abstract: A description is given of a photometer attachment to a monochromator; it records the logarithm of the ratio of two radiation fluxes by means of a logarithmic response diode that acts as the load of a photomultiplier. The ratio of the fluxes can extend up to $10^4:1$. An ÉPP-09 potentiometer recorder traces out the spectrum.

Measurement of the Group Velocity in the Retarding System of a Maser, by V. B. Shteinshleiger and G. S. Mizezhnikov, p. 989.



The following Russian abbreviations are retained in the figure: Π = tube, T_p = transformer, M = megohm, k = kilohm, v = volt, $\mu k = \mu f$ or μh , $M = m\mu f$ or $m\mu h$, and $n = \mu\mu f$ or $\mu\mu h$. For individual tube designations see appendix to No. 1 of this year.

Abstract: An apparatus with an equivalent noise resistance of 10 ohms for studying current noise in semiconductors over the range 20-20,000 cps is described.

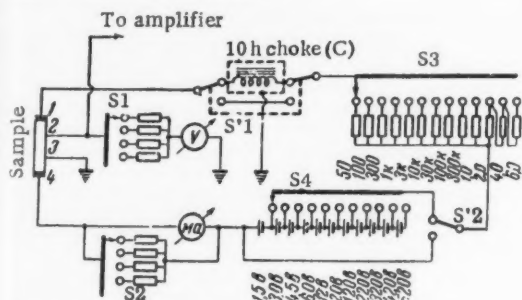


Fig. 1. Circuit of the supply for powering the sample.

The following Russian abbreviations are retained in the figure: Π = tube, T_p = transformer, M = megohm, k = kilohm, $M\mu$ = μf or μh , M = $m\mu f$ or $m\mu h$, μ = μf or μh , and v = volt. For individual tube designations see appendix to No. 1 of this year.

Fig. 2. Preamplifier circuit diagram.

conjunction with American Society of Mechanical Engineers, New York.

Vol. 23, no. 3, 1959.

The Formation of Equilibrium Cracks During Brittle Fracture. General Ideas and Hypotheses. Axially Symmetric Cracks, by G. I. Barenblatt, pp. 622-636.

Introduction: A large number of investigations has been devoted to the problem of the formation and the development of a crack during brittle fracture of solids. The first of these was the well-known work of Griffith devoted to the determination of the critical length of a crack at a given load, i.e., the length of a crack at which it begins to widen catastrophically. Assuming an elliptical form of a crack forming in an infinite body subjected to an infinitely homogeneous tension, Griffith obtained an expression for the critical length of a crack as that corresponding to the total of the full increase in energy (equal to the sum of the surface energy plus the elastic energy released due to the formation of the crack).

In the following study equilibrium cracks are considered, i.e., cracks forming in a brittle solid subjected to a given system of forces, constant and not decreasing in time. Apparently the first ideas concerning equilibrium cracks are met in the works of Mott and Frenkel'. These ideas are similar, but were arrived at independently. These works contain also a critical analysis of Griffith's theory. Both these authors, however, limited themselves to qualitative considerations, proceeding from the assumption of a crack of infinite length.

In our work the question concerning equilibrium cracks forming during brittle fracture of a material is presented as a problem in the classical theory of elasticity, based on certain very general hypotheses concerning the structure of a crack and the forces of interaction between its opposite sides, and also on the hypothesis of finite stresses at the ends of the crack, or, what amounts to the same thing, the smoothness of the joining of opposite sides of the crack at its ends. The latter hypothesis was first put forth by Khristianovich in his consideration of certain problems in the formation of cracks in rocks. Using this hypothesis it seemed possible to solve a series of problems related to the development of cracks in rocks.

Some Three-Dimensional Problems of Thermoelasticity, by Witold Nowacki, pp. 651-665.

Introduction: In this paper thermal stresses are investigated which are caused by the action of nonstationary sources of heat, arbitrarily distributed in elastic and visco-elastic media. The construction of Green's functions for stresses caused by an instantaneous point source of heat is considered. In Sections 1 and 2 the state of stress in absolutely elastic bodies is considered and in Section 3, in visco-elastic bodies.

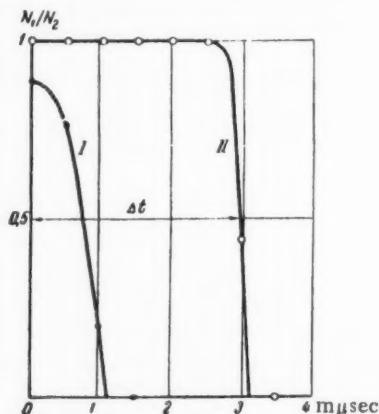


Fig. 2. Delayed-coincidence curves for photomultiplier FEU-2V. The pulse time delay is plotted along the X-axis and the ratio of coincidence counting rate (after the gate which is opened by the amplitude selector) to the pulse-counting rate at the output of the amplitude selector along the Y-axis. Curve I corresponds to the threshold value of the pulse amplitude, and curve II to the value of an amplitude three times greater than the threshold. The time of the pulse transition along the shaping cable is 1 μ sec.

The Direct Method of Liapunov in Stability Problems of Elastic Systems, by A. A. Movchan, pp. 686-700.

Introduction: Considered is the problem of stability of the plane state of an elastic thin plate of infinite length simply supported along two edges (beam), subjected to the action of constant forces in its plane, from the point of view of application of various methods of analysis, namely the methods of direct integration and the direct method of Liapunov. The definition of stability in the sense of Liapunov is given for the problem under discussion, and the theorems of the direct method of Liapunov regarding stability and instability are given; to this end an auxiliary metric space is introduced, in order to construct in it the corresponding functionals.

It is assumed, that the equations of motion for the dimensionless deflection $w(x, t)$, referred to the chord a of the plate, may be written in the form

$$\frac{\partial^4 w}{\partial x^4} - \frac{a^2 N}{D} \frac{\partial^2 w}{\partial x^2} + \frac{\partial^2 w}{\partial t^2} = 0 \quad w(x, t) = \frac{\partial^2 w(x, t)}{\partial x^2} = 0 \quad \dots \text{for } x = 0, 1 \quad [1]$$

Here x is the dimensionless space coordinate, referred to the chord ($0 < x < 1$); t is a dimensionless time, referred to the quantity $(\mu a^4/D)^{1/2}$; μ is the mass per unit of area; D is the rigidity; N is the force in the plane of the plate, positive in case of extension.

The Stability of MacLaurin Ellipsoids of a Rotating Fluid, by V. V. Rumiantsev, pp. 701-715.

Stability of Nonlinear Automatic Control Systems, by O. I. Komarnitskaia, pp. 716-729.

Introduction: There are many methods of stability analysis of nonlinear automatic control systems. As a basis of many investigations in this field the works of Lur'e were used in which he applied a special transformation to equations of motion of nonlinear automatic control systems and indicated a method of constructing Liapunov's function for them. Lur'e's method reduces the problem of stability of equilibrium positive in automatic control systems to the investigation of solvability of algebraic systems of quadratic equations. This method gives wide stability regions and is convenient when the number of equations is small. With the increase of degrees of freedom the application of the method becomes more complex because of the difficulty in establishing criteria for the solvability of systems of quadratic equations of higher order.

Malkin offered a different method of constructing Liapunov's function of equations of motion of automatic control systems which results in simpler stability conditions. The method of Malkin is as follows. Let the motion of an automatic control system with one control element be described by differential equations which in terms of canonic variables have the form

$$\dot{x} = \lambda x + f(\sigma)e \quad \dot{\sigma} = \beta x - r f(\sigma) \quad [0.1]$$

where x, β, e are column matrices of the n th order containing elements $x_i, \beta_i, e_i = 1$ ($i = 1, \dots, n$), respectively, and λ is a diagonal matrix with the elements λ_i . The scalars in Equation [0.1] have the following meaning: β_i are characteristic constants of the system; λ_i are roots of the characteristic equation with $\text{Re } \lambda_i < 0$; $r > 0$ is a constant called the feedback coefficient, σ is a parameter determining position of the control element, and $f(\sigma)$ is a function satisfying the following conditions:

(a) $f(\sigma)$ is continuous and is such that for given initial conditions the Equations [0.1] have a unique solution.

(b) $f(0) = 0, f(\sigma)\sigma > 0$ for $\sigma \neq 0$. Liapunov's function used is of the form

$$V = \frac{1}{2} A x x + \int_0^\sigma f(\sigma) d\sigma \quad [0.2]$$

where A is a symmetric positive definite quadratic form and is derived from the condition

$$\theta = \frac{1}{2} (A\lambda + \lambda'A) \quad [0.3]$$

(λ' is the transposition matrix of λ) and θ is some matrix of the negative-definite quadratic form.

Having calculated the derivative of V on the basis of [0.1] and taking into account the choice of θ , we obtain asymptotic

stability conditions for the equilibrium position for the Equations [0.1]

$$\Delta = \begin{vmatrix} -\theta & g \\ g' & r \end{vmatrix} > 0 \quad [0.4]$$

where the column matrix g is found from the formula

$$2g = -\beta - Ae \quad [0.5]$$

Malkin does not elaborate on how to select the θ matrix, so that the method will give good practical results; furthermore, he used this method only in the case of different roots of characteristic equation and one zero root of the second order not simple with respect to elementary dividers.

In this paper a form of the θ matrix is given, stability regions are investigated, and Malkin's method is used in the case of multiple zero roots both simple and not simple with respect to elementary dividers.

Asymptotic Solutions of Nonlinear Second-Order Differential Equations With Variable Coefficients, by G. E. Kuzmak, pp. 730-744.

Introduction: In this paper there are considered the asymptotic solutions of the equation

$$\frac{d^2 y}{dt^2} + \epsilon f(\tau, y) \frac{dy}{dt} + F(\tau, y) = 0 \quad [0.1]$$

where ϵ is a small parameter, $\tau = \epsilon t$ is slow time; by asymptotic solutions are meant the principal terms of asymptotic expansions of solutions.

Investigations of the asymptotic behavior of solutions of differential equations were made in other publications. Certain studies were devoted directly to the investigation of the asymptotic behavior of the solution of Equation [0.1] in certain special cases.

Shock Waves in Magnetogasdynamics, by M. N. Kogan, pp. 784-792.

Abstract: In this work the nature of the shock polar is investigated for various parameters of the stream and of the magnetic field.

Virtual Masses of Some Curvilinear Contours Immersed in Detached Flow, by S. I. Parkhomovskii, pp. 827-833.

Introduction: An exact solution in closed form of the problem of the detached flow past one of the family of curves $L(m, \nu)$ was given by Pykhtev. In this article we consider the impact upon the same family of curves of the detached streamlined flow of indefinite extent of an ideal incompressible fluid.

Finding the Shape of a Body From a Given Impact Pressure, by V. S. Rogozhin, pp. 834-838.

Introduction: It is required to determine the contour of a part of a body in contact with incompressible liquid from a given impact pressure. Let us examine the two-dimensional case of a liquid with infinite depth. The abscissa is assumed to be along the surface of the liquid and the ordinate is pointed vertically downward. Let the body intersect the abscissa axis at $x = \pm 1$. The velocity potential ϕ is related to the impulse pressure p_i by $\phi\rho = -p_i$, where ρ is the density of the liquid. Therefore, for any given pressure along the contour L there is a corresponding potential ϕ .

Let the projections of velocities upon the axes of coordinates be u_0 and v_0 , and the angular velocity ω_0 , then the stream function ψ along L will be

$$\psi_L = u_0 y - v_0 x - \frac{1}{2} \omega_0 (x^2 + y^2) \quad [1]$$

In formulating the reverse problem, let us assume that u_0, v_0 and ω_0 are given.

The choice of given ϕ along L depends upon the character of the motion of the body in the interval of time immediately after the shock.

Sufficient Conditions for Optimization, by N. N. Krasovskii, pp. 839-843.

Introduction: We will analyze the problem described in a previous publication¹ and dealing with the determination of an optimal trajectory. In our work we will observe the same

¹ Krasovskii, N. N., *PMM*, vol. 23, no. 1, 1959.

terminology and the same system of notations. In Section 4 of the previous paper those sufficient conditions (Theorem 4.1) are indicated which are such that a trajectory $x(x_0, t, \eta_0)$ in the system of equations

$$dx/dt = f(x, t) + q\eta(t) \quad [1]$$

is locally optimal (in the sense of the definition given in the previous work) in respect of the admissible governing functions $\eta(t)$, constrained by the condition

$$|\eta(t)| \leq 1 \quad [2]$$

Apart from conditions 1 to 4 (which are analogous to conditions given by the principle of a maximum, Theorem 4.1¹ contains some other limitations (shown by expression 5) on the second derivatives of $\partial^2 f_i / \partial x_j \partial x_k$. It is the aim of this note to prove that, without these additional limitations, conditions 1 to 4¹ fail to produce a locally optimal trajectory $x(x_0, t, \eta^0)$, and that even these conditions are insufficient for the trajectory to become optimal in respect of small variations of function $\eta^0(t)$ constrained by condition [2].

The Stability of Solutions of Differential Equations of Second Order, by Iu. M. Filimonov, pp. 846-849.

Introduction: In the present paper several theorems are proposed on the stability in the sense of Liapunov of the solutions of differential equations of second order. As a source for this paper other works are given.

The Stability of a Solution of a System of Differential Equations With Discontinuous Right-Hand Sides, by I. V. Livartovskii, pp. 850-859.

Introduction: The stability of the periodic solution of the system of equations

$$dz/dt = f(z, t) \quad [0.1]$$

with discontinuous periodic $[f(z, t + \tau) \equiv f(z, t)]$ right-handed sides $[z$ and f are n -dimensional vector columns with coordinates z_i and $f_i (i = 1, \dots, n)]$ has been investigated by Aizerman and Gantmakher. Establishing what should be understood by the linear approximation in this "discontinuous" case, the authors have proved theorems analogous to those of Liapunov.

The present paper deals with the stability of any solution (periodic or nonperiodic) of system [0.1] with discontinuous non-periodic right-hand sides. For this, use is made of the condition for the discontinuities of the solution of the linear approximation introduced in another paper for periodic systems. Two criteria of stability are established which are generalizations of the corresponding theorems of Persidskii and Perron, proved by these authors for continuous systems.

The Stability of Motion of a Gyroscope, by Chzhan Sy-In, pp. 860-863.

Introduction: In previous papers the authors considered the motion of a symmetric gyroscope with its center of gravity on the axis of spin, and derive by various methods the sufficient conditions of stability of motion in the two cases: (1) When the axis of the outer ring is vertical; (2) when the axis of the outer ring is horizontal.

In this note the author derives from Chetaev's theorem on the instability of motion the necessary condition of stability in case (2).

The Stability of the Unperturbed Motion of a Certain Mechanical System, by E. N. Berezkin, pp. 864-871.

Introduction: In this paper the author considers a problem related to the stability of the unperturbed motion of an airplane with an autopilot. The characteristic equation of the first approximation of the system has a pair of zero roots with one group of solutions. General methods of solving this kind of problem were investigated by Liapunov and Kamenkov. In the actual cases the construction of the Liapunov function which determines the region of permissible perturbations may be very difficult.

Integral Equations of Equilibrium of Thin Elastic Cylindrical Shells, by N. I. Remizova, pp. 872-879.

Introduction: In his contributions to the theory of shells, Kil'chevskii derives a general method of solving the static problem of the theory of shells by reducing this problem to the treatment of a certain system of integral equations. In the

following we give the results of further development of his method with reference and application to the case of cylindrical shells.

The system of the integro-differential equations of equilibrium of a cylindrical shell is obtained on the basis of the theorem of work reciprocity (theorem of Betti). According to this theorem we consider, in the well-known manner, two systems of forces and displacements: The first system consists of prescribed forces and sought displacements; the second one consists of auxiliary forces and auxiliary displacements.

We treat the cylindrical shell as a continuous three-dimensional medium. The middle surface of the shell is used as coordinate surface, and the position of a point on this surface is determined by the coordinates x and s ; these are the distance along a generator and the length of the arc of the directing curve, respectively. The third coordinate z is the distance, measured along the normal, between the point $M(x, s)$ of the middle surface and a point considered; z varies between the limits $-\frac{1}{2}h$ and $+\frac{1}{2}h$, where h is the constant thickness of the shell.

Vol. 23, no. 4, 1959.

The Theory of Optimum Control, by N. N. Krasovskii, pp. 899-919.

Abstract: In the present paper problems of optimum (in the sense of high speed action) control of systems containing a linear basic part and corresponding to certain basic types of restriction on the controlling actions are considered. Limit passages in the solutions are discussed which correspond to the passages from one type of restriction to another. On the basis of these limit passages, approximate methods are described for the computation of optimum trajectories and the construction of optimum systems.

Estimates of the Solutions of Systems of Differential Equations of the Accumulation of Disturbances and the Stability of Motion Over a Finite Time Interval, by Chzhan Sy-In, pp. 920-933.

Abstract: Problems on the stability of motion over a finite time interval are based on the estimates of the solutions of systems of differential equations. In this paper there is given a method for estimating the solutions in certain cases. The conditions for stability are also determined.

Some Problems of the Theory of Dynamic Programming, by Ia. N. Roitenberg, pp. 943-955.

Introduction: The theory of optimum processes in linear systems has been rigorously developed in recent years in the works of Pontriagin, Poltianskii and Gamkrelidze.

These studies were preceded by the work of Fel'dbaum, Lerner and others. Considerable contribution to this field was made by Bellman, the author of a fundamental paper on dynamic programming.

In this paper, one of the problems of the theory of dynamic programming is considered, namely, the problem of choosing the law of variation of the additional external forces by means of which one can insure realization of prescribed motion in a linear nonstationary system. This problem is considered for both continuous and impulsive systems.

New Concepts in Plasticity and Deformation Theory, by V. D. Kliushnikov, pp. 1030-1042.

Introduction: This paper contains a comparative analysis of some conclusions of three new theories of plasticity (Batdorf and Budiansky's slip theory; Sanders' theory based on linear loading functions and the theory proposed by Klinshnikov) and a model representation.

Temperature and Velocity Distributions in a Laminar Flow of a Fluid Between Rotating Coaxial Cylinders, by A. I. Borisenko and A. D. Myshkis, pp. 1054-1065.

Flow of Highly Rarefied Gases Around Oscillating Surfaces, by N. T. Pashchenko, pp. 1081-1089.

Abstract: In the present paper the total force, acting on a unit surface, which performs small unsteady motions while moving forward, is determined, as well as its projection in directions corresponding to normal pressure, friction, etc. An attempt is made to assess the validity of analysis of flows around concave surfaces with the usual free-molecular assumptions. In the process, conditions on the shape of such surfaces and on their motion are established. As a concrete example, the flow around an oscillating flat plate is analyzed. It is found that the expression

for the additional pressure due to the oscillation agrees, up to a multiplicative constant, with a known formula of the "piston theory," which can well be of theoretical interest.

Flow of a Gas Stream From a Container of Finite Width at Maximum Discharge, by B. A. Gushchin, pp. 1097-1106.

Introduction: We deal with a case of plane laminar gas flow. It is an adiabatic steady-state flow without vorticity. The method for solving such flows in the subsonic case with a specified reference velocity, has been given by Chaplygin. Fal'kovich extended the Chaplygin method to flows involving more than one characteristic velocity. The solution described here is based on this extension and also makes use of Frankel's results, where it is demonstrated that the flow problem of a gaseous stream at maximum discharge reduces to the Tricomi problem for the Chaplygin equation

$$4\tau^2(1 - \tau) \frac{\partial^2 \psi}{\partial \tau^2} + 4\tau[1 + (\beta - 1)\tau] \frac{\partial \psi}{\partial \tau} + [1 - (2\beta + 1)\tau] \frac{\partial^2 \psi}{\partial \beta^2} = 0 \quad [0.1]$$

The Problem of Symmetrical Flow Past a Given Symmetrical Profile With Subsonic Velocity at Infinity and Local Supersonic Velocities, by F. I. Frankl', pp. 1107-1114.

Spatial Transonic Gas Flows in Ducts, by O. S. Ryzhov, pp. 1115-1121.

The Propagation of Weak Waves in a Continuous Medium in the Presence of Radiant Energy Transfer, by Iu. S. Riazantsev, pp. 1126-1128.

Introduction: The problem of the nonadiabatic propagation of weak plane waves in a continuous medium was investigated in the papers of Prokof'ev, where a system of linearized equations of gas-dynamics was written out, in which the effects of viscosity, heat conduction and radiation were taken into account and some solutions of those equations were derived. In this note, the propagation of weak plane waves is considered in the presence of radiant energy transfer only. Two particular cases are noted, namely, for the case of motion only slightly different from adiabatic or isothermal motions, and for these cases the amount of attenuation of weak waves was worked out.

The Stability of Permanent Rotations of a Rigid Body With a Fixed Point Under the Action of a Newtonian Central Force Field, by G. K. Pozharitskii, pp. 1134-1137.

Vol. 23, no. 6, 1959.

Hypersonic Flow Past a Body in Magnetohydrodynamics, by M. D. Ladyzhenskii, pp. 1427-1443.

Introduction: Hypersonic flow is considered past a body from within which a magnetic field is excited. The field acts on the gas that becomes electrically conducting as a result of thermal ionization occurring on transition across the strong shock wave ahead of the body. In a majority of the papers appearing recently, the behavior of the flow of a conducting fluid is studied in the vicinity of the forward critical point of a blunt body; here, the effect of a strong imposed magnetic field on the general flow picture is studied. The cases of flow past bodies of rectilinear shape—the wedge and cone—are considered in detail when the magnetic field intensity vector is directed perpendicular to the surface of the body. The method of solution is based on the assumption that the perturbed zone between the body and the shock wave is narrow. The forces acting on the body are determined. As follows from the solution, for a sufficiently strong field the magnetic drag force has the same order of magnitude as the gasdynamic force, despite the narrowness of the zone of perturbed flow on which the magnetic field acts.

It is shown that under certain conditions the flow may separate from the wall. The point of magnetic separation from the surface of the body is determined. With increase of the imposed field this point moves upstream; therefore using strong fields leads to the possibility of creating a separated region around the body which leads to an increase in the drag of the body investigated, and, as might be expected, to a decrease in the heat transfer to the body.

Bodies of Minimum Wave Drag, by V. N. Zhigulev and Iu. L. Zhilin, pp. 1462-1475.

Introduction: Certain variational problems are considered for a

body that slightly disturbs a supersonic stream. It is found possible in the general case to separate the problem for the determination of the drag from the problem of the determination of the minimum drag body itself. For the solution of the first problem it is sufficient to express the properties of the body that are of interest (for example, forces, moments, volume, etc.) in terms of the values of the perturbation velocity potential on the characteristic surfaces enclosing the body. In this work, as an example, relations are found connecting the volume of the body with the values of the perturbation velocity potential on the characteristic surfaces enclosing the body.

It is shown that the perturbation velocity potential corresponding to flow past a body of minimum drag with arbitrary fixed leading and trailing sections and given volume satisfies, on the rear characteristic surface, Poisson's equation with mixed boundary conditions. Axisymmetric ducted bodies are found having minimum drag for fixed leading and trailing sections and given volume.

Also considered is the problem of the optimum choice of a fuselage having given length and volume with a given wing, and a lower estimate is obtained from the drag of the wing-fuselage system.

The method used in the work is that proposed by Nikol'skii for the solution of the problem of determining the contour of the body of revolution of minimum drag passing through two given points. We note that this method has been used to find the drag of the optimum wing with a straight trailing edge perpendicular to the free stream, and for the solution of the problem of finding the drag of an optimum wing of arbitrary planform.

The Stability of the Rotational Motions of a Solid Body With a Liquid Cavity, by V. V. Rumiantsev, pp. 1512-1524.

Introduction: The author here considers the stability of the rotation of a solid body with a cavity filled entirely or partially (containing a bubble) with an ideal incompressible homogeneous liquid.

Conclusions: In conclusion we emphasize once more that the stability of the rotational motion of a solid body with liquid content under the action of a tilting moment is attained by means of gyroscopic stabilization, and that the latter, as was shown by Kelvin, cannot occur when the system is acted upon by a dissipative force with a loss of energy under arbitrary displacements of the system. Since in real situations there always exist small dissipative forces, the gyroscopic stability will always be destroyed. In view of this, Kelvin suggested that a distinction should be made between "temporary" stability, which can be achieved with gyroscopic stabilization, and "secular" (or permanent) stability which exists under the action of potential forces only. It is obvious that the stability within our system has the character of the "temporary" stability, and that our system is unstable in the "secular" sense. Chetaev succeeded in proving a theorem on the instability of the motion of a solid body by taking into account dissipative forces. It seems that this theorem is also valid for the rotational motion of a solid with a cavity containing a liquid.

The Characteristic Exponents of the Solutions of a Second-Order Linear Differential Equation With Periodic Coefficients, by L. M. Markhashov, pp. 1525-1535.

A Stability Criterion for Creep, by S. A. Shesterikov, pp. 1574-1581.

Introduction: Stability in the presence of creep has been studied by different authors; some of these investigations were made as much as 10 years ago.

The majority of the published papers are concerned with problems of the stability of longitudinally compressed rods, since this represents the simplest formulation of the problem by which many of the particular characteristics of stability can be elucidated.

It has to be noted that there exists a series of principally different formulations of the problems of stability in the presence of creep. In this paper, consideration will be restricted to stability of rectilinear forms of equilibrium.

The Theory of Ideally Plastic Anisotropy, by D. D. Ivlev, pp. 1582-1592.

Abstract: The behavior of an ideally rigid plastic body is investigated under a generalized Tresca plasticity condition.

The Propagation of Elasto-Plastic Waves for Combined Stresses, by N. Cristescu, pp. 1605-1614.

Introduction: In his paper Rakhmatulin considered several problems of the propagation of elasto-plastic waves in the presence of combined stresses. He studied the case when the wave of the combined stress is a wave of a strong discontinuity, propagating with a velocity which is smaller than the velocity of the usual elasto-plastic waves (Riemann waves). Thus, Rakhmatulin assumed that in the case of a combined stress for a shock in a plastic body there propagates at first a group of plastic waves and then the wave of the strong discontinuity which is a wave of a combined stress.

The present paper studies the same problem on the basis of the equations established by Rakhmatulin; however, it also considers another possible case of propagation which may occur for certain materials. For example, it is shown that for such materials the combined dynamic stress is transmitted in a plastic body only by combined waves. These waves propagate in a body faster than the usual plastic waves. The presented study is rather qualitative than quantitative, since the theory of small elasto-plastic deformations, used in this investigation, has not yet been verified experimentally (and adapted in a proper manner) for dynamic problems.

The Stability of a Gyroscopic System, by I. Z. Pirogov, pp. 1623-1626.

Introduction: When using the second method of Liapunov in investigating the problem of stability of motion of a gyroscopic stabilizing system installed on a ship performing complex maneuvers, it is necessary to construct Liapunov's function for variational equations. These equations in this case will constitute a system of linear differential equations with variable coefficients. Successful methods of constructing Liapunov functions for such systems are given by Chetaev. Boundaries of the stable regions obtained by means of these methods are investigated by Razumikhin. In the paper by Roitenberg (closely related to the two mentioned) the Liapunov function is constructed by first transforming the original system of differential equations to new variables which are coordinates of some auxiliary system of differential equations. Utilizing this method, let us construct the Liapunov function for the differential equations of the gyroscopic system under consideration having the form

$$\begin{aligned} x_1 + x_2 - f_1(t)x_3 &= 0 & x_1' - m_1x_2 + f_1(t)x_4 - m_2x_5 &= 0 \\ -f_1(t)x_1 + m_1x_3 + x_4' + m_3x_4 &= 0 \\ f_1(t)x_2 + x_3' - [m_4 + f_2(t)]x_4 &= 0 \\ m_5x_2 + x_5' + m_5x_5 &= 0 \end{aligned} \quad [1]$$

Here x_1, \dots, x_5 are coordinates of the system; m_1, \dots, m_5 are constant coefficients; $f_1(t)$ and $f_2(t)$ are some time functions dependent on ship's movement.

Accumulation of Disturbances in Nonstationary Linear Impulsive Systems, by L. S. Gnoenskii, pp. 1627-1636.

Introduction: The problem of determining the maximum value of $y_{\max}(T)$ of the particular solution of the differential equation $L\{y(t)\} = f(t)$ subject to the conditions $|f(t)| \leq M_0, 0 \leq t \leq T$ at instant T has been solved by Bulgakov and Kuzovkova. An analogous problem for linear difference equations has been treated by Roitenberg. However, in a number of cases much more rigid conditions are imposed upon the right-hand side of the equation; i.e., in addition to the constants on the modulus of $f(t)$ there may be also constraints on the moduli of some of its derivatives such as $f'(t), f''(t)$. This situation may be observed in systems where position, velocity and acceleration of the controlled object are constrained. In the presence of such additional constraints on the right-hand side of the equation, the magnitude of $y_{\max}(T)$ may be considerably smaller than in the case of a single constraint on $|f(t)|$. In this paper a method of determining the maximum value of $y_{\max}(T)$ of the particular solution of the linear difference equation $L\{y(t)\} = f(t)$ is given for the cases

$$|f^{(m)}(t)| \leq M_m \quad m > 0 \quad [0.1]$$

$$|f(t)| \leq M_0 \quad |f'(t)| \leq M_1 \quad |f''(t)| \leq M_2 \quad [0.2]$$

Some Remarks on the Structure of a Normal Magnetohydrodynamic Shock Wave, by A. G. Kulikovskii and G. A. Liubimov, pp. 1644-1647.

Introduction: The structure of normal hydrodynamic shock waves in a viscous, heat-conducting gas has been dealt with. It is also interesting to study the limiting cases when one or two

of the dissipative coefficients are small enough to be neglected. The structure of a shock wave in the absence of thermal conductivity was dealt with in another work as was the structure of a shock wave in the absence of both conductivity and of viscosity. In this article we are dealing with the structure of a normal shock wave, taking into account the effects of thermal and electrical conductivity, but not of viscosity.

Vol. 24, no. 1, 1960.

Certain Questions Related to the Problem of the Stability of Unsteady Motion, by N. G. Chetaev, pp. 5-22.

Introduction: In modern engineering there arise new and increasingly more complex problems concerning the stability of motion. Looking at the past and anticipating the future, one can see that in order to keep up with technological progress it will be necessary to develop more and more precise methods for the investigation of these stability problems. The main difficulties in this direction are caused by the insufficient development of computation algorithms and of the procedures proposed already by Liapunov in his work "General Problem of the Stability of Motion."

Note on Classical Hamiltonian Theory, by N. G. Chetaev, pp. 40-42.

Introduction: The requirement that deviations of theoretical values from the natural values of observed functions be small imposes a series of conditions on the forces in a strict theoretical sense.

In rough engineering theories the requirement is that the undisturbed motion must be asymptotically stable in order that the equations of the disturbed motion represent the instrument or system to the first approximation. Then all the exciting forces of order of smallness above the first will not be able to make the undisturbed motion unstable. But this elementary consideration interests me little now.

Actual exciting forces, if they do make the undisturbed motion unstable, are detected by inadmissible deviations between theoretical and natural values of observed functions, with respect to which the undisturbed motion becomes unstable; and consequently such forces must be introduced into the theory if the latter is to satisfy the requirement of small deviations of theory from experiment. In a rigorous theory, real exciting forces must not cause a well-established stable equilibrium or an undisturbed motion of a mechanical system to become unstable.

The Relaxation of Material Systems, by V. I. Kirgetov, pp. 48-58.

Introduction: In 1829 Gauss found and described a remarkable property of material systems, namely to move with least constraint. Gauss discovered this property in connection with a transformation of material systems. The Gauss transformation consisted of a relaxation [removal] (the terminology stems from here) of all the constraints of the systems. After Gauss, attempts were made to find other forms of relaxation where a property similar to that formulated by Gauss would hold.

In his "Mechanics" Mach noted that the property of least constraint, which holds for systems with complete relaxation, possibly also holds for a relaxation of only a part of their constraints (partial relaxation of material systems). This assumption by Mach was verified by Bolotov, who proved it for a system with linear differential constraints of the first order. Later on this case was also extended to a system with nonlinear constraints.

In 1933 Chetaev developed a new point of view on the relaxation of material systems. He proposed to apply the term "relaxation" to any system transformation which satisfied some mathematical algorithm (parametric relaxation of material systems). Chetaev added to his proposition a proof of a corresponding minimum theorem.

In the present paper the problem of the relaxation of a material system is studied from the qualitative point of view. A sufficiently broad qualitative definition of the relaxation of a system is given, and a corresponding minimum theorem is established, after which its mathematical algorithm is derived from the given qualitative definition of the material systems.

A Theorem on the Stability of Motion, by V. V. Rumiantsev, pp. 59-69.

The Instability of the Motion of Systems With Retardation, by S. N. Shimanov, pp. 70-81.

Abstract: In this paper it is shown that the known theorems of Liapunov and of Chetaev concerning stability may be extended to systems with retardation. A criterion of instability in first approximation of motion of systems with retardation is given.

Optimum Control in the Presence of Random Disturbances, by N. N. Krasovskii, pp. 82-102.

Abstract: Considered is a problem of optimum control under the condition of minimum expected decay time of a transient process. A method is described for applying the Liapunov function to this problem. Assumed statement of the problem is generalized to include some problems of optimum application of high speed action on systems subject to random disturbances. Discussed are approximate methods for synthesizing optimum control.

Author notes that he discussed the theme of this work and the methods of solution of the considered problems with Chetaev who gave him a number of valuable suggestions. Especially, detailed remarks were made by Chetaev regarding the application of the Liapunov function to the problems of the investigated systems subject to random disturbances.

The Placing of a Gyroscopic Compass Into a Meridian During the Acceleration of the Rotors of the Gyroscopes, by Ia. N. Roitenberg, pp. 113-119.

Abstract: The placement of a gyrocompass after it has been started into a meridian is usually accomplished by means of application to the gyroscope of additional external forces. The selection of the law of control of these forces may be subjected to the requirement of placing the gyrocompass into a meridian within an interval of time given in advance. To accelerate the readiness of the gyrocompass, it is advisable to start placing it into the meridian when the rotors of the gyroscopes are still being accelerated.

The Turbulent Boundary Layer of an Imperfect Gas, by I. I. Mezhirov, pp. 120-128.

Abstract: We consider the derivation of the equation of the turbulent boundary layer of an imperfect gas (e.g., dissociated air). We show that the relations which hold for an ideal gas and which are consequences of the equations of motion, continuity and energy only can be generalized to include the case of an imperfect gas by formally replacing temperature with enthalpy. We give examples of such relations.

Some Solutions of the Equations of One-Dimensional Magneto-hydrodynamics and Their Application to Problems of Shock Wave Propagation, by V. P. Korobeinikov and E. V. Riazanov, pp. 144-158.

Abstract: This paper points out cases of integrability of the equations describing one-dimensional motion of an electrically conducting gas with cylindrical and plane symmetry, the case of cylindrical symmetry being considered in greater detail. For steady motions with infinite conductivity a general solution of the equations is found, and a short description is given of the corresponding flows.

Unsteady self-similar and non-self-similar motions associated with shock waves are considered. A method is given for joining the solutions to gas at rest by means of a shock wave. Concrete cases are solved which may have application to the theory of impulsive gaseous discharge.

Application of Integral Relationships in Problems of Propagation of Strong Shock Waves, by G. G. Chernii, pp. 159-165.

Utilization of Similarity Considerations for the Improvement of the Convergence of a Process of Successive Approximation in Shell Analysis, by I. V. Svirskii, pp. 177-190.

Abstract: This paper represents an extension of a previous paper; the idea of the work is connected, on the one hand, with the studies of the Chinese scientist Chien in which the deflections of circular plates are determined by means of expansions of the stresses in powers of the deflection of the center of the plate, and, on the other hand, with the work of Muskhelishvili on the semi-nonlinear treatment of the problem of the determination of deflections of shells. In Muskhelishvili's work the nonlinear equations are linearized with respect to the higher harmonics of the deflection in stress functions, and the nonlinearity with respect to the fundamental harmonic of the deflection having the largest amplitude is taken into account. This permits the inclusion of the principal part of the nonlinearity connected with the large deflections and considerably simplifies the calculations.

At each step of the consecutive approximations presented in this work the equations are likewise found to be comparatively satisfactory with respect to the fundamental harmonics of the larger amplitudes; the determination of the higher harmonics of the deflections and the stress function is reduced to the solution of linear equations. Since the higher harmonics are usually small and their frequencies high, in determining them the curvature of the shell and the nonlinearities of the problems have been disregarded.

The Integration of the Equations of Unsteady Creep of Solid Bodies, by P. S. Kuratov and V. I. Rozenblium, pp. 195-199.

A Solution to the Equations of Magnetogasdynamics, by I. M. Iur'ev, pp. 233-237.

Abstract: An investigation of strong and weak discontinuities in magnetohydrodynamics is contained in a series of papers and books. In the following, the equations of planar flow in a magnetic field parallel to the velocity field are transformed under certain initial restraints to a linear equation of the Chaplygin type. We will apply the result to a problem in which there are no strong discontinuities.

JOURNAL OF ACOUSTICS (Akusticheskii Zhurnal).
Published by American Institute of Physics, New York.

Vol. 6, no. 1, July-Sept. 1960.

Ultrasonic Luminescence: A Survey, by I. E. El'piner, pp. 1-11.

Introduction: The phenomenon of luminescence of liquids in a field of ultrasonic waves, first observed in 1935, has become the object of extensive investigations. The importance of these investigations is contained in the fact that luminescence in liquids usually takes place under those conditions of sound irradiation for which the initiation of chemical and physical-chemical reactions becomes inevitable. From the scientific-practical standpoint there remains the important question: Is there an inherent relationship between these phenomena? In this respect a study of the nature of ultrasonic luminescence, its localization, spectral composition, and, finally, the power of the luminescent flux is of the utmost value.

The route of investigation, then, is laid out quite clearly. The role of cavitation in the phenomenon of luminescence and the effect of that chemical impurity or gas on the spectrum and the luminescence brightness of the sound-irradiated liquid are very clearly present. Repeated attempts have been undertaken to establish a correlation between the physical parameters of the investigated liquid and its capacity for ultrasonic luminescence. Definite regularities, connected with the problems of the origination of luminescent radiation, its spectrum, brightness and dependence of the latter on the phase of the variable acoustic pressure, on the frequency and intensity of the ultrasonic waves, have been observed. A comparison of the data on ultrasonic chemical elementary processes with the elusive manifestations and peculiarities of ultrasonic luminescence is exceptionally important in explaining the mechanism for the origination of chemical and biological reactions under the action of ultrasonic oscillations.

Instruments for Plotting Refracted Rays, by O. P. Galkin and V. S. Grigor'ev, pp. 20-25.

Abstract: The paper examines the fundamental design principles of automatic continuous operation instruments capable of plotting an aggregate of sound rays in a laminar inhomogeneous medium on the basis of a given law for the velocity of sound distribution (or velocity of sound gradient) over the vertical coordinate.

Investigation of the Propagation of Low Frequency Sound in Shallow Water, by V. S. Grigor'ev and F. I. Kryazhev, pp. 30-37.

Abstract: A procedure is described for the experimental investigation of the propagation of sound at low frequencies in shallow water. Experimental data are cited, characterizing certain features of the wave guide propagation of sound under the conditions of a shallow water reservoir and a shallow sea.

Propagation Velocity of Finite Amplitude Ultrasonic Waves in a Liquid, by L. K. Zarembo and V. V. Shklovskaya-Kordi, pp. 42-46.

Abstract: In a solution of methyl alcohol and water with a temperature-velocity coefficient of $\sim 10^{-6} \text{ deg}^{-1}$ the change in the velocity of the zeros of a wave of finite amplitude with an

increase in the potential on the radiating quartz from 100 v to 1.5 kv at a frequency of 1.5 mc was determined. The maximum accuracy of the determination of change in velocity was 0.003 per cent. Measurements with a constant surplus pressure (~ 1 atm), when the initiation of cavitation is impeded, show that with an accuracy of ~ 0.007 per cent the velocity of a finite amplitude zero-order wave with acoustic Reynolds numbers ~ 10 and Mach numbers $\sim 10^{-4}$ remains constant. With the initiation of cavitation in water in the indicated solution over a certain interval of propagation of the wave a very large discontinuous jump in velocity is observed.

Limits of Applicability of the Method of "Smooth" Perturbations in the Problem of Radiation Propagation Through a Medium Containing Inhomogeneities, by V. V. Pisareva, pp. 81-86.

Abstract: The author considers the problem of finding the limits of applicability of the method of "smooth" perturbations in solving the problem of the propagation of radiation through a medium containing inhomogeneities. In this connection the results obtained in the papers of Obukhov, Chernov and Scheffler for the mean-square values of the phase and amplitude fluctuations and amplitude correlation function are discussed. The conditions under which the effect of a layer with inhomogeneities on the through radiation can be replaced by the perturbing action of an equivalent phase screen are determined.

Experimental Study of Acoustic Streaming in Water, by E. V. Romanenko, pp. 87-91.

Abstract: An experimental investigation is made on the dependence of the velocity of acoustic streaming in water due to waves of finite amplitude on the pressure amplitude and waveform. The dependence resembles a square law when the waveform is sinusoidal or sawtoothed. With the transition of a sinusoidal waveform to a sawtooth, an anomaly is observed in the increase in acoustic streaming velocity with increasing wave amplitude.

The Absorption of Ultrasound in Electrolytes, by M. I. Shliomis, pp. 112-115.

Abstract: Two mechanisms for the absorption of sound in electrolytes are considered. One of these is connected with the electro-acoustic effect. The other is caused by the relative motion of the ions and solvent that arises with the propagation of sound in the solution. An equation is obtained for the absorption coefficient and a numerical determination of the effects discussed is given.

Ultrasonic Method for Measuring the Height of the Fluid Level in a Vessel by Means of Flexural Oscillations of a Thin Elastic Strip, by N. S. Ageeva, pp. 116-117.

Introduction: The velocity of propagation of flexural waves in an elastic plate submerged in a liquid differs from the velocity of propagation in the free plate in a vacuum or gas. This phenomenon can be applied to measuring the height of the fluid level in a vessel. The proposed method is based on a measurement of the phase difference of ultrasonic flexural waves reflected from the end of a thin, elastic strip immersed in the fluid when the height of the fluid level is changed.

Connection Between the Magnetic Properties and Sensitivity of Magnetostrictive Nickel-Zinc Ferrite Pickups, by A. D. Sokolov and Ya. S. Shur, pp. 130-132.

MEASUREMENT TECHNIQUES (Izmeritel'naya Tekhnika). Published by Instrument Society of America, Pittsburgh, Pa.

No. 5, May 1959.

The Theory of Errors of a Self-Compensating Pressure Gage, by V. I. Bakhtin, pp. 314-320.

Piezoelectric Acceleration Transducers, by V. P. Nenyukov, A. S. Zhmur and G. L. Lyapin, pp. 323-326.

An Aspect of the Effect of Temperature on the Resistance of a Conductor Covering a Surface, by B. I. Puchkin, p. 329.

Text: It is often necessary in the course of physical experiments to study the electrical properties of thin conducting layers fixed to a hard surface, and obtained by means of sputtering, deposition in vacuum, galvanically or otherwise. In this study an important part is occupied by the effect of temperature on the electrical

resistance of these layers. The work published on this question does not mention, however, the effect on the resistance of different coefficients of linear expansion of the layer and the underlay.

Let us use the expression representing the effect of temperature on the resistance of the conductor (c) rigidly connected to the surface (s) of an underlay which is not mechanically loaded

$$\frac{dR}{R_0} = \left\{ \left(\frac{1}{\rho_0} \cdot \frac{\partial \rho}{\partial T} \right)_c - \left(\frac{1}{l_0} \cdot \frac{\partial l}{\partial T} \right)_c + k^+ \left[\left(\frac{1}{l_0} \cdot \frac{\partial l}{\partial T} \right)_s - \left(\frac{1}{l_c} \cdot \frac{\partial l}{\partial T} \right)_c \right] \right\} dT$$

where

R = resistance of the conductor
 l = conductor length
 ρ = conductor resistivity
 k^+ = conductor strain-response coefficient
 T = temperature.

Subscript 0 denotes that the variable is taken at its initial temperature T_0 .

In studies at a certain degree of accuracy it is obviously desirable to consider temperature changes due to the previously indicated cause, especially for substances with a small resistance temperature coefficient and a large temperature strain response. Despite the importance of this question its solution is made more difficult owing to the fact that the data on strain response is given in the technical literature only for wires. It seems therefore most expedient to develop on a wide scale the study of the temperature strain response of various thin conducting layers. This work is becoming increasingly important at present since the study of the temperature strain response of thin layers is finding practical application in measurement techniques.

Reproducibility of the Boiling Temperature of Oxygen, by M. P. Orlova, pp. 330-333.

Introduction: The low reference point of the international temperature scale is the temperature of equilibrium between liquid oxygen and its saturated vapor at an atmospheric pressure derived from the formula

$$t_p = t_{760} = 1.26 \cdot 10^{-2} \cdot (p - 760) - 0.065 \cdot 10^{-4} \cdot (p - 760)^2$$

where p is the pressure of the saturated vapor of pure oxygen.

With the development of work at low temperatures the requirement of accuracy of calibration at the temperature of liquid oxygen increased, and thus arose the problem of revising the method of reproducing this temperature.

Secondary thermometers are usually calibrated against a condensation thermometer filled with pure oxygen. The basic errors in this method of calibration are due to the instability of the temperature of the oxygen bath filled with industrial liquid oxygen which contains nitrogen (up to 0.7 per cent) as its main admixture. In the course of evaporation the content of nitrogen decreases and changes the boiling temperature of the bath, which acquires a temperature "drift." Moreover, the bottom layers of the oxygen bath acquire a considerably higher temperature (up to 1.5 deg) than that of liquid oxygen equilibrium under atmospheric pressure. The excess temperature is periodically equalized by the formation of a large number of vapor bubbles, which produces temperature fluctuations in addition to the even "drift." Since the condensation thermometers have a considerably greater inertia than the platinum resistance thermometers (the inertia of a platinum thermometer of Strelkov's design approaches 9 sec, whereas that of a condensation thermometer from 18 to 20 sec) the calibration of these secondary thermometers by means of such a bath is not sufficiently accurate.

In 1948-1949 the Moscow State Institute of Mechanical and Measuring Instruments laboratories developed, for producing the oxygen point, the required method and equipment, which were subsequently widely applied in precision measurements carried out in the same laboratory, and which proved to be satisfactory.

We describe the design of the equipment and give the results of calibrating platinum thermometers at the oxygen point.

Photoelectric Amplifiers F17, by A. M. Kasperovich, pp. 348-354.

Introduction: Only in the last few years have photocompensation systems acquired recognition as simple and reliable means of obtaining high sensitivity in measuring voltage or current with a small zero drift. These systems can be used for solving many

problems of measurement and control in technology, physics, chemistry, biology, etc.

However, in manufacturing various photocompensations systems difficulties arise in making the unit consisting of the galvanometer, the optical system and the photosensitive elements (this unit is usually known as the photoelectric amplifier). Difficulties in practice limited the application of the photocompensation system.

In this connection the "Vibrator" plant has since 1957 started producing universal photoelectric amplifiers type F17 for use with other equipment.

No. 6, June 1959.

Precision Microscope for the Measurement of Small Dimensions, by V. E. Kostin, pp. 412-413.

Introduction: A precision tool microscope for the measurement of small dimensions by the noncontact method has been developed in the Standardization Bureau of the Committee of Standards, Measures, and Measuring Instruments.

Application of an Optical Inner Base Range Finder in a Factory Arrangement for Checking Dimensions of Up to 25 m, by B. E. Kostich, pp. 413-415.

Introduction: The required accuracy in manufacturing large machined parts is characterized by tolerances which are, on the average, equal to 0.0001 of the length to be measured. Parts of dimensions exceeding 6 m are difficult to produce with the indicated accuracy due to considerable errors of common measuring instruments, which sometimes exceed the tolerance values.

The usually applied measurement method with additional bases, while satisfactory with respect to accuracy, has a number of drawbacks, including the necessity of additional machining of technological reference bases and the impossibility of checking a part after it has been taken off the lathe or the assembly stand.

The present article provides a description of a new noncontact method for the inspection of parts by means of the universal factory measuring device TsIZM which has been developed by TsNIITMASH.

Visual Method of Determining the Nonlinearity of Sawtooth Voltage, by D. I. Ataev, pp. 435-440.

Introduction: The existing methods of measuring the nonlinearity of sawtooth voltage (the method of standard oscillators, the method of the shift of scanning lines, etc.) do not secure a sufficient accuracy and speed in measurements.

The proposed method allows a quick, convenient, and more accurate determination of the nonlinearity of sawtooth voltage.

Measurement of Impedances at Audio Frequencies by the Method of Magnetically Coupled Circuits, by O. G. Malkina, pp. 440-445.

Stepping Up the Input Resistance of Semiconductor Amplifiers, by G. N. Novopashennyi and P. V. Novitskii, pp. 454-456.

Introduction: A large resistance which increases the sensitivity of measuring instruments and reduces errors at low frequencies is often required at the input of amplifiers used in measurement techniques.

Summary:

1 Semiconductor triodes provide the possibility of securing amplifier input resistances of the order of several hundreds of kilohms in a comparatively simple manner.

2 In practice, it is feasible to obtain amplifier input resistances of the order of several megohms, but the question whether the use of such amplifiers is advisable must be solved for each concrete case.

Discharge Coefficients of Diaphragms and Nozzles, by S. S. Kivlis, pp. 469-473.

Introduction: The present article considers some results of our investigations of discharge coefficients of flow contraction devices.

OPTICS AND SPECTROSCOPY (Optika i Spektroskopiia). Published by Optical Society of America, Washington, D. C.

Vol. 8, no. 2, Feb. 1960.

Calculation of Photo-Ionization Cross Sections of Aluminum and Gallium Atoms, by L. A. Vainstein and G. E. Norman, pp. 79-80.

A Possible Mechanism of Electronic Excitation in Slow Atomic Collisions, by E. E. Nikitin, pp. 82-84.

Abstract: As follows from the general theory of atomic collisions, the effective threshold E_{eff} of the cross section, σ for electronic excitation in the adiabatic approximation exceeds the real threshold E_0 by a significant amount. For intermediate energies E of the colliding atoms ($E_0 < E < E_{eff}$), σ varies exponentially with E , so that the cross section, averaged over the Maxwellian energy distribution of the colliding atoms, is characterized by a temperature dependence of the Landau-Teller type. The latter is well known for the theory of inelastic molecular collisions.

New Variant of the Metallic Model of a Molecule, by L. A. Borovinskii, pp. 99-102.

Abstract: A model of molecules with short chains of conjugate bonds is proposed. The molecular skeleton, which consists of the nuclei and the σ -electrons, is represented by a rigid charge evenly distributed along a straight line which is the same length as the conjugate bond chain. The motion of π electrons in the field of this model of the skeleton is examined. An approximate separation of the longitudinal and transverse motion of the π electrons is presented. In a zero approximate, the longitudinal part of the potential function can be replaced by the potential function of an harmonic oscillator, and, correspondingly, the energy levels are determined to be the energy levels of the harmonic oscillator. For a more precise representation of the potential function the problem is solved using the semiclassical method of quantum mechanics. Calculated wave lengths of absorption bands are found to be in good agreement with experimental data.

Photoelectric Investigation of Raman Spectra of Gases at Low Pressures, by P. A. Bazhulin and Iu. A. Lazarev, pp. 106-109.

Introduction: Up till now, investigations of line shapes and widths in Raman spectra of gases at low pressures have been almost completely absent from the literature. This is obviously due to the existence of serious experimental difficulties. However, the study of this very parameter as a function of the structure of the molecule, type of vibration, temperature, pressure and state of aggregation would make it possible to solve one of the most important problems of molecular spectroscopy, namely, the nature of line width in Raman spectra. The question of the nature of line width has been raised by many authors. Very thorough experimental investigations of Raman spectra of the gases N_2 and O_2 at high pressures have been performed recently by Mikhailov, who showed in particular that the line width in the vibrational spectrum changes very little between 10 and 100 atm, and that the observed shape of these lines can be explained by a splitting of the Q branch due to vibration-rotation interaction. However, up till now, the question of the nature of line width in Raman spectra has remained unsolved.

It is therefore of considerable interest to perform further detailed investigations, beginning with the simplest nonpolar molecules whose structure is well known and whose molecular constants have been accurately measured at pressures close to atmospheric, so that molecular interaction can either be neglected or corrected for.

We have constructed an instrument which allowed us to record spectra photoelectrically, and to measure the intensities, widths and shapes of the rotational and vibrational lines in the Raman spectra of vapors and gases between 1 and 10 atm at 30-250 C.

Fig
len
A,

Fig
the
tion
of
len
ph
fro
fla

Re

bul
2
Pro
3
in
198

to

it
in

et

N

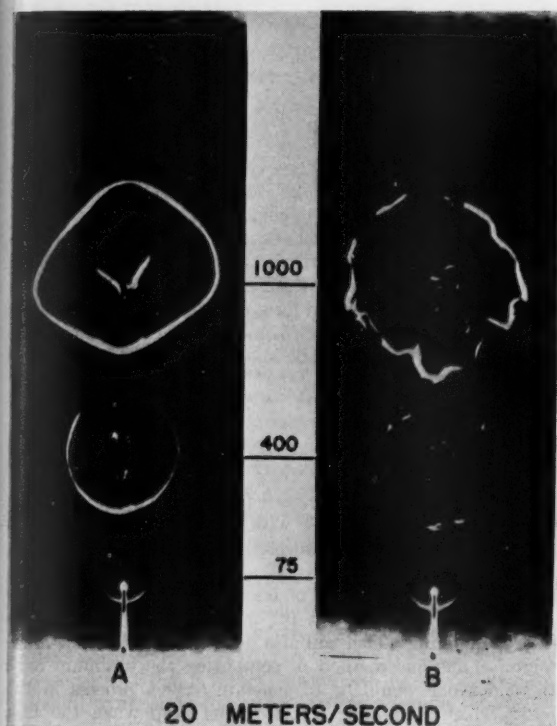


Fig. 1 Schlieren photographs of flames in laminar and turbulent flows of methane-air mixture. Flow speed 20 m per sec; A, laminar flow; B, isotropic turbulent flow. Delays in microseconds as indicated on vertical scale

Fig. 1 is presented. This is a Schlieren photograph taken at the Johns Hopkins Applied Physics Laboratory³ of a situation similar to that of (2). The figure shows the propagation of a flame kernel in laminar and in turbulent flow (turbulence intensity greater than in authors' experiments). The photograph shows no evidence of a thickening of the flame front and illustrates the increase in the wrinkling of the flame front with time.

References

1. Shefelkin, K. I., "Measurement of the Speed of Propagation of Turbulent Combustion," *ARS JOURNAL*, vol. 30, no. 1, Jan. 1960, pp. 76-77.
2. Bolz, R. E. and Burlage, H., "The Influence of Turbulence on Flame Propagation Rates," *JET PROPULSION*, vol. 25, no. 6, June 1955.
3. Seurlock, A. C. and Grover, J. H., "Propagation of Turbulent Flames," in "Fourth Symposium on Combustion," Williams and Wilkins Co., N. Y., 1953.

³ Courtesy of Dr. H. Lowell Olsen, Applied Physics Laboratory, The Johns Hopkins University.

Optimum Time to Rendezvous

JOHN M. EGGLESTON¹

NASA, Langley Research Center, Va.

When two vehicles are approaching one another in space, it is usually necessary to make small velocity corrections to insure that rendezvous occurs. These velocity corrections

Received June 6, 1960.

¹ Asst. Head, Flight Mechanics Branch, Aero-Space Mechanics Division. Member ARS.

NOVEMBER 1960

depend upon the instantaneous relative positions and velocities of the two vehicles, and the "time to rendezvous." The optimum time to rendezvous is that value of time requiring the smallest velocity correction. A method is presented for calculation of that optimum time.

IF ONE chooses a rotating set of rectangular coordinates fixed in the space station to define the relative motion of an approaching ferry vehicle, then it can be shown that the equations of relative motion of the ferry are given by

$$\begin{aligned}\ddot{x} - 2\omega\dot{y} + x\left(\frac{g_e r_e^2}{r_f^3} - \omega^2\right) &= \frac{T_x}{m} \\ \ddot{y} + 2\omega\dot{x} + (y + r_s)\left(\frac{g_e r_e^2}{r_f^3} - \omega^2\right) &= \frac{T_y}{m} \\ \ddot{z} + z\frac{g_e r_e^2}{r_f^3} &= \frac{T_z}{m}\end{aligned}\quad [1]$$

where $r_f = \sqrt{x^2 + (y + r_s)^2 + z^2}$. The coordinate system is shown in Fig. 1, and the assumption is made that the orbit of the space station is essentially circular, so that the radius r_s and the angular velocity ω are constant.

It can further be shown² that if r_f^{-3} is expanded into the Taylor series, so that

$$\begin{aligned}r_f^{-3} &= [x^2 + (y + r_s)^2 + z^2]^{-3/2} = \\ &= \frac{1}{r_s^3} \left[1 - 3\frac{y}{r_s} - \frac{3}{r_s^2} (x^2 - 4y^2 + z^2) + \dots \right]\end{aligned}\quad [2]$$

and the terms higher than first order are dropped, then the equations can be linearized in the form

$$\begin{aligned}\ddot{x} - 2\omega\dot{y} &= T_x/m \\ \ddot{y} + 2\omega\dot{x} - 3\omega^2 y &= T_y/m \\ \ddot{z} + \omega^2 z &= T_z/m\end{aligned}\quad [3]$$

where the angular velocity of the station is given by

$$\omega^2 = g_e r_e^2 / r_s^3 \quad [4]$$

² Clohessy, W. H. and Wiltshire, R. S., "Terminal Guidance System for Satellite Rendezvous," IAS Paper no. 59-93. Presented at the IAS National Summer meeting, Los Angeles, Calif., June 16-19, 1959.

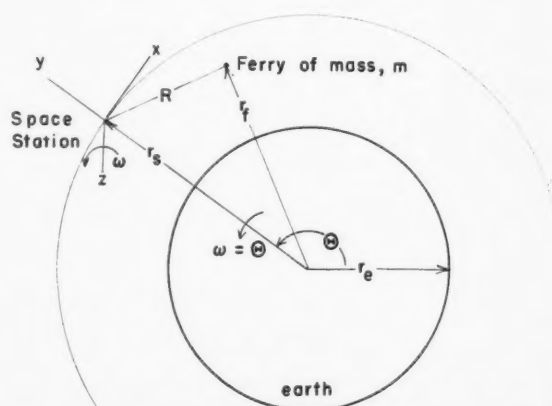


Fig. 1 Position of ferry vehicle with respect to rotating rectangular coordinate system of space station

The homogeneous solutions to these equations are

$$\begin{aligned}
 x &= 2 \left(2 \frac{\dot{x}_0}{\omega} - 3y_0 \right) \sin \omega t - 2 \frac{\dot{y}_0}{\omega} \cos \omega t + \\
 &\quad \left(6y_0 - 3 \frac{\dot{x}_0}{\omega} \right) \omega t + x_0 + 2 \frac{\dot{y}_0}{\omega} \\
 y &= \left(2 \frac{\dot{x}_0}{\omega} - 3y_0 \right) \cos \omega t + \frac{\dot{y}_0}{\omega} \sin \omega t + 4y_0 - 2 \frac{\dot{x}_0}{\omega} \\
 z &= z_0 \cos \omega t + (\dot{z}_0/\omega) \sin \omega t
 \end{aligned}
 \tag{5}$$

Note that z is uncoupled with x and y .

If it is desired that $x = y = z = 0$ at some time $t = \tau$ in the future, then the solutions of Equations [5] may be rearranged to give the required initial velocities (at $t = 0$) in terms of the initial position and the time until rendezvous. The expressions for the required velocities are

$$\frac{\dot{x}_0'}{\omega}(\tau) = \frac{1}{\Delta} [x_0 \sin \omega \tau + y_0 (6 \omega \tau \sin \omega \tau - 14 + 14 \cos \omega \tau)]$$

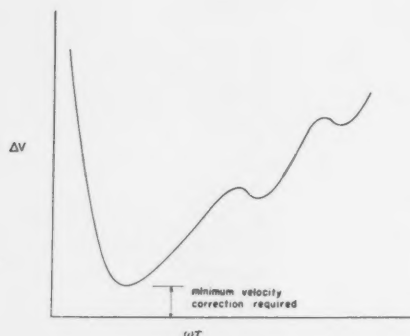


Fig. 2 Variation of total velocity change required to rendezvous as a function of time required for rendezvous

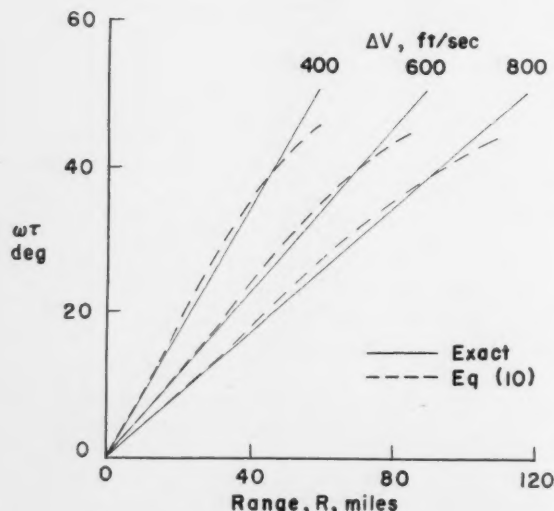


Fig. 3 Comparison of exact time until rendezvous (no velocity corrections required) and optimum time to rendezvous as computed by Equation [10]. Station in 300-mile circular orbit ($\omega = 0.001112$ rad/sec). Without terminal thrust control collision would occur at relative velocity ΔV

$$\frac{\dot{y}_0'}{\omega}(\tau) = \frac{1}{\Delta} [2x_0(1 - \cos \omega \tau) + y_0(4 \sin \omega \tau - 3\omega \tau \cos \omega \tau)]$$

$$\frac{\dot{z}_0'}{\omega}(\tau) = -z_0 \cot \omega \tau$$

where $\Delta = 3\omega \tau \sin \omega \tau - 8(1 - \cos \omega \tau)$. Primes are used to denote the fact that these are calculated velocities and not necessarily the actual relative velocities of the ferry.

Now at any particular instant during the approach of the ferry to the space station $x_0, y_0, z_0, \dot{x}_0, \dot{y}_0$ and \dot{z}_0 are specified (from radar or some other measurement). If, at that instant Equations [6] are computed for a particular value of τ (along with the specified values of x_0, y_0 and z_0), then the total change of velocity that must be made in order to rendezvous at time τ may be computed from

$$\Delta V =$$

$$\sqrt{[\dot{x}_0 - \dot{x}_0'(\tau)]^2 + [\dot{y}_0 - \dot{y}_0'(\tau)]^2 + [\dot{z}_0 - \dot{z}_0'(\tau)]^2} \tag{7}$$

Now if the process is repeated for a whole series of values of τ , then a variation of ΔV with τ may be plotted for that particular set of initial conditions ($x_0, y_0, z_0, \dot{x}_0, \dot{y}_0$ and \dot{z}_0). A typical plot is shown in Fig. 2. It may be noted that the curve will have a number of maxima and minima (one for each successive orbit), but the minimum of interest is the lowest minimum which will also usually be of the first minimum. Thus one method of computing the optimum time to rendezvous would be to generate such a process in the ferry vehicle and have the computer stop when the first minimum occurred. Another method would be to give the pilot an oscilloscope presentation of the plot and have him pick the minimum. In either case this particular value of τ or $\omega \tau$ would be used to compute the velocity corrections that must be made to effect the rendezvous.

Because these are an infinite number of extremums, the condition for directly computing the extremums, namely

$$\Delta V \frac{\partial \Delta V}{\partial \tau} = [\dot{x}_0 - \dot{x}_0'(\tau)] \frac{\partial \dot{x}_0'}{\partial \tau} +$$

$$[\dot{y}_0 - \dot{y}_0'(\tau)] \frac{\partial \dot{y}_0'}{\partial \tau} + [\dot{z}_0 - \dot{z}_0'(\tau)] \frac{\partial \dot{z}_0'}{\partial \tau} = 0 \tag{8}$$

leads to a very lengthy, complicated transcendental equation. However, if the optimum time to rendezvous is "small enough" (to be defined later), such that

$$\sin \omega \tau = \omega \tau - \frac{(\omega \tau)^3}{3!} + \frac{(\omega \tau)^5}{5!} - \dots$$

$$\cos \omega \tau = 1 - \frac{(\omega \tau)^2}{2!} + \frac{(\omega \tau)^4}{4!} - \dots$$

then this limits the infinite number of solutions to a finite number of solutions, only one of which will have any physical significance.

Such a calculation has been carried out, and the condition for the extremums was found to be

$$0 = a_0 + a_1(\omega \tau) + a_2(\omega \tau)^2 + a_3(\omega \tau)^3 + \dots \tag{9}$$

where

$$a_0 = x_0^2 + y_0^2 + z_0^2$$

$$a_1 = x_0 \frac{\dot{x}_0}{\omega} + y_0 \frac{\dot{y}_0}{\omega} + z_0 \frac{\dot{z}_0}{\omega}$$

Although the smallest positive roots of the cubic and quadratic expressions were computed, it was found that the sim-

plest and best results were obtained from using the one unique solution obtained from the linear expression $0 = a_0 + a_1 \omega\tau$, or

$$\tau_{\text{opt}} = \frac{(x_0^2 + y_0^2 + z_0^2)}{-(x_0\dot{x}_0 + y_0\dot{y}_0 + z_0\dot{z}_0)} = -\frac{R_0}{\dot{R}_0} \quad [10]$$

where R_0 is the line of sight range defined by

$$R_0 = (x_0^2 + y_0^2 + z_0^2)^{1/2}$$

Equation [10] then is an expression for the optimum time to rendezvous as determined from $(x_0, y_0, z_0, \dot{x}_0, \dot{y}_0, \dot{z}_0)$ or $(R_0 \text{ and } \dot{R}_0)$.

In order to determine the accuracy of the expression, the exact equations (i.e., Eqs. [1]) were solved for the case where the ferry vehicle was ejected from a space station (in a 300-mile circular orbit) at relative velocities of 400, 600 and 800 fps at time $t = 0$. The problem was run in negative time, so that the trajectories of the ferry vehicle prior to rendezvous would be computed. Thus for each value of $\omega\tau$ the solutions gave the values of $x, y, z, \dot{x}, \dot{y}$ and \dot{z} , and R and \dot{R} . The variation of R with $\omega\tau$ is shown in Fig. 3. It should be noted here that $\omega\tau$ represents the angular travel of the station around Earth, and as such it is more significant here than just elapsed time. Also shown (dotted lines in Fig. 3) are the values of $\omega\tau$ obtained from Equation [10] plotted as a function of R (the values of $\omega\tau$ were computed from the relative position and velocity of the ferry vehicle for each value of R). It can be seen in Fig. 3 that Equation [10] gave very good results out to an $\omega\tau = 40$ deg, and within 30 deg it continually improved as the time to rendezvous grew smaller. It can also be seen that the range of the ferry from the station was not important.

Tests on a digital computer using this equation in the guidance system to effect the rendezvous of a ferry vehicle

with a space station have shown this method of computing the optimum time to rendezvous to be very effective.

Conclusion

It is concluded that, if an optimum time to rendezvous exists during the latter stages of a two-body rendezvous, this condition can be computed with an approximation that improves as the time to rendezvous grows smaller. This expression, with its convergent characteristics, is very convenient for use with guidance systems that depend upon measurements of the relative range and range rate.

Nomenclature

a	= coefficients of polynomial in powers of $\omega\tau$
g_e	= acceleration due to gravity at Earth's mean surface
m	= mass of ferry vehicle
R	= line of sight range between ferry and station
r_f	= radial distance from center of Earth to ferry
r_s	= radial distance from center of Earth to station
r_e	= mean radius of Earth
T_x, T_y, T_z	= components of thrust in the x, y, z direction
t	= time
ΔV	= total velocity difference between ferry and station at rendezvous
x, y, z	= three components of rectangular coordinate system with center fixed in space station. z axis is perpendicular to plane of orbit with y always pointing away from the center of Earth (x and y rotate about z with angular velocity ω)
θ	= angular position of station as measured in plane of orbit about the center of Earth. ($\theta = \theta_0 + \omega\tau$)
τ	= time until rendezvous
ω	= $\dot{\theta}$
Sub zero used to denote initial or some particular instantaneous position and velocity.	
Dot over a variable denotes a derivative with respect to time.	

Approximate Solution for Rocket Flight With Linear-Tangent Thrust Attitude Control

JOHN S. MACKAY¹

NASA, Lewis Research Center, Cleveland, Ohio

An approximate solution to the equations of motion written with linear-tangent thrust attitude control is presented. The usefulness of this solution is evaluated by comparison with accurate numerical integration. This comparison shows that the solution gives accuracies sufficient for preliminary calculations for satellite boost vehicles and has a four-to-one speed advantage over numerical integration of the same accuracy level.

IN ORDER to perform preliminary design calculations for satellite boosting systems, a reasonably accurate estimate of the propellant requirements is necessary. Unfortunately, obtaining such an estimate usually requires the aid of trajectory calculations. When trajectory data are obtained by numerical integration of the nonlinear equations of motion, the computation time often seems excessive for preliminary calculations. This note, therefore, presents a closed form, approximate solution for the equations of motion which is about four times faster than stepwise numerical integration of equal accuracy.

Received June 2, 1960.

¹ Aeronautical Powerplant Research Engineer. Member ARS.

Since the approximate solution presented (details given in the Appendix) has been developed for use with satellite boosting systems, it utilizes an approximate form of the thrust attitude schedule that maximizes the mass in orbit. This schedule, as has been shown by Fried (1)² and other authors (2,3), is

$$\tan \psi = a - bt$$

This relation, usually referred to as the "linear-tangent" schedule, compares well with results obtained by numerical integration of the exact Euler-Lagrange differential equations.

Theoretically, the linear-tangent schedule should be followed through all phases of flight. However, the large angles of attack that can occur with this schedule preclude its use at low altitudes. Consequently, the first stage of powered flight, where aerodynamic forces are concentrated, must follow some other thrust attitude schedule, ordinarily a zero-lift schedule. It is therefore reasonable to neglect aerodynamic forces, for mathematical simplicity, during linear-tangent flight.

The vehicle burnout conditions for orbital missions are usually fixed (e.g., a circular orbit at a given altitude). For this case, it would be convenient if the closed form solution would allow an inverse-type calculation for the required trajectory parameters (e.g., a, b and t_f) from the known end conditions. This is not possible with the solution presented, and further simplifications do not appear profitable. For example, a somewhat simpler solution given in (3), which has about one tenth the accuracy of the present solution, also fails to allow an inverse computation. Consequently, the trajectory parameters must be solved for iteratively.

² Numbers in parentheses indicate References at end of paper.

Table 1 Error in flight parameters for a three-stage satellite boosting vehicle. Orbit altitude, 150 nautical miles

	Numerical integration	Approximate solution Error	% Error
r_3	2.3261208	-0.0459212	1.97
ψ_0	48.714°	+0.560°	1.30
b	0.00323681	+0.00004885	1.51

Accuracy

Usually, selection of a burnout altitude, velocity and attitude is necessary to specify an orbital mission. Therefore, at least that many vehicle and/or trajectory parameters must be variable to allow an iterative solution. One convenient set of variables is a , b and r_n with given first-stage burnout conditions.

Table 1 shows the resulting values of ψ_0 , b and r_3 for a typical three-stage vehicle and a 150-nautical-mile-orbit mission. Also shown are the results for the same case as computed by accurate numerical integration. The errors shown in Table 1 have been found acceptable for many preliminary design problems.

As will be seen in the Appendix, certain assumptions will be required which allow the error to increase with the burning time of any stage. As an example of the errors that can be caused by these assumptions, Fig. 1 shows the error in top-stage weight ratio for three-stage satellite boosting systems as a function of the total burning time of the upper two stages. The scatter in the points shown is due to other differences in the vehicles chosen, but the essential feature to be noted is that the error increases rapidly after $t = 400$ sec. This corresponds to about 200 sec per stage, which does not seem an unreasonable limitation for typical stages.

Appendix

Neglecting drag and using $\tan \psi = a - bt$, the equations of motion written for the coordinate system of Fig. 2 are

$$\begin{aligned} \ddot{x} + \frac{\mu x}{R^3} &= \frac{g_c F/W}{\sqrt{(a-bt)^2 + 1}} = f_x \\ \ddot{y} + \frac{\mu y}{R^3} &= \frac{g_c F(a-bt)}{W\sqrt{(a-bt)^2 + 1}} = f_y \end{aligned} \quad [1]$$

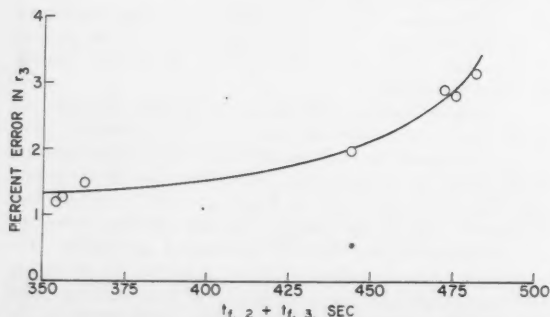


Fig. 1 Variation of third-stage weight ratio error with total upper-stage burning time for satellite boosting vehicles. Orbit altitude, 150 nautical miles

Assuming that the magnitude of R does not vary during one stage of powered flight, Equations [1] become

$$\begin{aligned} \ddot{x} + \mu x/R_0^3 &= f_x \\ \ddot{y} + \mu y/R_0^3 &= f_y \end{aligned} \quad [2]$$

where R_0 is the radius at the beginning of powered flight of the stage under consideration.

Using the method of variation of parameters, Equations [2] can be solved in the form

$$\begin{aligned} y_f &= (y_0 + A) \cos \omega t_f + (y_0/\omega + B) \sin \omega t_f \\ x_f &= (x_0 + D) \cos \omega t_f + (x_0/\omega + E) \sin \omega t_f \end{aligned} \quad [3]$$

where

$$\begin{aligned} A &= - \int_0^{t_f} \frac{f_y \sin \omega t}{\omega} dt \\ B &= \int_0^{t_f} \frac{f_y \cos \omega t}{\omega} dt \\ D &= - \int_0^{t_f} \frac{f_x \sin \omega t}{\omega} dt \\ E &= \int_0^{t_f} \frac{f_x \cos \omega t}{\omega} dt \end{aligned} \quad [4]$$

and

$$\omega = \sqrt{\mu/R_0^3}$$

Unfortunately there is no apparent way to integrate Equations [4] without some additional assumption. Considering the magnitude of ω , it can be seen that it will never exceed $\sqrt{\mu/R_0^3} = 1.2398 \times 10^{-3}$. Consequently, if $t < 200$ sec, which is a typical burning time for one stage, ωt will always be less than 15 deg. For such small angles, it is reasonable to assume

$$\sin \omega t \cong \omega t \quad \cos \omega t \cong 1.0 \quad [5]$$

Using Equations [5], Equations [4] can be integrated to give

$$\begin{aligned} A &= V_y(iG - iF \sin \bar{\psi} + H/b) \\ B &= V_y(F \sin \bar{\psi} - G)/\omega \end{aligned}$$

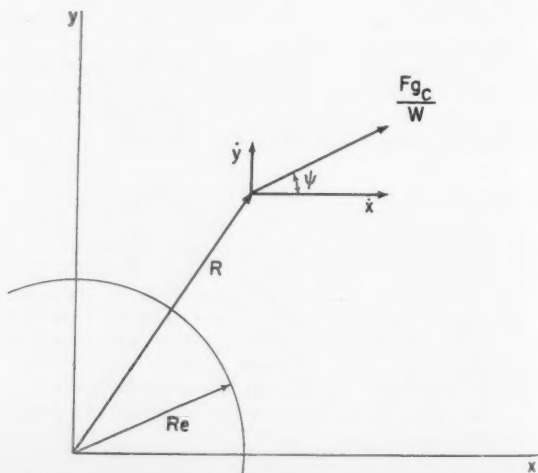


Fig. 2 Earth centered, nonrotating (inertial) coordinate system

$$D = V_j(\bar{t}F \cos \bar{\psi} + G/b)$$

$$E = V_j(F \cos \bar{\psi})/\omega$$

where

$$F = \ln \left\{ r \left[\frac{1 + \cos(\psi_f - \bar{\psi})}{1 + \cos(\psi_0 - \bar{\psi})} \cdot \frac{\cos \psi_0}{\cos \bar{\psi}} \right] \right\}$$

$$G = \ln \left(\frac{\sin \psi_f + 1}{\sin \psi_0 + 1} \cdot \frac{\cos \psi_0}{\cos \bar{\psi}} \right)$$

$$H = \frac{(\cos \psi_f - \cos \psi_0)}{\cos \psi_0 \cos \bar{\psi}}$$

Using the fact that the method of variation of parameters assumes

$$\dot{A} \cos \omega t + \dot{B} \sin \omega t = \dot{D} \cos \omega t + \dot{E} \sin \omega t = 0$$

the velocity components can be written as

$$\dot{y}_f = -\omega(y_0 + A) \sin \omega t_f + \omega(\dot{y}_0/\omega + B) \cos \omega t_f$$

$$\dot{x}_f = -\omega(x_0 + D) \sin \omega t_f + \omega(\dot{x}_0/\omega + E) \cos \omega t_f$$

Nomenclature

$a = \tan \psi_0$

$b = d(\tan \psi)/dt, 1/\text{sec}$

$F = \text{thrust, lb}$

$g_c = 32.174 \text{ fps}^2$

$I = \text{specific impulse, sec}$

$R = \text{radius from center of Earth} = \sqrt{x^2 + y^2}, \text{ ft}$

$r = \text{weight ratio} = W_0/W_f$

$t = \text{time measured from ignition of } i\text{th stage, sec}$

$V_j = g_c I, \text{ fps}$

$W = \text{weight} = W_0 - \dot{W}t, \text{ lb}$

$x = \text{distance along } x\text{-axis of Fig. 2, ft}$

$y = \text{distance along } y\text{-axis of Fig. 2, ft}$

$\mu = \text{gravitational constant} = 1.4077 \times 10^{16} \text{ ft}^3/\text{sec}^2$

$\psi = \text{angle between thrust vector and } x\text{-axis, deg}$

Subscripts

$e = \text{evaluated at surface of Earth}$

$f = \text{conditions at burnout of } i\text{th stage}$

$n = \text{nth stage}$

$0 = \text{conditions at } t = 0$

Superscripts

$(\cdot) = d/dt$

$(\bar{}) = \text{conditions at } t = W_0/\dot{W}$

References

1. Fried, B. D., "Powered Flight Trajectory of a Satellite," *JET PROPULSION*, vol. 27, no. 6, June 1957, pp. 641-643.
2. Okhotsimsky, D. E. and Eneyev, T. M., "Certain Variational Problems Connected with Launching of an Artificial Earth Satellite," Translated from *Progress in Physical Sciences* (in Russian), vol. 63, no. 1-2, Sept. 1957, by U. S. Joint Publications Research Service, Jan. 25, 1958.
3. Ross, S., "Composite Trajectory Yielding Maximum Coasting Apogee Velocity," *ARS JOURNAL*, vol. 29, no. 11, Nov. 1959, pp. 843-848.

Free Surface Condition for Sloshing Resulting From Pitching and Some Corrections¹

WEN-HWA CHU²

Southwest Research Institute, San Antonio, Texas

IN (1, 2 and 3)³ the free surface condition for pitching oscillations is valid, within the linearized theory, only for fixed gravitational field. If there is a tank fixed inertia field, corrections should be made. This note reports the more general free surface condition and the simple corrections needed in the final result on forces and moments.

Pitching oscillations may be expected to occur during vertical launching of a rocket. Let the acceleration resulting from thrust along the axis of rotational symmetry of the rocket be α_T' . The resultant acceleration \underline{a} in the gravitational field is $\underline{\alpha_T'} + \underline{G}$; the gravitational acceleration is \underline{G} , and the inertia acceleration is $-(\underline{G} + \underline{\alpha_T'})$; therefore the resultant

stead of α_T' along z . In a ground test, a is zero, and in the case of pitching motions first described, $\underline{G} = 0, a \rightarrow \alpha_T'$.

For simplicity, consider only a pitching oscillation, θ_y (Fig. 1). Neglecting the square of velocity, the pressure, in (x', y', z') coordinates, is

$$p' \cong -\rho \left[\left(\frac{\partial \phi'}{\partial t} \right)_{x', y', z'} + Gz' + z'a \cos(z', z) + x'a \cos(z, x') \right] \quad [1]$$

where an arbitrary function of time is absorbed in the definition of $\phi'(t)$. $\phi'(x', y', z', t) = \phi(x, y, z, t)$ is the velocity potential at the same point in (x', y', z') coordinates and (x, y, z) coordinates, respectively (Fig. 1). The position coordinates of the same point possess the relations

$$x = x' \cos(x', x) + z' \cos(z', x) \cong x' - \theta_y z'$$

$$z = x' \cos(z, x') + z' \cos(z, z') \cong z' + \theta_y x'$$

The velocity components at the same point are similarly related.

For small oscillations

$$\left(\frac{\partial \phi'}{\partial t} \right)_{x', y', z'} = \left(\frac{\partial \phi}{\partial t} \right)_{x, y, z} + \left(\frac{\partial \phi}{\partial x} \right)_{y, z, t} \left(\frac{\partial x}{\partial t} \right)_{x', y', z'} + \left(\frac{\partial \phi}{\partial y} \right)_{x, y, t} \left(\frac{\partial y}{\partial t} \right)_{x', y', z'} + \left(\frac{\partial \phi}{\partial z} \right)_{x, y, t} \left(\frac{\partial z}{\partial t} \right)_{x', y', z'} \cong \left(\frac{\partial \phi}{\partial t} \right)_{x, y, z},$$

body force is $-\rho \alpha_T' = -\rho a + \rho G$. In (1 and 3) and in the following discussion, a is assumed to be along the z axis in-

Received June 20, 1960.

¹ The results presented in this paper were obtained during the course of research carried out under the sponsorship of the Army Ballistic Missile Agency, Contract no. DA-23-072-ORD-1251.

² Senior Research Engineer, Department of Applied Mechanics.

³ Numbers in parentheses indicate References at end of paper.

hence

$$p'(x', y', z', t) = p(x, y, z, t) \cong -\rho \frac{\partial \phi}{\partial t} - \rho \alpha_T z + \rho G x \theta_y \quad [2]$$

where $\alpha_T = a + G$. In the space fixed coordinates, the free surface condition is

$$p' \cong 0 \text{ or } D'p'/D't = 0 \quad [3]$$

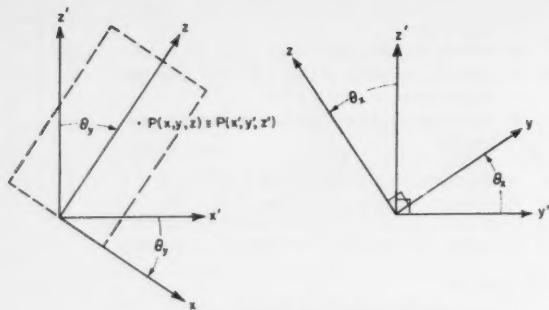


Fig. 1 Notation for pitching oscillations

Since

$$\begin{aligned} \left(\frac{\partial p'}{\partial t} \right)_{x', y', z'} &= \left(\frac{\partial p}{\partial t} \right)_{x, y, z} + \left(\frac{\partial p}{\partial x} \right)_{y, z, t} \left(\frac{\partial x}{\partial t} \right)_{x', y', z'} + \left(\frac{\partial p}{\partial z} \right)_{x, y, t} \left(\frac{\partial z}{\partial t} \right)_{x', y', z'} \cong \frac{\partial p}{\partial t} + \frac{\partial p}{\partial z} (x \dot{\theta}_y) \\ w' \left(\frac{\partial p}{\partial z} \right)_{x', y', t'} &= -\rho \alpha_T w \\ u' \left(\frac{\partial p'}{\partial x} \right)_{y', z', t} &= 0(\delta^2) \cong 0 \\ \frac{\partial p}{\partial t} &= -\rho \frac{\partial^2 \phi}{\partial t^2} + \rho G x \dot{\theta}_y \end{aligned}$$

thus, on the free surface

$$-\rho \frac{\partial^2 \phi}{\partial t^2} + \rho G x \dot{\theta}_y + x \dot{\theta}_y (-\rho \alpha_T) - \rho \alpha_T w \cong 0 \quad [4]$$

Similarly, if there is also a pitching angle $\theta_x(t)$, the free surface condition in the rotating axis is

$$\rho \frac{\partial^2 \phi}{\partial t^2} + \rho \alpha_T \frac{\partial \phi}{\partial z} + \rho (\alpha_T - G) x \dot{\theta}_y - \rho (\alpha_T - G) y \dot{\theta}_x \cong 0 \quad [5]$$

Only when there is no tank fixed acceleration a , $\alpha_T = G$, this condition reduces to

$$\frac{\partial^2 \phi}{\partial t^2} + \alpha_T \frac{\partial \phi}{\partial z} = 0 \quad [6]$$

Since this is the condition used in (1, 2 and 3), the results can only be applied to the case of fixed gravitational field without tank fixed acceleration. Corrections should therefore be made for the case $G = 0$, $a \rightarrow \alpha_T$.

Let

$$\phi = \phi_1 + \phi_2 + \left(\frac{-\theta_y}{i\omega} \right) x (\alpha_T - G) + \left(\frac{\theta_x}{i\omega} \right) y (\alpha_T - G)$$

so that ϕ_1 and ϕ_2 satisfy the boundary condition (Eq. [6]) for oscillatory motions

$$\theta_y = |\theta_y| e^{i\omega t} \quad \theta_x = |\theta_x| e^{i\omega t}$$

ϕ_1 is the potential obtained previously, and ϕ_2 is the correction potential such that

$$\frac{\partial \phi_2}{\partial \nu} = - \left\{ \cos(x, \nu) \left[(\alpha_T - G) \frac{\dot{\theta}_y}{\omega^2} \right] + \cos(y, \nu) \left[(\alpha_T - G) \left(\frac{-\dot{\theta}_x}{\omega^2} \right) \right] \right\}$$

where

$$\begin{aligned} \nu &= \text{normal to the tank wall} \\ \frac{\partial \phi_2}{\partial z} &= 0, \text{ at the tank bottom} \end{aligned}$$

This is equivalent to the addition of translational oscillations

$$x_b = -(\alpha_T - G) \frac{\dot{\theta}_y}{\omega^2} \quad y_b = +(\alpha_T - G) \frac{\dot{\theta}_x}{\omega^2}$$

in the notation of (3). The expressions for pressure become

$$\begin{aligned} p &= -\rho \left[\frac{\partial \phi_1}{\partial t} + \frac{\partial \phi_2}{\partial t} - \theta_y x (\alpha_T - G) + \theta_x y (\alpha_T - G) - G x \dot{\theta}_y + G y \dot{\theta}_x + \alpha_T z \right] \\ &= -\rho \left[\frac{\partial \phi_1}{\partial t} + \frac{\partial \phi_2}{\partial t} + \alpha_T z - x \alpha_T \dot{\theta}_y + y \alpha_T \dot{\theta}_x \right] \end{aligned}$$

Therefore, in the forces and moments of (3), x_b should be replaced by $x_b - (\alpha_T - G)(\dot{\theta}_y/\omega^2)$, y_b by $y_b + (\alpha_T - G)(\dot{\theta}_x/\omega^2)$, and in the terms due to static tipping, $G (= g)$ should be replaced by α_T . This includes the limiting case for a cylindrical tank. For cylindrical tank and $G = 0$, the corrected results agree with those in (4).

Mechanical analogy systems have been obtained for cylindrical tank with Earth fixed gravitational field, in (1 and 5). For tank fixed "gravitational" field, two different equivalent systems are given in (4 and 5), respectively. The latter includes the effect of damping and is consistent for simultaneous pitching and translation.

References

- 1 Schmitt, A. F., "Forced Oscillation of a Fluid in a Cylindrical Tank Undergoing Both Translation and Rotation," Convair Rep. ZU-T-069, Oct. 1956.
- 2 Bauer, H. F., "Fluid Oscillations in a Circular Cylindrical Tank," ABMA Rep. DA-TR-1-58, April 1958.
- 3 Chu, W. H., "Sloshing of Liquids in Cylindrical Tanks of Elliptic Cross-Section," ARS JOURNAL, vol. 30, no. 4, April 1960, pp. 360-363.
- 4 Schmitt, A. F., "Forced Oscillations of a Fluid in a Cylindrical Tank Oscillating in a Carried Acceleration Field—A Correction," Convair Rep. ZU-7-074, Feb. 1957.
- 5 Abramson, H. N., Chu, W. H. and Ransleben, G. E., Jr., "Representation of Fuel Sloshing by an Equivalent Mechanical Model," Technical Rep. no. 8, Contract no. DA-23-072-ORD-1251, Southwest Research Institute, June 1960.

Lateral Hydrodynamic Forces on an Airborne Missile Launched Underwater¹

THEODORE R. GOODMAN²

Allied Research Associates, Inc., Boston, Mass.

WHEN an airborne missile is propelled from a submerged submarine it must pass from the air environment of the submarine into the water environment of the sea. Subsequently, it must pass from the sea to the atmosphere. Both as it enters and leaves the sea it passes through a free surface. The hydrodynamic coefficients and the buoyancy are constant when the missile is fully submerged, but are time dependent when the missile is in the neighborhood of the free surface. The objectives of this note are to discuss when the free surface effects are significant and to derive the variation in the hydrodynamic coefficients during that time. The basic assumptions are:

- 1 Cavitation is absent.
- 2 The missile is a slender body of revolution.
- 3 The missile axis is almost normal to the interface.
- 4 The forward speed U is given.

It is to be emphasized that only the lateral force and moment will be considered; the longitudinal motion is already accounted for by assumption 4. That the missile is slender is essential to the theory; that it is a body of revolution is not essential, but it is sufficient to solve this case because the hydrodynamic forces on a symmetrical finned missile can be expressed, according to slender-body theory, in terms of an equivalent body of revolution.

If the Froude number is large, the boundary condition at the free surface is simply the condition that the velocity potential is constant. This boundary condition can be satisfied by placing a negative image above the free surface (see Fig. 1 for water exit case). Provided the trajectory is nearly normal to the free surface, the body and its image together may be taken to be one long slender body having positive area at the body, negative area at the image and no area in between. If the launch were not near-normal there would be a kink at the free surface in this combined body, and it could not be considered slender.

Now it is well known that slender-body theory implies that the lateral force at each section is independent of that at any other section. Hence, to within the approximation of slender-body theory, each section of the body is independent of the entire image, and the force on that section may be computed as though the image were absent and the body immersed in an infinite fluid. It may be shown that the body does not begin to feel the image until the time when the nose is within the order of a body radius of the free surface; during broach it continues to feel the image only in a layer of the order of a body radius from the free surface. Since the free surface effect is felt only in this small layer, and since the body is slender, this effect may be ignored, and the force per unit length computed as though the free surface were completely absent. The force per unit length for unsteady motions is given, for example, by Miles.³ The result for constant forward speed is

$$\frac{dF}{dx} = \rho \left(\frac{\partial}{\partial t} + U \frac{\partial}{\partial x} \right) S(x) w(x, t) \quad [1]$$

where

- ρ = mass density of water
 $S(x)$ = cross-sectional area distribution

- $w(x, t)$ = upwash velocity on body
 t = time from nose broach
 x = distance along body from nose

For rigid body motions

$$w(x, t) = w + q(x - x_0) \quad [2]$$

where

- w = normal velocity
 q = pitch rate
 x_0 = location of the c.g.

Equation [2] may be substituted into Equation [1] and the differentiations performed. The result is

$$\frac{dF}{dx} = \rho \dot{w} S(x) + \rho q (x - x_0) S(x) + \rho U w \frac{dS}{dx} (x) + \rho U q \frac{d}{dx} [(x - x_0) S(x)] \quad [3]$$

where the dot denotes differentiation with respect to time.

The moment per unit length taken about the center of gravity is obtained by multiplying Equation [3] by $-(x - x_0)$. The result is

$$\frac{dM}{dx} = -\rho \dot{w} S(x) (x - x_0) - \rho q (x - x_0)^2 S(x) - \rho U w (x - x_0) \frac{dS}{dx} (x) - \rho U q (x - x_0) \frac{d}{dx} [(x - x_0) S(x)] \quad [4]$$

If the body is fully submerged these equations may be integrated over the entire length of the body from zero to l . The result will be four contributions to the force, and four to the moment, proportional respectively to \dot{w} , q , w and q . The integrals which are obtained are the slender-body results for the various stability derivatives. During broach the integrations must be carried out only over the submerged portion of the body since the density of air is negligible compared with the density of water. Thus, for the water entry

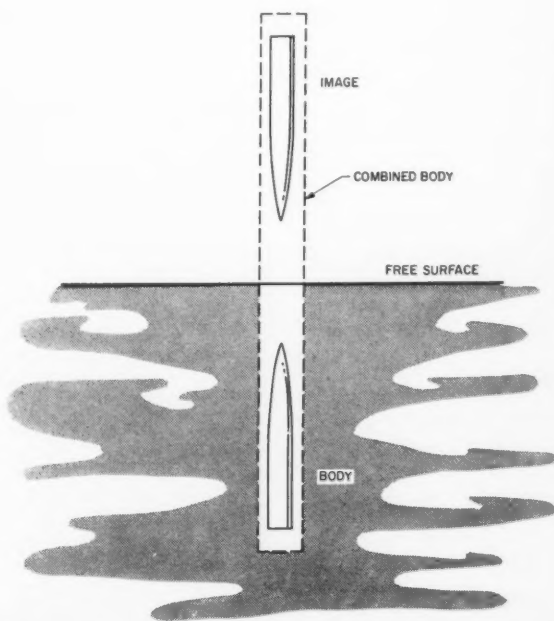


Fig. 1 Sketch of missile and image, showing the combined body

Received May 20, 1960.

¹ This work was performed under Contract Nonr-2343(00) for the Office of Naval Research.

² Manager, Department of Applied Mathematics.

³ Miles, J. W., "The Potential Theory of Unsteady Supersonic Flow," Cambridge University Press, 1959, chap. 12.

Table 1 Formulas for time variation of hydrodynamic stability derivatives

	F/F_s	M/M_s
w	$\frac{S(Ut)}{S(l)}$	$\frac{(Ut - x_0) S(Ut) - \int_0^{Ut} S(x) dx}{(l - x_0) S(l) - \text{volume}}$
\dot{w}	$\frac{\int_0^{Ut} S(x) dx}{\text{volume}}$	$\frac{\int_0^{Ut} (x - x_0) S(x) dx}{\text{volume moment}}$
q	$\frac{(Ut - x_0) S(Ut)}{(l - x_0) S(l)}$	$\frac{(Ut - x_0)^2 S(Ut) - \int_0^{Ut} (x - x_0) S(x) dx}{(l - x_0)^2 S(l) - \text{volume moment}}$
\dot{q}	$\frac{\int_0^{Ut} (x - x_0) S(x) dx}{\text{volume moment}}$	$\frac{\int_0^{Ut} (x - x_0)^2 S(x) dx}{\text{volume moment of inertia}}$

problem the integrations should be performed from zero to Ut which is the part that is submerged; for the water exit problem on the other hand, the integrations should be performed from Ut to l for the same reason. If this calculation is performed literally, then during complete submergence slender-body stability derivatives would have to be used, and it would be impossible to take advantage of the more accurate derivatives which may have been obtained experimentally. It is suggested, therefore, that the results be scaled up or down by using experimental values for the fully submerged body and that slender-body theory be used only to give the time dependence during broach.

As a typical example of the falloff or buildup of a derivative, consider the force due to pitch rate which may be obtained from the last term in Equation [3]. For water exit

apparent momenta. Upon integrating Equation [3] for water entry, this becomes

$$F = \frac{d}{dt} \left[w \rho \int_0^{Ut} S(x) dx \right] + \frac{d}{dt} \left[q \rho \int_0^{Ut} (x - x_0) S(x) dx \right] \quad [8]$$

with a similar result for water exit.

The quantity $\rho \int_0^{Ut} S(x) dx$ is, thus, a varying additional apparent mass, and so is $\rho \int_0^{Ut} (x - x_0) S(x) dx$. However, simply accounting for the variation of the various stability derivatives, as illustrated by Equation [6], for example, automatically accounts for the varying apparent mass. The formula for the moment can only be partly grouped in the same way. The result for water entry is

$$M = - \frac{d}{dt} \left[w \rho \int_0^{Ut} (x - x_0) S(x) dx \right] - \frac{d}{dt} \left[q \rho \int_0^{Ut} (x - x_0)^2 S(x) dx \right] + U \left[w \rho \int_0^{Ut} S(x) dx + q \rho \int_0^{Ut} (x - x_0) S(x) dx \right] \quad [9]$$

this becomes

$$F = \rho U q \int_{Ut}^l \frac{d}{dx} [(x - x_0) S] dx = \rho U q [(l - x_0) S(l) - (Ut - x_0) S(Ut)] \quad [5]$$

Normalizing with respect to the value for full submersion F_s , there is obtained

$$\frac{F}{F_s} = 1 - \frac{(Ut - x_0) S(Ut)}{(l - x_0) S(l)} \quad 0 < Ut < l \quad [6]$$

In a similar manner, for water entry

$$\frac{F}{F_s} = \frac{(Ut - x_0) S(Ut)}{(l - x_0) S(l)} \quad 0 < Ut < l \quad [7]$$

It is interesting to observe that the total integrated force can be grouped in the form of two exact differentials, or, which is the same thing, in terms of the rates of change of

It is recommended that in performing trajectory calculations during water entry or exit, the stability derivatives be allowed to grow and diminish, respectively, according to slender-body theory, as illustrated by Equation [6]. For the sake of completeness, the variation of all the stability derivatives is given in Table 1. Each of them has been normalized with respect to the fully submerged value so that an experimentally determined coefficient may be used. The results are given for water entry only, since, in general, the results for entry and exit are related by the equation

$$(F/F_s)_{\text{exit}} = 1 - (F/F_s)_{\text{entry}} \quad [10]$$

with a similar result for the moments.

The volume moment and volume moment of inertia are to be taken about the center of gravity. For variable forward speed simply replace Ut by distance traveled throughout.

Comparison of Gas-Turbine Cycles for Space Applications

ROBERT E. ENGLISH¹ and HENRY O. SLONE²

Lewis Research Center, NASA, Cleveland, Ohio

On the basis of the radiator area required for rejecting cycle waste heat, Rankine vapor cycles are far superior to the basic Brayton gas cycle for space turbogenerating powerplants. The present analysis considers modifications of the basic Brayton cycle and compares the modified cycles to the basic cycle with radiator area as the criterion of merit. The results indicate that reductions in radiator area attainable by modifying the basic Brayton cycle are small, and thus the competitive position of gas-turbine cycles relative to Rankine vapor cycles is unchanged.

A MOST important item in the design of a space turbogenerating powerplant is the weight of the overall unit. Studies have shown that the radiator necessary for rejecting the cycle waste heat is the largest and heaviest component of the powerplant (1).³ One means of obtaining a lightweight powerplant is to select a cycle working fluid and establish cycle operating conditions that will result in the smallest radiator area. Using the criterion of minimum radiator area per unit of power output, (1) showed that for a given turbine inlet temperature the minimum radiator area obtainable with a basic gas-turbine Brayton cycle is 10 times that attainable with Rankine vapor cycles. Similar results were obtained in (2 and 3). In general, these analyses considered that the cycle working fluid should be the vapor of a metal such as mercury, rubidium, potassium or sodium.

In order for the competitive position of gas-turbine powerplants to be better evaluated, the reductions in radiator area that could be obtained by modifying the basic Brayton cycle should be determined. The present analysis considers four modifications of the basic Brayton cycle: Regeneration, one reheat, two reheats and compressor intercooling. The modified Brayton cycles are compared with the basic cycle for a range of cycle component pressure losses, with minimum radiator area as the criterion of merit.

Computations

The procedure used for relating radiator surface area per kilowatt of electric power output and the various cycle parameters is like that used in (1) for the basic Brayton cycle, except that polytropic efficiencies were used for the compressor and turbine instead of adiabatic efficiencies. Radiator area is expressed in terms of the radiator-area parameter AT^4/P , where A is radiator area, ft^2 ; T is turbine inlet temperature, R ; and P is power output, kw . This parameter was chosen because it specifies radiator area in a form independent of turbine inlet temperature. The following component characteristics were assigned: Compressor and turbine polytropic efficiencies (0.88), product of generator and mechanical efficiencies (0.95), ratio of specific heats (1.66), regenerator effectiveness (0.90) and radiator emissivity (0.90). Increasing either the efficiencies, regenerator effectiveness or emissivity, reduces radiator area. Changing ratio of specific heats from 1.66 to 1.40 also reduces radiator area.

Since radiator area is sensitive to pressure loss in the various powerplant components, a range of pressure loss was assumed for each component. This pressure loss was expressed as the loss in pressure across the component divided by the pressure at the inlet to that component and is herein called

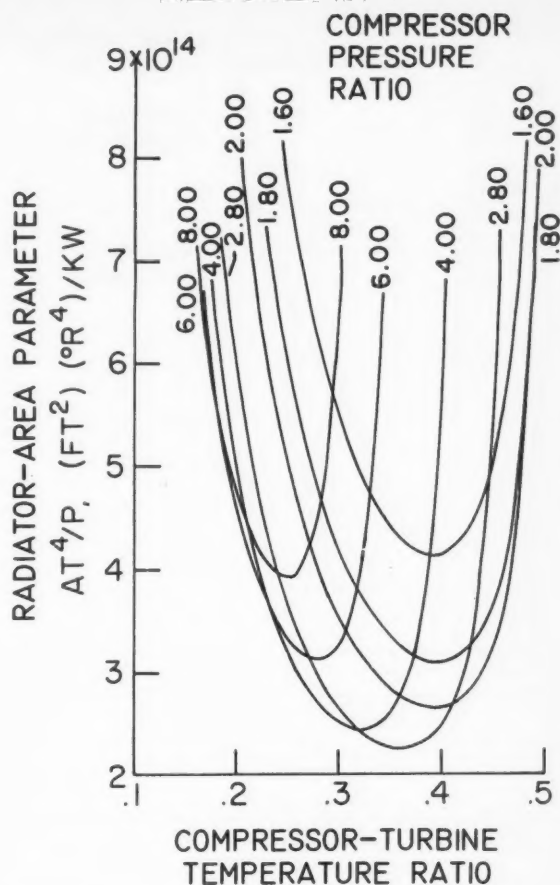


Fig. 1 Radiator area parameter for basic Brayton cycle with component pressure loss ratio of 0.05

"pressure loss ratio." Equal pressure loss ratios were assigned for each component, and the value was varied from 0.025 to 0.15. The following components were assigned pressure losses: Heat source, radiator, regenerator, reheater and intercooler. For those cycles that included either reheating or intercooling, an additional pressure loss was assumed for the ducting to or from the reheater or intercooler; for each duct, the value of pressure loss ratio was taken as half that for the reheater or intercooler.

Results and Discussion

Typical results are shown in Fig. 1 for the basic Brayton cycle. Minimum radiator area is obtained for one particular combination of compressor pressure ratio and cycle temperature ratio (defined as the ratio of compressor inlet temperature to turbine inlet temperature). Various such minima have been replotted in Figs. 2 and 3. Fig. 2 shows that none of the modified cycles is clearly superior to the basic Brayton cycle for any of the values of pressure loss ratio considered; in fact, the basic cycle is best except for the lowest values of pressure loss ratio. In most cases, the adverse effect of the component's pressure loss more than offsets the desirable effect of the improved cycle that otherwise might result. Although only division of turbine work into two equal parts is shown in Fig. 2 for the reheating cycles, division of turbine work in a manner that minimizes radiator area was also considered; the resulting radiator areas were essentially unchanged from those for equal splitting of the turbine work. Variation in

Received June 2, 1960.

¹ Associate Chief, Power Production and Shielding Branch, Nuclear Division.

² Aeronautical Research Scientist.

³ Numbers in parentheses indicate References at end of paper.

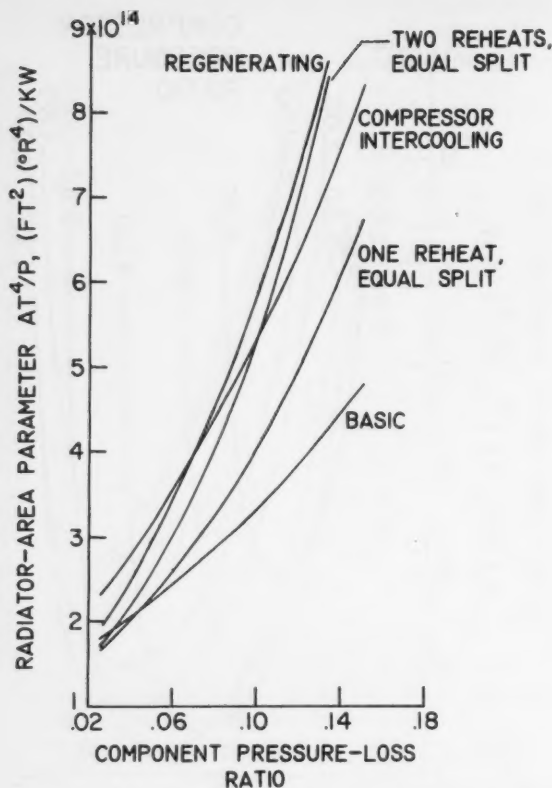


Fig. 2 Comparison of minimum radiator areas for various gas-turbine cycles

regenerator effectiveness from 0.90 to 0.70 affected minimum radiator area to only a small extent (7 per cent or less).

From Fig. 2, the superiority of the Rankine vapor cycles over the gas-turbine cycles can be inferred. For example, even for the lowest pressure loss ratio shown in Fig. 2, the radiator area parameter is about five times the value corresponding to that for the Rankine vapor cycle in Fig. 5 of (1).

In practice, the pressure loss ratio for the various heat exchanging components might not be equal as assumed. On this basis, the comparison in Fig. 2 may appear to be unfair to the modified cycles. In order that the value of radiator area parameter may be determined for any distribution of pressure loss among the powerplant components, Fig. 3 presents the results in terms of overall pressure loss ratio; overall pressure loss ratio is defined as 1.0 minus the product of the pressure ratios across the various heat exchanging components. Fig. 3 shows that, if the reheater and its attendant ducting have no pressure losses, the radiator area required for the reheat cycle is less than for the basic cycle.

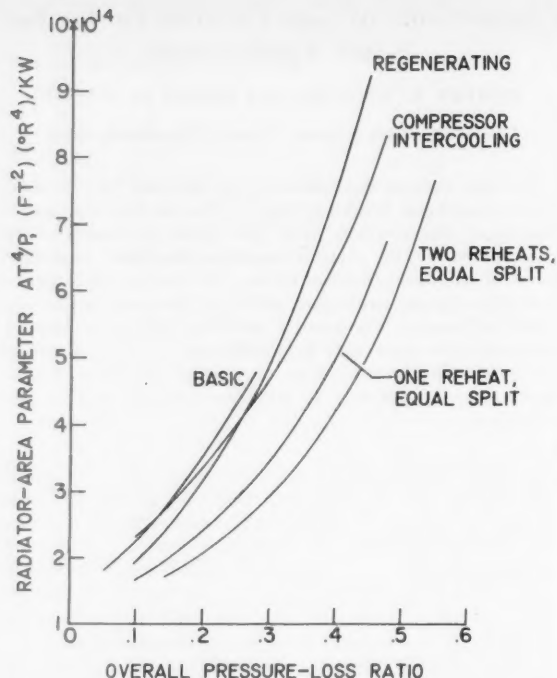


Fig. 3 Comparison of minimum radiator areas for various gas-turbine cycles on the basis of overall pressure loss ratio

If, for example, the overall pressure loss ratio for the basic cycle is 0.15, the radiator area parameter is 2.85×10^{14} ; a one-reheat cycle having the same radiator area parameter is allowed an overall pressure loss ratio of 0.245, and this corresponds to a total pressure loss in the reheater and its ducting to and from the turbine of 11 per cent [i.e., $1 - (1 - 0.245)/(1 - 0.15)$]. If the reheater has less than 11 per cent pressure loss, the required radiator area will be less than that for the basic cycle; and, conversely, if the pressure loss is higher, the required radiator area will also be higher for the reheating cycle.

Conclusion

On the basis of the results obtained in this analysis, reductions in radiator area attainable by modifying the basic Brayton cycle appear, at best, to be so small that the competitive position of gas-turbine cycles relative to Rankine vapor cycles for space power systems is not changed.

References

- 1 English, R. E., Slone, H. O., Bernatowicz, D. T., Davison, E. H. and Lieblein, S., "A 20,000-Kilowatt Nuclear Turboelectric Power Supply for Manned Space Vehicles," NASA Memo 2-20-59E, 1959.
- 2 Mackay, D. B., "Powerplant Heat Cycles for Space Vehicles," IAS Paper no. 59-104, 1959.
- 3 Martin, C. G., "Dynamic Heat Engines—Fundamental Concepts for Lightweight, Compact Application," Seminar on Advanced Energy Sources and Conversion Techniques, Nov. 1958, ASTIA no. Ad 208301.

Rocket Propulsion With Nuclear Power¹

E. L. RESLER Jr.² and N. ROTT³

Cornell University, Ithaca, N. Y.

A VERY attractive possibility for rocket propulsion with nuclear power involves the use of hydrogen as a "propellant," i.e., as the substance to be heated by nuclear energy and exhausted in the rocket. The well-known advantage of hydrogen is its inherent high specific impulse. One possibility for transmitting the energy to the hydrogen is direct heat transfer. It seems best for this purpose to carry liquid hydrogen under low pressure (to make the rather voluminous containers light) and to pressurize the liquid hydrogen before entering the reactor, so that the heat exchanger can be kept small. The liquid pump has only a small power requirement. It would be possible to lead the hot high pressure hydrogen gas, coming out of the reactor, into a turbine, then to reheat the hydrogen after leaving the turbine in the reactor, and then dump the turbine power (minus the small liquid pump power) into the gas, which therefore will become hotter than the maximum reactor temperature. The best way of "dumping" is presumably the use of a compressor. The scheme is illustrated in Fig. 1.⁴ The main engineering difficulty is reheating the gas after it leaves the turbine, at low pressure; this leads to an impractically large heat exchanger. Therefore another scheme is proposed which avoids this difficulty. (Actually, if this difficulty does not turn out to be insurmountable, both schemes can be used simultaneously.)

The new scheme calls for a closed-cycle regenerative gas turbine working between the reactor (as a heat source) and the liquid hydrogen, which serves as a heat sink. The power of the gas turbine is dumped electrically (or otherwise) into the hydrogen coming out of the reactor. The scheme is shown in Fig. 2.

The closed-cycle regenerative gas turbine is filled with high pressure gas (in this case helium must be used—the only gas which condenses below H_2). The pressurization of the closed cycle and the radical reduction of all heat transfer surfaces by this stratagem is the essence of the well-known invention, made by Akeret and Keller. The process (also called the AK process and described in many standard textbooks) calls for very large regenerators, which become manageable by the pressurization.

Before considering the details of the AK process, let the maximum gain be calculated which is obtainable from the scheme given in Fig. 2. Let Q_+ be the heat given by the reactor to the engine, and Q_- be the rejected heat which evaporates the hydrogen, so that $Q_- = GL$, where G is the hydrogen weight flux and L is the latent heat of H_2 . The enthalpy gain of the hydrogen by "dumping" the engine power is $Q_+ - Q_-$, so that the specific enthalpy of hydrogen after dumping will be

$$c_p T_F = c_p T_R + L(Q_+/Q_- - 1) \quad [1]$$

where

T_F = final temperature after dumping
 T_R = reactor temperature

This formula is exact and can be used for any engine; the gain is naturally given by the second term on the right. The maximum is obtained, when for a "reversible" process, fol-

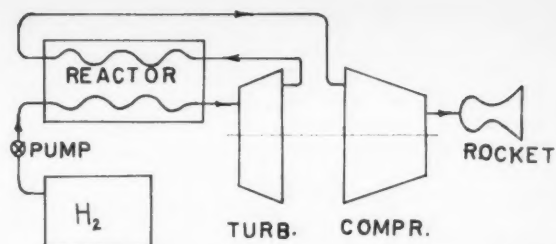


Fig. 1 Reheat scheme for nuclear powered rocket using hydrogen

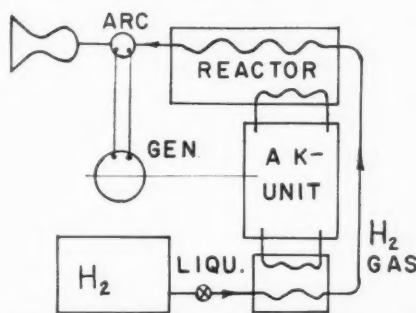


Fig. 2 New scheme for nuclear powered rocket using hydrogen. A closed cycle gas turbine (AK unit) works with the reactor as heat source and the liquid H_2 as heat sink. The power generated is dumped into the hydrogen

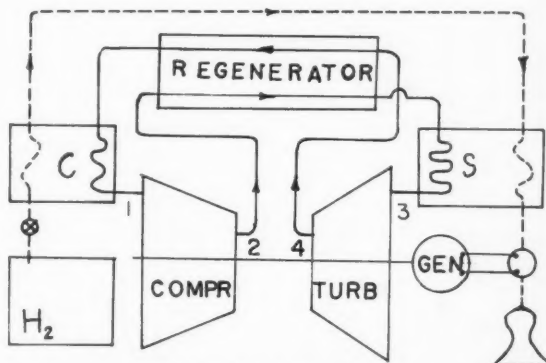


Fig. 3 Scheme of the closed cycle gas turbine. C = cooler, S = superheater (in the reactor). Numbers refer to the subscripts used for the corresponding temperatures and pressures

lowing the second law

$$\frac{Q_+}{Q_-} = \frac{T_R}{T_L} \quad [2]$$

where T_L is the temperature of the liquid hydrogen. With $T_R = 1300$ K (say) and $T_L = 20$ K, truly fabulous gains can be obtained. The purpose of this note is to show that even with a real AK process, the gain is interesting.

Fig. 3 shows the schematic AK process. The regenerator makes it possible for the turbine (and the compressor) to work with reasonably low pressure ratios, and yet keep the efficiency high, namely, near-Carnot, by use of the regenerative heat exchanger. For a perfect heat exchanger, with infinite surface and zero temperature difference across the exchanger,

Presented at the ARS Semi-Annual Meeting, Los Angeles, Calif., May 9-12, 1960.

¹ This work was carried out under contract with Thompson Ramo Wooldridge, Inc., Cleveland, Ohio.

² Professor of Aeronautical Engineering.

³ Now Professor of Engineering, UCLA.

⁴ This system was proposed by Akeret (unpublished); see also Goldsmith, M., ARS JOURNAL, vol. 29, no. 8, Aug. 1959, p. 600.

the process in the T - S diagram is given in Fig. 4. For this cycle

$$\frac{Q_+}{Q_-} = \frac{T_3 - T_4}{T_2 - T_1} \quad [3]$$

For 100 per cent efficiency machinery

$$\frac{T_3}{T_4} = \frac{T_2}{T_1} = \left(\frac{p_2}{p_1}\right)^{(\gamma-1)/\gamma} \quad [4]$$

so that

$$\frac{Q_+}{Q_-} = \frac{T_3}{T_2} = \frac{T_R}{T_2} \quad [5]$$

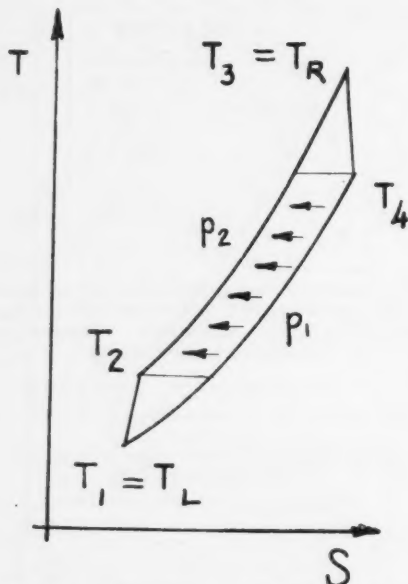


Fig. 4 Temperature-entropy diagram of the closed cycle process with ideal (infinite) regenerator

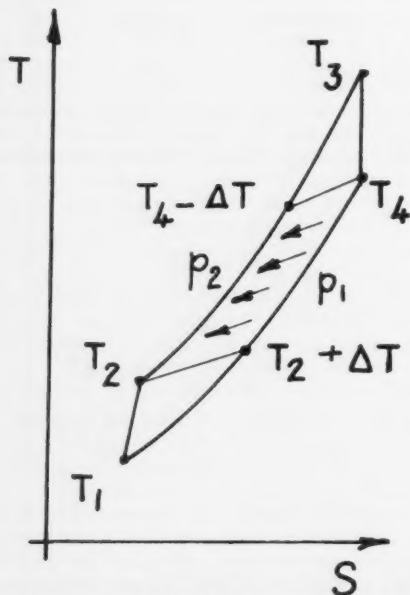


Fig. 5 T - S diagram of the closed cycle process with real (finite) regenerator

The increase of T_L to T_2 is the first correction to be applied to the optimal value, Equation [2]. A value of $T_2/T_1 = 1.75$ would lead, with $\gamma = \frac{5}{3}$, to a reasonable pressure ratio of about 4. With finite efficiency of the machinery, it is safer to calculate with $T_2/T_1 = 2$.

Now, the effects of the finite regenerator size are to be introduced. The effects are twofold: First, there will be pressure losses in the flow through the regenerator. For the configurations under consideration, these losses are not critical; one has to choose the ratio p_2/p_1 across the compressor big enough so that the pressure losses are small compared to this pressure ratio. On the other hand, the effect of p_2/p_1 on the process was already considered by replacing T_L with T_2 , and for the present preliminary estimates it will suffice to take only this loss into account.

The second loss in the regenerator, however, gives a very important contribution. A finite temperature difference ΔT (say) will be needed for the flow of the heat from the low pressure gas after turbine to the high pressure gas after compressor. In a perfect counterflow exchanger, with constant specific heats on both side, the difference ΔT can be taken as constant at any spot of the regenerator, so that the temperature is decreased to $T_4 - \Delta T$ before entering the superheater and increased to $T_2 + \Delta T$ before the cooler. The modified process is shown in Fig. 5. Now

$$Q_+ = c_p [T_3 - (T_4 - \Delta T)]$$

and

$$Q_- = c_p (T_2 + \Delta T - T_1)$$

so that $Q_+ - Q_-$ is the same as before, but

$$\frac{Q_+ - Q_-}{Q_-} = \left(\frac{T_3}{T_2} - 1\right) \frac{T_2 - T_1}{T_2 - T_1 + \Delta T} \quad [6]$$

Introduced in Equation [1], the formula for T_F is, using $T_2 = 2T_1 \equiv 2T_L$

$$T_F = T_R + \frac{L}{c_p} \frac{T_L}{T_L + \Delta T} \left(\frac{T_R}{2T_L} - 1\right) \quad [7]$$

For H_2 , L is 108 cal per gm and $c_p = 3.5$ cal/gm/deg, so that L/c_p equals 31 deg; it boils at $T_L = 20$ K. Take a reactor temperature of $T_R = 1300$ K, and assume $\Delta T = 20$ K. (The regenerator size necessary for this will be given later.) Then

$$T_F = 1790 \text{ K}$$

The corresponding specific impulse (with zero counterpressure) is

$$I_{sp} = 750 \text{ sec}$$

Now the size of a regenerator which is needed to accomplish the heat transfer with the value of ΔT assumed before will be estimated. The counterflow heat exchanger is assumed to consist of a bundle of pipes with diameter d and length l , carrying the high pressure helium, after the compressor (temperature T_2), to the superheater (temperature $T_4 - \Delta T$, see Fig. 5). The hot helium leaving the turbine is carried in the volume between the pipes and regenerator wall.

If the pressure loss in the pipe is, in conventional notation

$$\Delta p = \lambda \frac{l}{d} \frac{1}{2} \rho v^2 \quad [8]$$

then the film coefficient, according to the well-known Reynolds analogy, is

$$h = (1/8) \lambda c_p \rho v \quad [9]$$

Let ΔT_1 be the difference between the high pressure gas and

the pipe wall, a constant for counterflow along the tube. The heat balance is

$$\frac{\pi}{4} d^2 \rho v c_p (T_4 - \Delta T - T_2) = \pi d l h \Delta T_1 = \frac{\pi}{8} \lambda c_p \rho v d l \Delta T_1$$

or

$$\frac{l}{d} = \frac{2}{\lambda} \frac{T_4 - T_2 - \Delta T}{\Delta T_1} \quad [10]$$

For the present estimate, assume $\Delta T_1 = \frac{1}{2} \Delta T$, that is, the same temperature difference exists between the wall and the gas on either side. The temperature T_4 is about 660 K for the process represented in Fig. 4. Finally, for λ (which is a function of the Reynolds number) the "typical" value $\lambda = 0.02$ will be assumed. Thus

$$l/d = 6000$$

If the diameter is 0.5 cm, a length of 30 m is needed.

The number of tubes needed depends on the admissible pressure drop in the regenerator. Here, only the results of a preliminary but conservative estimate will be given. The number of tubes is proportional to the power level, and varies inversely with the pressure level in the closed system. For 1

megawatt generated by the AK unit, with a pressure $p_2 = 100$ atm (or 1470 psi), about 200 tubes are required. This is an extremely small number; it should be possible to "wrap around" the 30-m tubes so that the space requirements are small. Compressor and turbine are also "miniaturized" at such a high pressure level. Dimensions which are too small may cause technical difficulties; in such cases p_2 can be reduced so that reasonable dimensions are obtained. On the other hand, larger values of p_2 can make even high power levels manageable. This, in essence, is the advantage of the AK system, and in the present application use will be made of high pressurization for all heat transfer surfaces, even in the hydrogen system. Since the heat removal problem for the power output of reactors per unit weight is so critical, the advantage of reasonable heat transfer surfaces can be decisive. Such nuclear devices might even be used for missions which were once thought to be possible with chemical rockets only. Besides, the advantage of having a power source (without a radiator surface) is obvious for spaceflight applications. It is believed that the scheme proposed here is the only one which can make use of the liquid hydrogen as a heat sink. Any such process must have near-Carnot efficiency, and this can be achieved by the AK process even in the case of extreme temperature ratios.

Technical Comments

Air Torpedo—A Proposal of Dr. Eng. Albert Fono Dated 10 February 1915

W. H. AVERY¹

Applied Physics Laboratory,
The Johns Hopkins University, Silver Spring, Md.

Opening Remarks (by W. H. Avery)

AT THE close of a survey paper on ramjet development published in this Journal in 1955,² I invited readers to send supplementary information on the history of ramjet propulsion, which could be presented at a later date. In this connection, Dr. Theodore von Kármán has sent to me some interesting documents received from a long-time friend, Dr. Albert Fono of Budapest, who had only recently seen my paper. The forwarded material shows that Dr. Fono in February 1915 proposed the use of the ramjet principle for sustaining the velocity of an artillery shell with a device he called an air torpedo. Through detailed performance calculations he showed that the range of the shell could be more than doubled by ramjet propulsion.

Excerpts from a translation of Dr. Fono's proposal are presented here. The accompanying figures are photostats of the originals.

Introduction (by Albert Fono)

"The distance to which one can shoot a projectile is bounded in practice by the great increase in air resistance that occurs

with higher velocities . . . In order to achieve a greater distance, more work is necessary to overcome the total resistance. Also, more energy must be given to the shell as it leaves the gun. Since this energy is applied only in the form of kinetic energy, to achieve greater distances the initial velocity must be raised, but with this high velocity a part of the trajectory encounters excessive air resistance. The difficulty of achieving greater range evidently lies in the fact that the energy must be stored in the form of kinetic energy. If it were possible to store the necessary energy in another manner and make it available in overcoming air resistance, then an obvious improvement in the shooting distance would be possible.

"The accompanying description and analysis proposes that chemical energy instead of kinetic energy be introduced in the form of a combustible fuel in the projectile. This fuel is to be burned along the way with the approaching air, and the derived heat converted into work to overcome the air resistance. If in this way a forward acting force can be applied to the projectile, then it is evidently possible to accelerate the shell during flight . . . It would be possible with a relatively small initial velocity of the shell and with a relatively small reaction force on the shell to achieve very great range and an appreciable impact energy at the terminal point. It would also be possible with relatively light guns to shoot heavy shells to great distances."

Technical Description (by Albert Fono)

"The force acting on the shell will be obtained through burning of a fuel introduced into the shell. Heat released in the burning will raise the temperature of the air streaming through the shell. Because the specific volume of heated air is greater, the air volume leaving the shell will be greater, and therefore with a proper selection of cross section the heated air will exhaust with a greater velocity than the inlet

Received June 15, 1960.

¹ Research Development Supervisor. Fellow Member ARS.

² Avery, W. H., "Twenty-Five Years of Ramjet Development," *JET PROPULSION*, vol. 25, no. 11, Nov. 1955, pp. 604-614.

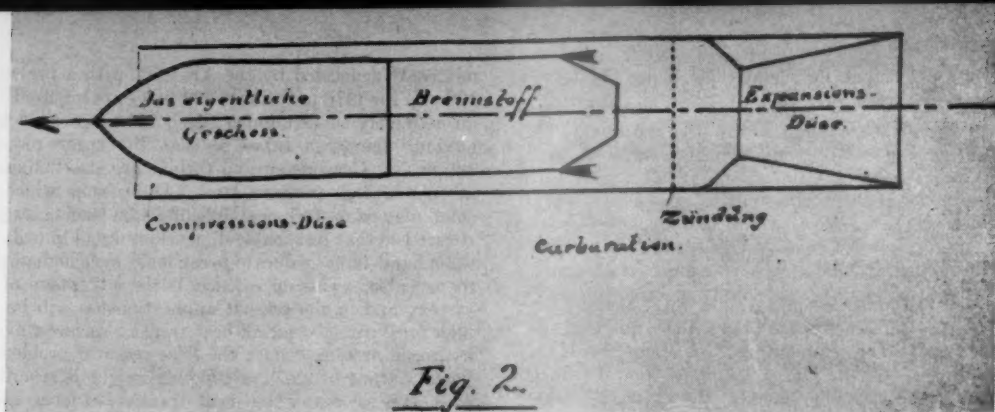


Fig. 2.

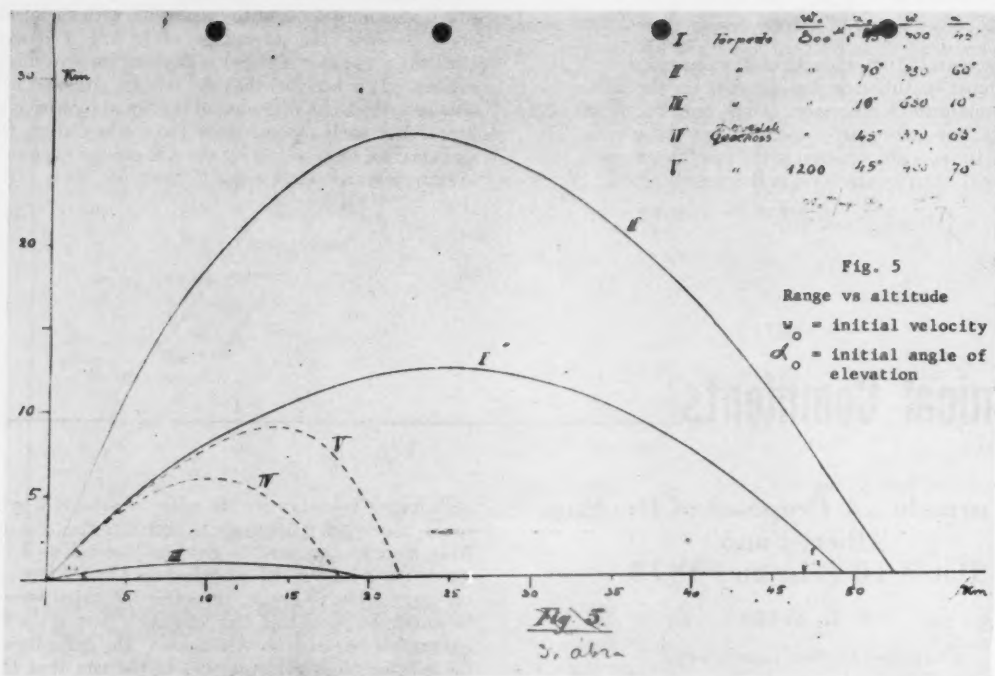


Fig. 5

Range vs altitude

v_0 = initial velocity
 α_0 = initial angle of elevation

Fig. 5.
 3. abn

MILITÄRKOMITEE.
 Sept. 1. 1915.
 Begründung: Lufttorpedo.

In der Antwort (auch Postbegleit-
 adresse Frachtbrief, Postanweisung)
 auf diese Zuschrift, die Nummer der
 Sektion, die Geschäftsnummer und
 die Jahreszahl genau anzuführen.

An
 Seine Wohlgeborenen den Herrn Dr. Ing. Albert FONO

in
 BUDAPEST.

Bism. am 7. April 1915.

Unter Rückschluß der theoretischen Ausarbeitung über ein
 Lufttorpedo wird mitgeteilt, daß von Ihrem Projekte kein prak-
 tischer Erfolg zu erwarten ist, aus welchem Grunde auf Ihre
 Vorschläge nicht weiter reflektiert werden kann.

Für den Präsidenten:
Radaiurosky

1 Beilage.

velocity. Since this air quantity enters with a small relative velocity and exhausts with a greater velocity, the exit momentum is greater than the inlet momentum. The resultant of the two forces acts on the shell. In the simplest case, this resultant is parallel to the flight direction, is equal to the difference between the two forces and acts in the forward direction. Thermodynamics shows that heat energy can be converted into mechanical work with good effectiveness if the heat is introduced under conditions of high pressure, and the heated gas is allowed to expand to a low pressure. The desired high pressure will be produced in the shell through the relative velocity of the air stream. This velocity will, by means of a diffuser, compress the air in a fashion similar to the operation of a turbocompressor. The air compressed in the shell, after heating by burning a fuel introduced into the flowing stream, will expand through a nozzle where the pressure again is converted into velocity. Figure 2 shows the proposed arrangement."

Closing Remarks (by W. H. Avery)

Dr. Fono then presents formulas for the ram pressure, the temperature rise in the combustor, the exit momentum, the inlet drag and external drag. From these he computes the net force, the acceleration and by stepwise integration the ve-

locity and distance of a ramjet propelled shell. The results are presented in his Figure 5. Note that the ramjet speed is 800 m per sec or roughly M 2.5.

The proposal was submitted on Feb. 10, 1915, to the military committee of the Austrian Government, who replied on April 7, 1915, that study of the aerial torpedo proposal indicated that no practical results were to be expected; consequently, the proposal could not be considered further. A photostat of the reply is attached.

The material received from Dr. Fono also includes an additional German patent no. 560075 issued in 1932 which was not found in my original literature search.

The documentation furnished by Dr. Fono indicates that he was the first person to visualize the possibilities of ramjet propulsion for supersonic flight. Although the work of Lorin³ was earlier, there is no indication in Lorin's published papers that he foresaw the use of ramjets at the high speeds needed by this type of engine to achieve useful thrust or efficient operation.

I feel sure that all ARS readers will be glad to accord Dr. Fono recognition for his pioneering studies of ramjet propulsion.

³ Lorin, R., "De la Turbine a Gaz au Propulseur a Reaction," *L'Aerophile*, May 15, 1913, p. 229.

Comment on "Solar Heating of a Rotating Cylindrical Space Vehicle"

JOHN W. TATOM¹

Lockheed Aircraft Corp., Marietta, Ga.

IN THEIR recent article (1),² Charnes and Raynor have investigated the quasi steady-state temperature distribution along the surface of a hollow rotating cylinder located in the solar radiation field. By linearizing the differential equation which describes the effects of surface conduction, radiation and solar energy reception, they were able to obtain an approximate analytical solution which was then applied to the case of a stationary cylinder. In their article (p. 483) the following example appears.

Given: A stationary cylinder with

$$\begin{aligned} R &= 1 \text{ ft} \\ l &= 0.005 \text{ ft} \\ k &= 100 \text{ Btu/hr ft R} \\ \epsilon_s &= 1 \\ \alpha_s &= 1 \\ S &= 442 \text{ Btu/hr ft}^2 \\ \sigma &= 0.1717 \times 10^{-8} \text{ Btu/hr ft}^2 \text{ R}^4 \end{aligned}$$

Then

$$\begin{aligned} T_0 &= 534.25 \text{ R} \\ T_{\max} &= 705.48 \text{ R} \\ T_{\min} &= 420.94 \text{ R} \end{aligned}$$

The temperature errors involved in this example were estimated to be approximately 5.7 per cent.

Recently a numerical integration (2) was completed of the differential equations describing the steady-state temperature distribution along the surface of:

- 1 A hollow sphere located in the solar radiation field.
- 2 An infinitely long nonrotating hollow cylinder, also located in the solar radiation field.

Received June 15, 1960.

¹ Thermodynamics Engineer. Member ARS.

² Numbers in parentheses indicate References at end of paper.

The equations, which for sake of generality are written in nondimensional form, include the effects of surface conduction, radiation, solar energy reception and also that of internal radiation. Both equations take the general form

$$\frac{d^2 \zeta}{d\theta^2} + A \cot \theta \frac{d\zeta}{d\theta} = K [\zeta^4 - B - C \cdot F(\theta)] \quad [1]$$

For a cylinder

$$\zeta = T/T_\infty$$

where

$$T_\infty = T_0 \left[\frac{\pi + \epsilon_i/\epsilon_s}{1 + \epsilon_i/\epsilon_s} \right]^{1/4} \quad T_0 = \left[\frac{S\alpha_s}{\pi\sigma\epsilon_s} \right]^{1/4}$$

and

$$\begin{aligned} A &= 0 \\ B &= (\epsilon_i/\epsilon_s)/(\pi + \epsilon_i/\epsilon_s) \\ C &= \pi/(\pi + \epsilon_i/\epsilon_s) \\ K &= \sigma(\epsilon_i + \epsilon_s)R^2T_\infty^3/kl \\ F(\theta) &= \cos \theta \quad \text{for } 0 \leq \theta \leq 90^\circ \\ &= 0 \quad \text{for } 90^\circ \leq \theta \leq 180^\circ \end{aligned}$$

This equation (Eq. [1]), in the special case of $\epsilon_i/\epsilon_s = 0$, reduces to essentially Charnes and Raynor's equation for no rotation, except that here the fourth-degree term is not linearized. Table 1 presents selected values of the numerical solution of this equation in the particular case of $\epsilon_i/\epsilon_s = 0$.

Applying these new methods and results to the previous example

$$\begin{aligned} T_0 &= 534.25 \text{ R} \\ T_\infty &= 711.25 \text{ R} \\ K &= 1.2356 \\ \zeta_{\theta=0} &= 0.9360 \quad \left. \begin{array}{l} \text{linearly} \\ \zeta_{\theta=\pi} = 0.5338 \end{array} \right\} \text{interpolated} \end{aligned}$$

Then

$$T_{\theta=0} = 665.7 \text{ R} \quad T_{\theta=\pi} = 379.7 \text{ R}$$

Table 1 Tabulation of ζ vs. θ for a cylinder, with $\epsilon_i/\epsilon_s = 0$

θ	$K = 0$	$K = 0.5$	$K = 1.0$	$K = 2.0$	$K = 5.0$	$K = 10$	$K = \infty$
0	0.7511	0.8854	0.9282	0.9611	0.9854	0.9932	1.0000
30	0.7511	0.8597	0.8934	0.9207	0.9446	0.9547	0.9646
60	0.7511	0.7919	0.7983	0.8021	0.8083	0.8159	0.8407
90	0.7511	0.7113	0.6816	0.6459	0.5961	0.5598	0
120	0.7511	0.6548	0.6036	0.5456	0.4675	0.4108	0
150	0.7511	0.6239	0.5628	0.4964	0.4103	0.3501	0
180	0.7511	0.6141	0.5500	0.4814	0.3934	0.3327	0

Comparison of Results

	$T_0 = 0$	$T_0 = \infty$
Linearized analytical solution	705.5 R	420.9 R
Exact numerical solution	665.7 R	379.7 R
Difference	39.8 R	41.2 R
Per cent difference	5.98	10.9

It appears, therefore, that the linearized solution in the case of no rotation may give errors of somewhat more than the estimated 5.7 per cent.

Nomenclature

$A, B, \{$	= nondimensional constants appearing in Equation [1]
$C, K \}$	
k	= thermal conductivity, Btu/hr ft R
R	= radius, ft
S	= solar constant, 442 Btu/hr ft ²
T	= temperature, R

l	= wall thickness, ft
α	= solar absorptivity
ϵ	= thermal emissivity
τ	= dimensionless temperature
θ	= angular position on cylinder (referred to point closest to the sun)
σ	= Stefan-Boltzmann constant, 0.1717×10^{-8} Btu/hr ft ² R ⁴

Subscripts

0	= average
∞	= conditions at $\theta = 0$ for $K = \infty$ ($k = 0$)
i	= interior
e	= exterior

References

- 1 Charnes, A. and Raynor, S., "Solar Heating of a Rotating Cylindrical Space Vehicle," ARS JOURNAL, vol. 30, no. 5, May 1960, pp. 479-484.
- 2 Tatom, J. W., "Shell Radiation," Master's Thesis, Georgia Institute of Technology, Atlanta, Ga., May 1960.

Nonequilibrium Reactions in Solid Propellant Gas Generator Systems

FRANK R. GESSNER Jr.¹

Rocketdyne Div., North American Aviation, Inc.,
McGregor, Texas

Nonequilibrium reactions during the combustion of solid propellants can result in gas temperatures several hundred degrees above those estimated by theoretical calculations. This paper presents results of an investigation of this phenomenon and shows the differences that can be expected in typical propellant systems.

WHEN it was found that burned gas temperatures observed in tests of certain solid propellant gas generator systems were several hundred degrees Fahrenheit above calculated values, a theoretical investigation was undertaken to explain the discrepancies. This study revealed the simple, but not generally appreciated, fact that incomplete reaction of the fuel in a fuel-rich propellant can cause an increase in burned gas temperature over the equilibrium value. More specifically, this report contains results of calculations for typical gas generator propellants, which illustrate the effects of formation of methane and carbon, and of failure of the water-gas reaction to follow equilibrium requirements. The calculations confirm that the actual gas temperature can differ considerably from the theoretical equilibrium temperature. Therefore, since temperature is of vital interest in gas generator applications, efforts must be made in the development of propellants for gas generation to attain combustion characteristics such that chemical equilibrium of the exhaust products is approached as closely as practicable.

In many applications of gas generators the temperature of the products of combustion is of prime importance, a relatively low limit being established by the high temperature mechanical properties of the materials used in structures upon which the hot gases are to impinge.

Normally in the design of moving equipment utilizing hot gases as the working medium, for instance gas turbines, it is reasonable to assume that, if the combustion of fuel does not attain equilibrium, the gas temperature will be lower than theoretical. Such failure to reach equilibrium in fuel-air systems is specified as a combustion efficiency, and is always

less than 100 per cent because the gas temperatures are lower than if true chemical equilibrium were attained. By analogy the nonequilibrium reactions in solid propellant gas generators might reasonably be expected to result in temperatures below the theoretical equilibrium values. However, the reverse is actually true in many instances.

Analysis

During the development and subsequent tests of certain types of composite propellants designed for gas generation, the temperatures actually attained by the products of combustion were found to be as much as 300 F above the theoretical equilibrium values. In an effort to explain this apparent discrepancy, a re-evaluation of the theoretical performance of the propellants was undertaken, with due consideration of the possibilities that, at these low temperatures, some of the constituents might react to form other compounds in addition to the normal products, CO, CO₂, H₂O, H₂ and N₂, and the normal products formed do not attain complete chemical equilibrium.

Since it was known that some methane could be formed at these low temperatures under normal equilibrium, a bias in favor of methane was applied to the performance calculations. The results, as can be seen in Curve A of Fig. 1, indicated that, as the methane content increased, the combustion temperature also increased. For a CH₄ content of 2 per cent by weight, the combustion temperature can be 300 F above the normal equilibrium value calculated on the assumption that no CH₄ is formed.

In many gas generator propellants carbon is used as a reinforcing agent and/or burning rate additive, and it is also

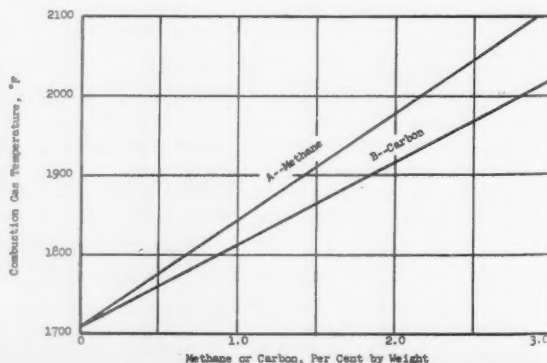


Fig. 1 Effect of methane and carbon on combustion temperature

Presented at the ARS Solid Propellant Rocket Research Conference, Princeton University, Princeton, N. J., Jan. 28-29, 1960.

¹ Research Specialist, Solid Propulsion Operations. Member ARS.

possible that carbon can be formed in the flames at these low temperatures from coking of the hydrocarbon fuel binder. In some instances residual carbon has been found in gas generators. Therefore, a calculation to determine the effect of such carbon formation was made, with results shown by Curve B of Fig. 1. At about 2 per cent carbon by weight, the increase in temperature was about 200 F.

It has been stated by many investigators that the normal water-gas equilibrium is not attained at temperatures below 1900 F. This phenomenon tends to lower the combustion temperature, since the resulting equilibrium is usually in the direction which produces lower energies. For a gas generator propellant with a theoretical exhaust temperature of about 1700 F, this abnormal equilibrium composition would lower the temperature only 20 F as can be seen in Fig. 2. Similarly, the possibility of formation of oxides of nitrogen can account for lowering the temperature by no more than 20 F when the concentration of nitric oxide is 2 per cent by weight. Results of calculations of this kind for a typical propellant are shown on Fig. 3.

The fact that the formation of methane or carbon increases the gas temperature is more easily understood if one considers the stoichiometry of the oxidizer and the fuel that actually reacts with it. Since the propellant is always fuel-rich, the removal of fuel, as methane or carbon, lowers the fuel-oxidizer ratio. The combustion temperature for a stoichiometric mixture of the carbon-hydrogen-oxygen-nitrogen system is about 3600 F. Therefore, as fuel is prevented from reacting in the system, the available energy is increased owing to increased production of carbon dioxide and water. Since the increase in the specific heat of the gas mixture is very small, the temperature goes up, approaching the stoichiometric temperature as an upper limit.

It is the purpose of this brief paper to point out a potential pitfall in the application of gas generator propellants to systems requiring control of the gas temperature. The possibility of higher temperatures than normally expected points up the importance of careful consideration of the combustion processes to insure complete reaction of all fuel and the use of propellants which can insure that combustion goes completely to equilibrium.

Although most solid propellants can be made to deliver the expected performance, designs which allow loss of energy from the burning surface in excess of that required for good combustion can possibly compromise this performance. No particular difficulty should be encountered in most designs if advance consideration is given to this phenomenon. This

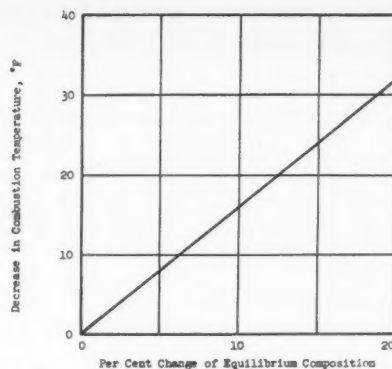


Fig. 2 Effect of equilibrium composition on combustion temperature

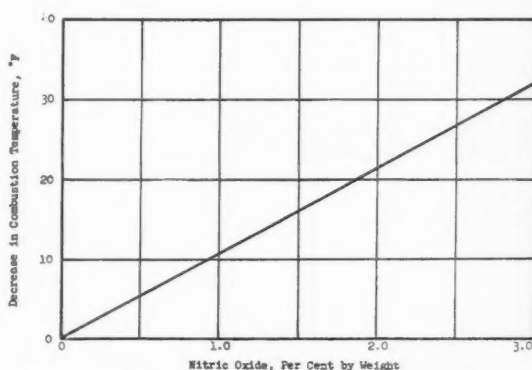


Fig. 3 Effect of nitric oxide on combustion temperature

study also illustrates the value of a complete analysis of the theoretical aspects of problems in chemical reactions, as well as those normally considered to be mandatory.

Until a better understanding of chemical kinetics is available, the possibility of nonequilibrium reactions should not be overlooked in the development and application of fuel-rich propellant systems.

Errata: "Hypervelocity Glider at Large Angles of Inclination"

W. H. T. LOH¹

Federal Technical Institute,
Zurich, Switzerland

THE FOLLOWING corrections are offered to the paper which appeared in this Journal, vol. 30, no. 2, Feb. 1960, pp. 200-201:

The term $d\theta/ds$ shown in the first equation should be $-d\theta/ds$ instead of $+d\theta/ds$.

Received June 23, 1960.

¹ National Science Foundation Senior Post Doctoral Fellow.

The second term in Equation [1] should have a minus instead of a plus sign.

The flight velocity expression should be $(\theta_f - \theta)$ instead of $(\theta - \theta)$.

In item 8, the total aerodynamic heat input equation should be

$$Q \cong \int_{\theta_f}^{\theta} \frac{C_b - C_b \cos \theta}{C_b - \beta \cos \theta} e^{-C_b \theta} d\theta$$

In the Nomenclature, C_1 should be $-2(D/L)$, and C_3 should be [usually use of negative (D/L) for large angle descent]

$$\left[\beta \cos \theta_f - \frac{C_D A \rho_f (L/D)}{2m} \right]$$

Erratum: "Aerodynamic Instability of Supersonic Inlet Diffusers"

C. C. CHANG¹

University of Minnesota, Minneapolis, Minn.

C. T. HSU²

Iowa State University, Ames, Iowa

THIS note presents a correction to an error in our paper which appeared in this Journal, vol. 30, no. 5, May 1960.

Received June 23, 1960.

¹ Professor of Fluid Mechanics, Aeronautical Engineering Dept. Member ARS.

² Associate Professor, Aeronautical Engineering Dept. Member ARS.

The neutral stability criterion obtained by Stoolman (10)³ and Mirels (11) for small Mach number in the plenum chamber should be written as

$$\left| \frac{1 - (\gamma - 1)M_c/2}{1 + (\gamma - 1)M_c/2} \right| \left| \frac{1 + \xi_1}{1 - \xi_1} \right| = 1 \quad [1]$$

The second bracket contains the amplitude ratio of the reflected wave to the impinging wave at the inlet of the plenum chamber. This ratio is possibly greater than 1 if the viscous term is considered in the equation of motion. Obviously instability may occur if $\xi_1 > (\gamma - 1)M_c/2$ for quasi-steady operation (11).

³ Numbers in parentheses indicate References in the original paper.

Book Reviews

Ali Bulent Cambel, Northwestern University, Associate Editor

The Exploration of Space, edited by Robert Jastrow, The Macmillan Co., New York, 1958, 160 pp. \$5.50.

Reviewed by C. C. MIESSE
Armour Research Foundation

This comprehensive review of the most recent developments in the space sciences is the result of the first nationally sponsored conference devoted to the special problems of space physics, which met in Washington on April 29-30, 1959, under the auspices of the National Academy of Sciences, the National Aeronautics and Space Administration, and the American Physical Society. The following ambitious objectives were admirably satisfied: To awaken the interest of the scientific community in the problems of space research; to present an estimate of our present and future capabilities for space exploration; and to acquaint the experimentalist with existing instrumentation in space physics.

Four chapters were devoted to the status of research in fields pertaining to the solar system. The chapter "Plasma and Magnetic Fields in the Solar System" by Thomas Gold attributes the transport of charged particles, from the sun to Earth, to the mutual effects of radial expansion of the solar cloud and the eruption of clouds of plasma from the surface of the sun. The resultant configuration of magnetic field loops traps the ionized particles and constrains them to travel back and forth within the cloud. "Extension of the Solar Corona into Interplanetary Space" by Eugene Parker explains the observed phenomena in terms of a simple hydrodynamic expansion of the solar corona, and terms this radial flow a "solar wind." "The Geomagnetically Trapped Corpuscu-

lar Radiation" by James A. Van Allen summarizes the known properties of the trapped particles, and presents new evidence which indicates particle fluxes of great magnitude observed shortly after unusually intense solar activity. "The Argus Experiment" by N. C. Christofilos describes the background and results of the geophysical experiment which was designed to study the trapping of the relativistic electrons in the geomagnetic field.

Two chapters summarize the recent and proposed research on meteors and meteorites. "Solid Particles in the Solar System" by Fred L. Whipple surveys the current meteorological results and outlines needed experiments based on space- and ground-based meteoritic studies: Impact phenomena and erosion on exposed surfaces; total velocity vectors of particles; study of meteorites, comets, asteroids, zodiacal clouds, and lunar surface; and perturbation studies of the motions of astronomical bodies. "Primary and Secondary Objects" by H. C. Urey discusses recent evidence for differences in the cosmic-ray ages of iron and stone meteorites, which indicates the initial formations at hundreds and tens of millions of years, respectively.

Three chapters consider the moon, the planets and their atmospheres. "The Moon" by G. P. Kuiper describes the formation of Earth's sole satellite by a process of accretion about 5.5 billion years ago, which caused heating and partial melting of the interior, resulting in the appearance of lavas on the lunar surface. "Remarks on Mars and Venus" by G. de Vaucouleurs concludes that the astronomical data are fairly complete; the astrophysical data are incomplete, particularly with respect to atmospheric composition; and the geo-

physical data are extremely sketchy. "Outer Atmospheres of the Earth and Planets" by R. Jastrow attributes the trace of lunar atmosphere to the argon formed by the decay of radioactive potassium, discusses the development of the Martian and Venusian atmospheres, and describes the discrepancies which exist between rocket data and satellite measurements of the density variations with latitude.

Four chapters on new facilities and techniques for space research complete the formal presentations. "Capabilities for Space Research" by H. E. Newell surveys the present and future capabilities of the NASA space research program, including chemical and nuclear rockets, space probes for radiation potential, and satellite-based astronomical observatories.

"Rocket Astronomy" by H. Friedman stresses the need for astronomical observations above an altitude of 300 km, provides a detailed description of the instrumentation necessary, and presents several radiation phenomena which depend upon refined techniques for the anticipated satisfactory explanation.

"Astronomy from Satellites and Space Vehicles" by L. Goldberg describes a few typical controlled experiments, outlines the plans and problems for imminent experiments in satellite astronomy, and forecasts future objectives in the field of astronomical observations from stabilized space platforms.

"Experimental Research Programs in the Space Sciences" by J. W. Townsend Jr. specifies the criteria for spaceworthy instrumentation, and describes the instrumentation included in each of the following satellites: Atmosphere structure, space probe, ionospheric measurements,

astronomical telescope and magnetometer probe.

In addition to the formal presentations summarized here, verbatim reports of three cross-fire roundtable discussions were included, so that an integrated cross section of the current status of space exploration is provided for the reader. Although each chapter represents an independent contribution, the insertion of the roundtable discussions serves as an ingenious method to bridge the occasional gaps between the authors' individual fields of interest, and serves to resolve any apparent differences in opinion. For those who prefer verbatim reports by the nation's experts in the field of space research, "The Exploration of Space" is an indispensable reference both for the current state of the art and for future plans and tools to instrument these plans.

Technical Communication, by George Harwell, The Macmillan Co., New York, 1960, 330 + x pp. \$5.

Reviewed by IRWIN HERSEY
American Rocket Society

The problem of technical communication has been with us for some time now and has grown in recent years to a point where any effort aimed at improving such communication must be welcomed. However, in judging the merits of books dealing with this problem, it is necessary to differentiate between those directed at students and those designed for working scientists and engineers.

This distinction has been overlooked by George Harwell in "Technical Communication." In his preface, the author tells us that "this textbook was written with the engineering student primarily in mind," although it can also "serve as a guide and reference work for the practicing engineer." This is somewhat questionable, since a book designed for one purpose can scarcely serve another purpose equally well. Thus, few, if any, engineers or scientists will have an interest in the exercises and assignments which conclude each chapter, or in the "manual of general composition" which serves as an appendix.

Within the bounds of his primary aim, however, which, in the opinion of this reviewer at least, was to write a textbook, Professor Harwell has done an admirable job, producing a well-written, straightforward volume which will be of considerable help to the engineering student who is just getting into this business of technical communication.

The text is divided into six sections. The first three chapters provide a definition of effective writing and cover organization of material and methods of exposition. Chapter 4 covers the business letter and is somewhat superfluous. The next three chapters form the heart of the book, covering in considerable detail the formal and informal technical report. Chapters 8 and 9 deal with technical articles and oral presentations, and the last chapter, one of the best in the book, covers the use of illustrative material in technical papers. The 60-page "manual of composition" referred to previously and a list of A.S.A. abbreviations of scientific and engineering terms serve as appendices, and a helpful index is also provided.

What the author has to say he says well. The three chapters devoted to the technical report cover fairly well, in less than a hundred pages, what any engineer or scientist needs to know about writing such reports, and the chapter devoted to illustrations has a number of helpful suggestions on how to best utilize graphs, tables, charts and figures of various types.

Since Professor Harwell has chosen the broadest possible title for his book, it is only natural that his coverage should also be broad. However, to the engineer or scientist working in the field, much of the material contained in the first four chapters will be old hat, and the chapter on technical articles will be of greater interest to the public relations people than to the working engineer.

It is unfortunate that the chapters dealing with technical reports and handling of illustrations have not been excerpted and turned into a thin manual on technical report writing, since it is a good manual of this kind which is most urgently needed today.

Proceedings of the Ninth International Astronautical Congress, Springer-Verlag, Vienna, 1959, two volumes, 970 pp. \$23.80.

Reviewed by E. V. LAITONE, G. LEITMANN
and A. K. OPPENHEIM
University of California

This volume was beautifully produced and includes an impressive collection of papers that were presented at the Amsterdam Congress in August of 1958. The reason for the two volumes is apparently mere convenience in binding, not subject division. In fact, it appears that in order to speed up the publication, the editor decided to put the papers together as they became available after the author's corrections, without any consideration of the sequence, and then to supply the first volume with an organized list of contents and complete list of authors. Because of this feature, one has to have both volumes available in order to follow any particular subject.

The subject matter is divided into seven chapters: Chapter I on astronautics general contains some five papers of essentially unrelated subjects ranging from the rudiments of relativistic astronautics to the description of an interplanetary navigation system. Chapter II on upper atmosphere research has only two papers, one on the mechanisms of atmospheric ablation and the other reporting on the data obtained by means of the third Soviet Sputnik. Chapter III on physics of spaceflight astrophysics consists of nine papers. One learns from them such facts as that the western hemisphere of the moon is probably less exposed to the meteoritic bombardment than the eastern one, and that the Groebner method of integrating differential equations may provide a complete solution of the n -body problems in astronautics. One can also find out from these papers about the influence of the sun on cosmic radiation in interplanetary space, the probable types of planets surrounding any sun, the estimate of physical conditions existing on the planet Mars, and the feasibility of using an astronautical telescope in a satellite orbiting around Earth.

Chapter IV on astronautical engineering contains 10 papers in the general subject area of space technology, ranging from flight mechanics to spaceship ecology. There are two papers dealing with trajectory optimization, one by variational techniques, the other by direct methods. Of the five articles in the field of guidance and control, three are concerned with apparatus for space navigation, one with orbital computations and one with the general concepts of guidance and control. There is also an interesting paper dealing with the aerodynamics of re-entry vehicles. Included in this group is a report on the environmental data that have been gathered in the flight of balloon capsules, viewed as prototypes of future space cabins.

By far the largest is Chapter V on propulsion. It consists of 30 papers. There are three papers on the fundamental aspects in magnetofluid-mechanics, one on internal energy of highly ionized gases, and one on the significance of atom recombination in energy exchange reactions. Then there are several papers concerned with various aspects of chemical propulsion systems, and the rest are devoted primarily to electrical propulsion, and the powerplant systems and requirements associated with it.

Chapter VI on artificial satellites is made up of 13 papers. It complements Chapter II with the historically most significant reports on the first results obtained from satellite programs both in the USSR and in the USA. It contains also a good deal of information on orbital techniques under the dynamics of the satellite motion.

The last chapter is concerned with the field of space biology and medicine. It contains articles whose subject matter ranges from a report on the biological observations of the effect of cosmic radiation on hordeum seeds that were kept at altitudes of 30,000 and 40,000 meters, to some general medical reflections on space travel.

All in all, there are 74 papers that have been written by 93 authors. The scope of the coverage is quite extensive, and the treatment, in most cases, is on a high scientific level.

Physics and Medicine of the Atmosphere and Space, edited by Otis O. Benson Jr. and Hubertus Strughold, John Wiley & Sons, Inc., New York, 1960, 645 pp. \$12.50.

Reviewed by WESLEY O. PIPES
Northwestern University

Space medicine and bioastronautics are highly speculative fields mainly because there have been only a few opportunities for direct observation and experimentation. Actually the best that a scientific writer in this field can do at present is to present some physical data collected by space probes or some biological data collected in terrestrial laboratories and then speculate on what will happen to biological materials when they are subjected to the environment of a space capsule. The speculations produced are more or less valuable according to whether or not they are based on the best available data and approach their subjects with a realistic attitude.

"Physics and Medicine of the Atmosphere and Space" is a collection of 42 papers which were presented at the Second International Symposium on Physics and Medicine of the Atmosphere and Space, in San Antonio, in November 1958. All of the papers are of the nature of speculative discussions on one or another of the medical-biological-logistics aspects of manned spaceflight. In general the authors have attempted to base their discussions on the best data available, although there are a few exceptions. Most of the papers maintain a high level scientific approach to their subjects; at the same time the topics are broad enough to attract widespread interest.

As is true of any book with a large number of authors, there is some lack of continuity from chapter to chapter. However, the editors have been able to achieve a degree of uniformity in the presentations and have so arranged the papers that the topics are grouped in an orderly fashion. The various areas of interest are only sampled and no attempt is made to cover any one area completely. A few of the papers are quite detailed in the treatment of a particular problem.

The physical and chemical environments of the upper atmosphere and nearby space are considered in a series of papers, most of which present some of the recently collected data. The articles on radiation hazards are followed by two articles on the biological effects of cosmic radiations, thus providing an approach to this subject which will be of interest to designers of space capsules (although much of the information presented is available elsewhere).

Several articles on weight limitations, propulsion systems, space vehicles and related subjects are included. These articles seem to be directed primarily toward those concerned with space medicine who are not really sure why the protective and environ-

mental systems which they are developing are limited by the capabilities of vehicles and propulsion systems. These papers do achieve their purpose.

Many of the problems of maintaining human beings in sealed environments are considered in individual articles. Actually, these articles serve mainly to indicate large areas of deficiency of information. These papers were presented over a year and a half ago, and there has been a great stimulation of interest and activity in the various fields of bioastronautics since that time. However, many critical areas still exist which have been very imperfectly explored.

The book is concluded by a series of highly speculative discussions mostly relating to interplanetary travel. In five years these articles will probably have more historic than scientific value; however, at the present time they represent some of the most authoritative conclusions that can be presented.

The book as a whole presents very little in the way of new data, and most of the authors have probably been more cautious than need be in their discussions. However, it should be of value in establishing the place of biological scientists in the space program. From a reading of the book it is readily apparent that an astronaut is more than just one component of a system.

Flames, Their Structure, Radiation and Temperature, by A. G. Gaydon and H. G. Wolfhard, The Macmillan Co., New York, 1960, second edition, revised, xii + 383 pp. \$14.

Reviewed by MELVIN GERSTEIN
National Engineering Science Co.

This book is essentially a reprinting of the first edition published in 1953; only a minimum of new material has been added.

The reader who has the first edition would find little advantage in getting this newer edition. For the scientist and engineer interested in problems of flames, this book still represents one of the most readable and useful books in the combustion field. It is highly recommended to those who would like a general summary of the status of knowledge on flames and particularly to people wishing to acquire a quick background in this field. This edition, as is true for the previous edition, presents principally a phenomenological discussion of flames and is weak in the mathematical and theoretical aspects of flames.

The first two chapters which introduce the subject and discuss premixed flames are essentially unchanged from the previous edition. The chapters on flow patterns, flame shapes and measurements of burning velocity present new material on the shadowgraph technique and flat flame technique. The remaining chapters, except the last two, have additional references and some updating of the discussions, but only to a minor degree. It is somewhat disappointing that the treatment of turbulent flames could not be changed more than was done.

The chapter on combustion processes of rocket-type fuels has been completely revised and presents new material on flames using oxidants other than air. The chapter title is somewhat misleading in the sense that rocket combustion problems are not treated as such. The last chapter on recent progress on some flame problems has also been completely revised, and the authors take the opportunity to make a very interesting comparison between the final chapter in the previous volume and progress made on those problems in the past seven years.

In summary, the current volume like the previous one presents an excellent discussion of the properties of flames and is a valuable reference.

1960-61 ARS Meeting Schedule

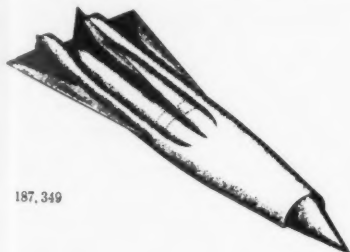
Date	Meeting	Location	Abstract Deadline
Dec. 5-8	ARS Annual Meeting and Astronautical Exposition	Washington, D.C.	Past
1961			
Feb. 1-3	Solid Propellant Rocket Conference	Salt Lake City, Utah	Past
March 13-16	Missile and Space Vehicle Testing Conference	Los Angeles, Calif.	Past
April 5-7	Lifting Re-entry Vehicles: Structures, Materials, and Design Conference	Palm Springs, Calif.	Past
April 26-28	Propellants, Combustion, and Liquid Rockets Conference	Palm Beach, Fla.	Past
May 22-24	National Telemetry Conference	Chicago, Ill.	Dec. 15
June 14-17	ARS Semi-Annual Meeting	Los Angeles, Calif.	Feb. 1
Aug. 21-23	International Hypersonics Conference	Cambridge, Mass.	Jan. 15
Aug. 23-25	Biennial Gas Dynamics Symposium	Evanston, Ill.	Jan. 15
Oct. 9-13	ARS SPACE FLIGHT REPORT TO THE NATION	New York, N.Y.	May 2

Send all abstracts to Meetings Manager, ARS, 500 Fifth Ave., New York 36, N.Y.

New Patents

George F. McLaughlin, Associate Editor

Aircraft design (187,349). I. H. Culver, H. Rosenzweig, D. H. Walters and E. G.



187,349

Ward, Glendale, Calif., assignors to Lockheed Aircraft Corp. (ARS corporate member).

Rocket ignition system (2,934,897). C. C. Waugh and W. C. Parrish, Puente, Calif., assignors to North American Aviation, Inc.

Diaphragm separating a pressure source from propellant tanks, and supported to prevent bursting. Removal of the support allows bursting of the diaphragm, preventing introduction of propellants into the chamber until the chamber reaches a temperature sufficient to ignite the propellants.

Aircraft design (187,823). W. Y. Gasaway, Sacramento, Calif.

Disk-like configuration with lifting vanes at the outer rim, and high dihedral stub wings at either side of an enclosed central cockpit.

Igniter compositions (2,935,839). H. A. Beatty and M. E. Gluckstein, Farmington, Mich., assignors to Ethyl Corp.

Introduction into a jet engine of a triethylaluminum mixture containing 5 to 40 per cent by weight of trimethylaluminum.

Fluid mixing chamber (2,935,840). F. Schoppe, Munich-Pasing, Germany, assignor to Metallbau Semlar G.m.b.H. Co.

Ramjet with a tubular combustion chamber fed with a combustible medium in a continuous flow rotating along the outer wall to create a large negative gradient of pressure from the wall to its axis.

Thrust chamber (2,935,841). H. S. Myers and J. R. Piselli, Buffalo, N. Y., assignors to Bell Aircraft Corp.

Hollow nozzle of one piece construction forming a highly heat-conductive material. Cooling passages extending in straight line form through the walls are equally spaced around the nozzle.

Fuel injection system for a ramjet (2,935,848). L. S. Billman, Lancaster, Calif., assignor to the U. S. Navy.

Valve comprising power-driven cam

wheels for metering fuel valves uniformly and at predetermined intervals during rotation.

Acceleration insensitive skin friction balance (2,935,870). W. C. Lyons Jr., Irving, Texas, assignor to the U. S. Navy.

Device for measuring skin friction on a missile. Counterweight system mounted on a base and surrounding a friction measuring system forming part of the missile surface.

Homing device (2,935,942). J. A. De Young, M. N. Fairbank, R. C. Jones and C. H. Matz, Cambridge, Mass., assignors to the U. S. Navy.

Eye-mirror-gyroscope unit in the nose-piece of a missile arranged to precess and constantly follow the path of a target, and means responsive to received signals to guide the missile to a target.

Telescoping ramjet (2,935,946). E. A. Gallo, D. B. Clark and E. W. Schwartz (ARS member), El Cajon, Calif., assignors to the U. S. Army.

Spin stabilized projectile with a stop member at the forward end of its shell to limit the forward movement of an air diffuser which becomes fully extended by aerodynamic pressure.

Three-axis gyroscopic aerodynamic damping system (2,935,947). L. T. Jagiello (ARS member), China Lake, Calif., assignor to the U. S. Navy.

Gyro wheel mounted within a control surface and rotatable on an axis perpendicular to the plane of the surface.

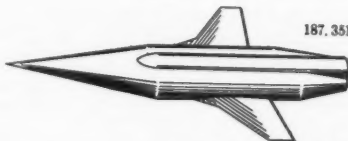
Rocket igniter pellets (2,935,948). S. J. Porter (ARS member), Scituate, Mass., assignor to American Potash & Chemical Corp. (ARS corporate member).

Sleeve of aluminum, magnesium, titanium and alloys encasing flat ended cylindrical pellets. The metal serves as part of the total metal requirements of the pellets, and enters into their burning mechanism.

Aircraft designs (187,350; 187,351 and 187,353). M. Dryer, J. R. Jack, R. W. Luidens and N. E. Samanich, Cleveland, Ohio, assignors to NASA.



187,350



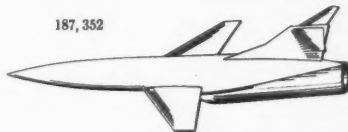
187,351



187,353

These are the first aircraft design patents assigned to the new National Aeronautics and Space Administration.

187,352



Aircraft design (187,352). M. Dryer, J. R. Jack, R. W. Luidens and N. E. Samanich, Cleveland, Ohio, assignors to the U. S. Navy.

Expandable liquid evaporate coolant system (2,925,722). C. M. Blackburn and W. W. Hagner, Silver Spring, Md., assignors to the U. S. Navy.

Coolant conveyed to passages in an aerial vehicle whereby heat generated by electronic components causes boiling of the coolant at lowered temperatures to cool the components.

Gyroscopic accelerometer (2,925,736). F. K. Mueller (ARS member), Huntsville Ala.

Compressed gas supplied to the clearance between the housing and casing of a gyroscope.

Manufacture of propellants (2,926,386). W. M. Hutchinson, Bartlesville, Okla., assignor to Phillips Petroleum Co.

Device for molding semi-solid propellant material having a high yield point.

Stress limiting control (2,926,488). H. F. Faught, Middletown Heights, Pa., assignor to the U. S. Navy.

Automatic maintenance of structural stress in a turbojet powerplant below a predetermined maximum value which is dependent on pressure regardless of ambient atmosphere temperature.

Laminated fluid-jacketed thrust chamber (2,926,490). C. C. Eaton (ARS member) and L. F. Arata, Whippany, N. J., assignors to Thiokol Chemical Corp. (ARS corporate member).

Jet motor thrust chamber comprising a stack of thin sheet metal laminations provided with rows of perforations to form coolant passages.

Powerplant using liquid decomposed into gas (2,926,492). R. M. Flanagan, Morris Plains, N. J., assignor to Bendix Aviation Corp. (ARS corporate member).

Catalyst chamber for converting hydrogen peroxide into steam. Metering valve controls flow of fuel to maintain the turbine at constant velocity.

Gas turbine with waste heat steam generator (2,926,493). A. J. Poole and C. B. Bayer, Fanwood, N. J., assignors to the Babcock & Wilcox Co.

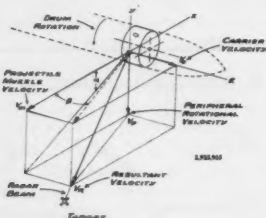
Steam generator and heater to heat exhaust gases and provide for their uniform distribution.

Rocket engine injector (2,928,236). H. J. Kircher and S. Lehrer (ARS member), Pompton Lakes, N. J., assignors to the U. S. Air Force.

A first propellant supplied through the openings in the side walls of alternate tubes in a tube bundle. A second propellant supplied through the remaining alternate tubes. Fuel flows through holes in the walls into the combustion chamber.

EDITOR'S NOTE: Patents listed above were selected from the Official Gazette of the U. S. Patent Office. Printed copies of patents may be obtained from the Commissioner of Patents, Washington 25, D. C., at a cost of 25 cents each; design patents, 10 cents.

Guided missile ordnance system (2,925,965). R. J. Pierce, Cedar Rapids, Iowa, assignor to Collins Radio Co. (ARS corporate member).



Radar controlling the firing of guns rotatable at a predetermined rate around the body of a missile.

Gas operated safety and arming mechanism (2,926,609). H. R. Van Goey and T. C. Campbell, Ventura, Calif., assignors to the U. S. Navy.

In a missile employing a rocket motor, a pressure responsive means at one side of the case moves a shutter to the armed position upon admission of a predetermined gas pressure.

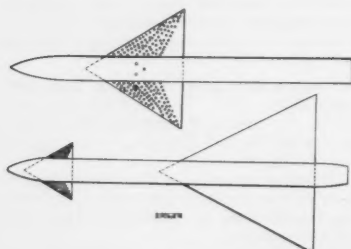
Composite rocket ramjet fuel (2,926,613). H. M. Fox (ARS member), Bartlesville, Okla., assignor to Phillips Petroleum Co.

Alternate disks of a solid rocket propellant and a solid ramjet fuel comprising methyl naphthalene and a powdered fuel consisting of carbon, alkali metals, beryllium, boron, magnesium and aluminum.

Aircraft with tiltable jets (2,926,868). I. A. Taylor, Davisburg, Mich.

Tabs carried by jet engines, and means for controlling their pivotal movement and line of thrust from fore and aft cavities in the body of the aircraft.

Stability compensator (2,926,870). W. Schwartz and R. H. Klepinger (ARS member), Dayton, Ohio, assignors to the U. S. Air Force.



Tail-less delta wing aircraft or missile for operation at supersonic speeds. Perforated lifting surfaces reduce the stability margin and thereby reduce the drag-due-to-trim.

Balloon world satellite (2,927,383). H. A. Longino, McLean, Texas.

Outer and inner spherical bodies with a movable member freely moving between them. Inner member has indicia simulating portions of the Earth. Air or vacuum pressure is supplied to the interior of the inner body and to the space between the bodies.

Multiple stage rocket (2,927,398). J. Kaye, E. F. Kurtz Jr. and G. F. Harper, Boston, Mass.

Acceleration of the rocket upon launching causes the second stage to uncouple and separate from the first stage.

Jet propelled propeller blade (2,927,647). C. A. Serriades, Chicago, Ill.

Integral system in the hollow portions of a propeller blade providing a continu-

ous air flow from the hub inlet to the outlets at the blade tips to turn the propeller.

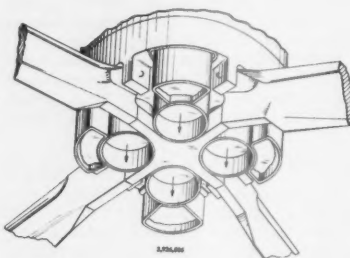
Toroidal aircraft (2,927,746). W. R. Mellen, Roslyn Heights, N. Y.

Circular hollow body with passenger compartments within. Air is directed inwardly beneath the bottom and upward and outward to alter the pressure beneath the bottom.

Path recording system (2,927,833). M. J. Maynard, Caldwell, N. J., assignor to IT & T Corp. (ARS corporate member).

Movable parallel transparent panels each representing a plane disposed in space. A marking device and means responsive to spacial position information for inscribing a visual path indicating the flight path of an object in space.

Sector tracer (2,926,606). G. E. Bangs, E. G. Loomis and R. Gregory, Altadena, Calif., assignors to the U. S. Navy.



Cups, at the after end of a rocket, filled with combustible material and ignited by the rocket exhaust to provide illumination.

Ramjet diffuser (2,928,237). C. H. Niles, Baltimore, Md., assignor to the U. S. Navy.

Inner wall of an outer body having longitudinal grooves extending the length of the diffuser section increasing in depth rearwardly from fuel injection means toward the combustor.

Jet deflector and orifice control (2,928,238). W. M. Hawkins Jr. (ARS member), N. Hollywood, Calif., assignor to Lockheed Aircraft Corp. (ARS corporate member).

Tailpipe terminating in a rectangular shape. Vertical and horizontal deflecting vanes provide pitch, roll and yaw control.

Control system for reaction motor igniters (2,928,240). H. W. Burton and E. W. Harslem (ARS member), Hackettstown, N. J., assignors to Thiokol Chemical Corp. (ARS corporate member).

Switch operable by a sensing relay coil upon expiration of a pre-established time interval to interpose a resistor in series with the coil and the ground.

Meteorological apparatus (2,928,277). R. T. Cavanaugh (ARS member) and W. Deichert, Jersey City, N. J., assignors to Allen B. Du Mont Laboratories, Inc.

Transmitters and receivers arranged to send and receive signals indicating relative magnitude and direction of wind, and density of air.

Stagnation air temperature measuring device (2,928,279). M. V. Schober, Fullerton, Calif., assignor to North American Aviation, Inc. (ARS corporate member).

Device having a very short response time for measuring total temperature of a high speed air stream. Heat sensitive member is located at a position where the air is at rest.

Aircraft propulsion systems (2,928,627). C. L. Johnson, Encino, Calif., assignor to

Lockheed Aircraft Corp. (ARS corporate member).

Propulsive gas stream led through tubes spanwise of an aircraft. Discharge exits for the stream lead aft over the control surfaces, and forwardly from the underside of the wing.

Propellants for rockets (2,929,697). J. W. Perry, W. R. Johnson and J. H. Frazer, Havre de Grace, Md.

Intimate mixture of potassium perchlorate, graphite, titanium, vinyl chloride, vinyl acetate and monobutyl ether of ethylene glycol.

Trajectory simulator (2,929,156). R. B. Reddy, Annapolis, Md., assignor to the U. S. Navy.

Device for simulating the constant velocity trajectory of a missile under the guidance of a radar beam program.

Airplane lift augmenting means (2,929,582). N. J. Munro, Victoria, Australia, assignor to the Commonwealth of Australia.

Hollow tubular members slidably mounted for partial extension and retraction at wing tips. Gaseous fluid is blown from the aircraft through the members for emission via slots.

Variable thrust rocket engine (2,930,187). C. W. Chillon (ARS member), M. Meyer (ARS member) and D. M. Lawrence, Wood-Ridge, N. J., assignors to the U. S. Air Force.

Two continuously variable chambers, each producing a different maximum thrust, one having a maximum thrust equal to the minimum thrust of the other.

Aircraft having vertical lift jet engines (2,930,544). A. R. Howell, Farnborough, England, assignor to the Government of Great Britain.

Apertures on the lower surface of the wing for the discharge of propulsive jet streams so as to produce an upwardly directed component of thrust.

Jet aircraft convertible for vertical ascent and horizontal flight (2,930,546). M. Wibault, New York, N. Y., assignor to Vibrane Corp.

Air compressors within the body with a discharge duct directed downward for developing lift under the fore-and-aft centerline of the aircraft.

Valved intermittent combustion reaction engine (2,930,196). A. Hertzberg and J. C. Logan Jr., assignors to Cornell Aeronautical Laboratory, Inc. (ARS corporate member).

Inlet and outlet valves phased to each other so as to generate a compression wave which is propagated toward the inlet end while the same is open, but closed in time to reflect the wave toward the outlet end.

Air intake for supersonic aircraft (2,931,167). René Leduc, Argenteuil, France.

Needle mounted in a tubular shell, with a substantially pointed portion extending forward and forming a compartment for the pilot.

Rocket projectile (2,926,608). E. F. Chandler (ARS member), Brooklyn, N. Y.



Charge to produce high pressure gas contained in a spider in the combustion chamber and adapted to resist breaking until a predetermined launching pressure has been reached.

Technical Literature Digest

M. H. Smith, Associate Editor

The James Forrestal Research Center, Princeton University

Propulsion and Power (Combustion Systems)

Analysis of Partial Admission Axial Impulse Turbines, by Hans D. Linhardt and D. H. Silvern, *ARS Preprint* 1202-60, May 1960, 16 pp.

On the Importance of Combustion Chamber Geometry in High Frequency Oscillations, in Rocket Motors, by J. R. Osborn and J. M. Bonnell, *ARS Preprint* 1108-60, May 1960, 35 pp.

Instrumentation for Studies of Unstable Burning Phenomenon, by G. W. Reissig and T. A. Angelus, *ARS Preprint* 1166-60, May 1960, 21 pp.

Some Instrumentation for Combustion Stability Research, by J. R. Osborn, *ARS Preprint* 1163-60, May 1960, 21 pp.

Instrumentation for Research on Combustion Instability in Solid Propellant Rocket Motors, by F. W. Spaid and E. M. Landsbaum, *ARS Preprint* 1162-60, May 1960, 10 pp.

An Integrated Combustion Instability Recordings and Analysis Installation, by Howland B. Jones Jr. and David T. Harrie, *ARS Preprint* 1164-60, May 1960, 10 pp.

High Frequency Pressure Instrumentation for Rocket Instability Studies, by Stanley W. Baker, *ARS Preprint* 1165-60, May 1960, 16 pp.

The Design of Movable Nozzles, by E. J. Hayes, S. F. Watanabe and D. S. Ernest, *ARS Preprint* 1169-60, May 1960, 6 pp.

Some Aspects of Underwater Jet Propulsion Systems, by C. A. Gongwer, *ARS Preprint* 1188-60, May 1960, 7 pp.

Limitations of a Rocket Propulsion System with Variable Exhaust Velocity Taking Into Consideration Nuclear Data, by Trutz Foelsche, *J. Astron. Sci.*, vol. 7, no. 2, Summer 1960, pp. 25-28.

Advances in Cryogenic Engineering, Vol. 5: Proceedings of the 1959 Cryogenic Engineering Conference (Univ. Calif., Berkeley, Calif., Sept. 2-4, 1959), K. D. Timmerhaus, ed., Plenum Press, N. Y., 1960, 584 pp.

Test Equipment and Procedures Used in the Development of Liquid Oxygen-Hydrogen Rocket Engines, by R. H. Anschutz, pp. 62-68.

Facilities for Testing Rocket Engine Components Using Cryogenic Fluids as Propellants, by B. Mandell and L. E. White, pp. 120-127.

Comparison of Localized Heat-transfer Rates in a Liquid Oxygen-heptane Rocket Engine Employing Several Injection Methods and Oxidant-fuel Ratios, by Richard F. Neu, *NASA TN D-286*, June 1960, 39 pp.

EDITOR'S NOTE: Contributions from Professors E. R. G. Eckert, J. P. Hartnett, T. F. Irvine Jr. and P. J. Schneider of the Heat Transfer Laboratory, University of Minnesota, are gratefully acknowledged.

Propulsion and Power (Non-Combustion)

Propulsion Requirements for Controllable Satellites, by Theodore E. Edelbaum, *ARS Preprint* 1228-60, May 1960, 17 pp.

On Rocket Propulsion with Nuclear Power, by E. L. Resler Jr. and N. Rott, *ARS Preprint* 1210-60, May 1960, 5 pp.

The Hybrid Rocket Motor and Its Unique Capabilities, by John Gustavson, *ARS Preprint* 1167-60, May 1960, 8 pp.

The Snap 2 Nuclear Space Power System, by J. R. Wetzel, H. M. Dieckamp and D. J. Cockeram, *ARS Preprint* 1203-60, May 1960, 11 pp.

Fluidized Solids as a Nuclear Fuel for Rocket Propulsion, by L. P. Hatch, W. H. Regan and J. R. Powell, *ARS Preprint* 1209-60, May 1960, 4 pp.

Design Considerations and Initial Evaluation of Model B Plasma Generator, by W. Lai, J. Gustavson and L. Talbot, *Univ. Calif., Inst. Engng. Res., Tech. Rep. HE-150-161*, Sept. 5, 1959, 13 pp.

Electro-gas-dynamical Considerations of a Pulsed Plasma Pinch Engine, by A. E. Kunen, I. Granet, W. J. Guman and W. McIlroy, *ARS Preprint* 1141-60, May 1960, 23 pp.

Electrical Power from Rockets, by John H. Huth, *ARS Preprint* 1147-60, May 1960, 11 pp.

Voltage-current Characteristics of Tungsten Electrode in Cesium Vapor, by L. H. Stauffer, *ARS Preprint* 1124-60, May 1960, 13 pp.

Design and Performance of Small Model Ion Engines, by G. R. Brewer, J. E. Etter and J. R. Anderson, *ARS Preprint* 1125-60, May 1960, 13 pp.

NASA Experimental Research with Ion Rockets, by E. E. Dangle and D. L. Lockwood, *ARS Preprint* 1126-60, May 1960, 15 pp.

Neutralization Experiments on Broad Cesium Ion Beams, by J. M. Sellen and H. Shelton, *ARS Preprint* 1161-60, May 1960, 12 pp.

Space Charge Measurements in Expanding Ion Beams, by J. M. Sellen and H. Shelton, *ARS Preprint* 1160-60, May 1960, 42 pp.

Propulsion by Composite Beams of Negative and Positive Ions, by M. A. Gilileo and S. W. Kash, *ARS Preprint* 1157-60, May 1960, 17 pp.

Effect of Electrode Refraction in Ion Beam Collimation and Neutralization, by G. C. Baldwin, *ARS Preprint* 1158-60, May 1960, 11 pp.

Experimental Studies of Cesium Ion Rocket Performance, by R. N. Edwards, P. E. Jasper, G. Kuskevics and R. A. Scheffer, *ARS Preprint* 1127-60, May 1960, 9 pp.

An Analysis of Mirror Accuracy Requirements for Solar Power Plants, by David H. Silvern, *ARS Preprint* 1179-60, May 1960, 7 pp.

Internal Design Considerations for

Cavity-type Solar Absorbers, by Charles W. Stephens and Alan M. Haire, *ARS Preprint* 1178-60, May 1960, 9 pp.

A Review of WADD Solar Programs, by William C. Savage, *ARS Preprint* 1178-60, May 1960, 9 pp.

Conversion of Heat to Electricity in Solids and Plasmas, by Werner B. Teutsch, *ARS Preprint* 1201-60, May 1960, 7 pp.

Photochemistry and Space Power Generation, by J. N. Pitts Jr., J. David Margerum and William E. McKee, *ARS Preprint* 1180-60, May 1960, 10 pp.

Global Asymptotic Stability for Non-linear Systems of Differential Equations and Applications to Reactor Dynamics, by J. J. Levin and J. A. Nohel, *Archive for Rational Mech. & Anal.*, vol. 5, no. 3, May 17, 1960, pp. 194-211.

Colloids May Cut Space Travel Time, by Milton Farber and Stanley Singer, *Missiles & Rockets*, vol. 7, no. 2, July 11, 1960, pp. 25-26.

Magnetic Plasma Propulsion by Means of a Travelling Sinusoidal Field, by Rudolf X. Meyer, *Space Tech. Labs., Phys. Res. Lab., Tech. Rep. 60-0000-09114*, April 1960, 17 pp.

Rotating Power Generation Machinery for Electrical Propulsion, by G. T. Harness, *North American Aviation, Rocket-dyne Div., Rep. R-1934*, May 1960, 24 pp.

Satellite and Space Propulsion Systems, by Wolfgang E. Moekkel, Lionel V. Baldwin, Robert E. English, Bernard Lubarsky and Stephen H. Maslen, *NASA TN D-285*, June 1960, 47 pp.

Power Generation by Means of the "Electric Wind," by Meredith C. Gour-dine, *CIT, Jet Prop. Lab., Tech. Rep. 32-6*, April 1960, 8 pp.

Performance of Nuclear Rocket for Large-payload Earth-satellite Booster, by Eldon W. Sams, *J. Aero/Space Sci.*, vol. 27, July 1960, pp. 481-492.

On the Question of Transforming Thermal into Electrical Energy by Utilization of Thermionic Emission, by N. D. Morgulis and A. G. Naumovets, *Radio Engng. & Electronics (transl. of Radiotekhnika i Elektronika)*, vol. 4, no. 6, June 1959, pp. 225-227.

Propellants and Combustion

The Catalytic Decomposition of Ammonium Perchlorate, by A. Hermoni and A. Salman, *ARS Preprint* 1107-60, May 1960, 10 pp.

High Energy Propellant Comparisons for Space Missions, by R. V. Burry, J. Jortner and J. K. Rosemary, *ARS Preprint* 1123-60, May 1960, 40 pp.

An Introduction to the Selection of High Performing Propellants for Torpedoes, by Leonard Greiner, *ARS Preprint* 1189-60, May 1960, 5 pp.

Diffusion and Heterogeneous Reaction, IV: Effects of Gas Phase Reaction and Convective Flow, by H. Wise and C. M. Ablow, *Princeton Univ., Proj. Squid, Tech. Rep. SRI-6-P*, May 1960, 32 pp. (Available on microcard only.)

Preliminary Report on the Thermodynamic Properties of Selected Light-element Compounds (Supplement to NBS Repts. 6297 and 6484), *Nat. Bur. Standards Rep.* 6645, April 1, 1960, 88 pp.

Infrared Spectra of Ion-producing Species in Hydrocarbons, by Andrew Gemant, *Appl. Sci. Res.*, vol. 8B, no. 3, 1960, pp. 149-158.

The Inhibition of the Hydrogen-oxygen Reaction by Methane, by R. R. Baldwin, N. S. Corney and R. W. Walker, *Trans. Faraday Soc.*, vol. 56, no. 6, June 1960, pp. 802-832.

Some Approximations in the Theory of Self-heating and Thermal Explosion, by P. H. Thomas, *Trans. Faraday Soc.*, vol. 56, no. 6, June 1960, pp. 833-839.

Cascade Time of π^- in Liquid Hydrogen, by T. H. Fields, G. B. Yodh, M. Derrick and J. G. Fetkovich, *Phys. Rev. Letters*, vol. 5, no. 2, July 15, 1960, pp. 69-70.

Maintained Detonations, by B. V. Voitsekhevskii, *Soviet Phys.: Doklady*, vol. 4, no. 6, May-June 1960, pp. 1207-1209.

Electron Capture and Detachment in Collisions of Fast Helium, Boron and Fluorine Atoms with Gas Molecules, by Ya. M. Fogel', V. A. Ankudnirov and D. V. Pilipenko, *Soviet Phys.: JETP*, vol. 11, no. 1, July 1960, pp. 18-22.

Advances in Cryogenic Engineering, Vol. 5: Proceedings of the 1959 Cryogenic Engineering Conference (Univ. Calif., Berkeley, Calif., Sept. 2-4, 1959), K. D. Timmerhaus, ed., Plenum Press, N. Y., 1960, 584 pp.

Cryogenic Engineering Advances in the Space Age, by R. F. Blanks and K. D. Timmerhaus, pp. 3-12.

Large-scale Production, Handling and Storage of Liquid Hydrogen, by P. C. Vander Arend, pp. 49-54.

A Study of the Hazards in the Storage and Handling of Liquid Hydrogen, by L. H. Cassutt, F. E. Maddocks and W. A. Sawyer, pp. 55-61.

Practical Storage and Distribution of Liquid Hydrogen and Helium, by W. E. Perkins and R. J. Frainier, pp. 69-74.

Handling Liquid Fluorine in Rocket Applications, by A. R. Kimball, pp. 77-84.

Handling Liquid Hydrogen on a Pilot-plant Scale, by H. L. Laquer, pp. 85-94.

Cryogenic Tankage for Space Flight Applications, by D. G. Driscoll, pp. 95-102.

Transfer of Liquid Hydrogen Through Uninsulated Lines, by R. J. Richards, W. G. Steward and R. B. Jacobs, pp. 103-110.

High-pressure Liquid-hydrogen and Helium Pumps, by C. F. Gotzman, pp. 289-298.

Single-phase Flow Tests with Liquid Hydrogen, by D. H. Pope, W. R. Killian and R. J. Corbett, pp. 441-449.

Gas-pressurized Transfer of Liquid Hydrogen, by R. W. Moore, A. A. Fowle, B. M. Bailey, F. E. Ruccia and R. C. Reid, pp. 450-459.

A Survey of Stratification in a Cryogenic Liquid, by R. Neff, pp. 460-466.

Transient Phenomena Associated with the Pressurized Discharge of a Cryogenic Liquid from a Closed Vessel, by J. A. Clark and G. J. VanWylen, pp. 467-480.

Pressure-temperature Histories of Liquid Hydrogen Under Pressurization and Venting Conditions, by P. M.

Ordin, S. Weiss and H. Cristenson, pp. 481-486.

An Experimental Study Concerning the Pressurization and Stratification of Liquid Hydrogen, by A. F. Schmidt, J. R. Purcell, W. A. Wilson and R. V. Smith, pp. 487-497.

Temperature Distribution in Liquid and Vapor Phases of Helium in Cylindrical Dewars, by R. T. Swim, pp. 498-504.

A Kinetics Study of Ortho-para Hydrogen Conversion, by R. N. Keeler, D. H. Weitzel, J. H. Blake and M. Konecnik, pp. 511-417.

Effective Density of Boiling Liquid Oxygen, by F. Herzberg, pp. 526-532.

Maximum-rate Theory of Impact Sensitivity, by A. Africano, pp. 533-544.

Composition and Analysis of Commercial Liquid Oxygen, by C. P. Smith, pp. 545-556.

Experimental Large-scale Equipment for Low-temperature Distillation Tray Studies, by B. R. Brown and J. B. Gardner, pp. 549-556.

A Compilation and Correlation of the P-V-T Data of Normal Hydrogen from Saturated Liquid to 80°, by R. B. Stewart and V. J. Johnson, pp. 557-565.

The Study of the Origin and Propagation of Disturbances in the Burning of Solid Propellants, by G. A. Agoston, *Stanford Res. Inst., Poulter Labs., Tech. Rep.* 003-60, Feb. 1960, 24 pp.

The Ignition Mechanism of Composite Solid Propellants, by Robert F. McAlevy III, *Princeton University, Dept. Aeron. Engng.*, June 1960, 78 pp., 89 refs. (Thesis, Ph.D.)

Erosive Combustion of Colloidal Powders, by P. Travernier and J. Boisson, *Gl. Brit., Tech. Info. & Library Series TIL/T* 4891, Dec. 1959, 10 pp. (transl. from *Chim. et Ind.*), vol. 78, no. 5, 1957, pp. 487-493.

Detonation of Secondary Explosives by Lead Azide, by D. B. Moore and J. S. Rice, *Stanford Res. Inst., Poulter Labs., Tech. Rep.* 004-60, March 4, 1960, 44 pp.

Photomicrographic Tracking of Ethanol Drops in a Rocket Chamber Burning Ethanol and Liquid Oxygen, by Robert D. Ingebo, *NASA TN D-290*, June 1960, 18 pp.

The Properties of Boron Compounds, compiled by Estal D. West, *U. S. Air Force Division of Res., Aeron. Res. Lab.*, TR 60-276, May 1960, 17 pp.

Burning Rates and Ignition Temperatures of Hydrogen Peroxide Solutions, by C. N. Satterfield, E. Kehat and Maria A. T. Mendes, *Combustion & Flame*, vol. 4, June 1960, pp. 99-106.

Studies of Combustion Processes Leading to Ignition in Hydrocarbons, by K. C. Salooja, *Combustion & Flame*, vol. 4, June 1960, pp. 117-136.

Theoretical Calculations in Gaseous Detonation, by C. L. Eisen, R. A. Gross and T. J. Rivlin, *Combustion & Flame*, vol. 4, June 1960, pp. 137-148.

The Passage of Explosions Through Narrow Cylindrical Channels, by H. G. Wolfhard and A. E. Bruszak, *Combustion & Flame*, vol. 4, June 1960, pp. 149-160.

The Theory of a Spherical Premixed Laminar Flame, by A. A. Westenberg and S. Favin, *Combustion & Flame*, vol. 4, June 1960, pp. 161-172.

An Approximate Solution of the Equation for Self-ignition, by Tosihiro Kinbara and Kazuo Akita, *Combustion & Flame*, vol. 4, June 1960, pp. 173-190.

Prediction of the Emissivity of Large Hydrocarbon Flames from the Mie Theory, by P. J. Foster and I. A. McGrath, *Combustion & Flame*, vol. 4, June 1960, pp. 191-192.

Instrumentation for Exploding Wire Research; Kerr Cell Camera Has 5-nanosecond Exposure Time, by N. Chase, N. Hankin and F. Webb, *Electronics*, vol. 33, July 1, 1960, pp. 43-45.

Some Models of Explosive Line Detonators, by A. Garsia, *J. Math. & Phys.*, vol. 39, April 1960, pp. 54-57.

Stable Combustion of a High-velocity Gas in a Heated Boundary Layer, by Donald L. Turcotte, *J. Aero/Space Sci.*, vol. 27, July 1960, pp. 509-516.

A Study of Supersonic Combustion, by Robert A. Gross and Wallace Chinitz, *J. Aero/Space Sci.*, vol. 27, July 1960, pp. 517-524.

Theory of Dielectric Constants of LiF, by Edwin R. Levin and Elmer L. Offenbacher, *Physical Rev.*, vol. 118, June 1, 1960, pp. 1142-1149.

Electric Conductivity of the Explosion Products of Condensed Explosives, by A. A. Brish, M. S. Tarasov and V. A. Tsukerman, *Soviet Phys.: JETP*, vol. 37 (10), no. 6, June 1960, pp. 1095-1100.

Materials and Structures

Neutron Flux Measurements for Materials Irradiation Experiments at Argonne National Laboratory, Brookhaven National Laboratory, Oak Ridge National Laboratory, and National Reactor Test Station, by L. E. Steele and J. R. Hawthorne, *Naval Res. Lab., Rep.* 5483, May 23, 1960, 10 pp.

Thermoelasticity, by E. W. Parkes, *Stanford Univ., Dept. Aeron. Engng., SUDAER* 91, Feb. 1960, 91 pp.

Heat Conduction and Thermal Stresses in a Solid Having Unequal Specific Heats, by E. W. Parkes, *Stanford Univ., Dept. Aeron. Engng., SUDAER* 90, Feb. 1960, 23 pp.

The Stresses in an Elasto-plastic Bar Subjected to a Sudden Change of Surface Temperature, by E. W. Parkes, *Stanford Univ., Dept. Aeron. Engng., SUDAER* 89, Jan. 1960, 20 pp.

A Theory of Small Deformations of Solid Bodies, by J. F. Besseling, *Stanford Univ., Dept. Aeron. Engng., Rep.* 84, Feb. 1959, 104 pp.

Mechanics Applied to Creep Testing, by N. J. Hoff, *Stanford Univ., Dept. Aeron. Engng., Rep.* 83, Dec. 1958, 80 pp.

A Survey of the Theories of Creep Buckling, by N. J. Hoff, *Stanford Univ., Dept. Aeron. Engng., SUDAER* 80, June 1958, 60 pp.

A Theory of Elastic, Plastic and Creep Deformations of an Initially Isotropic Material Showing Anisotropic Strain-hardening, Creep Recovery and Secondary Creep, by J. F. Besseling, *Stanford Univ., Dept. Aeron. Engng., SUDAER* 78, Dec. 1958, 36 pp.

The Idealized Columns, by N. J. Hoff, *Stanford Univ., Dept. Aeron. Engng., SUDAER* 82, Aug. 1958, 23 pp.

Buckling of a Thin Circular Cylindrical Shell Heated Along an Axial Strip, by D. W. Hill, *Stanford Univ., Dept. Aeron. Engng., SUDAER* 88, Dec. 1959, 91 pp.

A Note on the Impact Pressure Loading of a Rigid Plastic Spherical Shell, by R. Sankaranarayanan, *Brooklyn Polytech. Inst. PIBAL Rep.* 564, May 1960, 9 pp.

Yield Conditions of Plates and Shells by Mises-Hencky Criterion, by T. H. H.

Pian, MIT, *Aeroelastic & Structures Res. Lab., Tech. Rep. 76-3*, June 1960, 13 pp.

A Thermodynamic Analysis of the High-temperature Vaporization Properties of Silica, by Harold L. Schick, *Chem. Res.*, vol. 60, no. 4, Aug. 1960, pp. 331-362.

General Research in Flight Sciences; Jan. 1959-Jan. 1960, Vol. 2, Mechanics of Deformable Bodies, Lockheed Aircraft Corp., Missiles & Space Div., Rep. LMSD-288,139, vol. 2, Jan. 1960.

Buckling of a Cylindrical Shell of Arbitrary Length Under a Circumferential Band of Pressure, by B. O. Almrith and D. O. Brush, Paper 1, 33 pp.

Prebuckling Deflection Stresses in a Circular Cylinder Subjected to a Saddle-type Load, by B. O. Almrith, Paper 2, 26 pp.

Approximate Analysis of Damped, Linear Vibrations, by T. R. Beal, Paper 3, 10 pp.

Large Deflection and Buckling Analysis of Circular Cylindrical Shells, by D. O. Brush, Paper 4, 20 pp.

Approximate Buckling Loads by Energy Methods, by D. O. Brush, Paper 5, 15 pp.

On Determining Biaxial Stress Yield and Fracture Criteria for Hot Pressed Beryllium at Room and Elevated Temperature, by R. F. Crawford, Paper 6, 31 pp.

Stresses in Spherical Pressure Vessels, by O. Hoffman, Paper 7, 16 pp.

A Statistical Analysis of Axially Loaded Cylinder Buckling Data, by E. V. Pittner, Paper 8, 28 pp.

Shock Response of a Nonlinear Missile Suspension System, by E. Y. W. Tsui and P. Stern, Paper 9, 35 pp.

Elasto-plastic Analysis of Shells of Revolution Subjected to Heating and External Loads, by E. Y. W. Tsui and P. Stern, Paper 10, 19 pp.

Spring Characteristics of Long Tubular Air Cushions, by V. W. Coale, Paper 11, 15 pp.

The Initial Response of an Elastic Spherical Shell to a Step Pressure Wave, by P. M. Nachbar, Paper 12, 33 pp.

The Effect of Residual Stresses in the Critical Crack Length Predicted by the Griffith Theory, by W. E. Jahsman and F. A. Field, Paper 13, 17 pp.

Stresses Generated by Suddenly Introducing Moving Crack into a Stretched Elastic Sheet, by B. R. Baker, Paper 14, 62 pp.

General Research in Flight Sciences; Jan. 1959-Jan 1960, Vol. 1, Part 2, Fluid Mechanics, Lockheed Aircraft Corp., Missiles & Space Div., Rep. LMSD-288,139, vol. 1, Part 2, Jan. 1960.

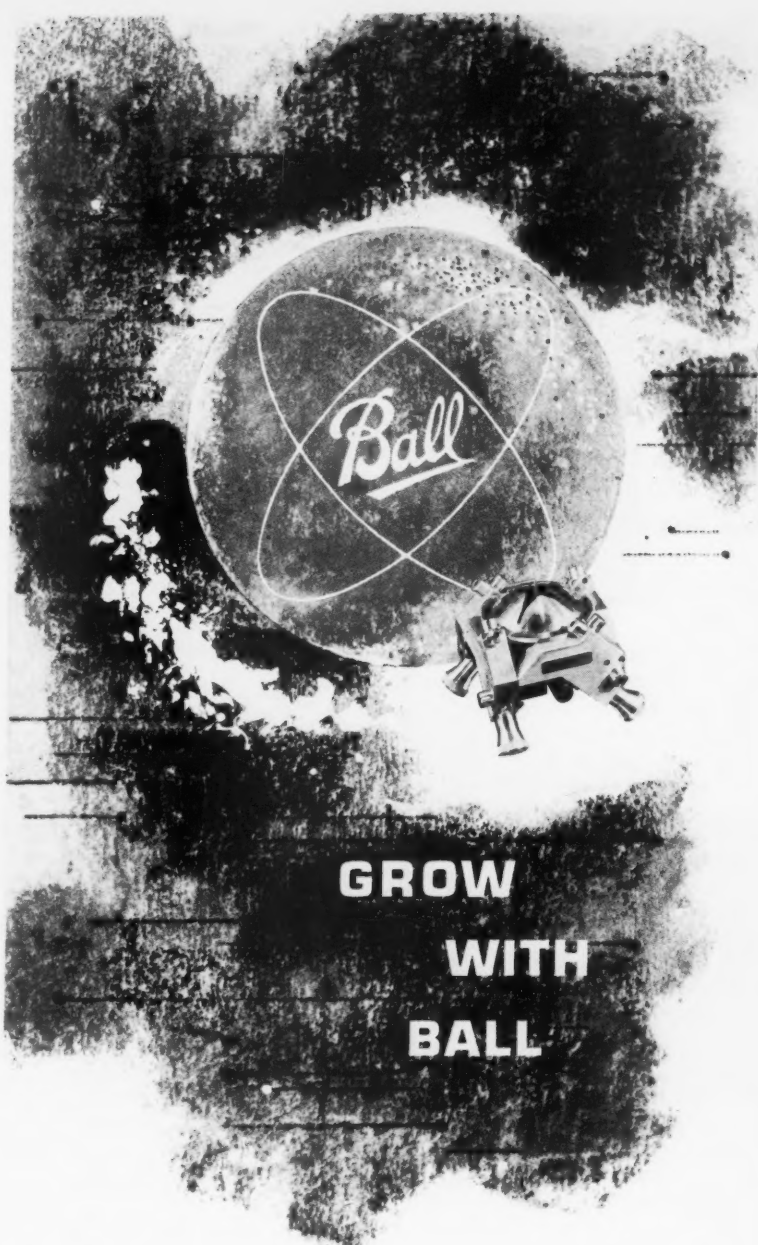
Studies of Sputtering by Beam Technique, by R. P. Stein and F. Hurlbut, Paper 5, 14 pp.

On Meteoritic Impact, by David B. Beard, Paper 10, 10 pp.

Advances in Cryogenic Engineering, Vol. 5: Proceedings of the 1959 Cryogenic Engineering Conference (Univ. Calif., Berkeley, Calif., Sept. 2-4, 1959), K. D. Timmerhaus, ed., Plenum Press, N. Y., 1960, 584 pp.

Flexibility Considerations for the Design of Cryogenic Transfer Lines, by W. G. Flieder, W. J. Smith and K. R. Wetmore, pp. 111-119.

Externally Bonded and Sealed Insulation for Liquid Hydrogen-fueled Rocket Tanks, by V. H. Gray and T. F. Gelder, pp. 131-138.



**GROW
WITH
BALL**



Opportunity... new brochure shows the capabilities and facilities which have enabled Ball Brothers Research to make such outstanding achievements in the satellite and related fields...shows the variety of company projects in research, development, and fabrication...shows why Ball Brothers Research presents an opportunity for scientists and engineers with above average abilities.

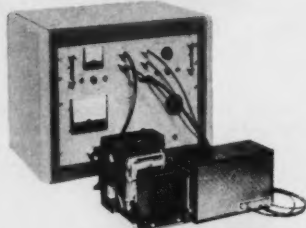
WRITE FOR YOUR COPY TODAY

BALL BROTHERS RESEARCH CORP.

DEPARTMENT R-4
INDUSTRIAL PARK—BOULDER, COLORADO
Hillcrest 2-2966

A Subsidiary of Ball Brothers Company, Inc.

5
BILLIONTHS
OF A SECOND



**KSC-51
KERR
CELL
CAMERA**

The KSC-51 Kerr Cell Camera is the fastest high-resolution photographic instrumentation camera in existence. This system is designed for ultra-high speed phenomena. Effective exposure is as brief as five nanoseconds. Optical shuttering can be synchronized with the experimental phenomenon to within one nanosecond. This instrumentation equipment is of prime interest to the MICRO-TIME oriented engineer or physicist working on...

- HYPERVELOCITY SHOCKS
- EXPLODING WIRES
- EXPLOSIVES
- PLASMA
- M.H.D.

EOI also supplies KERR CELL components for visual and ultra violet applications. We will be pleased to discuss your requirements. Contact the applications engineering group.

Your Kerr Cell Camera application problems are invited.



**ELECTRO OPTICAL
INSTRUMENTS INC.**

2612 E. FOOTHILL BLVD.
PASADENA • CALIFORNIA

Flat Panel Vacuum Thermal Insulation and the Super-Dewar Flask, by H. M. Strong, F. P. Bundy and H. P. Bovenkerk, pp. 139-145.

Metal Powder Additives in Evacuated-powder Insulation, by B. J. Hunter, R. H. Korpachot, J. E. Schrodt and M. M. Fulk, pp. 146-156.

Effect of Condensation on Conventionally Insulated Cryogenic Tanks, by S. W. Weiss and I. A. Goodman, pp. 157-161.

A Study of Condensing-vacuum Insulation, by D. A. VanGundy, L. O. Mullen and R. B. Jacobs, pp. 162-170.

Low-temperature Insulating Systems, by R. M. Christiansen, M. Hollingsworth Jr. and H. N. Marsh Jr., pp. 171-178.

Development of High-efficiency Insulation, by I. A. Black, A. A. Fowle and P. E. Glaser, pp. 181-188.

Multiple-layer Insulation, by R. H. Kropschot, J. E. Schroit, M. M. Fulk and B. J. Hunter, pp. 189-198.

Engineering Aspects of Heat Transfer in Multilayer Reflective Insulation and Performance of NRC Insulation, by M. P. Hnilicka, pp. 199-208.

Characteristics and Applications of Some Superinsulations, by P. M. Riede and D. I. J. Wang, pp. 209-215.

Cryogenic Insulation Development, by S. T. Stoy, pp. 216-221.

On the Evacuation of Plastic Foams to Reduce Their Thermal Conductivity, by L. R. Stoecker, pp. 273-281.

The Strength of Ten Structural Adhesives at Temperatures Down to -424°F, by W. M. Frost, pp. 375-384.

The Behavior of High-magnesium-content Aluminum Alloys at Room and Liquid Nitrogen Temperatures, by A. Everest, pp. 385-396.

Some Mechanical Properties of Magnesium Alloys at Low Temperatures, by R. P. Reed, R. P. Mikesell and R. L. Greeson, pp. 397-405.

The Low-temperature Mechanical Properties of Some Selected Austenitic Manganese Steels, by F. S. Death and H. M. Long, pp. 421-429.

The Tensile and Impact Properties of Plate and Welds of Aluminum Alloy 5083-H113 Between 75 and -320°F, by R. D. Olleman and G. C. Wolfer, pp. 430-438.

Vacuum Gaskets for Use at 20°K, by J. E. Harlow, E. L. Murley and H. L. Laquer, pp. 580-582.

Gamma Radiation of Fluorocarbon Polymers and Prototype Substances, by Leo A. Wall, R. E. Florin and D. W. Brown, *Wright Air Dev. Div., Tech. Rep.* 59-413, April 1960, 59 pp.

Dislocations and Twinning in Graphite, by A. J. Kennedy, *Cranfield Coll. Aeron., Co A Rep.* 130, April 1960, 7 pp.

Polarization Capacitance Determinations of Surface Roughness, by M. K. Testerman, *Wright Air Dev. Div., Tech. Rep.* 60-97, April 1960, 32 pp.

Dynamic Behavior of Cylindrical Shells Under Initial Stress, by G. Herrmann and A. E. Armenakas, *Columbia Univ., Dept. Civil Engng. & Engng. Mech., Inst. Flight Structures*, TN 5, CU-11-60-AF-430-CE, April 1960, 21 pp.

High Temperature Structures, by N. J. Hoff, *Stanford Univ., Dept. Aeron. Engng., SUDAER* 79, June 1958, 41 pp.

On Variational Principles in Thermoelasticity and Heat Conduction, by G.

Herrmann, *Columbia Univ., Dept. Civil Engng. & Engng. Mech., Inst. Flight Structures*, TN 4, CU-10-60-AF-430-CF, April 1960, 17 pp.

A Theory of Elastic, Plastic, and Creep Deformations of an Initially Isotropic Material, by J. F. Besseling, *Stanford Univ., Dept. Aeron. Engng., SUDAER* 78, April 1958, 31 pp.

Thermodynamic Foundations of the Theory of Deformation, by J. F. Besseling, *Stanford Univ., Dept. Aeron. Engng., SUDAER* 86, Aug. 1959, 26 pp.

Important Research Problems in Advanced Flight Structures Design, by Norris F. Dow, *NASA TN D-518*, June 1960, 49 pp.

Refractory Materials: Part II—High Temperature Behavior, by Robert I. Jaffee and Daniel J. Maykuth, *Aerospace Engng.*, vol. 19, July 1960, pp. 39-44.

Thermodynamic Inequalities for Elastic Solids, by James C. M. Li and Hsiao S. Kiang, *J. Chem. Phys.*, vol. 32, June 1960, pp. 1644-1651.

Fluid Dynamics, Heat Transfer and MHD

Prediction of Peak Temperature for Satellite Entries with Lift, by R. H. Edwards and G. S. Campbell, *ARS JOURNAL*, vol. 30, no. 5, May 1960, pp. 496-498.

Heating Penalty Associated with Modulated Entry into Earth's Atmosphere, by John V. Becker, *ARS JOURNAL*, vol. 30, no. 5, May 1960, pp. 504-505.

The Effect of an Aligned Magnetic Field on Oseen Flow of a Conducting Fluid, by G. S. S. Ludford, *Archive for Rational Mech. & Anal.*, vol. 4, no. 5, March 23, 1960, pp. 405-411.

Heat Transfer from Transverse and Yawed Cylinders in Continuum, Slip, and Free Molecule Air Flows, by L. V. Baldwin, V. A. Sandborn and J. C. Laurence, *J. Heat Transfer (ASME Trans.)*, vol. 82C, May 1960, pp. 77-86.

Magnetohydrodynamic Effects upon Heat Transfer for Laminar Flow Across a Flat Plate, by R. D. Cess, *J. Heat Transfer (ASME Trans.)*, vol. 82C, May 1960, pp. 87-93.

Conical Turbulent Boundary Layer Experiments and a Correlation with Flat Plate Data, by W. S. Bradfield, *J. Heat Transfer (ASME Trans.)*, vol. 82C, May 1960, pp. 94-100.

The Influence of Free Stream Turbulence on the Local Heat Transfer from Cylinders, by R. A. Seban, *J. Heat Transfer (ASME Trans.)*, vol. 82C, May 1960, pp. 101-107.

Heat Transfer to Fully Developed Laminar Flow in a Circular Tube with Arbitrary Circumferential Heat Flux, by W. C. Reynolds, *J. Heat Transfer (ASME Trans.)*, vol. 82C, May 1960, pp. 108-112.

Pressure Drop and Heat Transfer in a Duct with Triangular Cross Section, by E. R. G. Eckert and T. F. Irvine Jr., *J. Heat Transfer (ASME Trans.)*, vol. 82C, May 1960, pp. 125-138.

Heat Transfer in Flow Through Rotating Ducts, by C. Y. Kuo, H. T. Iida, J. H. Taylor and F. Kreith, *J. Heat Transfer (ASME Trans.)*, vol. 82C, May 1960, pp. 139-151.

Comparisons of Turbulent Heat-transfer Results for Uniform Wall Heat Flux and Uniform Wall Temperature, by R. Siegel and E. M. Sparrow, *J. Heat Transfer (ASME Trans.)*, vol. 82C, May 1960, pp. 152-153.

Remarks on Transition in a Round Tube, by A. M. O. Smith, *J. Fluid Mech.*, vol. 7, April 1960, pp. 565-576.

The Linearized Flow of a Dissociating Gas, by J. F. Clarke, *J. Fluid Mech.*, vol. 7, April 1960, pp. 577-595.

Curvature of Attached Shock Waves in Steady Axially Symmetric Flow, by E. Bianco, H. Cabannes and J. Kutzmann, *J. Fluid Mech.*, vol. 7, April 1960, pp. 610-616.

Losses Incurred in Turning a Gas Flowing in an Annular Duct Back into the Central Tube, by F. Cheers, *J. Nuclear Energy*, Part B, vol. 1, no. 1, March 1960, pp. 173-180.

Critical Heat Fluxes for Water Flowing in Tubes, by I. T. Aladiev, L. D. Dodonov and V. S. Udalov, *J. Nuclear Energy*, Part B, vol. 1, no. 1, March 1960, pp. 181-183.

Calculation of the Thermal Conductivity of Molten Metals, by G. F. Butenko and M. I. Radchenko, *J. Nuclear Energy*, Part B, vol. 1, no. 1, March 1960, pp. 184-185.

Excitation of Plasma Oscillations, by P. A. Sturrock, *Phys. Rev.*, vol. 117, March 15, 1960, pp. 1426-1429.

Ion-electron Relaxation of Plasmas in a Magnetic Field, II, by Taro Hihara and Yukio Midzuno, *J. Phys. Soc., Japan*, vol. 15, April 1960, pp. 684-687.

A Theory of Decaying Homogeneous Turbulence, by Robert G. Deissler, *Phys. Fluids*, vol. 3, March-April 1960, pp. 176-187.

Entropy Production and Pressure Waves, by Gerald Rosen, *Phys. Fluids*, vol. 3, March-April 1960, pp. 188-190.

Relaxation Theory of Thermal Conduction in Liquids, by R. E. Nettleton, *Phys. Fluids*, vol. 3, March-April 1960, pp. 216-224.

Kinetic Equations for Plasma and Radiation, by Albert Simon and E. G. Harris, *Phys. Fluids*, vol. 3, March-April 1960, pp. 245-254.

Coherent and Incoherent Radiation from a Plasma, by E. G. Harris and Albert Simon, *Phys. Fluids*, vol. 3, March-April 1960, pp. 255-257.

On Unsteady Gas Flows in Laval Nozzles, by O. S. Ryzhov and G. M. Shefter, *Soviet Physics-Doklady*, vol. 4, no. 5, March-April 1960, pp. 939-942.

The Heating of a Heat-conducting Wall Behind a Moving Compression Shock, by G. A. Tirsikii, *Soviet Physics-Doklady*, vol. 4, no. 5, March-April 1960, pp. 981-984.

Heat Wave, Radiating Energy from Front, by E. I. Andriankin, *Soviet Physics-Tech. Phys.*, vol. 4, no. 11, May 1960, pp. 1258-1262.

An Estimate of the Influence of Free Convection upon Turbulent Flow, by E. I. Yantovskii, *Soviet Physics-Tech. Phys.*, vol. 4, no. 11, May 1960, pp. 1280-1282.

Exact Solution for a Problem in Magnetohydrodynamics, by Ya. S. Uflyand and I. V. Chekmarev, *Soviet Physics-Tech. Phys.*, vol. 4, no. 11, May 1960, pp. 1301-1304.

Heat-transfer Near the Stagnation Point of a Body of Revolution in the Presence of a Magnetic Field, by R. X. Meyer, *Zeitschrift für Angewandte Math. und Phys.*, vol. 11, no. 2, March 25, 1960, pp. 127-145.

Summary of Technical Reports, January-June 1959, Vol. I, Gas Dynamics, General Electric Co., Missile & Space Vehicle Dept., Aero-Sci. Lab., 1959, 1 vol.

The Thermal Protection of Re-entry Satellites, by S. M. Scala, *Paper 2*, 22 pp.



DA VINCI AND THE BIRDMAN WARP

LEONARDO DA VINCI (1452-1519) was an intellectual giant who loved to discourse on the subject of "Natural and Mechanical Flight!" He propounded a theory of aerodynamics and recognized the importance of wing warp and airframe stresses. In his treatise on the mechanical birdman he cautions that, "...its joints should be made of strong tanned hide, and sewn with cords of strong raw silk. And let no one encumber himself with iron bands, for these are very soon broken..."

Here at CEA, our scientists and engineers analyze advanced systems. For example, we supply missile and ground support equipment manufacturers with detail data on the response of their structures to thermal and aerodynamic environments. In our studies, we use an invention that would have delighted the probing intellect of Da Vinci: our Direct Analog Computer.



COMPUTER ENGINEERING ASSOCIATES, INC.

350 N. Halstead

Pasadena, California

Elgin 5-7121

- A Contribution to the Theory of Meteor Ablation**, by F. W. Sutton, *Paper 3*, 12 pp.
- Laboratory Experimental Studies in Re-entry Aerothermodynamics**, by W. Warren, *Paper 4*, 22 pp.
- A Solution for Heat Transfer in Laminar Separated and Wake Flow Regions**, by W. D. Carlson, *Paper 5*, 14 pp.
- Transport and Thermodynamic Properties in a Hypersonic Laminar Boundary Layer**, by S. M. Scala and C. W. Baulknight (Part I. Properties of the Pure Species; Part II. Applications), *Paper 6*, 19 pp.
- The Quasi-one Dimensional Flow of an Electrical Conducting Gas for the Generation of Electrical Power**, by G. W. Sutton, *Paper 7*, 15 pp.
- Vaporization Process in the Hypersonic Boundary Layer**, by G. L. Vidale and S. M. Scala, *Paper 8*, 71 pp., 55 refs.
- Turbulent Boundary Layer Equations with Binary Diffusions**, by N. Ness and H. G. Lew, *Paper 9*, 28 pp.
- Combustion of a Gas Injected into a Hypersonic Boundary Layer**, by G. W. Sutton, *Paper 10*, 29 pp.
- The Application of Pressure and Force Transducers in Shock Tunnel Aerodynamic Studies**, by C. J. Harris and E. M. Kaegi, *Paper 11*, 19 pp.
- Stable Shapes of Slender Ablating Graphite Body**, by G. W. Sutton, *Paper 12*, 8 pp.
- Jet Flows with Shocks**, by Mildred M. Moe and B. Andreas Troesch, *ARS JOURNAL*, vol. 30, no. 5, May 1960, pp. 487-489.
- Wake of a Satellite Traversing the Ionosphere**, by S. Rand, *Phys. Fluids*, vol. 3, March-April 1960, pp. 265-273.
- Supersonic Flow Around Right Circular Cones; Tables for Small Angle of Attack**, by Joseph L. Sims, *Army Ballistic Missile Agency, Redstone Arsenal, Ala., Rep. DA-TR-19-60*, April 1960, 432 pp.
- Effect of Localized Mass Transfer near the Stagnation Region of Blunt Bodies in Hypersonic Flight**, by Paul M. Chung, *NASA TN D-141*, May 1960, 16 pp.
- Some Effects of Surface Curvature on the Laminar Boundary Layer Flow**, by K. Toba, *Rensselaer Polytech. Inst., Dept. Aeron. Engng., TR AE 5904*, March 1960, 20 pp.
- Dissociation Effects upon Compressible Turbulent Boundary Layer Skin Friction and Heat Transfer**, by William H. Dorrance, *Convair Sci. Res. Lab., Res. Rep. 6*, April 1960, 27 pp.
- An Approximation Method for the Integration of the Equations of a Non-stationary Laminar Boundary Layer in an Incompressible Fluid**, by L. A. Rozin, *NASA Tech. Transl. F-22*, May 1960, 12 pp. (transl. from *Prikladnaya Matematika i Mekhanika*, vol. 21, 1957).
- Boundary-layer Equations and Their Boundary Conditions in the Case of Motion at Supersonic Velocities in a Moderately Rarefied Gas**, by Yu. N. Lunkin, *NASA Tech. Transl. F-28*, May 1960, 12 pp. (transl. from *Prikladnaya Matematika i Mekhanika*, vol. 21, 1957).
- Annular Nozzles for Missile Base Flow Testing**, by C. E. Peters, *Arnold Engng. Dev. Center, ARO, Inc., AEDC-TN-60-62*, May 1960, 27 pp.
- Sublimation of a Hemisphere in Supersonic Flow**, by Robert Weiss, *MIT, Naval Supersonic Lab, TR 391*, July 1959, 61 pp.
- The Complex Conductivity of Plasma of an Arc Discharge Supported by a Direct Current**, by Jiri Kracik, *NASA Tech. Transl. F-24*, May 1960, 15 pp. (transl. from *Czechoslovak J. Physics*, no. 6, 1956).
- Advances in Applied Mechanics**, ed. by H. L. Dryden, Th. von Kármán and G. Kuerti, vol. 6, Academic Press, N. Y., 1960, 294 pp.
- The Theory of Unsteady Boundary Layers**, by K. Stewartson, pp. 1-37, 75 refs.
- Boundary-layer Theory with Dissociation and Ionization**, by G. Ludwig and M. Heil, pp. 39-118, 59 refs.
- The Propagation of Shock Waves Along Ducts of Varying Cross Section**, by W. Chester, pp. 119-152, 19 refs.
- Similarity and Equivalence in Compressible Flow**, by Klaus Oswatitsch, pp. 153-171.
- Karman Vortex Streets**, by R. Wille, pp. 273-287, 36 refs.
- Oscillations of an Inhomogeneous Plasma in a Magnetic Field**, by L. I. Rudakov and R. Z. Sagdeev, *Soviet Physics-JETP*, vol. 37(10), no. 5, May 1960, pp. 952-954.
- Plasma Sheath Characteristics About Hypersonic Vehicles**, by H. G. Lew and V. A. Langelo, *General Electric Co., Missile & Space Vehicle Dept., TIS R60SD356*, April 1960, 29 pp.
- Effect of Slight Blunting of Leading Edge of an Immersed Body on the Flow Around It at Hypersonic Speeds**, by G. G. Chernyi, *NASA Tech. Transl. F-35*, June 1960, 19 pp.
- Non-similar Solutions of the Compressible Laminar Boundary Layer Equations with Applications to the Upstream Transpiration Cooling Problem**, by A. Pallone, *Avco Corp., Res. & Advanced Dev. Div., Wilmington, Mass., Tech. Rep. RAD-TR-9-60-8*, May 1960, 46 pp.
- Boundary-layer Measurement on 15-deg and 24.5-deg Cones at Small Angles of Incidence at $M = 3.17$ and 3.82 and Zero Heat Transfer**, *Gl. Brit., Aeron. Res. Council, Reps. & Mem. 3133* (June 1957), 1959, 26 pp.
- Some Instabilities Arising from the Interactions Between Shock Waves and Boundary Layers**, by N. C. Lambourn, *Gl. Brit., Aeron. Res. Council, Current Papers 473* (Feb. 1958), 1960, 15 pp.
- Measurements of the Effect of Surface Cooling on Boundary Layer Transition on a 15 Degree Cone**, by J. G. Woodley, *Gl. Brit., Aeron. Res. Council, Current Papers 479*, June 1959, 22 pp.
- On the Turbulent Boundary Layer with Fluid Injection**, by Donald L. Turcotte, *Cornell Univ., Grad. School. Aeron. Engng.*, July 1959, 6 pp.
- Induced Mass Flows in Jet Apparatus**, A. V. Krasnikova, ed., Moscow, Gos. Izdatel. Oboronnoi Prom., 1958, 238 pp. (*Aviatsionnyi Institut imeni Sergo Ordzhonikidze, Trudy 97*). (In Russian.)
- Initial Phase of Mixing Flow in Ejectors**, by I. S. Bogoliubov, pp. 5-42.
- Investigation of Flows in Two-dimensional Jets and Nozzles**, by S. V. Mikhailov, pp. 43-86.
- Injection in Reacting Nozzles in Steady Flow**, by A. V. Kozlov, pp. 87-97.
- Pulsating Reactive Jets with Induced Mass Flow**, by O. I. Kudrin, pp. 98-180.
- Experimental Investigation of a Fluid Ejector**, by Ia. G. Shapiro, pp. 191-236.
- Schaaf, Samuel A. and Talbot, Lawrence, *Mechanics of Rarefied Gases* (Handbook of Supersonic Aerodynamics), *NavOrd Rep. 1488*, vol. 5, Section 16, Washington, D. C., U. S. Govt. Printing Office, Feb. 1959, 90 pp.
- Cylindrical Shock Waves from Exploded Wires of Hydrogen-charged Palladium**, by F. D. Bennett, *Aberdeen Proving Ground, Ball. Res. Labs., BRL Rep. 1063*, Jan. 1959, 25 pp.
- Calculation of the Recoil of a Shock Tube**, by B. A. Woods, *Gl. Brit., Aeron. Res. Council, Current Papers 486*, 1960, 10 pp.
- Errors Associated with a Method for the Experimental Determination of Heat Transfer Coefficients in Uncooled Rocket Nozzles**, by J. D. Clem Jr., *Rohm & Haas Co., Redstone Arsenal Div., Rep. P-60-5*, May 10, 1960, pp. 30-40.
- Variation in Heat Transfer During Transient Heating of a Hemisphere at a Mach Number of 2**, by Roland D. English and Howard S. Carter, *NASA TN D-399*, June 1960, 26 pp.
- Review on the Cooling of Nozzles**, by Jacques Cornillon, *France, Service de Documentation et d'Information Technique de l'Aéronautique SDIT 44/E*, Feb. 1960, 67 pp. (In French.)
- Elements of Cascade Flow**, by H. H. Schlichting, *Belgium, Training Center for Experimental Aerodynamics, Tech. Mem. 4*, March 1959, 16 pp.
- Potential Flows in the Approximation of Viscous Acoustics**, by William Joseph Rae, *Cornell Univ., Grad. School of Aeron. Engng.*, June 1960, 107 pp.
- Stagnation-point Heat-transfer Rate Measurements in the Unexpanded Flow of the NPL Hypersonic Shock Tunnel**, by B. D. Henshall, *Gl. Brit., Aeron. Res. Council, Current Papers 468*, 1960, 6 pp.
- Flow Studies in an Arc-heated Low-density Supersonic Wind Tunnel**, by C. L. Brundin, L. Talbot and F. S. Sherman, *Univ. Calif., Berkeley, Inst. Engng. Res., Tech. Rep. HE-150-181*, April 1960, 25 pp.
- Ballistic Research Laboratories' New Hypersonic Tunnel**, by J. Sternberg, *Aberdeen Proving Ground, Ball. Res. Labs., BRL Rep. 1076*, Jan. 1960.
- On the Separation Phenomenon of Binary Gas Mixture in Axisymmetric Jet**, by Reuben T. Chow, *Univ. Calif., Berkeley, Inst. Engng. Res., Tech. Rep. HE-150-175*, Nov. 1959, 52 pp.
- Design, Fabrication, and Evaluation of Axisymmetric Nozzles**, by Larry L. Lynes, *Univ. of Calif., Berkeley, Inst. Engng. Res., Tech. Rep. HE-150-174*, Sept. 1959, 34 pp.
- The Sputtering of Molecules of a Thin Layer by a Low Density Supersonic Flow in Free Molecular Regime**, by F. Marcel Devienne and George M. Forestier, *Laboratoire Méditerranéen de Recherches Thermodynamiques*, Dec. 1959, 25 pp.
- The Surface Ablation of Fiber Reinforced Plastics Parallel to an Oxyacetylene Flame**, by Robert B. Greene, *Univ. Calif., Berkeley, Inst. Engng. Res., Tech. Rep. HE-150-179*, Feb. 1960, 58 pp.
- Mollier Diagram for Nitrogen**, by R. L. Humphrey, W. J. Little and L. A. Seeley, *Arnold Engng. Dev. Center, AEDC-TN-60-83*, May 1960, 39 pp.
- The Free-free Continuum of Oxygen**, by R. G. Breene Jr. and M. C. Nardone, *General Electric Co., Missile & Space Vehicle Dept., TIS R60-SD365*, May 1960, 11 pp.
- High-temperature Heat-contents, Heat-capacity, and Entropy Data for the Elements and Inorganic Compounds**, by Kenneth Keith Kelley, *Bureau of Mines, Bull. 584*, 1960, 232 pp. Bibliography, pp. 211-232.
- Determination of the Internal Temperature in Satellite 1959 Alpha (Vanguard II)**, by V. R. Simas, J. B. Martin and E. C.

Humphrey, *NASA TN D-357*, June 1960, 18 pp.

Thermal Application of Catalytic Chemical Kinetic Theory, by Alvin R. Saltzman, *Aero/Space Engng.*, vol. 19, June 1960, pp. 28-31, 37.

A Review of the Development of High Enthalpy Aerodynamic Test Facilities, by B. D. Henshall, *Appl. Mech. Revs.*, vol. 13, June 1960, pp. 387-390, 42 refs.

Unsteady Incompressible Couette Flow in a Uniform Transverse Magnetic Field, by C. C. Mei, *Appl. Sci. Res., Section A.*, vol. 9, no. 4, 1960, pp. 275-284.

Estimating Transient Temperature Distributions During Ablation, by M. Richard Denison, *ARS JOURNAL*, vol. 30, no. 6, June 1960, pp. 562-563.

Isentropic Compression of Shock Tube Driver Gas, by R. J. Stalker, *ARS JOURNAL*, vol. 30, no. 6, June 1960, p. 564.

Analog Network to Convert Surface Temperature to Heat Flux, by G. T. Skinner, *ARS JOURNAL*, vol. 30, no. 6, June 1960, pp. 569-570.

Comparison of Transpiration and Ablation Cooling, by Curtis C. Beusman and Joel Weisman, *ARS JOURNAL*, vol. 30, no. 6, June 1960, pp. 573-574.

Thermal Conductivity of Simple Molecules in the Condensed State, by J. K. Horrocks and E. McLaughlin, *Trans. Faraday Soc.*, vol. 56, Feb. 1960, pp. 206-212.

The Stability of Inverse Bubbles, by M. H. I. Baird, *Trans. Faraday Soc.*, vol. 56, Feb. 1960, pp. 213-219.

Highly Intensive Heat and Mass Transfer in Dispersed Media, by Y. Mikhailov, *Internat. J. Heat & Mass Transfer*, vol. 1, no. 1, June 1960, pp. 37-45.

Turbulent Boundary Layer on a Flat Plate in a Stream of Dissociating Gas, by S. I. Kosterin and Yu. A. Koshmarov, *Internat. J. Heat & Mass Transfer*, vol. 1, no. 1, June 1960, pp. 46-49.

An Unsteady Process of the Measurement of Heat Transfer from Fluids and Gases, by P. Grassmann and W. Straumann, *Internat. J. Heat & Mass Transfer*, vol. 1, no. 1, June 1960, pp. 50-54. (In German.)

Evaluation of Bulk Velocity and Temperature for Turbulent Flow in Tubes, by G. F. C. Rogers and Y. R. Mayhew, *Internat. J. Heat & Mass Transfer*, vol. 1, no. 1, June 1960, pp. 55-67.

Convection in the Laminar Regime for the Case of Pressure Gradient and Any Wall Temperature; the Fluid Having Constant Physical Properties, by B. le Fur, *Internat. J. Heat & Mass Transfer*, vol. 1, no. 1, June 1960, pp. 68-80. (In French.)

One-dimensional Energy Transfer in Radiant Media, by Robert and Madeleine Goulard, *Internat. J. Heat & Mass Transfer*, vol. 1, no. 1, June 1960, pp. 81-91.

Heat Transfer by Natural Convection in Materials at the Critical State, by Ernst Schmidt, *Internat. J. Heat & Mass Transfer*, vol. 1, no. 1, June 1960, pp. 92-101. (In German.)

Heat Transfer Bibliography, by E. R. G. Eckert, J. P. Hartnett and T. F. Irvine Jr., *Internat. J. Heat & Mass Transfer*, vol. 1, no. 1, June 1960, pp. 102-112.

Electrostatic Acceleration of Microparticles to Hypervelocities, by H. Shelton, C. D. Hendricks Jr. and R. F. Wuerker, *J. Appl. Phys.*, vol. 31, July 1960, pp. 1243-1246.

Dynamics of a Dissociating Gas, Part 2.

Quasi-equilibrium Transfer Theory, by M. J. Lighthill, *J. Fluid Mech.*, vol. 8, Part 2, June 1960, pp. 161-182.

An Improved Perturbation Theory for Shock Waves Propagating Through Non-uniform Regions, by M. P. Friedman, *J. Fluid Mech.*, vol. 8, Part 2, June 1960, pp. 193-209.

On the Effect of the Molecular Diffusivity in Turbulent Diffusion, by P. G. Saffman, *J. Fluid Mech.*, vol. 8, Part 2, June 1960, pp. 273-283.

The Compressible Viscous Heat-conducting Vortex, by Leslie M. Mack, *J. Fluid Mech.*, vol. 8, Part 2, June 1960, pp. 284-292.

Mass Transport in the Boundary Layer at a Free Oscillating Surface, by M. S. Longuet-Higgins, *J. Fluid Mech.*, vol. 8, Part 2, June 1960, pp. 293-306.

Design Precepts for High-temperature Heat Exchangers, by A. P. Fraas, *Nuclear Sci. & Engng.*, vol. 8, no. 1, July 1960, pp. 21-31.

The Propagation of Sound in Monatomic Gas Mixtures, by R. Holmes and W. Tempest, *Proc., Phys. Soc., London*, vol. 75, Part 6, June 1, 1960, pp. 898-904.

Compression Waves in a Plasma in a Static Magnetic Field, by N. Anderson, *Proc., Phys. Soc., London*, vol. 75, Part 6, June 1, 1960, pp. 905-912.

On Steady Axially Symmetric Solutions of the Idealized Hydromagnetic Equation for a Compressible Gas in Which There Is No Diffusion of Vorticity, Heat, or Current, by T. V. Davies, *Quart. J. Mech. & Appl. Math.*, vol. 13, Part 2, May 1960, pp. 169-183.

Certain Solutions of the Heat Conduction Equation, by H. Poritsky and R. A. Powell, *Quart. Appl. Math.*, vol. 18, no. 2, July 1960, pp. 97-106.

Gas-ionizing Magnetohydrodynamic Shock Waves, by A. G. Kulikovskii and G. A. Lyubimov, *Soviet Phys.: Doklady*, vol. 4, no. 6, May-June 1960, pp. 1185-1188.

The Simplest Problems Concerning Gas-ionizing Shock Waves in an Electromagnetic Field, by A. G. Kulikovskii and G. A. Lyubimov, *Soviet Phys.: Doklady*, vol. 4, no. 6, May-June 1960, pp. 1195-1198.

Influence of a Magnetic Field on Boundary Layer Stability, by V. N. Arkhipov, *Soviet Phys.: Doklady*, vol. 4, no. 6, May-June 1960, pp. 1199-1201.

Fusion of a Heat-conducting Wall Behind a Moving Compression Shock, by G. A. Tirsii, *Soviet Phys.: Doklady*, vol. 4, no. 6, May-June 1960, pp. 1202-1206.

Asymptotic Behavior of Solutions in Heat Transfer, by M. M. Nazarchuk and N. I. Pol'skii, *Soviet Phys.: Doklady*, vol. 4, no. 6, May-June 1960, pp. 1227-1229.

Selected Problems in the Theory of Radiation Diffusion, by V. V. Sobolev, *Soviet Phys.: Doklady*, vol. 4, no. 6, May-June 1960, pp. 1235-1242.

The Motion of Gaseous Bubbles in a Liquid Under the Influence of Bjerknes Forces Arising in an Acoustic Field, by V. F. Kazantsev, *Soviet Phys.: Doklady*, vol. 4, no. 6, May-June 1960, pp. 1250-1254.

Electrical Conductivity of Dielectrics in Strong Shock Waves, by A. A. Brish, M. S. Tarasov and V. A. Tsukerman, *Soviet Phys.: JETP*, vol. 11, no. 1, July 1960, pp. 15-17.

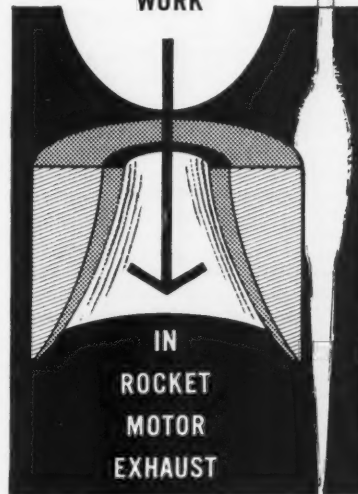
Certain Special Features of Ohmic Heating of Electron Gas in a Plasma, by A. V. Gurevich, *Soviet Phys.: JETP*, vol. 11, no. 1, July 1960, pp. 85-88.

example ...

FIBERITE

COMPOSITE
MOLDED
INSULATION

AT
WORK



Minimum erosion and ablation resistance are needed in exit areas to resist over 5000° F. and high velocities. Excellent results were achieved with Fiberite MX 2630 and MX 2630A. The mechanical strength and thermal insulation were provided by Fiberite MX 2625 with 2630 giving the ablation resistance. By molding these two formulations into a composite structure a superior insulation was developed. Fiberite compression molded high temperature insulating materials are designed for MIL-M-19536 applications: chopped fiber impregnated phenolic with special reinforcement materials, i.e., fiberglass, graphite cloth, ceramic and quartz. Fiberite insulation is specified in the Lar, Bull Pup, Polaris, Minute Man, Nike Zeus, Red Eye and many others.

EXPLORE FIBERITE

Missile engineers will find our research helpful in solving problems requiring materials for special performance. Write factory for bulletin "Fiberite High Temperature Insulating Materials."



SALES OFFICES IN
PRINCIPAL CITIES

**THE FIBERITE
CORPORATION**

Dept. ARS-11
510-520 West 4th Street
Winona, Minnesota

Effect on Conductivity Anisotropy in a Magnetic Field on the Structure of a Shock Wave in Magnetogasdynamics, by S. A. Kaplan, *Soviet Phys.: JETP*, vol. 11, no. 1, July 1960, pp. 183-184.

Isothermal Discontinuities in Magneto-hydrodynamics, by V. I. Tselyayev, *Soviet Phys.: JETP*, vol. 11, no. 1, July 1960, pp. 185-187.

Advances in Cryogenic Engineering, Vol. 5: Proceedings of the 1959 Cryogenic Engineering Conference (Univ. Calif., Berkeley, Calif., Sept. 2-4, 1959), K. D. Timmerhaus, ed., Plenum Press, N. Y., 1960, 584 pp.

Transient Phenomena Associated with the Pressurization of Liquid Nitrogen Boiling at Constant Heat Flux, by S. K. Fenster, G. J. VanWylen and J. A. Clark, pp. 226-234.

Recent Developments of the Reversing Exchanger, by M. C. Sze and E. Cimlar, pp. 235-243.

Design, Construction and Testing of a Helium-to-hydrogen Heat Exchanger, by C. C. Wright, pp. 244-253.

Boiling Heat Transfer to Liquid Hydrogen from Flat Surfaces, by C. R. Class, J. R. DeHaan, M. Piccone and R. B. Cost, pp. 254-261.

Nucleate- and Film-boiling Studies with Liquid Hydrogen, by U. H. von Glahn and J. P. Lewis, pp. 262-269.

A Closed Infrared Detector Cooling System, by F. E. Altoz and J. R. Eargle, pp. 317-323.

Miniature Joule-Thomson Refrigeration Systems, by J. M. Geist and P. Lashmet, pp. 324-331.

Continuous Refrigeration Between 4.2 and 1°K, by K. J. Nicol and H. V. Bohm, pp. 332-337.

Design, Construction and Performance of a Laboratory-size Helium Liquefier, by D. B. Mann, W. R. Bjorkland, J. Macinka and M. J. Hiza, pp. 346-353.

A New Low-temperature Gas Expansion Cycle, Part I, by H. O. McMahon and W. E. Gifford, pp. 354-367.

A New Low-temperature Gas Expansion Cycle, Part II, by H. O. McMahon and W. E. Gifford, pp. 368-372.

Measuring Vapor-liquid Ratios During Flow by a Capacitance Method, by W. R. Killian and J. O. Simpson, pp. 505-508.

Refrigeration Below -100°C, by J. W. L. Kohler, pp. 518-525.

Recent Hypersonic Studies of Wings and Bodies, by Michel H. Bertram and Arthur Henderson, *ARS Preprint* 1131-60, May 1960, 23 pp.

Flight Mechanics

On the Problem of the Interaction Between a Satellite and the Earth's Magnetic Field, by Yu. V. Zonov, *NASA Tech. Transl. F-35*, May 1960, 11 pp.

Motion of a Slender Blunted Body in the Atmosphere with High Supersonic Speed, by V. V. Lunev, *ARS JOURNAL*, vol. 30, no. 4, April 1960, *Russian Suppl.*, pp. 414-416.

Solar-lunar Perturbations of the Orbit of an Earth Satellite, by Mildred M. Moe, *ARS JOURNAL*, vol. 30, no. 5, May 1960, pp. 485-487.

Initial Azimuths and Times for Ballistic Lunar Impact Trajectories, by W. C. Riddell, *ARS JOURNAL*, vol. 30, no. 5, May 1960, pp. 491-493.

Electrically Charged Missile in Vertical Descent, by Marvin H. Hewitt, *ARS JOURNAL*, vol. 30, no. 5, May 1960, pp. 505-506.

Lunik III, Trajectory Predictions, by J. E. Michaels, M. Wachman and A. Petty, *Astron. Sci. Rev.*, vol. 2, no. 1, Jan.-March 1960, pp. 13-16.

Establishment of a Circular Satellite Orbit by Double Impulse, by G. Leitmann, *J. Brit. Interplanet. Soc.*, vol. 17, Jan.-Feb. 1960, pp. 194-198.

On the Drag of a Spherical Satellite Moving in a Partially Ionized Atmosphere, by H. H. C. Chang and M. C. Smith, *J. Brit. Interplanet. Soc.*, vol. 17, Jan.-Feb. 1960, pp. 199-205.

Program Costs for a Manned Space Station, by R. H. Lundberg and T. E. Dolan, *Aero/Space Engng.*, vol. 19, May 1960, pp. 82-83, 108.

Economic Aspects of Developing and Orbiting a Space Station, by Milton A. Margolis, *Aero/Space Engng.*, vol. 19, May 1960, pp. 84-85.

Evaluation of Preflight Risks by Means of Very High Speed Digital System Simulation, by Jesse R. Brinkerhoff, *ARS JOURNAL*, vol. 30, no. 5, May 1960, pp. 493-495.

Real-time Analysis, New Approach in Flight Testing, by Guenther Hintze, *ARS JOURNAL*, vol. 30, no. 5, May 1960, pp. 500-502.

Trajectories with Constant Tangential Thrust in Central Gravitational Fields, by W. E. Moeckel, *NASA Tech. Rep. R-53*, 1960, 73 pp.

The Libration of a Satellite, by V. V. Beletskiy, *NASA Tech. Transl. F-10*, May 1960, 34 pp. (transl. from *Iskusstvennyye Sputniki Zemli*, no. 3, Moscow, Acad. Sci. USSR, 1959).

Artificial Earth Satellites, Vols. I & II, ed.

by I. V. Kurnosova, translated from Russian, Plenum Press, N. Y., 1960, 120, 107 pp.

Motion of an Artificial Earth Satellite About Its Center of Mass, by V. V. Beletskiy, vol. I, pp. 30-54.

Dynamic Effects During the Motion of Artificial Earth Satellites, by L. I. Sedov, vol. II, pp. 3-11.

Satellite Perturbations from Extra-terrestrial Gravitation and Radiation Pressure, by F. T. Geyling, *J. Franklin Inst.*, vol. 269, May 1960, pp. 375-407.

Probing Interplanetary Space, by S. W. Greenwood, *J. Roy. Aeron. Soc.*, vol. 64, May 1960, pp. 299-301.

Interactions of Rapidly Moving Bodies in Terrestrial Atmosphere, by K. P. Chopra, *Southern Calif. Univ., Engng. Center, USCEC Rep. 56-212*, March 1960, 147 pp., 103 refs.

Longitudinal Dynamics of a Lifting Vehicle in a Circular Orbit, by B. Etkin, *Inst. Aerophys., Univ. Toronto, UTIA Rep. 65*, Feb. 1960, 21 pp.

Analysis of Low-acceleration Lifting Entry from Escape Speed, by Frederick C. Grant, *NASA TN D-249*, June 1960, 21 pp.

Analytic Solutions of Planar Reentry Trajectories with Lift and Drag, by Kenneth Wang and Lu Ting, *Brooklyn Polytech. Inst., Dept. Aeron. Engng. & Appl. Mech., PIBAL Rep. 601*, April 1960, 67 pp.

Interim Definitive Orbit for the Satellite 1958-Gamma, Explorer III, Theory and Analysis Staff, Goddard Space Flight Center, *NASA TN D-356*, June 1960, 490 pp.

Vehicle Design, Testing and Performance

Effects of Jet Billowing on Stability of Missile-type Bodies at Mach 3.85, by Reino J. Salmi, *NASA TN D-284* June 1960, 17 pp.

Comments on the Use of Guns to Launch High Altitude Probes, by L. C. MacAllister and J. W. Bradley, *Aberdeen Proving Grounds, Ball. Res. Labs., BRLM 1252*, March 1960, 30 pp.

Ideal Performance of Multistage Rockets, by Richard D. Geckler, *ARS JOURNAL*, vol. 30, no. 6, June 1960, pp. 531-536.

Observation Satellites: Problems and Prospects, by Amrom H. Katz, *ASTRONAUTICS*, vol. 5, June 1960, pp. 26-29, 52, 54.

The Transit Program, by Richard B. Kersher, *ASTRONAUTICS*, vol. 5, June 1960, pp. 30-31, 104-105.

Tiros I—Meteorological Satellite, by Sidney Sternberg and William G. Stroud, *ASTRONAUTICS*, vol. 5, June 1960, pp. 32-34, 84-86.

The Tiros I Timer, by John D. Freeman, *ASTRONAUTICS*, vol. 5, June 1960, pp. 35, 78-79.

Key Equipment for Tiros I, by E. A. Goldberg and V. D. London, *ASTRONAUTICS*, vol. 5, June 1960, pp. 36-37, 98-99.

Tiros I Spin Stabilization, by Harold Perkel, *ASTRONAUTICS*, vol. 5, June 1960, pp. 38-39, 106.

Thermal Design for Tiros, by Milton Titter, *ASTRONAUTICS*, vol. 5, June 1960, pp. 40-41, 92, 94.

Structural Design of Tiros I, by Carl C. Osgood, *ASTRONAUTICS*, vol. 5, June 1960, pp. 42-43, 90-91.

Scientific Experiments for Space Probes Near the Earth, Mars and Venus, by Marcia Neugebauer, *ARS Preprint* 1195-60, May 1960, 10 pp.

The Artificial Earth Satellite—A New

CHANGE-OF-ADDRESS NOTICE

In the event of a change of address, it is necessary to include both your old and new addresses, as well as your membership number and coding, when notifying ARS headquarters in order to insure prompt service. If you are moving or have moved, send the following form to Membership Dept., American Rocket Society, 500 Fifth Ave., New York 36, N. Y.:

Name _____
Membership Card No. _____ Coding _____
Old Address _____
New Address _____

Geodetic Tool, by Bruce C. Murray, *ARS Preprint* 1221-60, May 1960, 12 pp.

Launch Vehicles for Lunar Flight, by Ernst Stuhlinger, *ARS Preprint* 1115-60, May 1960, 9 pp.

Lunar Landing Vehicle Propulsion Requirements, by Richard J. Wrobel and Robert R. Breshears, *ARS Preprint* 1121-60, May 1960, 16 pp.

Optimization of Vehicles and Trajectories for the Twenty-four Hour Equatorial Satellite Mission, by Abraham Fiul and Harold Braham, *ARS Preprint* 1120-60, May 1960, 47 pp.

Missile Prelaunch Confidence Check-out: Content and Equipment Design Criteria, by S. I. Firstman and B. J. Voosen, *Rand Corp., Res. Mem.* RM-2485, Feb. 22, 1960, 107 pp.

Search Rules for Automatic Fault Location, by Sidney I. Firstman and Brian Gluss, *Rand Corp., Res. Mem.* RM2514, Jan. 15, 1960, 36 pp.

The Role of Man in the Maintenance of Earth Satellites, by David Mesiter and R. B. Wilson, *ARS Preprint* 1214-60, May 1960, 12 pp.

Evaluation of an Experimental Troubleshooting Technique, by Trindel J. Ferguson, *ARS Preprint* 1217-60, May 1960, 19 pp.

Electrostatic Tape Camera for Satellite Inspection, by Spencer Spaulding, *ARS Preprint* 1199-60, May 1960, 6 pp.

Design and Maintainability of the Able-Baker Bio-capsules, by Wallace G. Kistler Jr., *ARS Preprint* 1226-60, May 1960, 13 pp.

Maintaining Space Vehicles, by Nicholas A. Bond Jr., *ARS Preprint* 1218-60, May 1960, 6 pp.

Automatic Test Equipment Checks Missile Systems, by D. B. Dobson and L. L. Wolff, *Electronics*, vol. 33, July 15, 1960, pp. 74-78.

M/R's Fourth Annual World, Missile-Space Encyclopedia, Including for the First Time a Directory of Rocket Engines, Missiles & Rockets, vol. 7, no. 3, July 18, 1960, pp. 107-154.

Development of the Arcas Rocketsonde System, by R. C. Webster, W. C. Roberts Jr. and E. P. Donnell, *Atlantic Res. Corp., Alexandria, Va., Final Rep.*, Feb. 1960, 26 pp.

Support Systems. Part I—Scope and Techniques, by Beal M. Teague, *Aero-Space Engng.*, vol. 19, July 1960, pp. 16-19.

A Method for the Determination of the Thrust in Flight, by M. Cassetti, *L'Aerotecnica*, vol. 39, no. 6, Dec. 1959, pp. 309-315. (In Italian.)

Observation Satellites: Problems and Prospects, by Amrom H. Katz, *ASTRONAUTICS*, vol. 5, July 1960, pp. 28-29, 80, 82-84.

Rocket Power—Key to Space Supremacy, by Don R. Ostrander, *ASTRONAUTICS*, vol. 5, July 1960, pp. 22-23, 80-91.

The Shape of Tomorrow, by Clifford I. Cummings, *ASTRONAUTICS*, vol. 5, July 1960, pp. 24-25, 91.

The Saturn Project, by William A. Mrazek, *ASTRONAUTICS*, vol. 5, July 1960, pp. 26-27, 74, 76.

Rocket Catapult Facts and Fables, by Michael Stoiko and John W. Dorsey, *ASTRONAUTICS*, vol. 5, July 1960, pp. 30-31, 93-94.

On Target for Tomorrow—the Explorer Scout Space Science Exposition, by Vincent S. Haneman Jr. and Laurel van

der Wal, *ASTRONAUTICS*, vol. 5, July 1960, pp. 53, 68-69.

On Bodies of Minimum Wave Drag, by V. N. Zhigulev and Iu. L. Zhilin, *PMM: J. Appl. Math. & Mech. (transl. of Prikladnaya Mat. i Mek.)*, vol. 23, no. 6, 1959, pp. 1462-1475.

What Price Weight for Advanced Aerospace Vehicles? by Herbert C. Sanders, *Space/Aeron.*, vol. 34, July 1960, pp. 67-68, 70, 72.

The Exploration of Outer Space, by A. C. B. Lovell, *Spaceflight*, vol. 11, no. 7, July 1960, pp. 194-203.

Skylark, by Maurice Allward, *Spaceflight*, vol. 11, no. 7, July 1960, pp. 204-208.

Exploration of the Moon: 1. The Lunar Objective, by Patrick Moore, *Spaceflight*, vol. 11, no. 7, July 1960, pp. 209-211.

Exploration of the Moon: 2. The Robot Explorers, by K. W. Gatland, *Spaceflight*, vol. 11, no. 7, July 1960, pp. 212-219.

Guidance and Control

On the Optimum Response of Third Order Contactor Control Systems, by I. Flügel-Lotz and Mith Yin, *Stanford Univ., Div. Engng. Mech., Tech. Rep.* 125, April 25, 1960, 135 pp.

Rudimentary Launch Guidance Methods for Deep Space Missions, by C. G. Pfeiffer, *ARS Preprint* 1172-60, May 1960, 19 pp.

On the Propagation of Errors in a Schuler-type Inertial Navigation System, by Joseph G. Gurley, *ARS Preprint* 1173-60, May 1960, 3 pp.

On the Adequacy of ICBM Guidance Capability for a Mars Launch, by William N. Spence, *ARS Preprint* 1174-60, May 1960, 20 pp.

Evaluation of Precision Gyros for Space Boost Guidance Applications, by Louis K. Jensen, H. Evans Bowman and Richard Clark, *ARS Preprint* 1175-60, May 1960, 11 pp.

An Investigation of a Terminal Guidance System for a Satellite Rendezvous, by N. J. Niemi, *ARS Preprint* 1176-60, May 1960, 29 pp.

General Research in Flight Sciences; Jan. 1959-Jan. 1960, Vol. 3, Flight Dynamics and Space Mechanics, Lockheed Aircraft Corp., *Missiles & Space Div., Rep.* LMSD-288,139, vol. 3, Jan. 1960.

Fuel Requirements for Crude Interplanetary Guidance, by J. V. Breakwell, Paper 3, 16 pp.

Error Analysis Considerations for a Satellite Rendezvous, by W. M. Duke, E. A. Goldberg and I. Pfeffer, *ARS Preprint* 1198-60, May 1960, 15 pp.

On the Stability of a Gyroscopic System, by I. Z. Pirogov, *PMM: J. Appl. Math. & Mech. (transl. of Prikladnaya Mat. i Mek.)*, vol. 23, no. 6, 1959, pp. 1623-1626.

Passage of Signal and Noise Through a Non-linear Inertial System, by Iu. E. D'iaikov, *Radio Engng. & Electronics (transl. of Radiotekh. i Elektronika)*, vol. 4, no. 6, June 1959, pp. 38-46.

Long Range Radio Navigation Extended for Advanced Vehicles, by William B. Leaf, *Space/Aeron.*, vol. 34, July 1960, pp. 118-124.

Ceramic Gas-bearing Gyro for Space Guidance (Design Digest), by Bernard Kovit, *Space/Aeron.*, vol. 34, July 1960, pp. 131-132.

Important New Volumes in the Series PRINCIPLES OF GUIDED MISSILE DESIGN

AIRBORNE RADAR SYSTEMS

by Donald J. Povejsil, Robert S. Raven, Peter Waterman

This brand new addition to the series, provides an understanding of basic radar technology and its relation to overall weapons system design. Emphasis is placed on the basic principles and systems analysis techniques and how mathematical models may be developed to solve radar design problems. Important material for all weapons systems engineers, military personnel and graduate students.

700 pages, prob. \$14.50

SYSTEMS PRELIMINARY DESIGN

by Joseph Jerger

Covered at length in this important unifying volume are the various interrelationships that exist in the preliminary systems design of a guided missile. Useful data from important branches of engineering and science involved in missile design are presented in convenient form, and illustrative problems are carried out in complete numerical detail.

640 pages, \$14.75

SPACE FLIGHT

Volume I: Environment and Celestial Mechanics

by Kraft A. Ehricke

Here are the concepts of space flight, its environment, astronomy from the viewpoint of the astronautical engineer, and principles and methods of celestial mechanics. Comprehensive data, tables, graphs, many derivations and equations of notion are helpfully included.

650 pages, \$14.50

Volume II: Dynamics (Early 1961)

Van Nostrand



Publishers Since 1848
PRINCETON, NEW JERSEY

MAN

his ideas . . .

...and their fulfillment

Between an original concept and scientific achievement, the engineer, working with an unequaled array of experimental and test facilities at Los Alamos, makes significant contribution to space science.

For employment
information write:
Personnel Director
Division 60-101

los alamos
scientific laboratory
OF THE UNIVERSITY OF CALIFORNIA
LOS ALAMOS, NEW MEXICO

Index to Advertisers

ACADEMIC PRESS, INC.	998
AEROJET-GENERAL CORP.	Back cover
<i>D'Arcy Advertising Co., Los Angeles, Calif.</i>	
ALLIED CHEMICAL CORP., NITROGEN Div.	Second cover
<i>G. M. Basford Co., New York, N. Y.</i>	
BALL BROTHERS RESEARCH CORP.	1113
<i>Walter L. Schump, Denver, Colo.</i>	
COMPUTER ENGINEERING ASSOC.	1115
<i>Guerin, Johnstone, Jeffries, Inc., Los Angeles, Calif.</i>	
ELECTRO-OPTICAL INSTRUMENTS.	1114
<i>Soltys Associates, Los Angeles, Calif.</i>	
FIBERITE CORP.	1117
<i>Harold C. Walker Advertising, Minneapolis, Minn.</i>	
LORAL ELECTRONICS CORP.	996, 997
<i>Smith, Winters Mabuchi, Inc., New York, N. Y.</i>	
LOS ALAMOS SCIENTIFIC LABORATORY.	1120
<i>Ward Hicks Advertising Agency, Inc., Albuquerque, N. Mex.</i>	
RCA-DEFENSE ELECTRONIC PRODUCTS.	993
<i>Al Paul Lefston Co., Inc., Philadelphia, Pa.</i>	
SPACE TECHNOLOGY LABORATORIES.	995
<i>Gaunor & Ducas, Inc., Beverly Hills, Calif.</i>	
D. VAN NOSTRAND CO., INC.	1119
<i>R. W. Westervelt & Co. Advertising, Princeton, N. J.</i>	
WYMAN-GORDON CO.	Third cover
<i>The Davis Press, Inc., Worcester, Mass.</i>	

